CVR JOURNAL OF SCIENCE AND TECHNOLOGY

Vol.No. 25, December 2023
P-ISSN 2277 - 3916
DOI 10.32377/CVRJST25
E-ISSN 2581 - 7957

CVR COLLEGE OF ENGINEERING

In Pursuit of Excellence

CVR JOURNAL OF SCIENCE AND TECHNOLOGY

Indexed by

- Google Scholar
- Directory of Research Journals Indexing (DRJI)
- Scientific Indexing Services (SIS)
- International Institute of Organised Research (I2OR)
- Scholar Impact - Journal Index
- Citefactor
- Member Crossref / DOI

Accredited by NAAC with 'A' GRADE

CVR COLLEGE OF ENGINEERING

(UGC Autonomous - Affiliated to JNTU Hyderabad)
Mangalpalli (V), Ibrahimpatnam (M),
R.R. District, Telangana. – 501510
http://cvr.ac.in

EDITORIAL

The editorial team of the Biannual CVR Journal of Science and Technology is very happy to bring out Vol.25, very much in time. This has become a practice to bring out the journal in time, despite various hurdles including Carona Pandemic, sometime back. For the last 6 months the team has been working tirelessly to complete the task on time. We thank the authors, reviewers and all others involved in this task.

We are taking care to see that standard practices are followed in the publication of the Journal. Blind review is done, and a number of iterations are done till the reviewers are fully satisfied with the standard of the research paper. Senior faculty of English language Department, take care of the language issues. Template verification and typographical errors are checked before the articles go for publishing. Hope the researchers appreciate this effort. Many research articles published in the journal are being referred to by other researchers across the globe, as indicated by DOI, Crossref data.

This Volume covers research articles in the following disciplines:

CIVIL–2, ECE–6, EIE–4, ET–1, MECH–2, H & S–3 (Stats-1, Chem-1, Env. Sc.-1)

In this issue, a research article on Fiber-reinforced Lightweight Self Compacting Concrete (FRSCC) with fly ash is presented. The study consisted of substituting conventional natural aggregates with sintered fly ash. The outcome of this research yielded valuable insights into improving the mechanical and thermal properties of FRSCC. One paper on Image Inpainting using Efficient Patch Selection Technique is presented. New patch selection is proposed using the combination of Sum of Squares Difference (SSD) and Logarithmic Similarity (LS). The results obtained, according to the authors, are excellent and outperformed the state-of-art works reported in the literature. Another paper presents analysis of application of various machine learning models for plant leaf identification. Authors applied Weiner filter for noise reduction in the data. Morphological operations are utilized for feature extraction.

GSM based Patient Healthcare Monitoring System is proposed in another article. This system is claimed to be the most effective and cost-efficient solution compared to other methods available worldwide. Some other articles published are An IoT based Low-cost Artificial Mechanical Ventilator for Patients, IoT based power theft detection system, Novel approach to design a portable mobile charging device using wind energy. Hope the research articles published make interesting reading for researchers working in those areas. One article on Cloud and IoT based Monitoring System for Analytical Instruments, authored by a Scientific Officer from BARC and a student from BITS Pilani is also published in this issue. Some of the research articles have potential to develop gadgets, which can be used and released into the market by industries.

Students are being encouraged to publish research papers based on the project work done by them. P.G. students spend almost one year on the project work. So, this should result in significant work suitable for publication in a journal. Project supervisors guiding the students must give research orientation for the work of the students. Selected research papers of U.G. students are also published in this volume. It is heartening to see that U.G. students are also showing enthusiasm for publishing papers. Hope this trend will continue.

Thanks are due to **HOD, H & S,** and the staff of English Department for reviewing the papers. I am also thankful to **Dr. S. Venkateshwarlu, Assoc. Editor and Smt. A. Sreedevi, DTP Operator** in the Office of Dean Research, for the preparation of research papers in Camera - Ready form.

For further clarity on waveforms, graphs, circuit diagrams and figures, readers are requested to browse the soft copy of the journal, available on the college website www.cvr.ac.in wherein a link is provided. Authors can also submit their papers through our online open journal system (OJS) www.ojs.cvr.ac.in or www.cvr.ac.in/ojs

Prof. K. Lal Kishore
Editor

International Review Board:

CONTENTS Page No.

E-ISSN 2581 – 7957
P-ISSN 2277 – 3916
CVR Journal of Science and Technology, Volume 25, December 2023
DOI: 10.32377/cvrjst2501

Effect of Elevated Temperature on the Lightweight Aggregate Fibre Reinforced Self-Consolidating Concrete

N. Ramanjaneyulu[1], M.V. Seshagiri Rao[2] V. Bhaskar Desai[3]
[2]Research Scholar, JNTUA College of Engineering/Anantapuram and Sr. Asst. Professor, CVR College of Engineering/Civil Engg. Department, Hyderabad, India
Email: rams.613@gmail.com
[3]Professor, CVR College of Engineering/Civil Engg. Department, Hyderabad, India
Email: rao_vs_meduri@yahoo.com
[3]Retd. Professor & Rector, JNTU Anantapur, Civil Engg. Department, Anantapur, A.P, India
Email: vbdesaijntu@gmail.com

Abstract: **This study comprehensively investigates fiber-reinforced self-compacting concrete (FRSCC) behavior across multiple grade variations, namely M20, M30, and M40. The study encompasses substituting conventional natural aggregate with sintered fly ash, exploring replacement percentages of 10%, 20%, and 30%. The primary objective of this study is to identify the optimum Strength achieved through a 20% replacement ratio. The assessment of fresh properties of FRSCC was undertaken through rigorous testing protocols involving the L box, J ring, and V funnel tests, following the guidelines stipulated by the European Guidelines for Self-Compacting Concrete (EFNARC). Furthermore, the research extensively analyzed vital mechanical properties, including compressive Strength, split tensile Strength, and flexural Strength. These evaluations provided insights into the influence of sintered fly ash incorporation on the structural performance of FRSCC. The investigation extended to a post-curing temperature study, subjecting the concrete specimens to varying temperatures of 100 °C, 300 °C, 600 °C, and 900 °C, followed by exposure to a 1000 °C heating furnace for 3 hours at each designated temperature. The outcomes of this research yield valuable insights into the potential improvements in the mechanical and thermal properties of FRSCC by integrating sintered fly ash. This study is pertinent for professionals and researchers engaged in optimizing the formulation and utilization of fiber-reinforced self-compacting concrete, with implications for sustainable construction practices and enhanced resilience in diverse thermal conditions.**

Index Terms: **Fibre reinforced lightweight self-compacting concrete, Fly Ash, Sintered fly ash Aggregate, Lightweight Sintered fly ash aggregate concrete, lightweight self-consolidating concrete, Crimped steel fiber.**

I. INTRODUCTION

To provide engineers greater freedom during creating concrete structures that are both affordable and quick to create, lightweight self-compacting concrete aims to integrate the benefits of both lightweight concrete (LWC) and self-compacting concrete (SCC). Self-compacting concrete (SCC) does not require vibration for installation or compaction. Fiber-reinforced lightweight Aggregate Concrete (FRLWAC) focuses on its mechanical Strength, durability, and thermal behavior. The study contributes to optimizing FRLWAC's applications in construction and engineering. [1-4] Even amid packed reinforcement, it can pour with its weight, filling formwork and reaching full compaction without separating material components. Microcracks in the motor-aggregate interface cause plain concrete to be weak. In the concrete technology industry, self-compacting concrete (SCC) has become a groundbreaking substance because it provides remarkable flowability and self-consolidation without needing external compaction. Characteristics of Lightweight Expanded Clay Aggregate (LECA) used instead of some of the coarse aggregate in Lightweight Self-Compacting Concrete (LWSCC) regarding Strength and durability. The research aims to assess the feasibility and performance of LWSCC in various construction applications. [5-8]. To further enhance its mechanical properties and performance, researchers have investigated the potential of incorporating steel fibers as reinforcement within SCC Self-Compacting Concrete (SCC) by partially replacing coarse aggregate with Pumice Lightweight Aggregate (PLA). The research aims to evaluate the mechanical and structural properties of SCC with PLA, exploring its potential as a sustainable construction material. [9-12] The strength characteristics of concrete incorporating Sintered Fly Ash Aggregate (SFAA) as a partial replacement for conventional coarse aggregate. The study explores the viability and performance of SFAA-based concrete for sustainable construction applications. [13]. The fresh and hardened behavior of lightweight self-consolidating concrete (LWSCC) was made with sintered fly ash aggregate (SFAA). The research aims to assess the workability and mechanical properties of LWSCC with SFAA for potential structural applications. [14]. Steel fibers can be added to the mixture to minimize this weakness. To make concrete more durable or capable of resisting the development of cracks, composite materials can also be made from different fibers, such as glass, polymer, etc., which presents valuable insights into the properties and performance of this novel composite material. [15] The experimental study delves into the effects of steel fiber reinforcement on the properties and behavior of SCC, providing crucial knowledge for optimizing the mix design and harnessing the full potential of this advanced concrete material in construction applications. The combination of SFAA and LWSCC presents an exciting avenue for sustainable construction. The lightweight nature of SFAA reduces the overall dead load of structures, which is especially beneficial in applications like high-rise buildings and bridges. Additionally, LWSCC offers increased construction efficiency by eliminating the need for manual

Received on 17-10-2023, Revised on 14-11-2023, Accepted on 28-11-2023

compaction, resulting in reduced labor costs and faster construction cycles. [16] This paper explores the effects of fiber reinforcement on lightweight aggregate concrete, providing crucial knowledge for advancing sustainable and high-performance construction practices.

II. Literature Review

Hajime Okamura, Masahiro Ouchi (9999): Concrete that compacts by itself was created in 1988 to prevent vibrational compaction. Such that the author established a logical approach mix design before beginning the inquiry. At the work site, the rational mix design technique is determined to be suitable for SCC. With this method, we may investigate and suggest novel approaches to structural design.

Thomas Paul, Habung Bida, Bini Kiron (2016). The study aimed to identify and contrast the differences in the properties of regular concrete, or SCC, when steel fibers are added in various amounts. The experimental examination aimed to determine the compressive strength, flexural Strength, and split tensile Strength of concrete reinforced with steel fibers and containing fibers with volume fractions of 0%, 0.4%, 0.8%, and 1.2% end-hooked steel fibers. The aspect ratio of the steel fiber was 75. The data from the results has been examined and contrasted with a specimen that contains no steel fiber. As the fiber dosage rate rises, the workability of SCC is considerably diminished. The research article suggests that because of these characteristics, steel fiber-reinforced self-compacting concrete can be utilized to build curved forms and in locations where compaction is not feasible.

Siddharth Anand, Mohammad Afaque Khan, Abhishek Kumar (2016). At a certain point, adding steel fiber increases compressive Strength, preventing cracks from forming and giving greater Strength. The hardened condition has steel fibers added to it. Fiber-reinforced concrete is required when restricted durability, narrow fracture widths, or safety considerations are design criteria. With each additional steel fiber added to the SFR-SCC, compressive Strength rises. Workability in SFR-SCC significantly declines as steel fiber content rises. Flexural Strength in SFR-SCC rises as steel fiber content rises. As the amount of steel fiber in SFR-SCC grows, the tensile Strength also rises. 5. Self-compacting concrete is easy to use and straightforward.

S. Ramesh Reddy, I.Krisharchana, Dr. V. Bhaskar Desai (2017). An effort is made to create lightweight concrete made of ions by substituting sintered fly ash for 100% of the natural aggregate and using three different pozzolanic materials to replace a portion of the cement (11%), including equal amounts of slag, fly ash, and silica fume, as well as varying amounts of Nano Aluminium Oxide. M20 concrete is intended to have a mean strength of 26.6N/mm2. When Nano Al2O3 is raised by up to 1%, the altered concrete rises to 42.80N/mm2, enhancing its flexural Strength and Young's modulus. Sintered fly ash aggregate can be utilized as coarse aggregate, cutting down on cement usage by 11%.

Dilip Kumar, Arvind Kumar, Ashish Gupta (2014). In the current study, a mix design for concrete of the M25 grade was finished utilizing the IS technique. Sintered fly ash aggregates, a waste product of coal-firing thermal power plants (TPPs) and their accumulation near power plants, were formed by combining sintered fly ash with cement and water. Ordinary Portland cement of 43 Grades was used in the process. The Compressive Strength and Flexural Strength Test results of the concrete at ages 3, 7, 14, 28, 56, and 90 days are examined by the author in this study. Replace 10%, 20%, 30%, 40%, and 50% of the fly ash aggregate with coarse aggregate. Using it as a raw material to make cubes or bricks will benefit our economy and environment. 30% replacement of sintered fly ash aggregate in concrete resulted in the most value gain, whereas 50% replacement of sintered fly ash aggregate in concrete resulted in the lowest increase. At 30% replacement, the highest compressive Strength measured was 43.12 N/mm, while the lowest Strength was 26.24 N/mm. When concrete was used with a 30% less sintered fly ash aggregate, a maximum flexural strength of 11.16 N/mm was found.

Concrete reached a minimum strength of 2.10 N/mm at 50% substitution of sintered fly ash aggregate. Using lightweight concrete can expedite construction while enhancing the green construction environment. By partially replacing coarse aggregate with sintered fly ash aggregate, thermal power stations can produce waste materials.

III. Experimental Study

Materials

This section provides information about the different materials used in experimental investigation.

A. Cement:

In this investigation, ordinary Portland cement of grade 53 cement is used. This cement is found to various specifications. The physical properties are tested according to IS 4031-1998, and results are tabulated in Table 1.

TABLE I.
Physical Properties of Cement

Test	Result
Specific gravity	3.14
Standard consistency	33%
Initial setting time	45 min
Final setting time	680 min
Bulk density	1440 kg/ m^3
Fineness of cement	2.14 %

B. Fly-Ash

The non-combustible, finely divided waste called fly ash collected from the exhaust gases of industrial furnaces is one of the most expensive by-products used in the construction industry. Simple concrete has a flaw because the mortar-aggregate interface has tiny cracks. Steel fibers can be added to the mixture to eliminate or significantly lessen this weakness. Fibers are typically utilized in concrete to prevent shrinkage cracking caused by plastic. Additionally, they lessen the concrete's permeability, lessening water leaking. The number of fibers added to a concrete mix is expressed as a percentage of the composite's overall volume (concrete plus fibers), or volume fraction; this percentage usually falls between 0.1 and 3%. Concrete's ability to withstand cracks increases by adding steel fibers (or ductility). While steel fibers are beneficial for multidirectional reinforcement, traditional

rebars are typically employed to increase the tensile Strength of the concrete in a specific direction.

C. Coarse Aggregate

This investigation uses aggregates passed 12mm and retained on 10 mm aggregates. The properties of coarse aggregates are tabulated in Table 2

TABLE II.
COARSE AGGREGATES PHYSICAL PROPERTIES

Property	Coarse aggregate
Fineness modulus	6.39
Water absorption	0.58 %
Specific gravity	2.21
Bulk density	1419 kg/ m^3

D. Fine Aggregate

In this investigation, fine aggregate, which is locally available river sand free from all impurities, is used. The requirements of sand are confirming 'IS: 383-1970', and the properties of fine aggregate are tested, and results are tabulated in Table 3

TABLE III.
FINE AGGREGATE PHYSICAL PROPERTIES

Test	Results
Fineness modulus	2.91
Water absorption	1.1%
Specific gravity	2.61
Bulk density	1569 kg/ m3

E. 'Sintered Fly Ash' Aggregate

Concrete's dead weight decreases of natural stone aggregate. The concrete with sintered fly ash aggregate is spherical, with a 5–20 mm size range and a light grey hue. Bulk density is 640-750 kg/m3, aggregate crushing Strength is 5-8.5 t, and water absorption is 15-20% in uncrushed material and 40-50% in crushed material.

F. Water

The most crucial component of concrete is water, which aids in the binding of the aggregates and cement.

G. Super Plasticizer

In this investigation, CONPLAST SP430 is used to improve the workability of concrete.

H. Crimped Steel Fibre

Short, irregular steel fibers, termed crimped steel fibers, can be utilized in concrete to improve the mechanical qualities of the material. These fibers, generally constructed of low-carbon steel, are intended to boost the tensile Strength of concrete to enhance its performance.

CRIMPED STEEL FIBRE

Physical Properties
Diameter (d) - 0. 4 mm
Length of Fibre (l)- 12 mm
Aspect ratios (l/d) - 30

Figure 1. Crimped steel fibers

I. Mix Design

In this investigation, the mix design of SCC lightweight aggregates was finished using the rational mix design method. Pumice aggregate is replaced partially by coarse aggregate in concrete with different percentages such as 10%, 20%,30%, and 40%.

J. Curing of Specimens

All the specimens of pumice self-compacted lightweight aggregates were cast and cured by placing the specimens in a curing tank for 7 and 28 days.

IV. EXPERIMENTAL METHODOLOGY

A. Compressive Strength

Cubes size of 100*100*100mm specimens were cast, cured for 7 and 28 days, and tested below an automatic testing machine. In compressive strength tests, cylindrical or cubical samples are subjected to axial loads until failure, measuring their ability to withstand compression.

Figure 2. Compressive testing machine

B. Split Tensile Strength

The split tensile test, carried out per IS 5816-1999, is an indirect test used to measure the tensile strength of concrete. The average split tensile strengths of M40 grade lightweight self-consolidating concrete, with varying levels of sintered fly ash aggregate replacement (0%, 10%, 20%, and 30%), show an interesting trend. As the percentage of replacement increases, there will be a gradual decrease in split tensile Strength (6.06 MPa for 0% replacement, 6.31 MPa for 10% replacement, 5.12 MPa for 20% replacement, and 4.05 MPa for 30% replacement) as shown in figure 10. Cylinder size of the 150*300mm specimens was cast, cured, and tested under a CTM machine for 7 and 28 days. Measure the diameter of the cylinder or cube at the midpoint of its height using a measuring tape or digital calipers. This is the average diameter, denoted as 'D.'Calculate the split tensile Strength using the formula:

Split Tensile Strength (fsp) = (2 * Load at Fracture)/

CVR Journal of Science and Technology, Volume 25, December 2023
DOI: 10.32377/cvrjst2501

(π *D* L)Where L is the length of the cylinder or cube.

Figure 3. Split Tensile testing machine.

TABLE IV.
RESULTS OF HARDENED PROPERTIES OF SCC SINTERED FLY ASH AGGREGATE REPLACED CONCRETE.

GRADE	%	CEMENT	FA	CA	SFA	FLY-ASH	SP	WATER
M20	10%	263	960	594	17.5	316	17.3	238
	20%	263	96	528	35	316	17.3	238
	30%	263	960	462	52	316	17.3	238
M30	10%	374	942	617	18	383	22.7	206
	20%	374	942	549	36	383	22.7	206
	30%	374	942	480	54	383	22	206
M40	10%	432	942	617	18	349	11	228
	20%	432	942	549	36	349	11	228
	30%	432	942	480	54	349	11	228

C. Flexure Strength

Flexural test specimens are determined using flexural Strength by IS 516-1959. Prism size of 150*100*100mm samples were cast and cured for 7 and 28 days under a testing machine. Flexural strength tests assess the resistance of prismatic concrete beams to bending forces.

Figure 4. Flexure testing Machine

IV Tests on Temperatures up to 900˚C: The cubes underwent tests for compressive Strength and weight after a 28-day curing period. The lightweight sintered fly ash has been self-compacted and cured. Temperatures ranging from 100˚ to 1000˚c were experienced by classes M20, M30, and M40 to ascertain how resistant concrete specimens are to external factors, including heat generated during a volcanic eruption.

V. EXPERIMENTAL RESULTS

TABLE V.
QUANTITIES OF MATERIALS FOR CASTING PUMICE

Grade of concrete	Designation	Compressive Strength Mpa		flexural Strength Mpa		split tensile strength Mpa	
		7 Days	28 Days	7 Days	28 Days	7 Days	28 Days
20	NWSCC	25.6	37.8	5.12	7.4	5.92	8.06
	10%	22.83	36.76	4.96	6.37	4.84	6.37
	20%	21.73	33.2	4.28	5.84	4.26	5.12
	30%	14.79	25.6	3.01	4.01	3.14	4.05
30	NSCC	36.3	39.6	5.73	9.5	5.98	8.62
	10%	28	38.33	5.12	8.92	5.02	7.05
	20%	37.06	32.12	5.07	7.02	4.92	5.22
	30%	31.26	25.9	3.48	6.12	3.91	4.28
	40%	30.3	25.16	3.12	6.12	3.11	4.14
40	NSCC	46.8	44.9	6.20	9.7	6.12	8.69
	10%	47.56	42.96	6.18	9.26	5.18	7.58
	20%	48.62	44.8	5.23	9.73	6.26	8.73
	30%	42.7	38.2	5.01	8.68	4.98	5.27

TABLE VI.
FRESH PROPERTIES OF SCC

Grade of concrete	% of Replacement	Fresh Properties		
		Slump flow T50cm Test Sec	V Funnel Test Sec	L-Box Test H2/H1
20	10%	4	4	0.82
	20%	4.3	5.94	0.85
	30%	4.8	9.78	0.87
30	10%	5	6.8	0.78
	20%	5.2	7.4	0.84
	30%	5.7	8	0.87
40	10%	4.8	5.8	0.81
	20%	5	6	0.87
	30%	5.5	6.4	0.9

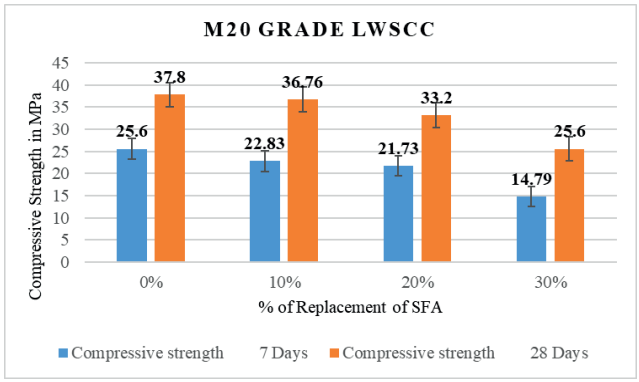

Figure 5. Compressive Strength for 7 and 28 days of M20 grade

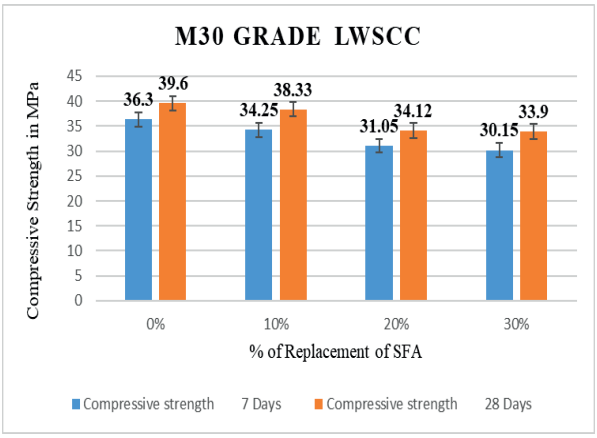

Figure 6. Compressive Strength for 7 and 28 days of M30

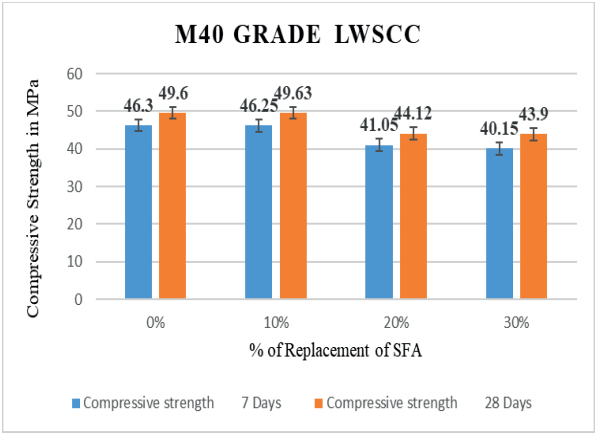

Figure 7. Compressive Strength for 7 and 28 days of M30

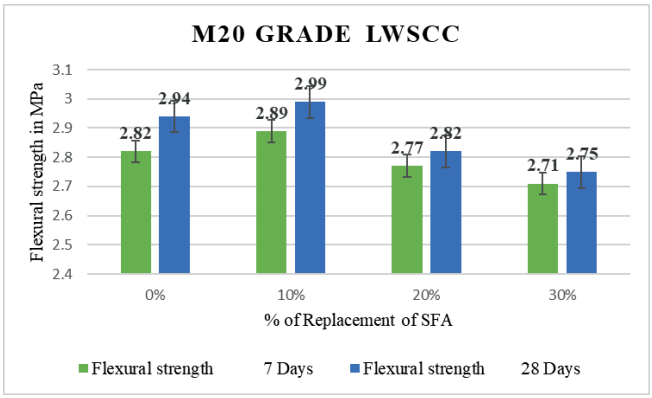

Figure 8. Flexural Strength for 7 and 28 days of M20

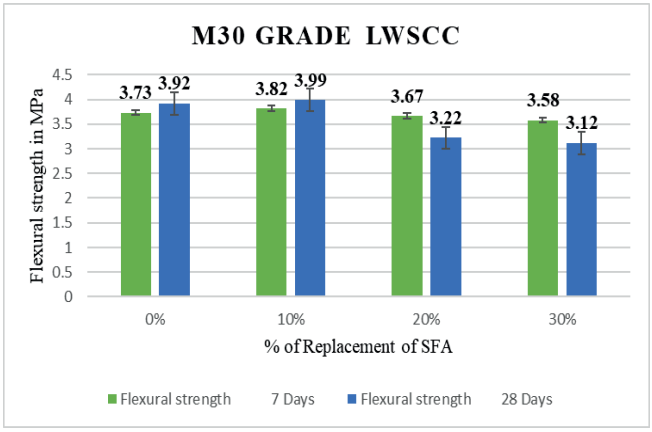

Figure 9. Flexural Strength for 7 and 28 days of M30

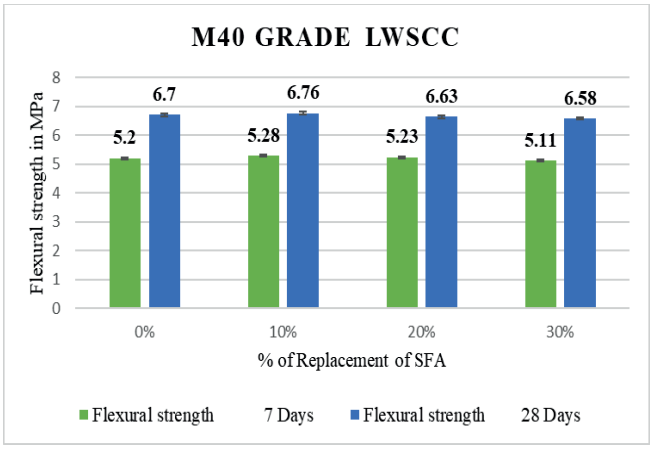

Figure 10. Flexural Strength for 7 and 28 days of M40

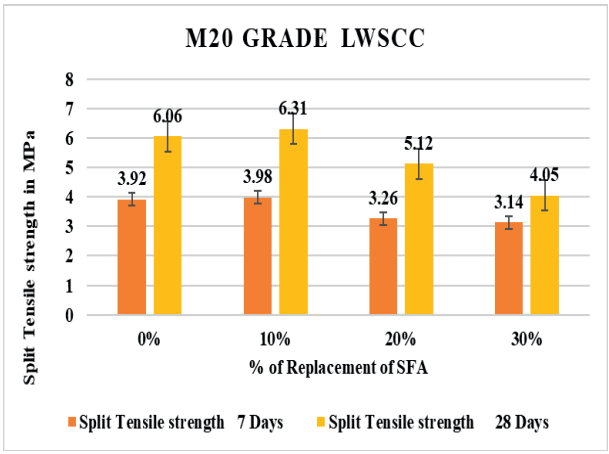

Figure 11. Flexural Strength for 7 and 28 days of M30 grade

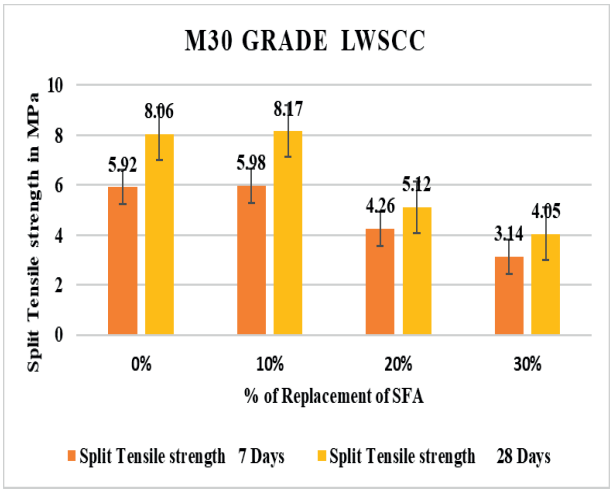

Figure 12. Flexural Strength for 7 and 28 days of M40

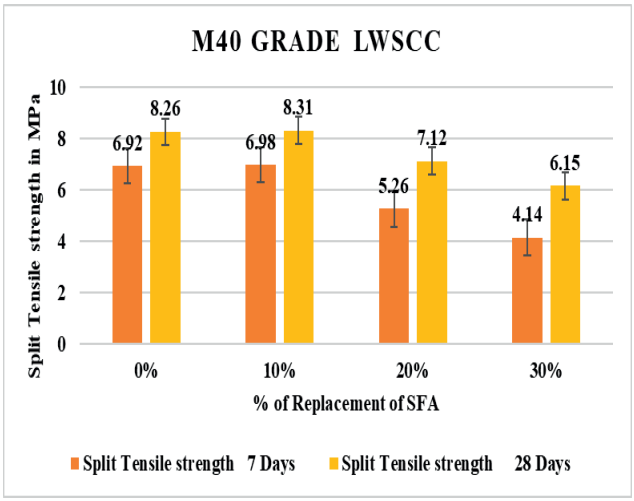

Figure 13. Tensile Strength for 7 and 28 days of M20

TABLE VII.
COMPRESSIVE STRENGTH OF LWSCC FOR 28 DAYS AT 100˚C

Grade of Concrete	Coarse Aggregate %		Hardened properties
	Gravel %	SFA %	Compressive Strength 28 days (MPa)
M20	100	-	27.2
	90	10	25
	80	20	26.3
	70	30	24.7
M30	100	0	38.9
	90	10	35
	80	20	36.1
	70	30	34.5
M40	100	-	49.5
	90	10	46.2
	80	20	45.1
	70	30	41.6

TABLE VIII.
COMPRESSIVE STRENGTH OF LWSCC FOR 28 DAYS AT 300˚C

Grade of Concrete	Coarse Aggregate %		Hardened properties
	Gravel %	SFA %	Compressive Strength 28 days (MPa)
M20	100	0	27.2
	90	10	26.3
	80	20	25
	70	30	24.7
M30	100	0	38.9
	90	10	35
	80	20	36.1
	70	30	34.5
M40	100	0	49.5
	90	10	46.2
	80	20	45.1
	70	30	41.6

TABLE IX.
COMPRESSIVE STRENGTH OF LWSCC FOR 28 DAYS AT 600˚

Grade of Concrete	Coarse Aggregate %		Hardened properties
	Gravel %	SFA %	Compressive Strength 28 days (MPa)
M20	100	0	27.2
	90	10	23.1
	80	20	24.0
	70	30	23.3
M30	100	0	38.9
	90	10	29.1
	80	20	29.5
	70	30	20.8
M40	100	0	49.5
	90	10	35.4
	80	20	38.7
	70	30	30.4

TABLE. X.
COMPRESSIVE STRENGTH OF LWSCC FOR 28 DAYS AT 900˚C

Grade of Concrete	Coarse Aggregate %		Hardened properties
	Gravel %	SFA %	Compressive Strength 28 days (MPa)
M20	100	0	27.2
	90	10	Failed
	80	20	Failed
	70	30	11.8
M30	100	0	38.9
	90	10	Failed
	80	20	21.4
	70	30	17.9
M40	100	0	49.5
	90	10	Failed
	80	20	Failed
	70	30	28.5

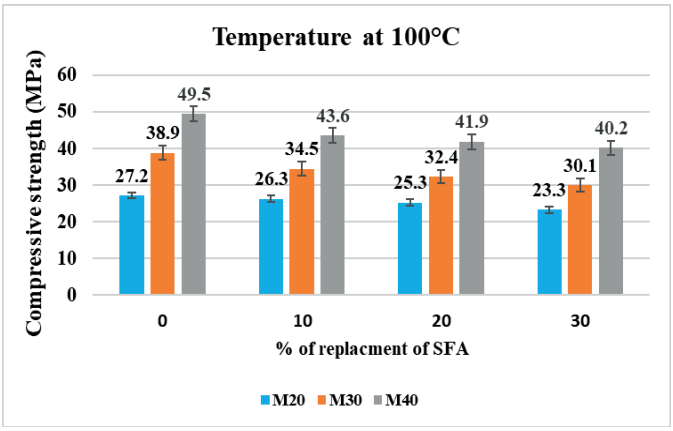

Figure 14. compressive strength subjected to different temperatures and replaced with 10% M40 grade of concrete.

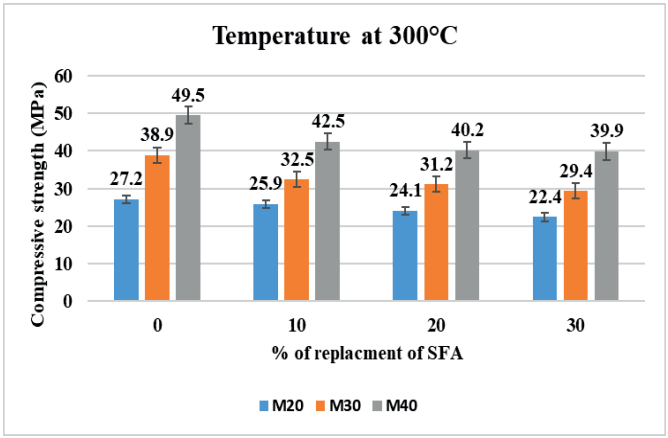

Figure 15. compressive Strength subjected to different temperatures replaced with 10%,20%, and 30% SFA of M20

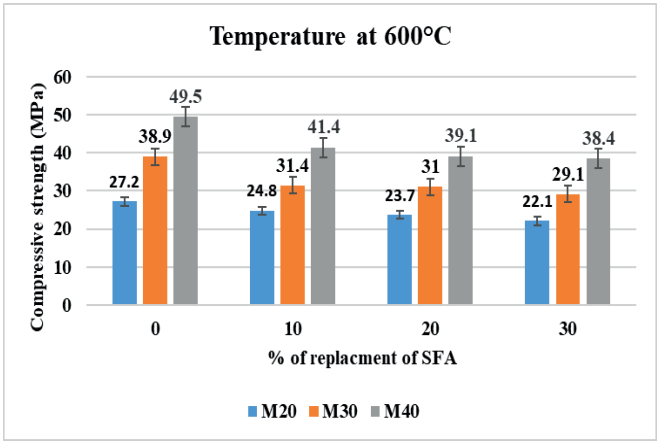

Figure 16. compressive strength subjected to different temperatures replaced with 10%,20%, and 30% SFA of M30 grade of concrete.

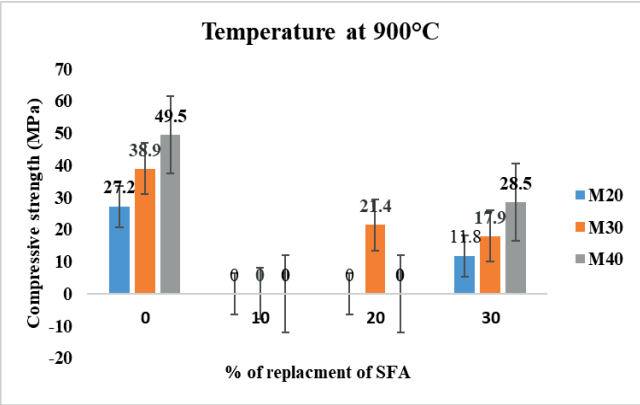

Figure 17. compressive strength subjected to different temperatures replaced with 10%,20%, and 30% SFA of M20, M30 and M40 grade of concrete.

VI. Results and Discussions

Table 6 displays the new characteristics of FRSCLWC made with sintered fly ash aggregates. The test results demonstrate that every blend complies with the specifications (EFNARC 2005). "A 20% substitution of SFA aggregate in the M20 grade of concrete led to an increase in split tensile Strength of 3.7%, flexural Strength of 1.4%, and compressive Strength of 11.4%. A 20% substitution of Sintered Fly Ash aggregate in the M30 grade of concrete increased its compressive Strength by 2.27%, flexural Strength by 2.3%, and split tensile Strength by 3.2%. A 30% substitution of SFA aggregate in the M40 grade of concrete increased the flexural Strength, split tensile Strength, and compressive Strength by 2.11%, 2.26%, and 1.41%, respectively. When 20% of the concrete aggregate in the M20 grade was replaced with sintered fly ash, the compressive Strength improved 6.6% at 100˚C and declined steadily as the temperature rose. When 20% of the Sintered Fly Ash aggregate in the M30 grade of concrete was substituted, the compressive Strength increased by 1.28% at 100˚C and declined gradually as the temperature rose. When 10% of the Sintered Fly Ash aggregate in the M40 grade of concrete was substituted, the compressive Strength increased 2.8% at 100˚C and declined gradually as the temperature rose. Because self-compacting concrete offers a number of advantages over regular conventional concrete, steel fibers are used to reinforce it.

VII. Conclusions

The conclusions and suggestions that may be drawn from this experimental investigation are outlined below.

1. Increased Strength with SFA Aggregate Replacement: The results indicate that including SFA (sintered fly ash Aggregate) in concrete mixes led to overall improvements in compressive, flexural, and split tensile strengths across different grades of concrete. Notably, a 20% replacement of conventional aggregate with SFA resulted in significant strength enhancements, particularly in the M20 grade.
2. Grade-Specific Response: The effect of SFA aggregate replacement on concrete Strength varied with different concrete grades. While the M20 grade exhibited the most significant improvements in Strength with a 20% replacement, the M30 and M40 grades showed more minor but still notable enhancements with 20% and 30% replacements, respectively.
3. Temperature-Dependent Behavior: The study also explored the behavior of SFA-reinforced concrete at elevated temperatures (100 The findings revealed that the compressive Strength initially increased with SFA replacement in all grades but gradually decreased as the temperature rose. This observation suggests that the performance of SFA-reinforced concrete may be sensitive to high-temperature conditions.
4. Superior Performance of SCC with Steel Fiber: The discussion highlights the advantages of Self-Compacting Concrete (SCC) over conventional concrete, particularly when reinforced with steel fiber. Although the specific benefits of SCC are not explicitly mentioned, it implies that SCC with steel fiber reinforcement offers superior properties to regular concrete mixes.
5. Optimal SFA Replacement Ratios: Based on the results, replacing 20% of conventional aggregate with SFA is a good choice for M20 and M30 grades, leading to significant strength improvements without affecting other properties. For the M40 grade, a 30% SFA aggregate replacement may be preferred, as it provides a reasonable strength enhancement while avoiding potential diminishing returns on Strength with higher SFA content.
6. The results of this study show that adding SFA aggregate, especially in the best replacement ratios, can improve the mechanical properties of different grades of concrete. This is an excellent way to improve concrete performance in various settings, including those with high temperatures. Additionally, the study highlights the suitability of SCC reinforced with steel fiber, further supporting its use in concrete construction where self-compaction and enhanced mechanical properties are desired.

References

[1] R. Kalpana P.S. Kothai, “Study on Properties of Fibre Reinforced Light Weight Aggregate Concrete," International Journal for Scientific Research and Development (IJSRD), vol.3, issue 2, 2015, ISSN:2321-0613.
[2] Hajime Okamura And Masahiro Ochi "Self-Compacting Concrete" Journal of Advanced Concrete Technology Vol.1, No 1.5-15. April2003.
[3] Bouzoubaa. N, And Lachmi.M, "Self-Compacting Concrete Incorporating High Volumes of Class F Fly Ash, Preliminary Results" Cement and Concrete Research, Vol.31, No.3, PP.413–420, March 2001.
[4] Thomas Paul, Habung Bida, Bini Kiron, Shuhad A K, Martin Varghes” Experimental Study on Self Compacting Concrete with Steel Fibre Reinforcement” Volume 5, Issue 4, April 2016.

[5] Siddharth Anand, Mohammad Afaque Khan, Abhishek Kumar" Effect of Steel Fiber on Self-Compacting Concrete" Volume: 03 Issue: 03, Mar-2016.
[6] Scrams Reddy, I.Krishnarchana, Dr. V. Bhaskar Desai," An Experimental Study On Sintered Fly Ash Aggregate Concrete Modified With Nano Aluminium Oxide (Al2o3)" Volume: 04 Issue: 03, Mar -2017.
[7] M. K Dipti Kanta Rout "Investigation on the Development of Light Weight Concrete with Sintered Fly Ash Aggregate and Activated Fly Ash in Blended Cement" Vol. 4 Issue 04, April-2015.
[8] Ramanjaneyulu, N., Seshagiri Rao, M V & Bhaskar Desai.,V. Strength and Durability Studies on Light Weight Self-Compacting Concrete with LECA as Partial Replacement of Coarse Aggregate (2018) https://doi.org/10.1007/s41062-020-00371-2.
[9] Arvind Kumar, Dilip Kumar," Use of Sintered Fly Ash Aggregates as Coarse Aggregate in Concrete," Volume 1 Issue 4, 2014.
[10] Farhad Aslani, M. ASCE; and Guowei Ma "Normal and High-Strength Lightweight Self-Compacting Concrete
[11] Incorporating Perlite, Scoria, and Polystyrene Aggregates at Elevated Temperatures", Volume 30, Issue 12, December 2018.
[12] Ramanjaneyulu, N., Seshagiri Rao, M V & Bhaskar Desai., V Behavior of Self-Compacting Concrete Partial Replacement of Coarse Aggregate with Pumice Lightweight Aggregate in the journal International Journal of Recent Technology and Engineering (IJRTE) ISSN: 2277–3878, Volume-7, Issue-6C2, April 2019
[13] C.L.Verma, S.K.Handa, S.K.Jain, R.K.Yadav " Techno-commercial perspective study for sintered fly ash lightweight aggregates in India.
[14] Arvind Kumar and Dilip Kumar "Strength Characteristics of Concrete with Sintered fly ash Aggregate" Journal of IJSRD Volume 2, Issue 7, Sept- 2014.
[15] Ramanjaneyulu, N., Seshagiri Rao, M V & Bhaskar Desai., Comprehensive Study on Fresh and Hardened Behaviour of Sintered Fly Ash Aggregate based Lightweight Self-Consolidating Concrete in the IJSRD (International Journal of Scientific Research and Development) | Vol. 9, Issue 8, 2021 | ISSN (online): 2321-0613
[16] Prakash Desai, B.K.Raghu Prasad and V. Bhaskar Desai conducted Mode-II fracture of cementitious materials- part IV: Fracture toughness, shear Strength, and fiber-reinforced cement mortar and concrete slip. Journal of structural engg. Vol. 26, No. 4, Jan 2000, pp. 267–273.

E-ISSN 2581 – 7957
P-ISSN 2277 – 3916

CVR Journal of Science and Technology, Volume 25, December 2023
DOI: 10.32377/cvrjst2502

Comparative Study on the Mechanical Properties of Steel Fiber Reinforced Self-Compacting Concrete

Vijaykumar Thadaka[1] and M. R. Rajagopal[2]
[1]PG Scholar, CVR College of Engineering/Civil Engg. Department, Hyderabad, India
Email: vijaykumarvk319@gmail.com
[2]Assoc. professor, CVR College of Engineering/Civil Engg. Department, Hyderabad, India
Email: mr.rajagopal@cvr.ac.in

***Abstract*: Self-compacting concrete (SCC) is a flowable concrete which can consolidate under its own weight without the need of external vibration. The highly fluid nature of SCC makes it suitable for placing in difficult environments like congested reinforcement and thinner sections. Use of SCC can also help in decreasing noise pollution at worksites which is caused by vibration of concrete. SCC is used in bridges, buildings, and tunnel construction.**

The addition of small closely spaced and uniformly dispersed fibres to concrete would act as a crack resistor and would substantially improve its properties. This type of concrete is known as fibre reinforced concrete. In fact, the fibre reinforcement mechanisms can convert the brittle behaviour of this cement-based material into a pseudo-ductile behaviour up to a crack width that is acceptable under the structural design point-of-view. Fibre addition, however, increases the complexity of the mix design process, due to the strong perturbation effect that steel fibres cause on fresh concrete flow.

In the present study, the effect of steel fibres on fresh and hardened properties are studied by adding steel fibres of different percentages such as 0%, 1% and 2% for M70 grade of concrete. An experimental investigation has been carried out to determine different properties like workability and strength of Fiber Reinforced Self Compact Concrete and Self- Compacting Concrete (SCC). For testing the properties of SCC and Fiber Reinforced SCC (FRSCC) in fresh state slump-flow, T50 Test, L-box, U-box, and V-funnel tests were conducted. Whereas for testing the properties in hardened state compressive strength, split tensile strength and flexural strengths are carried out.

Detailed studies have revealed that the Steel Fiber Reinforced Self Compacting Concrete made with the Steel fibres displays a better performance. The investigations and results are presented from the study.

***Index Terms*: Self compacting concrete, Steel fibre reinforced concrete, Super plasticizer, Silica fume, Fly ash, Steel fibre.**

I. Introduction

Concrete is the predominant, most popular and widely used construction material. Self-Compacting Concrete (SCC) or Self-Consolidating Concrete is one of the most important innovations. When a large quantity of heavy reinforcement is to be placed in reinforced concrete, that is fully compacted without voids or honeycombing, compaction by manual or by mechanical vibration is extremely challenging in that situation [1-3]. Underwater concreting always required fresh concrete which should be placed without the need for compacting and in such circumstances, vibration is simply impossible [4]. This problem can now be solved with Self Compacting Concrete. This type of concrete flows easily around the reinforcement and into all concerns of formwork. Self-Compacting Concrete is described as concrete with the ability to compact itself only by its own weight without the reinforcement of vibration. Self-Compacting Concrete is also known as Self-Consolidating concrete. Self-Compacting Concrete is a concrete mix with a low yield stress, high deformability, good segregation resistance (prevents separation of particles in the mix), and moderate viscosity (necessary to ensure uniform suspension of solid particles during transportation, placement (without external compaction), and thereafter until the concrete sets [5-7]. In everyday terms, when poured, SCC is an extremely fluid mix with distinctive practical features - it flows very easily within and around the form work, can flow through obstructions and around corners measured using “passing ability”, is close to self-compacting (although not actually self-levelling), does not require vibration or tamping after pouring, and follows the shape and surface texture of a mould very closely once set [4]. The typical method of compaction, vibration generates delays and is an additional cost to the project. In this project SCC is used along with steel fibre for increasing strength of the concrete [8-10]. Steel fibre has high elongation property i.e., tensile strength, by the addition of steel fibres in SCC an increase in the Compression Strength, Flexural Strength and Split Tensile Strength of Concrete was achieved.

II. Characteristic of Fresh SCC

SCC mixes must meet three key properties:

1. Ability to flow into and completely fill intricate and complex forms under its own weight.
2. Ability to pass through and bond to congested reinforcement under its own weight.
3. High resistance to aggregate segregation.

The main characteristics of SCC are.

i) Passing ability
ii) Filling ability
iii) Resistance to Segregation

CVR College of Engineering
Received on 20.03.2023, Revised on 18.05.2023, Accepted on 26.05.2023.

III. Objective of the Work

In the present study, it is proposed to study the following on M70 grade concrete using steel fibres of different percentages by weight of cementitious material, silica fume and fly ash:

- Comparison of different properties like workability and strength of Self-Compacting Concrete (SCC) with Steel Fiber Reinforced Self Compacting Concrete (SFRSCC).
- Tests involving various fibre proportions for a particular mix of SFRSCC.
- Test methods used to study the properties of fresh concrete were Slump test, V – funnel, T50, and L – Box.
- To determine Hardening properties like Compressive Strength, Flexural Strength, Split tensile strength for cubes, prisms and cylinders.
- To determine the load vs deflection curves of beams by varying percentage of steel fibres.

IV. Materials & Methodology

Cement: Ordinary Portland Cement OPC 53 Grade available in the local market was used. The below test properties according to IS: 4031-1988 and found confirming to IS: 12269-1987 was used. Normal Consistency 32%, Specific Gravity 3.10, Initial and Final Setting time of 45 min and 580 min respectively, Fineness 2.37% and Soundness of 4 mm was measured on Le-Chatelier's apparatus.

Fine aggregate: Sand is a naturally occurring granular material composed of finely divided rock and mineral particles. It is defined by size being finer than gravel and coarser than silt. Fine aggregate (sand) used for this investigation is river sand conforming to zone-II of IS 383-1970 and it was well graded, passing through 4.75mm sieve.

Coarse Aggregate: Crushed angular granite material available from the local market was used as coarse aggregate in this investigation. The coarse aggregate (passing through IS Sieve 12mm and retained on IS Sieve 10mm was tested for its characteristics as per IS: 2386-1963 and found to be confirming to the specifications.

Fly Ash: Fly ash is one of the most widely used by- product materials in the construction field resembling Portland cement. The physical and chemical properties of the fly ash as used in the investigation confirm to grade, I fly ash of IS: 3812-2003. Specific Gravity 2.20 and Specific Surface area 420m^2/kg. The chemical composition was SiO2 68%, Al2O3 23%, Fe2O3 4%, CaO 1.1% and MgO 0.5%.

Silica Fume: Silica Fume is a byproduct of producing silicon metal or ferrosilicon alloys. The quality of silica fume used was as specified by ASTM C 1240 and AASHTO M 307. Powdered Silica Fume with a Specific Gravity of 2.2 and bulk density of 220 Kg/m^3 was used.

Steel Fibres: Hooked end steel fibres of 0.4mm diameter and Aspect ratio of 30 and 12-mm length were used. Here in the present study, steel fibres hooked at both ends were used.

Water: Ordinary portable water of normal PH 7 was used for mixing and curing the concrete specimen.

Admixtures: CONPLAST SP430 confirming the requirement of IS: 9103-1979 as a high range water reducing admixture was used.

V. Mix Design

Mix design is the process of selecting suitable ingredients of concrete and determining their relative proportion for producing concrete of certain minimum strength and durability as economically as possible for Grade M70 using the Code IS 10262:2019[11]. The proportions of the mix are listed in Table I.

VI. Tests on Fresh Concrete

Different test methods were used to characterize the properties of SCC.

1. Slump flow & T50 test,
2. V- funnel test & V-funnel at T5 minutes
3. L- box test

The acceptance criteria as per EFNARC is mentioned Table II.

TABLE I.
Mix Proportion for SCC

W/C	Cement	Fly Ash	SF	CA	FA	WC	Super plasticizer (1.8% by weight of Cement)
0.31	421*	78.9	26.3	945.23	720	148	7.58

*All quantities in kg/m3. SF-Steel Fibers, WC-Water Content

TABLE II.
Acceptance Criteria for SCC

Sl. No	Method	Unit	Typical rangeof values Minimum	Maximum
1	Slump flowby Abram's cone	mm	650	800
2	Time increase, V-funnel at T5minutes	Sec	2	5
3	V-funnel	Sec	6	12
4	L-box	mm	0.8	1

VII. Tests on Hardened Concrete

Testing of hardened concrete plays an important role in controlling and confirming the quality of concrete work. Systematic testing of raw materials, fresh concrete and hardened concrete are inseparable parts of any quality control programmed for concrete, which helps to achieve higher efficiency of the material used and greater assurance of the performance of the concrete with regards to both strength and durability [12-13]. The hardened property test such as compression test by using compression testing machine, split tensile test by using compression testing machine and flexural test by using ultimate testing machine were conducted using the specimen cast as shown in Fig. 1 and Fig. 2. The results obtained for the various mixes of SCC, SCC with 0%, 1%, and 2% Steel Fibres is listed in the results section.

CVR Journal of Science and Technology, Volume 25, December 2023
DOI: 10.32377/cvrjst2502

Behaviour In Flexure of Beams: Experimental investigation is carried out on beams to determine its flexural behaviour. The beams are tested using a 1000kN capacity Load Frame under midpoint load setup to get the flexural behaviour.

Beams casted were tested by placing them on the load frame to draw the load versus deflection curves.

VIII. Results & Discussion

The results were obtained by experimentally testing the specimen in the Fresh state and Hardened state and are detailed and discussed in the subsequent text below.

A. Fresh Properties

Fresh properties of various mixes of M70 grade plain self-compacting concrete (SCC) based on various combinations of steel fibre contents using various workability test methods are presented below in Table III. The filling ability, passing ability and segregation resistance values, which are the basic requirements for SCC in fresh state, were found to be satisfying as per EFNARC.

Figure 1. Casting of Cube, Cylinder & Prism Specimen

Figure 2. Casting of Beams

B. Hardened Properties

Compressive Strength

From the compressive strength results of cubes shown in Table IV, the 90 days compressive strength of SCC mixes when Steel fibres are added from 0%, 1% and 2 % the strength observed was 71.23 MPa, 75.14 MPa, and 58.53 MPa that is an increase of 5.49%, from adding 1% steel fibres to 0% steel fibres and a decrease of 18.25% by adding 2% steel fibres to 0% steel fibres as shown in the Fig. 3 and Fig. 4.

TABLE III.
FRESH PROPERTY RESULTS FOR SCC

Grade	Fresh Properties			Remarks	Designation (% of SP)
	Slump flow T50 cm Test Sec	V-Funnel Test Sec	L-Box Test H2/H1		
M70	8(600)	12	0.6	Not withinlimits	SCC (0.5%)
	6 (600)	12	0.7	Not withinlimits	SCC (1%)
	5(620)	11	0.90	Within limits	SCC (1.5%)
M70	4(650)	7	0.9	Within limits	SCC (1.8%)

TABLE IV.
COMPRESSION TEST RESULTS AFTER 90 DAYS FOR M70

Mix	0% SF	1% SF	2% SF
Compressive Strength(N/mm2)	71.23	75.14	58.53

Figure 3. Failure of Cube

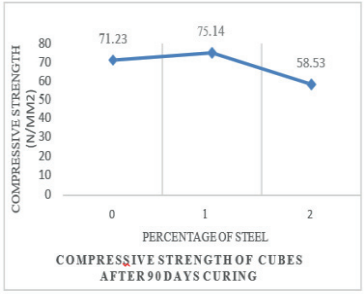

Figure 4. Graph representing Compressive Strength of Cubes

Split Tensile Strength

From the Split Tensile strength results of cylinders shown in Table V, the 90 days Split Tensile strength of SCC mixes when Steel fibres are added as 0%, 1% and 2 % the strength observed was 10.86 MPa, 11.30 MPa, and 11.86 MPa that is an increase of 4.05% and 9.20% by adding 1% to 0% and adding 2% to 0% steel fibres as shown in Fig. 5 and Fig. 6.

TABLE V.
SPLIT TENSILE TEST RESULTS AFTER 90 DAYS FOR M70

Mix	0% SF	1% SF	2% SF
Split Tensile Strength (N/mm2)	10.86	11.30	11.86

Figure 5. Failure of Cylinder

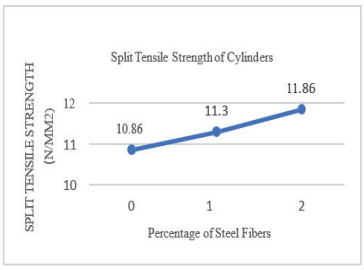

Figure 6. Graph representing Split Tensile Strength of Cylinders

Flexural Strength

From the Flexural strength results of prisms shown in Table VI, the 90 days Flexural strength of SCC mixes when Steel fibres are added from 0%, 1% and 2 % the strength observed was 5.86 MPa, 6.69 MPa, and 7.5 MPa that is an increase of 14.16% and 27.98% from adding 1% to 0% and adding 2% to 0% steel fibres as shown in Fig. 7 and Fig. 8.

TABLE VI.
FLEXURAL TEST RESULTS AFTER 90 DAYS FOR M70

Mix	0% SF	1% SF	2% SF
Flexural Strength (N/mm2)	5.86	6.69	7.5

Figure 7. Failure of Prism

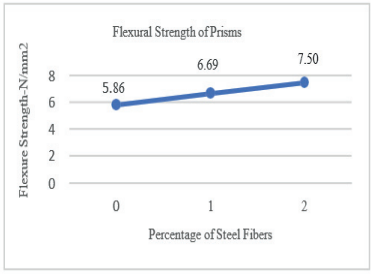

Figure 8. Graph representing Flexural Strength of Cylinders

Flexure of Beams (Load vs Deflection)

The load-deflection results from the Loading Frame using two LVDTs for different SCC mixes after 28 days of curing are listed in Table VII and the Load vs Deflection for the three specimen PSCC, PSCC+1%SF and PSCC+2%SF are shown in Fig. 9 and Fig. 10.

TABLE VII.
LOAD & DEFLECTION VALUES

Sl. No	Method	Ultimate load (KN)	Ultimate Deflection mm
1	Plain SCC	112.50	9.95
2	PSCC+1%SF	195.50	5.58
3	PSCC+2%SF	165.13	6.33

Figure 9. Failure of Beam

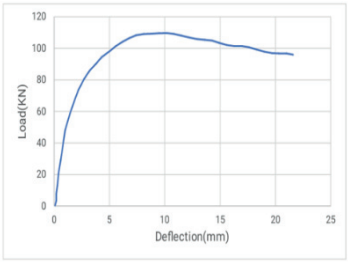

Figure 10. Load vs Deflection PSCC

From overall results of the testing, the ultimate load for self- compacting concrete beams with 1% and 2% steel fibres has increased by 71% and 46% when compared with the plain self-compacting concrete beams. Whereas deflection for self-compacting concrete beams with 1% and 2% steel fibres has decreased by 43.9% and 50% when compared with the plain self-compacting concrete beams.

IX. CONCLUSIONS

Based on the experimental work conducted on SCC mixes and SFRSCC mixes of different grades are the following specific conclusions are drawn from this experimental study:

1. Fibre reinforced self-compacting concrete can be produced by incorporating Steel fibres to improve its performance. However, the use of appropriate dosage of super plasticizer is essential to maintain the fresh properties of self-compacting concrete.
2. Addition of steel fibres has decreased fresh properties for M70 grade SCC but are within the EFNARC specifications.
3. With increase of fibre dosage, the workability decreases. This problem of workability and flow properties of concrete can be overcome by adding superplasticizers.
4. Overall slump flow diameter (flow ability) decreases with the increase in steel fibre content of concrete mixtures with respect to plain mixtures.
5. V-funnel flow time increased with the increase in steel fibre content of the concrete mixtures with respect to plain mixtures.
6. To retain high level workability or fluidity with fibre reinforcement, the amount of paste in the mix should be increased to provide better dispersion of fibres. It can be done by increasing cement content or increasing fine aggregate content or using pozzolanic and chemical admixtures (High range water reducing admixture).
7. By the number of trials mixed, the dosage of the super plasticizer at 1.8% by weight of cementitious material was concluded as optimal.
8. In M70 grade concrete the compressive strength of the Steel Fiber Reinforced Self-compacting concrete was found to have increased in its strength by 5.49% with a dosage of 1% steel fibres by weight of cementitious material and has decreased by 18.25% by an addition of 2% steel fibres when compared to plain self- compacting concrete.

9. Addition of fibres has a marginal increase in the split tensile and flexural strengths as dosage of fibres increased. The split tensile strength increased by 4.05%, 9.20% and flexural strength by 14.16% and 27.98%, when compared to plain SCC with 1% and 2% dosage of steel fibre .
10. In beams, the ultimate load value is maximum for SCC with 1% steel fibres and the deflection decreases when compared with the plain SCC and SCC with 2% steel fibres .
11. From the above experimental investigation, it is observed that Ultimate load will increase with increase in fibre content.
12. With increasing fibre content, mode of failure is observed changing from brittle to ductile failure when subjected to compression and bending.
13. From the overall investigation 1% steel fibres give an enhanced compression strength, split tensile, flexure strength and for load vs deflection.

REFERENCES

[1] Ch. Sukesh Kumar and Dr. M.V. Seshagiri Rao: Durability Studies on Glass Fibre Reinforced Self Compacting Concrete- CVR Journal of Science and Technology, Volume 16, June 2019, DOI: 10.32377/cvrjst1601.

[2] B. Ramesh, V. Gokulnath, V. Vijay Vignesh : A review on fibre reinforced self-compacting concrete addition with M-Sand- https://doi.org/10.1016/j.matpr.2019.11.312 2214-7853/ 2019 Elsevier Ltd

[3] Mahir Mahmoda, Ammar N. Hanoona, c, Haitham J. Abed, "Flexural behaviour of self-compacting concrete beams strengthened with steel fibre reinforcement."

[4] M. Mastali, Ph.D; and A. Dalvand: Fresh and Hardened properties of Self-Compacting Concrete Reinforced with Hybrid Recycled Steel–Polypropylene Fiber- DOI: 10.1061/(ASCE)MT.1943-5533.0001851. © 2017 American Society of Civil Engineers.

[5] Biswajit Jena, Kirtikanta Sahoo, Bipin Bihari Mohanty: Comparative study on self- compacting concrete reinforced with different choppedfibers- http://dx.doi.org/10.1680/jcoma.16.00076, 2017, Proceedings of the Institution of Civil Engineers

[6] Subhan Ahmad, Arshad Umar, Amjad Masood: Properties of Normal Concrete, Self- Compacting Concrete and Glass Fiber Reinforced Self-Compacting Concrete-doi: 10.1016/j.proeng.2016.12.106, 1877-7058 © 2017 The Authors. Published by Elsevier Ltd.

[7] Abhishek Sachdeva, Pankaj Singla: Strength Evaluation of Steel Fiber Reinforced Self Compacting Concrete- International Journal of Engineering Research & Technology (IJERT), ISSN: 2278-0181, Vol. 4 Issue 09, September-2015.

[8] Rahmat Madandoust, Malek Mohammad Ranjbar, Reza Ghavidel, S. Fatemeh Shahabi: Assessment of factors influencing mechanical properties of steel fibre reinforced self- compacting concrete.

[9] http://dx.doi.org/10.1016/j.matdes.2015.06.024, 0264-1275/2015 Elsevier Ltd.

[10] K.C Dinesh: Experimental Study on Fiber Reinforced Self Compacting Concrete- International Journal of Engineering Research & Technology (IJERT), ISSN: 2278-0181, Vol. 3 Issue 9, September- 2014

[11] Mohamed I. Abukhashaba, Mostafa A. Mostafa, Ihab A. Adam: Behaviour of self- compacting fibre reinforced concrete containing cement kiln dust- http://dx.doi.org/10.1016/j.aej.2014.03.006, 1110-0168 ª 2014 Production and hosting by Elsevier.

[12] T. Suresh Babu, M.V. Seshagiri Rao and D. Rama Seshu: Mechanical Properties and Stress- Strain Behaviour of Self Compacting Concrete with and Without Glass Fibres- Asian Journal of Civil Engineering (Building and Housing) Vol. 9, NO. 5 (2008).

[13] Eduardo N. B. Pereira; Joaquim A. O. Barros; and Aires Camões: Steel Fiber-Reinforced Self- Compacting Concrete Experimental Research and Numerical Simulation- Journal of Structural Engineering © ASCE /August 2008-10.1061/ASCE0733-9445-2008-134:8-1310.

E-ISSN 2581 – 7957
P-ISSN 2277 – 3916
CVR Journal of Science and Technology, Volume 25, December 2023
DOI: 10.32377/cvrjst2503

Performance Analysis of Hybrid Comparator using 45nm Technology

Racha Ganesh[1], K. Lal Kishore[2] P. Srinivasa Rao[3]
[1]Ph. D Scholar, JNTUH University, CVR College of Engineering/ECE Department, Hyderabad, India.
Email: rachaganesh@gmail.com[1]
[2]Professor, CVR College of Engineering/ECE Department, Hyderabad, India.
Email: lalkishore@cvr.ac.in[2]
[3]Professor, CVR College of Engineering/ECE Department, Hyderabad, India.
Email: psrao.cvr@gmail.com[3]

Abstract: **In the present real-time world, due to the improvements and innovations of System on Chip (SoC) applications, there is a requirement to integrate multiple technology design topologies. The electronic system design is classified as analog, digital, and mixed-signal design. The comparator is the major building block used in the datapath of System on Chip (SoC) application device. The usage of these devices depends on not only functionality but also on the non-functionality parameters considering different performance estimation metrics. The nonfunctional performance metrics for a transistor level design depends on the number of transistors, switching activities of logic level voltages and delay between input and outputs. These performance metrics are improved by considering the multiple logic families for multiple output generations instead of using a single logic family topology.**

The comparator is the major component in the arithmetic circuits for SoC applications and can be realized by using various design topologies. The vividly used topologies are Conventional CMOS logic, Pass Transistor Logic (PTL), Gate Diffusion Input (GDI) Logic, Stacking technique, Quantum-dot cellular automata, etc. The selection of the design topology for the comparator is made based on the non-functional parameters. The performance of non-functional parameters is improved by combining the topology architectures of different design techniques. In this paper, the comparator is designed using conventional CMOS logic, PTL, GDI, and a hybridized topology for best performance and the same is implemented using 45nm technology. These circuits are designed by using Cadence Virtuoso Electronic Design Automation (EDA) design tools. Non-functional performance parameters are analyzed for different topologies.

Index Terms: **VLSI Design, Comparator, Datapath, EDA tools, CMOS Logic, GDI Logic, PTL Logic.**

I. Introduction

In the present System on Chip (SoC) applications era, there is a requirement to design any system using both datapath and control path. The selection of the electronic system and software elements for data and control paths will decide the improvement in the nonfunctional metrics along with the system design functionality. Hence, the electronic systems related to datapath elements are designed by using arithmetic elements, computational elements for Small Scale Integration (SSI), Large Scale Integration (LSI), Very Large Scale Integration (VLSI), Digital Signal Processing (DSP) AND Embedded Systems application areas.

The Very-Large-Scale Integration (VLSI) is the combination of thousands of transistors that are integrated into a single device called a VLSI chip. The introduction of VLSI technology made a great improvement in the design of electronic systems. This Electronics system VLSI chip consists of data and control path using arithmetic elements, computational elements, memory elements like RAM, ROM, and other logic.

The VLSI technology along with software design together with an integrated single chip device made the possibility of application domain area as System on Chip (SoC) devices. This System on Chip (SoC) application area made the electronic systems design a new development for different system design applications. The different applications for System on Chip applications include Embedded systems, Data Computation systems, Image enhancement and processing applications, communication devices with software applications etc. This cutting edge System on Chip (SoC) application era made the VLSI system design as more important and dominant design technology to meet the needs of present technology applications. Hence, the present VLSI system design based electronic system is an integration of analog, digital, and mixed-signal design components. All the above-mentioned components except ASIC come under digital design, whereas ASIC is the combination of Analog and mixed-signal designs. In ASIC, there are two types of designs semi-custom designs and full-custom designs. The semi-custom uses pre-designed logic cells and libraries known as standard cells. Full-custom design in VLSI is a method of creating integrated circuits that specifies the architecture of each transistor as well as their interconnections. To design a system, there is a requirement for inputs, outputs, datapath and a control unit. The datapath consists of computational elements like arithmetic and logical elements. The control unit consists of control logic using states or algorithms.

This paper implements the design of a basic data path element i.e., comparator using different logic family topologies. The different logic design family topologies used are Conventional CMOS, PTL, GDI and this designed system proposes a hybridized logic model which makes a better design methodology to meet the functionality and nonfunctional metrics. The selection of the logic family is done as per the comparison input output logic and performance metrics for best results.

An overview of the existing design topologies and different arithmetic applications is given in section II. Section III explores the design and modeling of the comparator. Section IV shows the design of a comparator using EDA tools. The simulation input, output relations and performance

Received on 09-10-2023, Revised on 30-10-2023, Accepted on 11-11-2023.

analysis of the comparator are discussed in section V. The conclusions are given in section VI followed by references.

II. Design Topologies and Arithmetic Applications

Overview of the comparator's properties, architecture, and different parameters that must be considered while designing a device, including delay, offset voltage, output impedance, and voltage gain [1]. However, the application and requirements of system design determine which topology to be chosen. The design presents an enhanced technique for designing CMOS comparator based on a preamplifier-latch circuit controlled by a clock [2]. The primary benefit of this design is its ability to boost an ADC's speed while consuming less power. The design is simulated using the Cadence environment in 0.18-micron CMOS technology. The suggested design has high accuracy and uses only roughly 102 W of power when operating at a 125 MHz sampling frequency and a 1.8 V supply. The construction of a 1-bit reverse comparator employing reversible L and M gates and simulation using the TANNER EDA tool is proposed in [3]. The Reverse logic gates are used in digital comparator circuits to cut down on the number of transistors, size, and power consumption. To develop the suggested 1-bit reverse comparator circuit utilizing 180nm technology, L and M reverse logic gates were downscaled using constant electrical field scaling. Power dissipation at 5V supply voltage was estimated to be 0.162mW, which is 10% better than the CMOS circuit design [3]. To provide low power in digital circuits, one of the unique designs (XOR circuit using only n-MOS) has been proposed in [4]. The GDI cell has been used to realize a variety of circuit combinations. Their waveforms have been examined, and numerous performance metrics have been determined based on the results of the simulation. Then, these parameters are contrasted with conventional CMOS logic. The layout and schematics are created using the Dsch tool and 120nm technology file. Microwind 3.1 and the BSIM simulator are used to analyze the results. Utilizing TANNER S-EDIT, the GDI approach has been applied to 250 nm manufacturing technology [5]. After studying several solutions, a multiplexer based magnitude comparator is eventually suggested with optimum VLSI design limitations. The optimal design that results in the lowest transistor count was provided after considering all the potential designs employing multiplexers with a wide range of main inputs as selection inputs. In comparison to current GDI comparators, the transistor count is reduced by 70%, 33%, and 9%, respectively. Two key design strategies are shown in [6]. The former compares CMOS and GDI logic in terms of nonfunctional metrics and provides the design solution using newly designed basic logic cells. The latter discusses the performance concerning the installation of five various modified GDI full adders. In contrast to the current GDI method, CMOS, and pass transistor logic at 250nm technology. The proposed system performance shows improvement in the power and delay parameters using GDI technology. The design summary of the MGDI technology, uses fewer transistors to make digital circuits that use less power and chip space [7]. The complete adder is introduced in this study utilizing the MGDI approach. Using GDI the approach, 2-bit comparator, and complete subtractor were introduced. Then, these digital circuits' power dissipation, transistor count, size, speed, and latency were contrasted with those of conventional CMOS transistors. The S-GDI approach, which is more power-efficient than DCMOS (Differential CMOS) and Energy Economized Pass Transistor Logic, is presented in the work [8]. (EEPL). In comparison to the GDI approach, S-GDI exhibits power efficiency of 96.20%, 93.65%, 97.88%, and 98.22% for XOR, 1-bit adder, 1-bit comparator, and 4-bit up-down counter, respectively. S-GDI exhibits area efficiency of 17.16% and 28.1% for XOR, 41.26% and 53.89% for 1-bit adder, 7.6% and 21.76% for 1-bit comparator, and 6.7% and 28% for up-down counter over EEPL and DCMOS techniques, respectively. S-GDI may be utilized effectively for low-power applications because of its efficiency in terms of the factors that are taken into consideration. The PTL technology reduces the number of transistors required for the design of logic gates. The performance analysis of PTL with CMOS is discussed in [9]. The 2-bit comparator layout is created using semi-automated and automatic methods. The result demonstrates that the semi-custom PTL logic layout uses 35% less space than the CMOS design to give an area-efficient solution [9]. In [10], the circuit methods for constructing a high-speed adder with PTL are discussed. The Double Pass-Transistor logic (DPL) improves the design performance even at a low power supply. The speed is improved because of its symmetrical design and double-transmission properties. This improvement in the gate speed is achieved without increasing input capacitance. The issue of series-connected pass transistors in the carry propagation channel is solved using a Conditional Carry Selection (CCS) carry propagation circuit approach. Combining these methods can decrease a 32-b ALU's addition time from a typical CMOS ALU by 30%. Using these circuit approaches, a 32-b ALU test chip is created in 0.25-um CMOS technology and has a 1.5 ns addition time at a 2.5 V supply. Additionally, it is discovered in [11] that when the threshold voltage is 0.4 V, the low-voltage performance of nMOS-based pass-transistor logic is superior to that of traditional CMOS circuits down to 1 V. [12] proposed a novel methodology for synthesizing large PTL circuits. This also pointed out the need for CAD algorithms for PTL circuit design. It outlined a comprehensive synthesis flow and proposed logic level optimization, that could directly provide efficient PPA.PTL is a natural partner for ambipolar field-effect transistors, and [13] suggests a circuit that uses compact PTL and ambipolar FETs for better energy delay performance compared to the traditional static CMOS logic structure. By combining PTL and GDI approaches, the paper provides a 17T 1-bit hybrid comparator design. Nine NMOS transistors and eight PMOS transistors make up the comparator architecture [14]. This space-efficient 9T full adder module serves as the foundation for the suggested hybrid architecture. DSCH 3.1 and Microwind 3.1 were used to develop and simulate the comparator on a 120nm chip. On the LEVEL-3 and BSIM-4 models, the simulation results are displayed. The suggested design in [14] has an area of 329.3 m2 and uses 120nm technology. The suggested 1-bit comparator circuit operates effectively over a broad frequency range of 2MHz to

400MHz and requires a minimum voltage supply of 0.4V. The 1-bit comparator simulation results demonstrate that the power consumption and current are lower.[15] presented the design of a 2-bit magnitude comparator using Conventional CMOS and PTL. The proposed design in [15] used a PTL-based circuit at input terminals & CCMOS-based circuit at output terminals. The results displayed satisfactory PPA and design efficiency for present microprocessor designs.

In [16], the design of the comparator is implemented by using conventional CMOS logic, GDI logic and PTL topologies. Four P-channel MOSFETs and four N-channel MOSFETs are used in the efficient design. DSCH-3.1 and Microwind-3.1 are the software programs that are being used. Using the 45 nm manufacturing technique, the circuit is developed using DSCH-3.1 and subsequently simulated using Microwind-3.1.

The non-functional parameters considered are power, the area covered, and transistor count. The GDI logic uses less power than the traditional MOS design by around 85.9% and has a smaller latency of roughly 42.1%. Compared to PTL, GDI-Logic uses less power (43.4%) and has an 89% shorter latency. [17] investigates the performance of the fundamental NAND gate utilizing several CMOS approaches. These approaches include Gate Diffusion Input (GDI), Transmission Gate, Domino Logic, and Pass Transistor Logic (PTL). [18] reviewed the performance & efficiency of various design implementation techniques like PTL, GDI, and conventional CMOS by designing a full adder. On comparison of their performance in terms of PPA, showed that an adder designed with PTL & GDI provides less delay & less power dissipation when operated at a higher speed. [19] presented the efficient design of a 2-bit hybrid magnitude comparator using various design topologies. It proved that PTL-GDI techniques provide efficient results in terms of PPA. The simulations are carried out using Tanner EDA tools. The hybrid PTL/CMOS Logic approach produces the best performance at the circuit level when compared to CMOS solo and PTL only. The proposed design in [20] has small power dissipation and low area over various supply voltages. Simulations are built on the BSIM 3V3 90nm CMOS platform. [21] suggests an effective approach for optimizing circuits with closely spaced sequential cycles that concurrently use Shannon decomposition and retiming. Even though the technique can only enhance a small percentage of the circuits (approximately half of the benchmarks are examined), the performance improvement can be significant (7%–61%) with just a little (1%–12%) increase in area.

The algorithm is a useful addition to a synthesis flow since it is also quick. Although retiming is a potent method for accelerating pipelines, it is hampered by close consecutive cycles. It is common practice for designers to manually combine Shannon decomposition and retiming to target such cycles; however, this manual decomposition is error prone. With these above findings in the background, the proposed comparator is designed by using Cadence EDA tools [21].

The design of comparators is used in the applications of image processing for skeletonization using different edge and corner detection algorithms. [22,23]

III. Design and Modeling of Comparator

The electronic system design consists of a data path and a control path. The data path is designed by using arithmetic and logical units in which the comparator is the major building block. The basic design diagram of the comparator is shown in Figure 1. This comparator design diagram consists of A and B as inputs and produces the outputs as A<B, A=B and A>B. This comparator is used mainly in all computational units to calculate the addresses, the table indices for encryption and security application areas.

Figure 1. Block diagram of the comparator

The design of comparators is done by using basic digital logic primitive gates to produce proper input and output relations. The basic input and output relations of a comparator of Figure 1 is shown in Table 1 with all test case possibilities.

TABLE I.
Truth Table of Comparator

INPUT		OUTPUT		
A	B	A=B	A>B	A<B
0	0	1	0	0
0	1	0	0	1
1	0	0	1	0
1	1	1	0	0

Logic Families

The Logic families used in the design of the comparator are classified into three topologies i.e., Conventional CMOS, GDI and PTL. Finally, the proposed system is designed using Hybrid Logic family to model comparator.

A. Conventional CMOS Logic Style

The conventional CMOS design technique makes use of many transistors. In this logic style three different transistor topologies are used to produce the outputs of comparator. The design of a basic conventional CMOS comparator is shown in Figure 2. This designed comparator consists of a greater number of transistors which results in an increased power analysis. As a result of increase in area and power the overall circuit speed is largely reduced. The main advantages are large fan-out capability (>50), very high noise margins and noise immunity.

CVR Journal of Science and Technology, Volume 25, December 2023
DOI: 10.32377/cvrjst2503

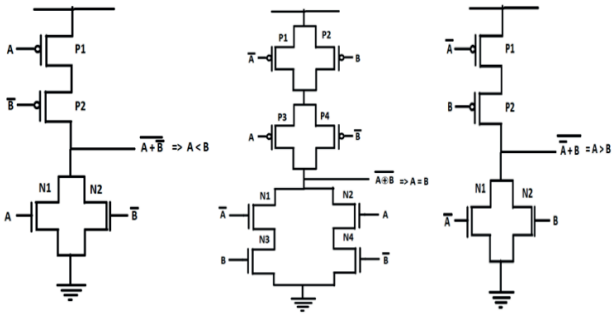

Figure 2. Conventional CMOS Comparator Design

The limitations of this topology are increased cost, less packing density due to a greater number of transistors and their interconnections, which also require the protection for avoiding short circuits among the interconnecting wires.

B. GDI Logic Style

The GDI logic style is used as a new method for digital circuits to achieve low power by considering less complexity in circuit topology. The basic GDI logic design technique makes use of a smaller number of transistors along with different transistor topologies to produce the outputs of comparator. The Figure 3 shows the GDI based comparator design for different output combinations.

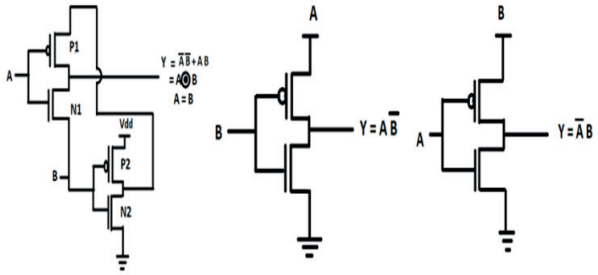

Figure 3. GDI based Comparator Design

The advantages are smaller transistor count, reduced supply voltage, area, power, and delay. This designed GDI logic consists of N, P, G terminals which are connected to VDD, Ground and input or outputs to produce the required logic cell functions. The basic GDI cell functions are listed in Table 2. The GDI logic based output boolean equations along with the logic functions are shown in Table 2.

This designed comparator using GDI has not fixed the problem of low voltage swing which is the major drawback in this topology.

TABLE II.
BASIC GDI CELL FUNCTIONS

N	P	G	OUT	Function
0	B	A	A'B	F1
B	1	A	A'+B	F2
1	B	A	A+B	OR
B	0	A	AB	AND
C	B	A	A'B+AC	MUX
0	1	A	A'	NOT

C. PTL Logic Style

The Pass Transistor Logic (PTL) is used as an alternative logic family compared with Conventional CMOS and GDI logic family. This PTL logic family uses a reduced number of transistors to design the input and output logic function relation. The design of PTL based comparator is shown in Figure 4.

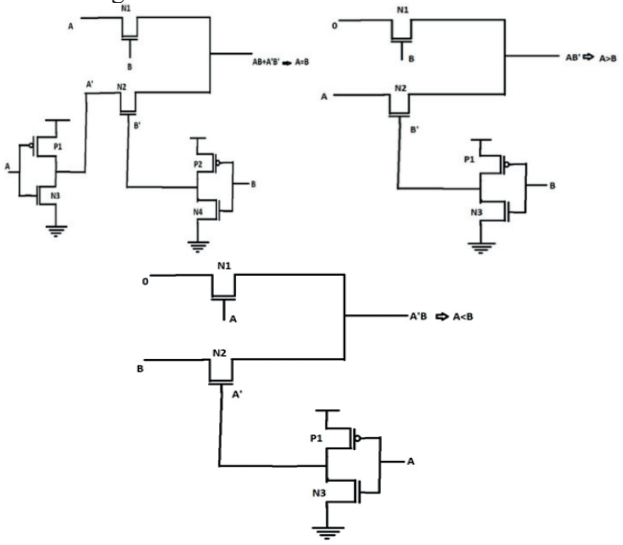

Figure 4. PTL based Comparator Design

The advantages of Pass Transistor Logic are small area and smaller power dissipation. Limitations is larger delay.

D. Proposed Hybrid Comparator

The hybrid model is an advanced technique of designing circuits using two or more design topologies for achieving efficient performance. PTL and GDI have some advantages over static CMOS, such that they can implement a logic function with a smaller number of transistors, smaller delay, and less power dissipation. For full-swing output, level-restoring logic may be required at the PTL and GDI output gates, and this level-restoring logic will slow down the PTL circuits and increase the power dissipation as well. Depending on the application and requirement, the topology for outputs is decided. The block diagram of Hybrid comparator is shown in Figure 5. This hybrid comparator consists of CMOS based design, PTL based design and GDI based designs for different output generations. The advantages of this topology are low-power, delay, power delay product.

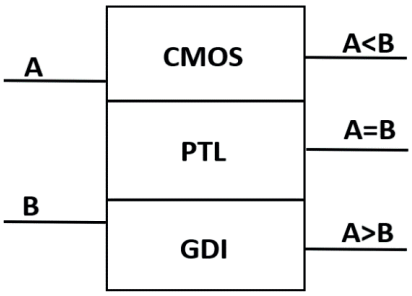

Figure 5. Block diagram of the Hybrid Comparator

E-ISSN 2581 – 7957
P-ISSN 2277 – 3916

DOI: 10.32377/cvrjst2503

IV. Design of Comparator using EDA Tools

The comparators are designed by using Cadence Virtuoso Design suite EDA tools environment. These comparators are designed by using Conventional CMOS topology, GDI topology, PTL topology and proposed hybrid model.

The Conventional CMOS comparator schematic designs for different output conditions A<B, A=B and A>B are shown in Figure 6.

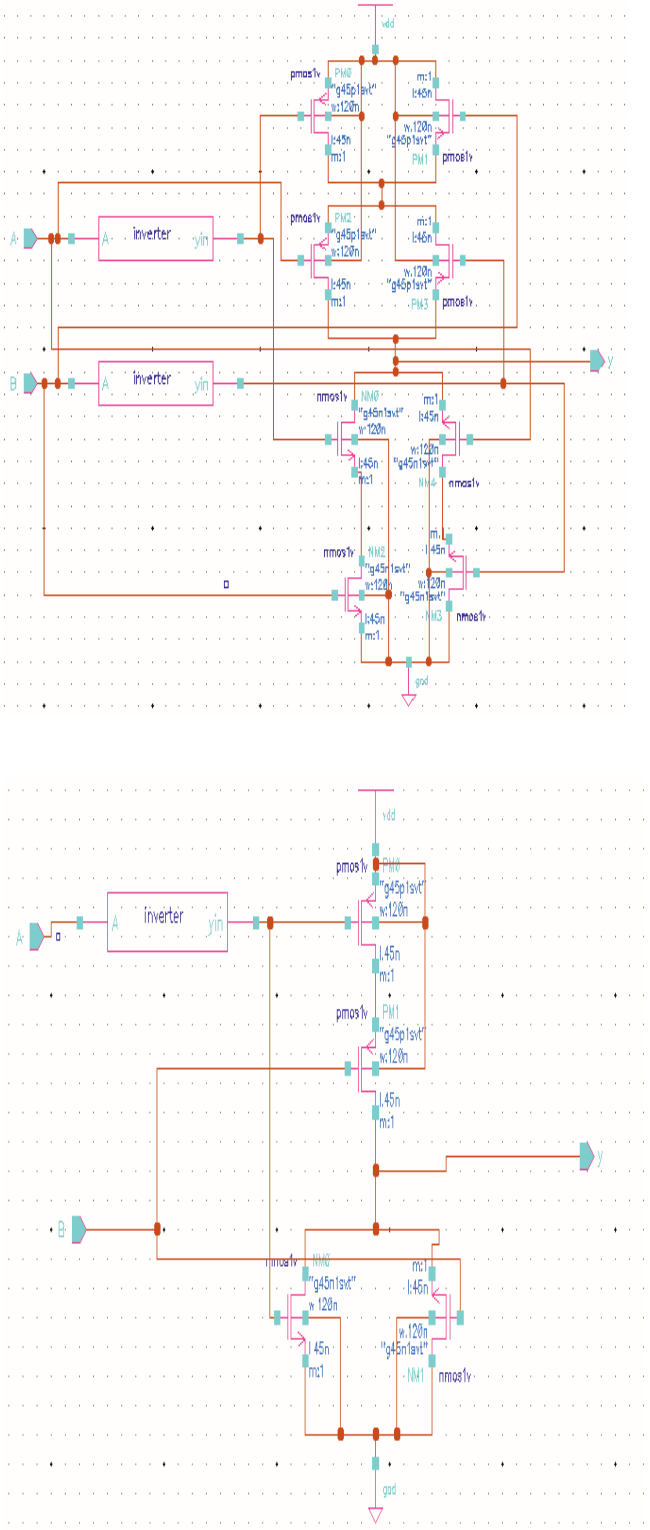

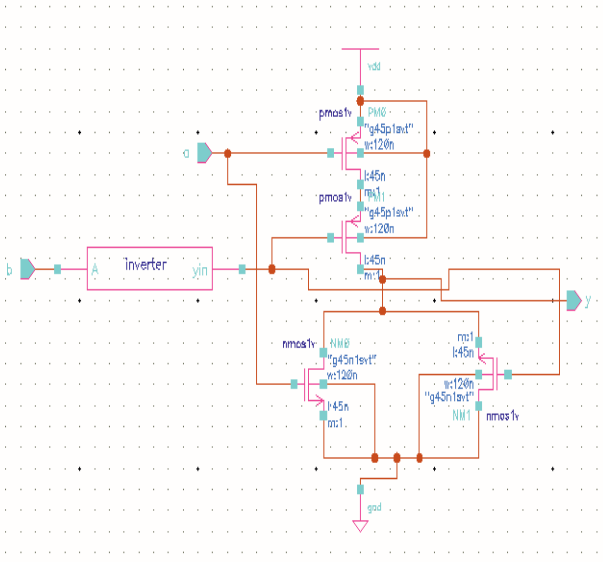

Figure 6. Schematic designs of Conventional CMOS Comparator

The GDI based comparator schematic designs for different output conditions A<B, A=B and A>B are shown in Figure 7.

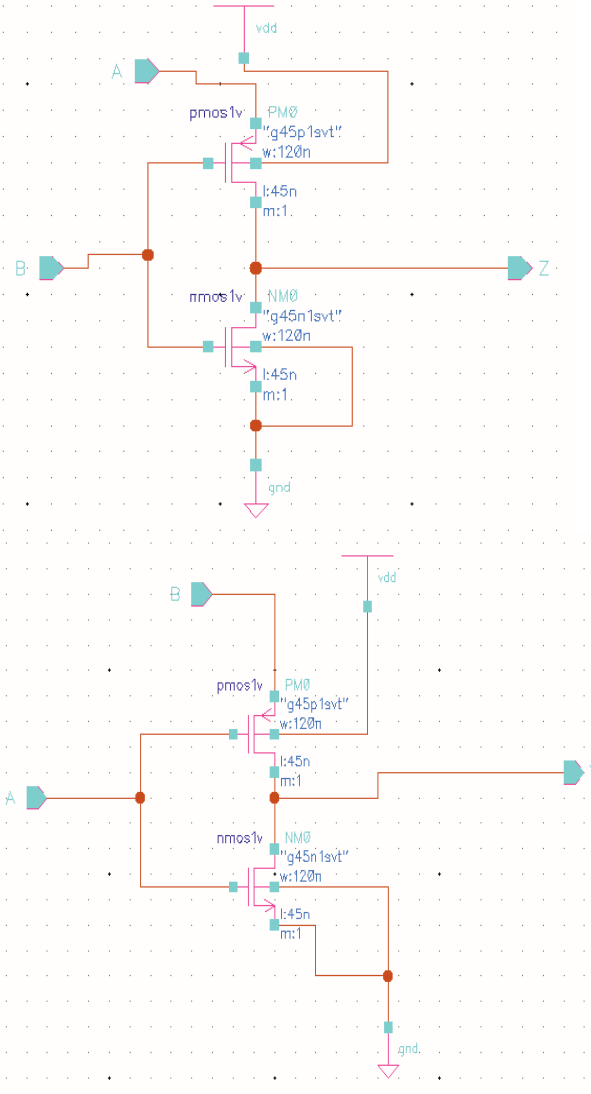

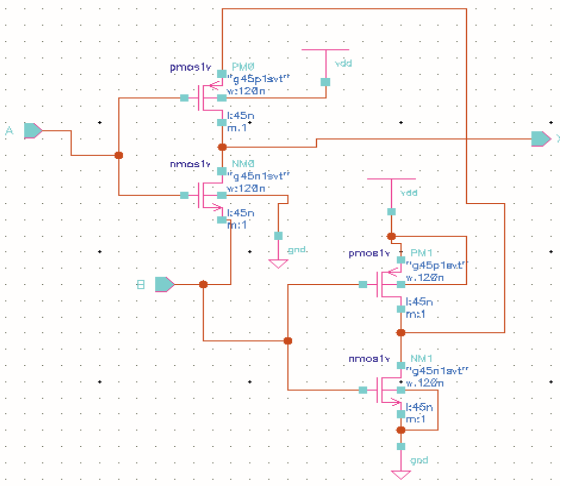

Figure 7. Schematic designs of GDI based Comparator

The PTL based comparator schematic designs for different output conditions A<B, A=B and A>B are shown in Figure 8.

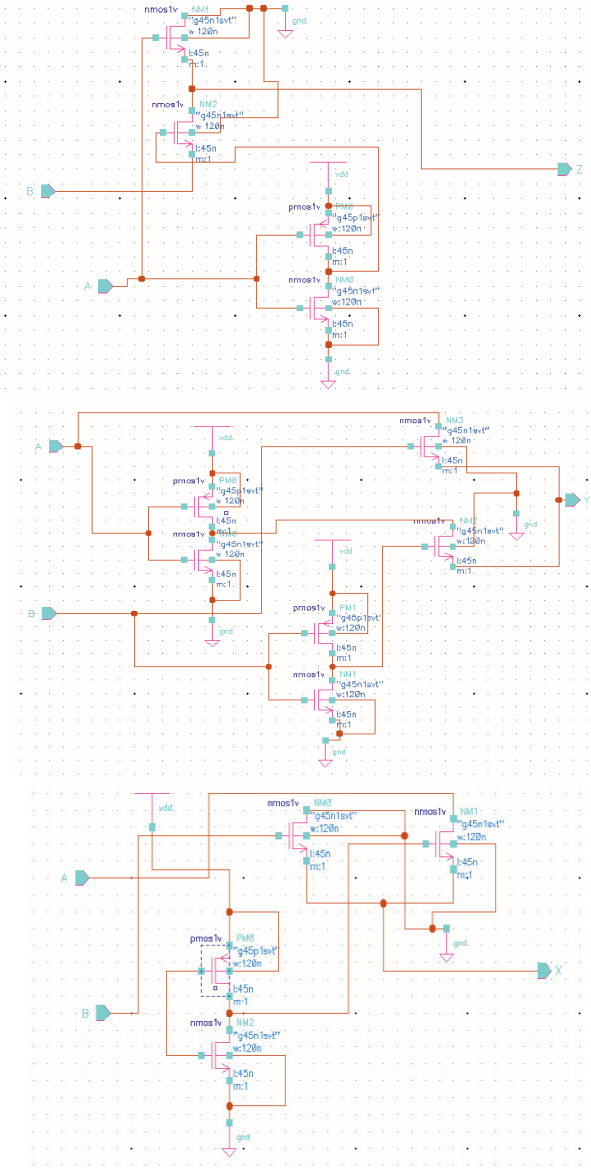

Figure 8. Schematic designs of PTL based Comparator.

The hybrid comparator schematic design using Conventional CMOS, GDI and PTL logic styles for different output conditions A<B, A=B and A>B is selected based on the nonfunctional performance metrics of IC design topologies is shown in Figure 9.

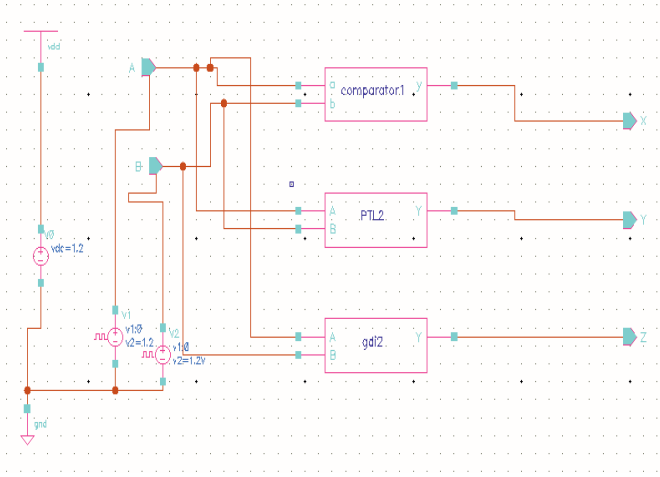

Figure 9. Schematic design of Hybrid Comparator

V. Simulation Results

The simulation results of Conventional CMOS based comparator design are shown in Figure 10.

Figure 10. Simulation of CMOS comparator for A<B, A=B and A>B

E-ISSN 2581 – 7957
P-ISSN 2277 – 3916

CVR Journal of Science and Technology, Volume 25, December 2023
DOI: 10.32377/cvrjst2503

The simulation results of GDI based comparator design are shown in Figure 11.

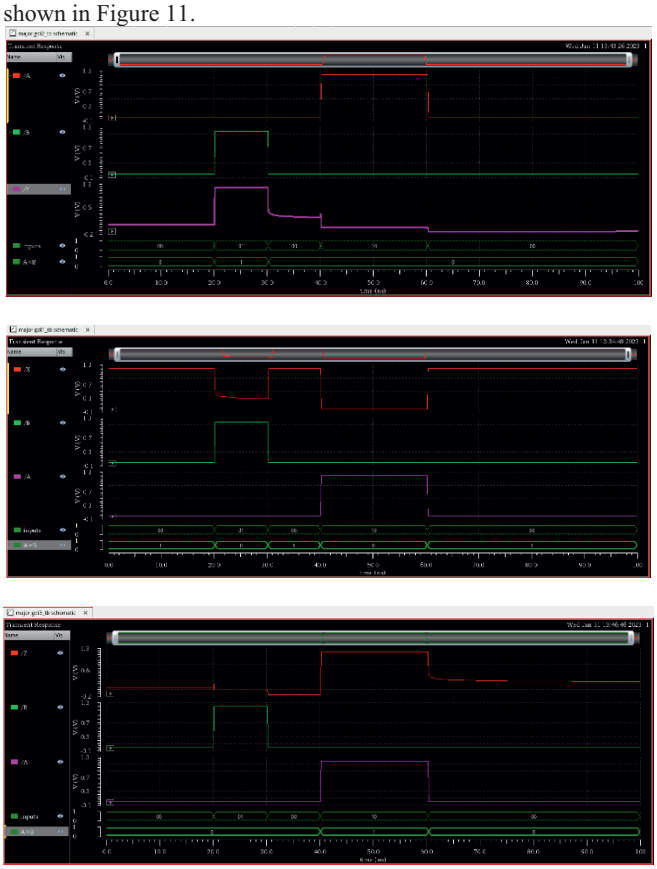

Figure 11. Simulation of GDI based comparator for A<B, A=B and A>B

The simulation results of PTL based comparator design are shown in Figure 12.

Figure 12. Simulation of PTL based comparator for A<B, A=B and A>B

Figure 13. Simulation of Hybrid comparator for A<B, A=B and A>B

Performance Analysis of Comparator

The Performance Analysis of comparator for area is shown in table III. The Performance Analysis of comparator for delay is shown in table IV and Figure 14. The Performance Analysis of comparator for power is shown in table V and Figure 15.

TABLE III.
AREA COMPARISON OF COMPARATOR

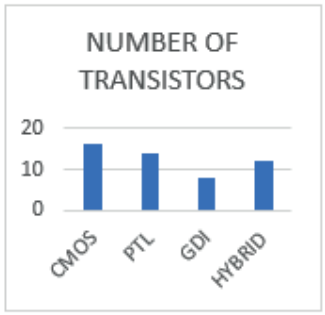

Design Style	Area (Number of Transistors)
MOS	16
PTL	14
GDI	8
HYBRID	12

Performance Analysis of Comparator in terms of Delay

TABLE IV.
DELAY COMPARISON OF COMPARATOR

Design Style	Delay for A<B (ns)	Delay for A>B (ns)	Delay for A=B (ns)
CMOS	9.9	0.056	20
PTL	20	0.351	0.017
GDI	0.02	0.042	19.94
HYBRID	20	20	0.0175

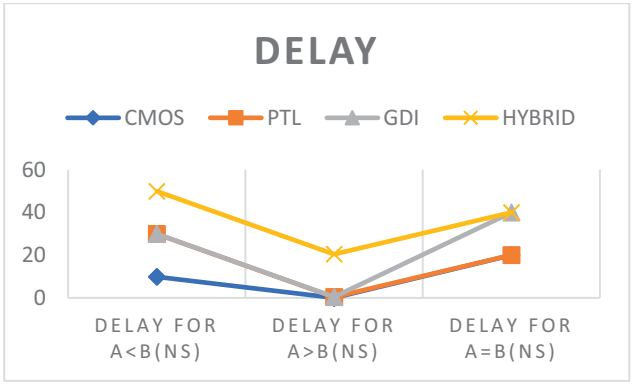

Figure 14. Delay Comparison of Comparator for MOS Logic families

CVR Journal of Science and Technology, Volume 25, December 2023
DOI: 10.32377/cvrjst2503

Performance Analysis of Comparator in terms of Power

TABLE V.
POWER COMPARISON OF COMPARATOR

TOPOLOGY	POWER FOR A<B (nW)	POWER FOR A>B (nW)	POWER FOR A=B (nW)
CMOS	1.62	2.32	36.5
PTL	4.25	30	10
GDI	4.21	7.56	2.1
HYBRID	1.048	0.004	1.04

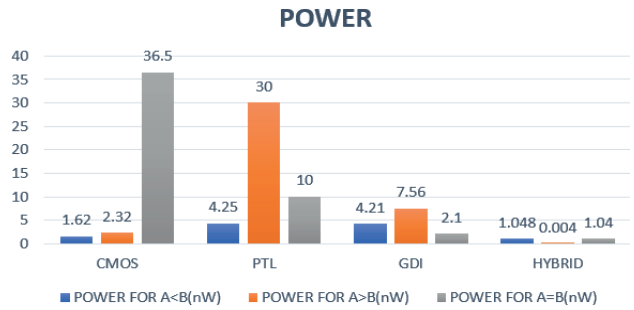

Figure 15. Power Comparison of Comparator for MOS Logic families

VI. CONCLUSIONS

The comparator for arithmetic applications is designed by using Conventional CMOS topology logic, Pass Transistor Logic (PTL), Gate Diffusion Input (GDI) Logic and Mixed hybrid topology logic. The comparators are designed by using Cadence Virtuoso EDA tools with 45nm technology. The nonfunctional area in terms of number of transistors for CMOS logic is 16, PTL is 14, GDI is 8 and Hybrid logic is 12 transistors. The delay and power parameters are also analyzed for the selection of hybrid logic topology. Hybrid logic is having best delay performance for equality comparison, and it also provides low power consumption for equality and inequality conditions compared to CMOS, PTL and GDI logic topologies.

REFERENCES

[1]. Chandrahash Patel, Dr. Veena C.S. Study of Comparators and their Architectures, International Journal of Multidisciplinary Consortium Volume – 1 Issue – 1 June 2014
[2]. Shubhara Yewale, Radheshyam Gamad. Design of Low Power and High-Speed CMOS Comparator for A/D Converter Application, Wireless Engineering and Technology, 2012, 3, 90-95 doi:10.4236/wet.2012.32015 Published Online April 2012
[3]. Sukhdeep Kaur, Hardeep Kaur, Er. Poonam Rani. Design and Optimization of GDI Based 1-bit Comparator using Reverse Logic, International Journal of Recent Research in Electrical and Electronics Engineering (IJRREEE) Vol. 2, Issue 2, pp: (6-10), Month: April 2015 - June 2015
[4]. Shashank Gupta, Subodh Wairya. A GDI Approach to Various Combinational Logic Circuits in CMOS Nano Technology, International Journal of Engineering and Computer Science ISSN: 2319-7242 Volume 5 Issue 4 April 2016, Page No. 16243-16247
[5]. Bhaskara Rao Doddi, Y E Vasanth Kumar, G Sai Kiran, K Sri Sravya, V Pruthivi. Optimized VLSI Design of 2-Bit Magnitude Comparator using GDI Technique, International Journal of Recent Technology and Engineering (IJRTE) ISSN: 2277-3878 (Online), Volume-7, Issue-6, March 2019
[6]. R. Uma, P. Dhavachelvan. Modified Gate Diffusion Input Technique: A New Technique for Enhancing Performance in Full Adder Circuits, 2nd International Conference on Communication, Computing & Security [ICCCS-2012]
[7]. Divya Soni, Mihir V. Shah. Review on Modified Gate Diffusion Input Technique, International Research Journal of Engineering and Technology (IRJET) Volume: 04 Issue: 04 | Apr -2017
[8]. Anjali Sharma, Harsh Sohal. Sleepy- Gate Diffusion Input (S-GDI) — Ultra Low Power Technique for Digital Design, International Journal of Innovative Technology and Exploring Engineering (IJITEE) ISSN: 2278-3075 (Online), Volume-9 Issue-1, November 2019
[9]. Jyoti, Rajesh Mehra. Area Efficient Layout Design of CMOS Comparator using PTL Logic, International Journal of Computer Applications (0975 – 8887) Volume 122 – No.16, July 2015
[10]. Makoto Suzuki, Norio Ohkubo, Toshinobu Shinbo, Toshiaki Yamanaka, Akihiro Shimizu, Katsuro Sasaki, Yoshinobu Nakagome.A 1.5-ns 32-b CMOS ALU in Double Pass-Transistor Logic, IEEE JOURNAL OF SOLID- STATE CIRCUITS, VOL. 28, NO. 11, NOVEMBER 1993
[11]. Kazuo Yano, Yasuhiko Sasaki, Kunihito Rikino, Koichi Seki. Top-Down Pass-Transistor Logic Design, IEEE JOURNAL OF SOLID-STATE CIRCUITS, VOL. 31, NO. 6. JUNE 1996
[12]. Premal Buch, Amit Narayan, A. Richard Newton, A. Sangiovanni-Vincentelli. Logic Synthesis for Large Pass Transistor Circuits, 0-89791-993-9/97, 1997 IEEE
[13]. Xuan Hu, Amy S. Abraham, Jean Anne C. Incorvia, Joseph S. Friedman. Hybrid Pass Transistor Logic with Ambipolar Transistors, IEEE TRANSACTIONS ON CIRCUITS AND SYSTEMS—I: REGULAR PAPERS, VOL. 68, NO. 1, JANUARY 2021
[14]. Anjali Sharma, Richa Singh, Pankaj Kajla. Area Efficient 1-Bit Comparator Design by using Hybridized Full Adder Module based on PTL and GDI Logic, International Journal of Computer Applications (0975 – 8887) Volume 82 – No.10, November 2013
[15]. Afran Sorwar, Elias Ahammad Sojib, Md. Ashik Zafar Dipto, Md. Mostak Tahmid Rangon, Md. Sabbir Alam Chowdhury, Abdul Hasib Siddique. Design of a High-Performance 2-bit Magnitude Comparator Using Hybrid Logic Style, 11th ICCCNT 2020 July 1-3, 2020 - IIT - Kharagpur, IEEE – 49239
[16]. Ashima Singh, Akanksha Mishra, Rajesh Mehra, Srishtee Chaudhary. Design Analysis of 1-bit Comparator using different Logic Techniques, 2019 JETIR March 2019, Volume 6, Issue 3
[17]. Aneela Achu Mathew, Juney M George. Comparative Analysis of a NAND Gate and a 2-bit Magnitude Comparator using GDI Technique, Proceedings of 2018 International Conference on Emerging Trends and Innovations in Engineering and Technological Research (ICETIETR)
[18]. Nidhi Dubey, Divyanshu Rao. Design of Full Adder Using PTL & GDI Technique and Comparison with Conventional Designs, International Journal of Modern Engineering and Research Technology Volume 4 | Issue 1 | January 2017
[19]. Mahitha M. Das, Greshma Mohan, Greeshma, Aneesh K. A Novel Design of Hybrid 2 Bit Magnitude Comparator,

International Research Journal of Engineering and Technology (IRJET), Volume: 06 Issue: 05 | May 2019

[20]. Geetanjali Sharma, Uma Nirmal, Yogesh Misra. A Low Power 8-bit Magnitude Comparator with Small Transistor Count using Hybrid PTL/CMOS Logic, IJCEM International Journal of Computational Engineering & Management, Vol. 12, April 2011 ISSN (Online): 2230-7893

[21]. Cristian Soviani, Olivier Tardieu, Stephen A. Edwards. optimizing sequential cycles through shannon decomposition and retiming, IEEE Transactions on Computer-Aided Design of Integrated Circuits and Systems, vol. 26, no. 3, march 2007

[22]. P. Srinivasa Rao, Yedukondalu Kmatam, Racha Ganesh. FPGA implementation of digital 3-D image skeletonization algorithm for shape matching applications, International Journal of Electronics, 2021, 108(8), pp. 1326–1339

[23]. P. Srinivasa Rao, Yedukondalu Kmatam. FPGA implementtation for skeletonization of 2-D images 2018 3rd IEEE International Conference on Recent Trends in Electronics, Information and Communication Technology, RTEICT 2018 - Proceedings, 2018, pp. 1698–1702, 9012576

E-ISSN 2581 – 7957
P-ISSN 2277 – 3916

DOI: 10.32377/cvrjst2504

Image Inpainting using Efficient Patch Selection Technique

B. Janardhana Rao[1], Venkata Krishna Odugu[2], G. Harish Babu[3]
[1]Asso. Professor, CVR College of Engineering/ECE Department, Hyderabad, India
Email: janarhdan.bitra@gmail.com
[2]Assoc. Professor, CVR College of Engineering/ECE Department, Hyderabad, India
Email: venkatakrishna.odugu@gmail.com
[3]Sr. Asst. Professor, CVR College of Engineering/ECE Department, Hyderabad, India
Email: harish.sidhu12@gmail.com

Abstract: **Image inpainting is a well growing research area in the field of image processing. It is used to reconstruct the spoiled images due to aging. It can also reproduce the images by removing any unwanted objects in the image. Exemplar inpainting methods gain the most attention for object removal applications. The major difficulty observed in these methods includes mismatching of patches while selecting the exemplar patches, which leads to fill by miscellaneous objects in the target region. In this paper, the new patch selection is employed to overcome the above stated issue. The combination of Sum of Squared Difference (SSD) and Logarithmic Similarity (LS) is proposed in this paper. The results generated from the proposed work are compared to the available method in the literature qualitatively. It shows that proposed work outperformed the state-of-art works.**

Index Terms: **Mismatch, Exemplar, SSD, Logarithmic Similarity, qualitative**

I. Introduction

Image inpainting refers to the procedure of restoring a damaged image or eliminating an object within an image [3], [4]. The underlying principle of image inpainting involves the utilization of the surrounding information within a certain region to complete or restore the missing portions of an image. Image inpainting techniques have a wide range of applications, including the automatic removal of text and objects in images or films for special effects [5]. These techniques can also be used to delete blurs caused by dust in an image, correct red eye, create inventive effects by removing objects [6], [7], remove logos from videos [8], restore old images or films [9], and correct missing or distorted information in medical images [10]. Typically, image inpainting approaches can be classified into five primary categories, namely: (1) inpainting based on partial differential equations, (2) inpainting based on texture synthesis, (3) exemplar-based inpainting, (4) semi-automatic and fast inpainting, and (5) hybrid inpainting [11], [12]. Each category possesses distinct benefits and constraints, and each category restores the impaired areas based on specific expectations for the restored visual material. This study primarily centers on the third category, specifically exemplar-based image inpainting.

Exemplar-based image inpainting is widely recognized as a crucial category of inpainting techniques, having demonstrated superior efficacy compared to other forms of inpainting methods [13]. Exemplar-based image inpainting primarily comprises two fundamental stages. The initial stage involves prioritizing the assignment. During this stage, a single patch from the outer edge of the region that is lacking must be chosen based on a priority function. This patch is then filled in as the first step. The second stage entails conducting a search for the most suitable patch by employing one of the available search algorithms. Within the realm of this particular field of study, scholars' endeavor to enhance either one or both of these processes in order to achieve superior outcomes in relation to the caliber of the rebuilt image. This study aims to enhance the search method by leveraging the spatial proximity between the patch to be inpainted and the other most suitable matching patches.

The main contributions of the proposed work are as follows:

- Exemplar based image inpainting technique is proposed using efficient patch matching.
- A new patch selection method is proposed to avoid the mismatching patches problem.
- This patch selection method is implemented using cumulative distance of SSD and LS.
- The experimentation is performed on Berkely Segmentation Dataset.
- The qualitative results are compared with the state-of-art methods of inpainting in literature.

The subsequent sections of the paper are structured in the following manner: Section II of the document encompasses the presentation of the related works of the image inpainting. The proposed inpainting methodology is described in detail in section III. In section IV, the experimental results are discussed. The conclusions are presented in Section V.

II. Related Work

The previous section discusses many classifications of image inpainting. The focus of this study is on exemplar-based image inpainting. As a result, this part will provide a review of significant methodologies that are relevant to exemplar-based image inpainting.

Criminisi et al. [13] introduced a technique that effectively addressed the processing of images containing comprehensive structural and texture information, while also effectively filling in wide areas of unknown regions. The present approach involves filling the patches located at the periphery of the unknown region by prioritizing the patches

Received on 30-09-2023, Revised on 30-10-2023, Accepted on 10-11-2023.

with the highest similarity to an exemplar patch from the source region. Liang et al. [14] introduce a proficient technique for detecting forgeries in object removal with the use of exemplar-based inpainting. This approach incorporates three key components: center pixel mapping (CPM), greatest zero-connectivity component labeling (GZCL), and fragment splicing detection (FSD). The CPM algorithm enhances the efficiency of identifying suspicious blocks by effectively comparing blocks with comparable hash values and subsequently identifying pairs that exhibit suspicious characteristics. In order to enhance the accuracy of detection, the technique of GZCL is employed to identify the manipulated pixels inside the suspected block pairings. The use of FSD serves the purpose of differentiating and precisely identifying manipulated areas from their corresponding regions with the highest degree of similarity. Tiang et al. [15] introduced a novel approach to image inpainting that utilizes exemplars, aiming to preserve geometric structures and effectively reproduce textures, resulting in aesthetically pleasing results. In order to enhance the efficiency of the filling order, a novel adaptive two-stage structure-tensor based priority function is introduced. Zhang et al. [16] introduced a highly effective technique for image inpainting, utilizing surface fitting as the underlying prior knowledge and incorporating angle-aware patch matching. In order to enhance the accuracy of patch matching, we propose the utilization of a Jaccard similarity coefficient. In order to alleviate the burden of the task, we employ a dynamic approach to determine the sizes of both target patches and source patches. Instead of exclusively choosing a single source patch, our approach involves a global search for numerous source patches using an angle-aware rotation strategy. This strategy is employed to ensure the preservation of both structural and textural consistency. In their study, Janardhana Rao et al. [17-19] proposed an enhanced method for calculating priorities, which encompasses the regularization factors and adaptive coefficients. The exemplary patch is chosen through the use of SSE and SAD metrics. Yao [20] implemented a priority calculation that took into account how similar the target patch was to its neighbors. They also made a change, switching addition for multiplication. To further improve the restoration's efficiency, also created a novel similarity calculating function. In their study, Zhang et al. [21] utilized a similarity metric that combined the mean squared difference and the square of mean differences in order to identify the example patch. In their study, Wang et al. [22] proposed the incorporation of a space-varying updating function to enhance the confidence term. The estimation of the priority function was achieved by using a matching confidence term. The target patch was populated through the utilization of structural consistent patch matching. In their study, Wang et al. [23] put out a novel approach for calculating priorities in exemplar-based inpainting. This method incorporates a regularization component to mitigate the dropping effect. The source region was subjected to a patch search using a combination of SSD and Normalized Cross-Correlation (NCC). Ahmed and Abdulla [24] introduced a novel approach for identifying the optimal similar patch inside the source region. Their method involves the integration of Euclidean distance and positional or locational distance measures between the patches. The aforementioned procedure is iteratively executed until the process of inpainting is successfully accomplished inside the designated target area. Further the exemplar-based methods are employed for implementing video inpainting techniques for object removal applications [25-28] along with spatio-temporal coherence.

III. Proposed Work

A. Annotations of the work

The annotations corresponding to the different components involved in the application of exemplar-based image inpainting are displayed in Figure 1. The symbol Ø represents the source region that is employed to populate the target region, Ω which is created subsequent to the removal of undesired objects. The boundary of the target region (∂Ω) refers to the region's outermost edge. A patch on the border of the target region is a small section located on this edge. The number of patches will be considered on the boundary with pixels on the boundary as center. Out of these patches, priority of the patch to fill initially is decided based on sophisticated methods. This prioritized patch is filled with patches taken on the source region($\Psi_{q1}\Psi_{q1}$, $\Psi_{q2}\Psi_{q2}$, Ψ_{q3} Ψ_{q3}) considering the similarity checking between these patches. The patch with high similarity is used for filling the high priority patch on the boundary. Later the boundary is updated, and the process will continue till it completes the target region.

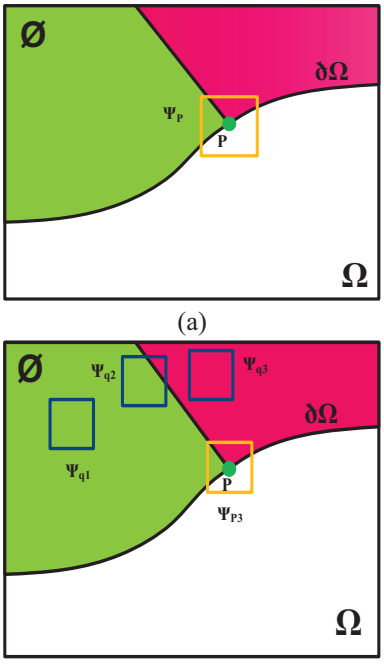

Figure 1. Diagram of Annotations.

From the above literature survey, the patch similarity verification methods produce matching error. While comparing the similarity between existing pixels of highly prioritized patch and the pixels in the source region patch there is a high difference of similarity value. Which leads to generating miscellaneous objects in the place of holes in the

target region, which means that the inpainting process has not taken place properly. In order to avoid the matching error occurring in the available methods, the new patch similarity computation method is proposed in this paper. In the exemplar based inpainting technique, highest priority patch computation and exemplar patch selection without matching error is the vital part. The proposed work for the two vital parts is described in this section.

B. Patch Priority Computation

The decision of the filling order in image inpainting is predicated upon the assignment of priority values to the different patches extracted from the boundary of the target region. The methodology utilized in this study entails employing to calculate the priority of patches. The selection of this specific method is based on its capability to assign elevated priority values to patches that are situated along prominent edges, hence maintaining structural coherence.

$$Prty = R_C(p) * D_p \quad (1)$$

where, $R_C(p)$ represents the confidence term with regularization factor (β) and D_p represents the data term.

$$R_C(p) = (1-\beta)C_p + \beta \quad (2)$$

where, C_p denotes the confidence term. It is given by,

$$C_p = \frac{\sum_{t\epsilon(\Psi_p \cap \Phi)} C(t)}{|\Psi_p|} \quad (3)$$

where, tt indicates the coordinates of the pixels of Ψ_p and Ø. $|\Psi_p|$ was the number of pixels in the target patch.
The data term D_p is taken as,

$$D_p = \frac{|\nabla I_P^{\perp} \cdot n_P|}{255} \quad (4)$$

where, $\nabla I_P^{\perp}$ indicates the isophote vector and n_p was the unit vector orthogonal to boundary of target region at pixel p.

C. Patch Matching Methodology

This study presents a novel matching rule for evaluating the similarity between the highest priority patch and the exemplar patch. The given information is provided as,

$$\Psi_{q'} = \arg\min_{\Psi_{qi}\epsilon\emptyset}\left[SSD(\Psi_p, \Psi_q) + LS(\Psi_p, \Psi_q)\right] \quad (5)$$

where, $SSD(\Psi_p, \Psi_{q1})$, is the Sum of Squared Difference (SSD) and $LS(\Psi_p, \Psi_{q1})$ is the Logarithmic Similarity (LS) Index.
The patches that exhibit the lowest distance value while employing the combination SSD and LS method are recognized as the most optimal matching patches.

The SSD distance between the patches is computed as,

$$SSD(\Psi_p, \Psi_q) = \sum(\Psi_p - \Psi_q)^2 \quad (6)$$

The SSD is the efficient distance matching method for images, which produces values ranging from 0 to 100. The value 0 indicates the highest correlation and 100 means the lowest matching between the patches.
The logarithmic similarity between the patches is generated with equation,

$$LS(\Psi_p, \Psi_q) = \log\{\Psi_p - \Psi_q\} \quad (7)$$

The logarithmic similarity between the two images yields a numerical number within the range of 0 to 100. A number 0 denotes a complete absence of similarity between the image in question, while a value of 100 signifies a 100% similarity.

IV. Results and Discussion

The proposed methodology is executed using the MATLAB software on a machine equipped with a 2.7GHz processor and 12GB of RAM. The evaluation of the suggested methodology is conducted through experiments on the Berkeley Segmentation Dataset [30]. The findings are subjected to qualitative analysis by comparison with existing works of high scholarly significance in literature. The visual quality of the proposed methodology of inpainting is compared to the available methods of inpainting in state-of-art works, it is described in figure 2. In figure 2, column (a) is input image with object, column (b) depicts the mask of the object to remove, column (c) shows the results obtained from the Criminisi et al. [13], column (d) given the results produced by Zhang et al. [21], and column (e) represents the results of inpainting from proposed method. The restored image by removing the unwanted object after filling is indicated in the white color box in figure 2. It is clearly showing that methods in the literature had some blur or not filled properly, our proposed method generated the results exceptionally good compared to other works.

V. Conclusions

The exemplar-based image inpainting techniques play a vital role in large object removal applications. The priority of the patches is estimated with an efficient available method in the literature to overcome the dropping effect and completely focused on similar patch selection from source region. This is implemented by employing cumulative distance of SSD and LS. The experimentation is performed on Berkely Segmentation Dataset, the qualitative results are superior compared to existing methods of inpainting in the literature.

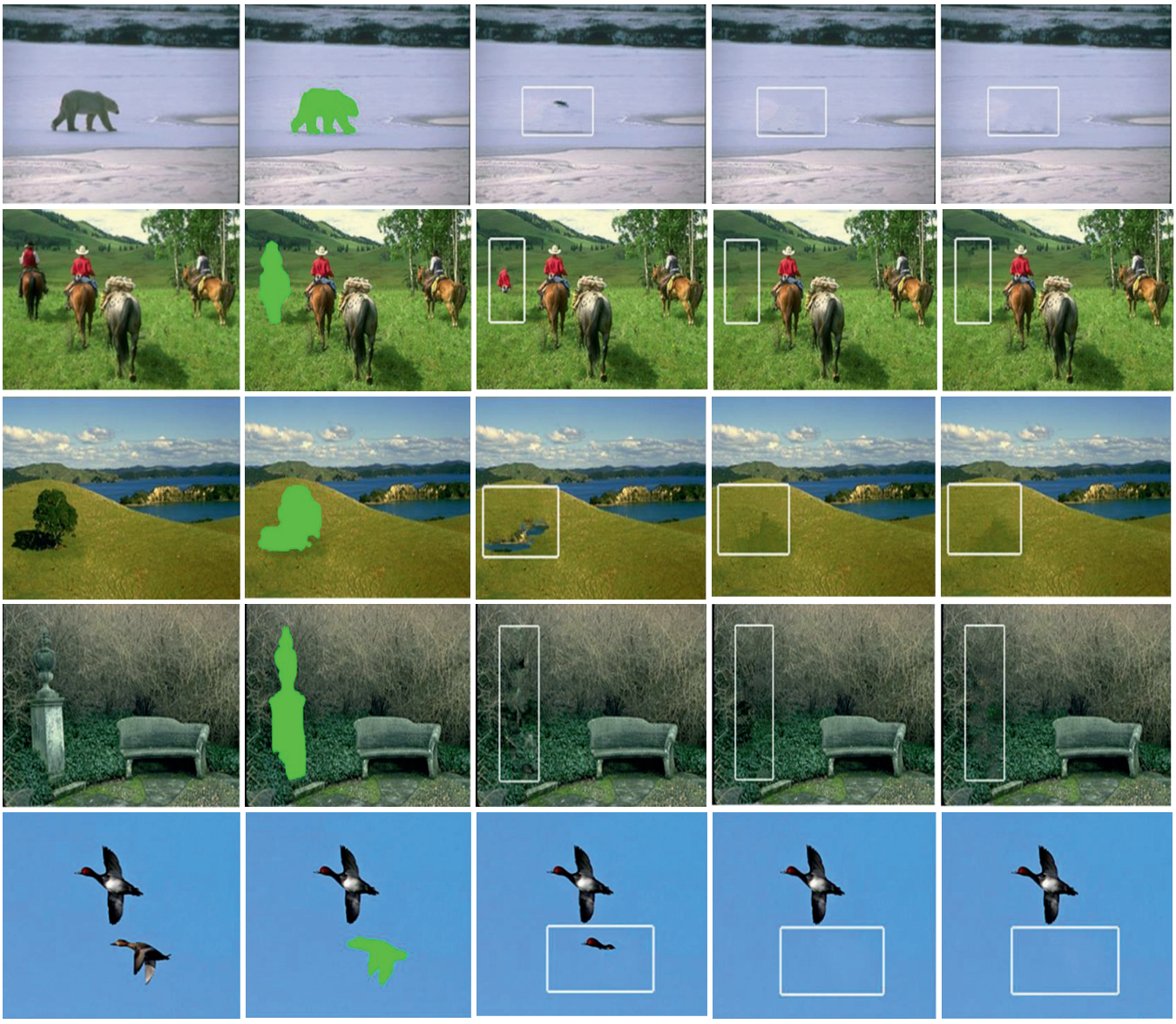

(a) (b) (c) (d) (e)

Figure 2. Comparison of the proposed method with available works in the literature

REFERENCES

[1] A. A. Abdulla. “Exploiting Similarities between Secret and Cover Images for Improved Embedding Efficiency and Security in Digital Steganography,” Department of Applied Computing, University of Buckingham, PhD Thesis, 2015.

[2] C.Guillemot and O. Meur. “Image Inpainting: Overview and Recent advances”. IEEE Signal Processing Magazine, vol. 31, no. 1, pp. 127-144, 2014.

[3] L. Cai and T.Kim. “Context-driven hybrid image inpainting”. IET Image Processing, vol. 9, no. 10, pp. 866-873, 2015.

[4] B. Nizar, H. A. Ben and M. Ali. “Automatic inpainting scheme for video text detection and removal. IEEE Transactions on Image Processing, vol. 22, pp. 4460-4472, 2013.

[5] J. K. Chhabra and V. Birchha. “An enhanced technique for exemplar based image inpainting”. International Journal of Computer Applications, vol. 115, pp. 20-25, 2015.

[6] R. H. Park and Y. Seunghwan. Red-eye detection and correction using inpainting in digital photographs”. IEEE Transactions on Consumer Electronics, vol. 55, pp. 1006-1014, 2009.

[7] M. S. Kankanhalli and W. Q. Yan. “Erasing Video Logos Based on Image Inpainting”. Vol. 2. IEEE, Lausanne, Switzerland, pp. 521- 524, 2002.

[8] Wu, Y., K. Zhonglin and Z. Hongying. "An Efficient Scratches Detection and Inpainting Algorithm for old Film Restoration”. Vol. 1. IEEE, Kiev, Ukraine, pp. 75-78, 2009.

[9] Y. Mecky, G. Sergios, Y. Bin and A. Karim. “Adversarial Inpainting of Medical Image Modalities”. IEEE, Brighton, United Kingdom, pp. 3267-3271, 2019.

[10] M. B. Vaidya and K. Mahajan. “Image in painting techniques: A survey”. IOSR Journal of Computer Engineering, vol. 5, no. 4, pp. 45-49, 2012.

[11] Jain, L., A. G. Patel and K. R. Pate. "Image inpainting-a review of the underlying different algorithms and comparative study of the inpainting techniques". International Journal of Computer Applications, vol. 118, no. 10, 2015. Available from:http://www.citeseerx.ist.psu.edu/viewdoc/download?doi =10.1.1.695.9341&re p=rep1&type=pdf.

[12] B. Limbasiya and N. Pandya. "A survey on image inpainting techniques". International Journal of Current Engineering and Technology, vol. 3, no. 5, pp. 1828-1831, 2013.
[13] A. Criminisi, P. Perez, K. Toyoma, Region filling and object removal by exemplar-based inpainting, IEEE Trans. Image Process. 13 (9) (2004) 1200-1212.
[14] Liang, Zaoshan, Gaobo Yang, Xiangling Ding, and Leida Li. "An efficient forgery detection algorithm for object removal by exemplar-based image inpainting." *Journal of Visual Communication and Image Representation* 30 (2015): 75-85.
[15] Xu, Ting, Ting-Zhu Huang, Liang-Jian Deng, Xi-Le Zhao, and Jin-Fan Hu. "Exemplar-based image inpainting using adaptive two-stage structure-tensor based priority function and nonlocal filtering." *Journal of Visual Communication and Image Representation* 83 (2022): 103430.
[16] Zhang N, Ji H, Liu L, Wang G (2019) Exemplar-based image inpainting using angle-aware patch matching. EURASIP J Image Video Process 70:1–13.
[17] Janardhana Rao, B., Chakrapani, Y. and Srinivas Kumar, S., 2018. Image inpainting method with improved patch priority and patch selection. *IETE Journal of Education*, *59*(1), pp.26-34.
[18] Revathi, K., and B. Janardhana Rao. "Analysis and Implementation of Enhanced Image Inpainting method using adjustable patch sizes." *International Journal* 9, no. 3 (2021).
[19] Rao, B. Janardhana, and O. Venkata Krishna. "Evaluation of Image Inpainting Algorithms." *CVR Journal of Science and Technology* 7 (2014): 48-52.
[20] Yao F (2019) Damaged region filling by improved criminisi image inpainting algorithm for thangka. Clust Comput 22(6):13683–13691.
[21] Zhang, L., & Chang, M. (2021). An image inpainting method for object removal based on difference degree constraint. *Multimedia Tools and Applications*, *80*, 4607-4626.
[22] H. Wang, L. Jiang, R. Liang, and X. X. Li, "Exemplar-based image inpainting using structure consistent patch matching," *Neurocomputing*, *269*, pp. 90-96, 2017.
[23] J. Wang, K. Lu, D. Pan, N He, and B. Bao, "Robust object removal with an exemplar-based image inpainting approach," Neurocomputing, pp. 150-155, 2014.
[24] M. W. Ahmed and A. A. Abdulla, "Quality improvement for exemplar-based image inpainting using a modified searching mechanism," *UHD Journal of Science and Technology*, *4*(1), pp. 1-8, 2020.
[25] Janardhana Rao, B., Chakrapani, Y., & Srinivas Kumar, S. (2022). MABC-EPF: Video in-painting technique with enhanced priority function and optimal patch search algorithm. *Concurrency and Computation: Practice and Experience*, *34*(11), e6840.
[26] B Janardhana Rao, Y Chakrapani, S Srinivas Kumar, An Enhanced Video Inpainting Technique with Grey Wolf Optimization for Object Removal Application, Journal of Mobile Multimedia (2022), Vol. 18, Issue 3, pp. 561-582.
[27] Janardhana Rao, B., Chakrapani, Y., & Srinivas Kumar, S. (2022). Video Inpainting Using Advanced Homography-based Registration Method. *Journal of Mathematical Imaging and Vision*, *64*(9), 1029-1039.
[28] Janardhana Rao, B., Chakrapani, Y., & Srinivas Kumar, S. (2022). Hybridized cuckoo search with multi-verse optimization-based patch matching and deep learning concept for enhancing video inpainting. *The Computer Journal*, *65*(9), 2315-2338.
[29] Rao, B. J., Revathi, K., & Babu, G. H. (2022). Video Inpainting using self-adaptive GMM with Improved Inpainting Technique. *CVR Journal of Science and Technology*, *22*(1), 42-46.
[30] Arbelaez P, Maire M, Fowlkes C, Malik J (2011) Contour detection and hierarchical image segmentation. IEEE Trans Pattern Anal Mach Intell 33(5):898–916.

E-ISSN 2581 – 7957
P-ISSN 2277 – 3916
CVR Journal of Science and Technology, Volume 25, December 2023
DOI: 10.32377/cvrjst2505

Enhancing Plant Leaf Identification: A Comparative Study of Machine Learning Models

D. Bhanu Prakash[1] and G. Santhosh Kumar[2]
[1]Assoc. Professor, CVR College of Engineering/ECE Department, Hyderabad, India
Email: pbhanududi@gmail.com
[2]Sr. Asst. Professor, CVR College of Engineering/ECE Department, Hyderabad, India
Email: santhoshemwave@gmail.com

Abstract: **In this paper, we present a comprehensive analysis of the application of various machine learning models to the task of plant leaf identification. A Weiner filter is applied for noise reduction in the data, and morphological operations are utilized for feature extraction. Subsequently, evaluated the performance of eight different classification models: Quadratic Discriminant Analysis (QDA), Extra Trees Classifier, Random Forest Classifier, Linear Discriminant Analysis, SGD Classifier, Bagging Classifier, Perceptron, and AdaBoost Classifier. These models are assessed in terms of their accuracy, balanced accuracy, ROC AUC, F1 Score, and time taken for predictions. The results reveal that QDA emerges as the top-performing model, achieving remarkable accuracy and balanced accuracy of 93%, along with an F1 Score of 93%. Extra Trees Classifier and Linear Discriminant Analysis also exhibit strong performance with high accuracy and balanced accuracy scores. The SGD Classifier, Bagging Classifier, and Perceptron yield competitive results as well. However, the AdaBoost Classifier falls short in terms of accuracy and F1 Score, indicating challenges in plant leaf identification. The Random Forest Classifier, while achieving an accuracy of 87%, shows slightly lower balanced accuracy and F1 Score.**

Index Terms- **Plant leaf identification, Wiener Filter, Extra Trees classifier, Bagging classifier, Balanced accuracy.**

I. Introduction

In addition to humans, plants are also important for other living creatures. They play a significant role in maintaining the world's climate and biodiversity. They can transform the light energy that comes from the sun into food for humans and other living things [1]. Unlike plants, animals cannot produce their own food. They rely on vegetation to supply them with the energy they need to survive. Plants also provide all the oxygen that organisms need. More coal and gas used by humans are extracted from the plants that lived hundreds of years ago. Unfortunately, people are destroying these natural environments, which will lead to the emergence of different plant types and the yearly death of plants [2].

Various effects of ecological disasters can also be seen in the form of land flooding, desertion, and weather anomalies [3]. These can result in lower survival rates for people and their habitat.

The field of machine learning and computer vision has gained more attention in the recognition of plants. There have been numerous studies on how to classify different kinds of plants. Before the invention of digital cameras and computer systems, people had to thoroughly study the classification of medical plants [4].

In the past, the lack of experience when it comes to the classification of plants has led to fatal errors, which have increased the mortality rate of patients [5]. Using artificial intelligence, machine vision, and digital videos, it has been shown that the classification of plants has improved significantly. This has motivated computer scientists and botanists to improve the systems used for plant classification. Computer vision and image processing are still being studied in various areas since they have numerous practical applications [6].

The plant leaves are regarded as essential features when it comes to performing the classification process. These provide computer models with valuable information about the plant. Furthermore, the textures found on the leaves are also known to play a vital role in determining the classification of the plant.

Due to the increasing importance of plants, various measures have been implemented to safeguard their resources. Understanding the characteristics of plants is very important to protect their populations.

Most of the time, the non-professional scientists are focused on performing plant classification [7]. This process involves identifying the various types of plants. There are around 4 lakhs plant types. These are given with names and recognized by experts.

The field of plant classification is regarded as the most demanding part of the biological and the agriculture industry. It involves identifying new plant species and developing a computerized system for their administration. There are also various requirements that are needed to perform the classification process for the benefit of agriculturists.

Plant recognition is a process that involves identifying all the plants and performing a plunging arrangement based on their similarities. This is beneficial for various applications, such as environmental protection and education.

There are various challenges that occur while performing the plant classification process. To overcome these issues, researchers use a sample image of the plant leaf to help them identify the plant category. This method also eliminates the need for the plant to be identified using the whole body. The goal of this paper is to use leaf recognition to automatically identify plants.

II. Literature Survey

A new technique [8] for classification of plant leaves based on their various invariants. The seven new invariants were developed using an area-oriented approach. The other

Received on 17-10-2023, Revised on 14-11-2023, Accepted on 28-11-2023.

CVR Journal of Science and Technology, Volume 25, December 2023
DOI: 10.32377/cvrjst2505

six were performed using a newer one based on the Geometric distribution of the first two Hu moment invariants.

Authors [9] developed small-scale disease clusters on plant leaves to detect the early signs of plant diseases using ANN. They used a contrast enhancement method before implementing the model. Later, they categorized the collected data into the various features of the model. The researchers then used a wrapper-based approach to select the best features of the model. The ANN was able to classify the collected data into two categories: normal and abnormal. It was developed on low-end smartphones for farmers.

The researchers [10] developed a diagnosis system that allows a computer-aided study of the various leaves of medicinal plants. It was able to classify the performance of different types of plants by distinguishing their texture features. The system was then used to extract the necessary features for five classes of leaves.

In 2008, authors [11] proposed a variety of classification models that were made using LBP operator and filters, including global and local features. The local attributes of the images were then obtained using LBP. They [12] presented a method that allows the identification of plant species using the images of occluded leaves and a dataset of complete leaves. They then used the b-spline curve as a 2D point representation of the data.

Yang [13] presented a novel method of identifying plant leaves by incorporating the shape and texture characteristics. The plant leaf classification framework utilized the MTD technique to study the plant leaves' shape information, and the LBP-HF extraction procedure was used to extract the texture feature. Weighted distance was used to calculate the texture and shape attributes of the images of the plant leaves. The chi-square and L1 distances were then utilized to determine these features.

Authors [14] introduced a new model for plant identification. It was divided into three phases: image gathering, pre-processing, and feature extraction. The latter stage involved removing the irregularities, noise, and irregularities from the collected images. A high-resolution camera was utilized for capturing the images, and various morphological constraints were then extracted from the data.

III. Methodology

A plant's identification can be performed automatically using a computer to learn how to identify the leaves. This method can also be used to determine the species of the plant. The efficiency of different plant identification techniques has been compared with that of molecular biology and cell biology. The flexibility and robustness of photographic sampling leaves can be attributed to the use of digital cameras. The general steps in identifying plant leaves are shown in Figure 1.

A. Dataset

The classification model uses the data collected from the D-leaf dataset. The D-leaf database [15] contains data samples taken from different kinds of tropical plants. It has a collection of over 30 leaf images from each of the 43 species. Figure 3.3 shows the database's sample images.

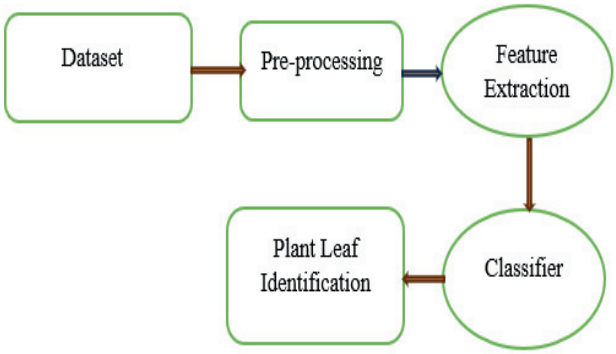

Figure 1. Block diagram of proposed method

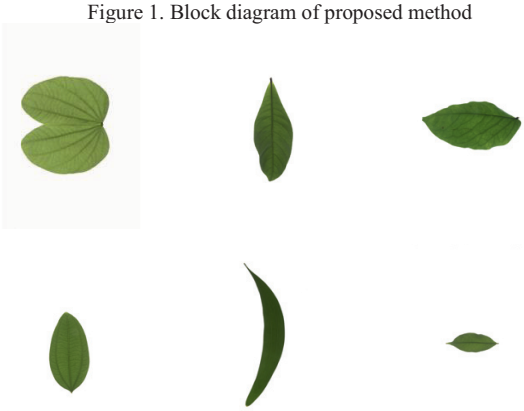

Figure 2. sample images of D-leaf dataset

B. Pre-Processing

The technique known as Wiener filtering [16] considers the image's original characteristics and the noise's statistical model. It can reduce the noise by estimating its original source.

C. Feature extraction

The characteristics of an object or plant that are related to its size, shape, and structure are referred to as morphological features [17]. They are often extracted from images of a plant.

- Counting the number of pixels in the leaf's boundary can determine its total area.
- A leaf's perimeter or outline is the length of its boundary.
- The aspect ratio of a leaf's major and minor axes is shown by comparing their length to the length of its bounding ellipse.
- The circularity of a leaf is computed by comparing its area to that of a circle with a similar perimeter.
- Commonly used to refer to the inverse of circularity, the roundness quotient is calculated as 1/circle.
- The elongation or length of a leaf is determined by comparing its major and minor axis lengths.
- The convex hull area is the area of the smallest polygon that can enclose a leaf.

- The solidity of a leaf is determined by comparing its area to the convex hull's area.
- The Feret's diameter is the maximum distance between a leaf's boundary points.
- The number of linked components in a leaf's image can be identified by the Euler Number, a topological feature. It can be utilized to differentiate complex and simple leaf shapes.
- A leaf skeletonization algorithm can be used to extract the central axis of a leaf. This process is useful in determining the leaf's branching patterns.
- The spread or compactness of a leaf is calculated by comparing its area to its perimeter.
- The leaf's curvature can be measured at various points along its curved surface to get a better understanding of its shape's complexity.
- The symmetry of a leaf can be studied to gain a deeper understanding of its bilateral symmetry, a characteristic present in numerous plant species.
- A leaf's aspect ratio is determined by comparing its width to the height of its smallest boundary.
- The different textures exhibited by a leaf, such as contrast, energy, and entropy, can provide data on its overall structure and appearance.

D. Classifiers

A machine learning classifier is a fundamental component of supervised learning [18]. It helps predict and make decisions based on the input data. These models or algorithms are trained to categorize the data into predefined classes or categories according to the features and patterns they learn.

(i) Extra Tree Classifier: The goal of the Extra Trees Classifier is to provide a more random and robust decision tree structure. It includes features such as random selection and feature splitting. This type of classifier can help improve the robustness and generalization of various data types [19].

(ii) Logistic Regression: This algorithm is a linear classification method that predicts the likelihood of a given outcome based on the logistic function. This is generally applicable to problems where the link between outcomes and features is linear [20].

(iii) Linear Discriminant Analysis: A linear discriminant analysis is a type of classification that seeks to find features that are most likely to separate groups. It is related to PCA and is useful in extracting features and reducing dimensionality [21].

(iv) SGD Classifier: The SGD classifier is a type of linear classification that's trained using the stochastic gradient descent method. It can be used for various applications, such as searching for groups of features [22].

v) Bagging Classifier: A bagging classifier is an ensemble method that combines several base models. It can reduce variance by averaging each model's predictions across different sets of data [23].

(vi) Perceptron: Linear classifier known as the Perceptron is simple and can be used to make decisions on features that are in a linear combination. It is a widely used model for machine learning [24].

(vii) AdaBoost Classifier: It is a framework that combines various weak classifiers to form a powerful one. It aims to improve accuracy by focusing on examples that have been misclassified [25].

(viii) Quadratic Discriminant Analysis (QDA): A QDA is a method for classifying data points that considers the various characteristics of each class's covariance matrix. The algorithm uses Bayes' Theorem to classify the data points. Although a QDA is useful for identifying complex decision boundaries, it is not ideal for handling large sets of features [26].

IV. Results

Table I shows the performance of different machine learning models when it comes to identifying plant leaves. The explanation for each column is provided below.

The column named model highlights the different kinds of machine learning approaches utilized to identify plant leaves.

The percentage of correctly classified plant leaves is referred to as accuracy, and it is a standard metric used in classification.

TABLE I.
Classifier's Performance on D-Datasets

Model	Accuracy (%)	Balanced Accuracy (%)	ROC AUC	F1 Score (%)	Time Taken (sec.)
Quadratic Discriminant Analysis	0.93	0.93	None	0.93	0.04
Extra Trees Classifier	0.88	0.88	None	0.88	0.28
Random Forest Classifier	0.87	0.86	None	0.86	0.70
Linear Discriminant Analysis	0.84	0.84	None	0.83	0.05
SGD Classifier	0.84	0.83	None	0.83	0.15
Bagging Classifier	0.81	0.81	None	0.81	0.33
Perceptron	0.77	0.77	None	0.77	0.06
AdaBoost Classifier	0.11	0.09	None	0.03	0.40
Support Vector Machine	0.82	0.81	None	0.81	0.13
K-Nearest Neighbors	0.83	0.82	None	0.82	0.07
Decision Tree	0.79	0.78	None	0.79	0.05
Naïve bayes	0.75	0.75	None	0.75	0.02

CVR Journal of Science and Technology, Volume 25, December 2023
DOI: 10.32377/cvrjst2505

The Balanced Accuracy metric considers the imbalanced classes in the dataset. It is calculated by averaging the sensitivity and specificity of the classes.

The ROC AUC is a measure of the model's ability to differentiate between classes. It considers the trade-off between the false positive and true positive rates. A value of 1 indicates that the model is perfect at discriminating, while a value of 0.5 indicates random guessing.

The F1 Score, which is a harmonic representation of recall and precision, is useful when trying to balance these two measures in an imbalanced dataset. A higher score indicates that the model has a better chance of achieving a better balance.

The time taken by each model to make predictions is shown in this column. It shows the model's computational efficiency and is useful in large-scale applications.

This classification system has a balanced and high accuracy rate, which shows it can identify plant leaves. Its F1 Score is also impressive at 93%, indicating that it can strike a good balance between recalling and precision. It can do calculations in only 0.04 seconds.

The Extra Trees classifier has an excellent accuracy rate of 88% and a balanced accuracy of 88%. Its F1 Score of 88% indicates that it can strike a balance between recalling and precision, and it can perform predictions in around 0.28 seconds.

Although it has an overall accuracy rate of 87%, the Random Forest classifier has a slightly lower balance of 86. Its F1 score of 86% indicates that it can manage between recalling and precision while still being able to perform accurate predictions.

This linear discriminant analysis can provide an accuracy of 84% and a balanced accuracy of 84%. Its F1 score of 83% indicates that it can maintain a good balance between recalling and precision. It is very fast, taking only 0.05 seconds.

The SGD Classifier is comparable to a linear discriminant analysis in terms of its accuracy and balanced accuracy. It has an F1 score of 83%, and it takes around 0.15 seconds to complete.

The Bagging Classifier can achieve an accuracy of 81% and a balanced accuracy of 81%. Its F1 score of 81% indicates that it can maintain a good balance between recalling and precision. It takes around 0.33 seconds to complete predictions.

The Perceptron can provide an F1 score of 77% and a balanced accuracy of 77%. This implies that it can maintain a balance between recalling and precision while still being efficient. It only took around 0.06 seconds to perform its tasks.

The Adaboost classifier has a balanced accuracy of 9%) and a lower accuracy of 11.1%. But its F1 score of 3% indicates that it has a hard time identifying plant leaves. Its prediction rate of 0.40 seconds is slower than other models.

The Support Vector Machine (SVM) in the provided table exhibits a respectable performance with an accuracy of 82%, a balanced accuracy of 81%, and an F1 score of 81%, making it a reliable choice for classification tasks.

The K-Nearest Neighbors (KNN) model demonstrates competitive results, achieving an accuracy of 83%, a balanced accuracy of 82%, and an F1 score of 82%. Its relatively short training time of 0.07 seconds suggests computational efficiency.

The Decision Tree classifier performs adequately, with an accuracy of 79%, a balanced accuracy of 78%, and an F1 score of 79%. Decision Trees are known for their interpretability, making them valuable in certain applications.

Lastly, the Naïve Bayes classifier shows a moderate performance with an accuracy of 75%, a balanced accuracy of 75%, and an F1 score of 75%, coupled with a very short training time of 0.02 seconds, indicating simplicity and efficiency, though the model's assumptions may affect its suitability for diverse datasets.

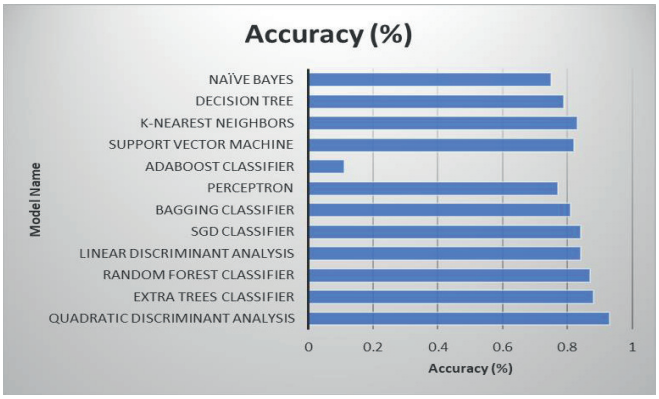

Figure 3. Model vs Accuracy

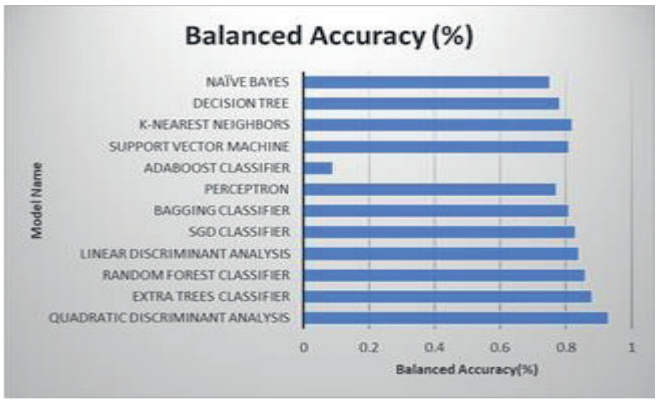

Figure 4. Model vs Balanced Accuracy

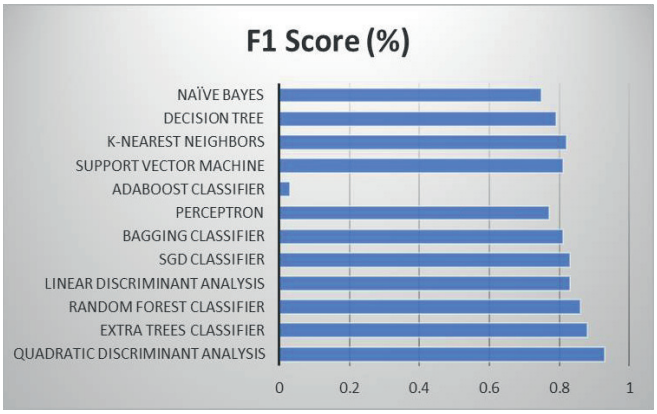

Figure 5. Model vs F1 Score

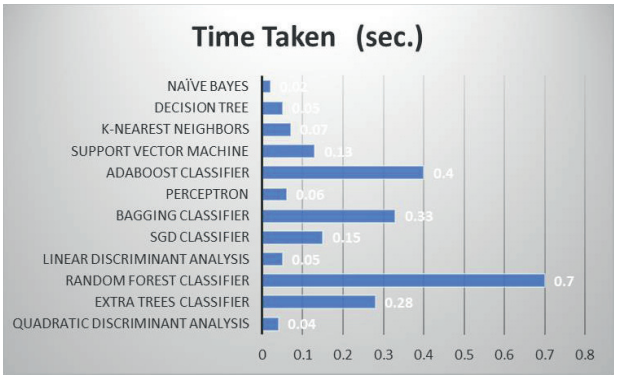

Figure 6. Model vs Time

Figures 3 to 6 indicate the performance measures of various classifiers. The best-performing model when it comes to identifying plant leaves is the Quadratic Discriminator Analysis. It has balanced accuracy and high accuracy. Other models such as the Linear Discriminant and the Extra Trees Classifier provide strong results. But it's crucial to consider the computational efficiency of the model when choosing one for practical applications.

V. Conclusions

This paper provides a comprehensive examination of machine learning models for the challenging task of plant leaf identification. Through a structured approach involving pre-processing, feature extraction, and classification, we shed light on key factors influencing the success of this domain-specific problem. Our study underscores the critical role of the chosen classification model. Notably, Quadratic Discriminant Analysis (QDA) emerged as a standout performer, achieving remarkable accuracy, balanced accuracy, and F1 Score of 93%. Extra Trees Classifier and Linear Discriminant Analysis also demonstrated robust capabilities, making them attractive choices for plant leaf identification tasks.

However, we observed certain challenges associated with specific models. The AdaBoost Classifier struggled to correctly identify plant leaves, resulting in lower accuracy and F1 Score, while the Random Forest Classifier, although delivering an accuracy of 87%, exhibited comparatively lower balanced accuracy and F1 Score.

In summary, this research contributes to the understanding of effective methodologies for plant leaf identification and underscores the adaptability of these techniques to diverse image classification applications. This work will serve as a valuable reference for future endeavors in the realm of computer vision and machine learning.

References

[1] M. Kumar, S. Gupta, X. -Z. Gao and A. Singh, "Plant Species Recognition Using Morphological Features and Adaptive Boosting Methodology," IEEE Access, vol. 7, pp. 163912-163918, 2019.

[2] J. Huixian, "The Analysis of Plants Image Recognition Based on Deep Learning and Artificial Neural Network," IEEE Access, vol. 8, pp. 68828-68841, 2020.

[3] Bhanuprakash Dudi & Dr. V. Rajesh (2023) A computer aided plant leaf classification based on optimal feature selection and enhanced recurrent neural network, Journal of Experimental & Theoretical Artificial Intelligence, 35:7, 1001-1035.

[4] J. Yang et al., "Excitation Wavelength Analysis of Laser-Induced Fluorescence LiDAR for Identifying Plant Species," IEEE Geoscience and Remote Sensing Letters, vol. 13, no. 7, pp. 977-981, July 2016.

[5] L. Li, S. Zhang and B. Wang, "Plant Disease Detection and Classification by Deep Learning—A Review," IEEE Access, vol. 9, pp. 56683-56698, 2021.

[6] B. Liu, C. Tan, S. Li, J. He and H. Wang, "A Data Augmentation Method Based on Generative Adversarial Networks for Grape Leaf Disease Identification," IEEE Access, vol. 8, pp. 102188-102198, 2020.

[7] Y. Wu, X. Feng and G. Chen, "Plant Leaf Diseases Fine-Grained Categorization Using Convolutional Neural Networks," IEEE Access, vol. 10, pp. 41087-41096, 2022.

[8] Mohamed Ben Haj Rhouma, Joviša Žunić, Mohammed Chachan Younis, "Moment invariants for multi-component shapes with applications to leaf classification", Computers and Electronics in Agriculture, vol. 142, pp. 326-337, November 2017.

[9] N. Pham, L. V. Tran and S. V. T. Dao, "Early Disease Classification of Mango Leaves Using Feed-Forward Neural Network and Hybrid Metaheuristic Feature Selection," IEEE Access, vol. 8, pp. 189960-189973, 2020.

[10] Diksha Puri, Abhinav Kumar, Jitendra Virmani & Kriti "Classification of leaves of medicinal plants using laws' texture features," International Journal of Information Technology, 2019.

[11] S. Sladojevic, Marko Arsenovic, Andras Anderla, D. Culibrk, Darko Stefanovic "Deep Neural Networks Based Recognition of Plant Diseases by Leaf Image Classification," Computational Intelligence and Neuroscience, Vol. 2016, 2016.

[12] A. Chaudhury and J. L. Barron, "Plant Species Identification from Occluded Leaf Images," IEEE/ACM Transactions on Computational Biology and Bioinformatics, vol. 17, no. 3, pp. 1042-1055, 1 May-June 2020.

[13] Chengzhuan Yang, "Plant leaf recognition by integrating shape and texture features," Pattern Recognition, Vol. 112, April 2021.

[14] Skanda H N, Smitha S Karanth, Suvijith S, Swathi K S, "Plant Identification Methodologies using Machine Learning Algorithms," International Journal of Engineering Research & Technology (IJERT), Vol. 8 Issue 03, March-2019.

[15] Dudi, B., Rajesh, V. Optimized threshold-based convolutional neural network for plant leaf classification: a challenge towards untrained data. J Comb Optim 43, 312–349 (2022).

[16] Dogariu L-M, Benesty J, Paleologu C, Ciochină S. An Insightful Overview of the Wiener Filter for System Identification. Applied Sciences. 2021; 11(17):7774.

[17] Hirata NST, Papakostas GA. On Machine-Learning Morphological Image Operators. Mathematics. 2021; 9(16):1854.

[18] Cherian, I.., Agnihotri, A.., Katkoori, A. K.., & Prasad, V. . (2023). Machine Learning for Early Detection of Alzheimer's Disease from Brain MRI. International Journal of Intelligent Systems and Applications in Engineering, 11(7s), 36–43.

[19] Geurts, P., Ernst, D. & Wehenkel, L. Extremely randomized trees. Mach Learn 63, 3–42 (2006).

[20] Alzen, J.L., Langdon, L.S. & Otero, V.K. A logistic regression investigation of the relationship between the Learning Assistant model and failure rates in introductory STEM courses. IJ STEM Ed 5, 56 (2018).

[21] Adebiyi MO, Arowolo MO, Mshelia MD, Olugbara OO. A Linear Discriminant Analysis and Classification Model for Breast Cancer Diagnosis. Applied Sciences. 2022; 12(22):11455.
[22] Kabir, Fasihul, et al. "Bangla text document categorization using stochastic gradient descent (sgd) classifier." 2015 International Conference on Cognitive Computing and Information Processing (CCIP). IEEE, 2015.
[23] Sreng S, Maneerat N, Hamamoto K, Panjaphongse R. Automated Diabetic Retinopathy Screening System Using Hybrid Simulated Annealing and Ensemble Bagging Classifier. Applied Sciences. 2018; 8(7):1198.
[24] Morariu, Daniel, Radu Crețulescu, and Macarie Breazu. "The weka multilayer perceptron classifier." International Journal of Advanced Statistics and IT&C for Economics and Life Sciences 7.1 (2017).
[25] Zhang, Yanqiu, et al. "Research and application of AdaBoost algorithm based on SVM." 2019 IEEE 8th joint international information technology and artificial intelligence conference (ITAIC). IEEE, 2019.
[26] Ghojogh, Benyamin, and Mark Crowley. "Linear and quadratic discriminant analysis: Tutorial." arXiv preprint arXiv:1906.02590 (2019).

E-ISSN 2581 – 7957
P-ISSN 2277 – 3916

CVR Journal of Science and Technology, Volume 25, December 2023
DOI: 10.32377/cvrjst2506

Low Power MIPS-RISC Processor: A Survey

V.Priyadarshini[1], M. Kamaraju[2], U.V. RatnaKumari[3]
[1]Ph.D scholar, JNTUK, Kakinada & Asst. Professor, SR Gudlavalleru Engg. College/ ECE Department. A.P India
Email: darshiniv708@gmail.com
[2]Professor & Mentor (AS&A), SR Gudlavalleru Engg. College/ECE Department, A.P., India
Email: profmkr@gmail.com
[3]Professor of ECE & Vice Principal, UCEK, JNTUK, Kakinada, A.P. India
Email: vinayratna74@gmail.com

Abstract: **This paper describes how low power strategies were used in the design and implementation of low power RISC processors. With the growing demand for energy- efficient computing devices, reduced power usage is now a crucial design factor. The paper provides a detailed analysis of the many low power strategies that can be implemented to lower RISC Processors power consumption. Clock gating, power gating, dynamic voltage and frequency scaling, and instruction set architectural optimizations are a few of these methods. The paper also discusses the impact of these techniques on CPU performance. These techniques introduce the design and implementation of a low-power RISC processor. The results of the experiments demonstrate that the suggested strategies are capable of reducing power usage by up to 50% without adversely compromising processor performance. This paper demonstrates the feasibility of designing low power RISC processors using low power techniques, making them suitable for use in portable and battery-operated devices.**

Index Terms: **MIPS, RISC, Low Power, Clock Gating, Xilinx.**

I. INTRODUCTION

This paper aims to discuss several design methodologies of RISC processor design and to give an overview of low power VLSI techniques that have been employed in the various components of the complete architecture of a processor.

The processor is a crucial component of any device and can significantly affect the battery life. Processors that consume more power will drain the battery life faster than those that consume less power. The battery life of a device is heavily dependent on the type of the processor used. The processors with low power consumption are generally the most battery-friendly. Therefore, choosing a processor that strikes the right balance between performance and power consumption is essential to achieving the desired battery life for a particular device.

Researchers are increasingly calling for surveys and studies to be conducted on low-power processor design with low-power techniques. The main goals of this survey are to identify the most effective low-power design approaches and methodologies, as well as to assess the performance and power consumption of various CPU designs. Based on the results of this survey, the researchers can choose an appropriate method for low-power processor design. This method is essential for advancing processor design and guaranteeing that upcoming gadgets use as little energy as feasible.

The data path is one of the key elements that significantly affect power usage. The power consumption has significantly grown recently since the integrated circuit being built was made to handle heavy computations where data pathways are crucial. As a result of the increased power usage, cooling circuitry will be utilized, which takes up more space. Therefore, a variety of approaches must be employed to lessen the consequences of power dissipation. The circuit is stated to have higher efficiency if the power dissipation is lower. The CMOS logic family is chosen above others due to its low power consumption, which is a straightforward analogue for the aforementioned statement. The consumption of CMOS power can be decreased by introducing a new technique. In this paper, an innovative method for lowering CPU power usage is presented.

The major element of a microprocessor that uses more power is the ALU. Therefore, novel strategies to lessen power dissipation are proposed. There are numerous logic styles available for ALU design. In essence, CMOS logic style (static) can result in lower static power usage. The ALU performs mathematical operations such as addition, subtraction, inversion, shifting, etc., as well as logical operations such as AND, OR, NAND, etc.

The circuits developed with CMOS technology [1], are more power efficient than those developed with other technologies. The power consumption of CMOS technology is superior to that of other technologies.

A CMOS component consumes power only when it switches from one state to another (switching activity). The higher the switching activity, the greater the power consumption.

As predicted by Gordon Moore, co-founder of Intel, transistors getting incorporated into a silicon wafer doubled approximately every 18 months until today. A reduction in the size of transistors results in continuous growth of the semiconductor industry. By improving the performance of the devices, it is transforming the technological world. Typically, a circuit operating at 100 -200 MHz will consume between 15-30 watts of power, and if it operates at 500 MHz, it will consume about 300 watts.

The circuit's operating speed is determined by frequency. Power consumption and frequency requirements are higher for devices that operate at fast speeds. It will become more expensive to cool and pack because of the heat caused by excessive power consumption, which will also degrade the system's performance.

Since 1965, Moore's law has been the driving force behind the fabrication of integrated circuits; however, with the

Received on 31-03-2023, Revised on 03-10-2023, Accepted on 18-11-2023.

CVR Journal of Science and Technology, Volume 25, December 2023
DOI: 10.32377/cvrjst2506

advent of 10 nm technology, the transistor size and atomic size were getting closer, making it difficult to maintain Moore's law, as depicted in figure 1. Power dissipation problems were raised as a result of device scaling. There is a need for alternatives to CMOS technology for the creation of Logic devices in order to address power issues.

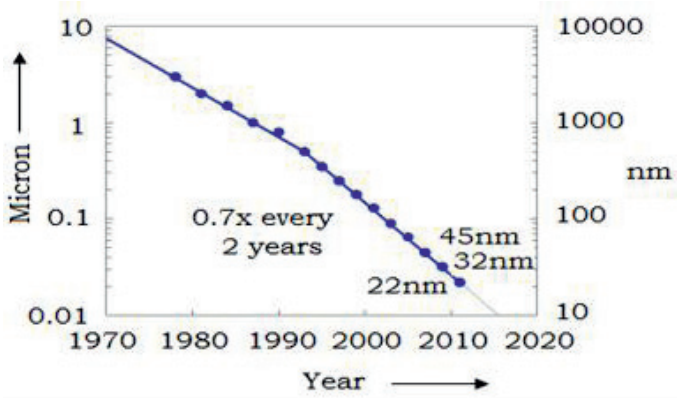

Figure 1. Transistor dimensions scale to improve performance, reduce power and reduce cost per transistor.

High-frequency integrated circuits have been made feasible by the advent of CMOS technology and the ability to fit millions of transistors onto a single sheet of wafer. Additionally, it has decreased the gate latency, increased transistor density, and decreased energy consumption per transistor. According to technical reports, each circuit generation saw a reduction in delay and voltage usage by a factor of 30 percent, a reduction in transistor threshold voltage of 15%, and a doubling of the transistor density on the chip every two years. Despite these benefits, power consumption becomes a problem due to the strong correlation between frequency and dynamic power consumption, which results in a 15% increase in battery's power consumption and 35% percent in overall power consumption.

The size of the devices has been reduced due to technological developments, and now a whole system may be integrated on a single layer of silicon. As a result of their small size and ability to be used anywhere, portable gadgets were in popular demand. However, because they were battery-operated, an increase in power consumption hampered their development. The working frequency of integrated circuits in desktops and servers is being lowered due to overheating, which is reducing chip performance. Power usage has been negatively impacted by the development of portable devices. The frequency of the circuit is also impacted because of the direct relationship between power consumption and frequency of operation. The tremendous need for the creation of portable devices with high computational capability and low battery consumption necessitates power consumption reduction. A sizable amount of the total power consumption is attributed to the data route and clock signal. One of the most important factors in the development of integrated circuits, particularly CPU design, has emerged as power consumption.

II. Motivation

Transistor switching speed has greatly increased in recent years. Despite these benefits, there were several drawbacks as well, including high power consumption and energy waste.

These drawbacks will grow more significant in the future, necessitating the development of further cooling solutions to lower chip package overheating. The transistor density in an integrated circuit has significantly increased, regardless of its size or the application for which it is being created, which results in power consumption of the order of thousands of watts. Systems are overheating and performing worse as a result. Therefore, there is a great need for novel methods that can reduce the system's overall temperature and power dissipation.

The size of the computer system has gradually shrunk from that of a room to a hand-sized device as a result of technical breakthroughs, supporting portability. Power dissipation is one of the performance aspects of these portable gadgets, which is why portability necessitates other features like charged or battery-operated devices.

Data paths are crucial to the operation of processors and power consumption in integrated circuits. There should be some new approaches to lower the power consumption of the data path because it will be higher if the processor is being used for high computational applications. Another criterion for the performance of portable devices is less space. It takes up additional space if cooling circuitry is added to minimize heating and power consumption. New methods that can lower power consumption are therefore needed.

III. Literature Survey

A. Power Management Strategies

The design of a system's flow is composed of several levels of abstraction. The design of a system must be optimized at every stage of the design process in order to run with low power consumption. Power saving can be carried out into any design at three different levels: System level, Logical level, and Technology level. Figure 2 depicts the overall design flow of a system in a bottom-up organization, originating at the lowest abstraction level and working its way up to the highest level.

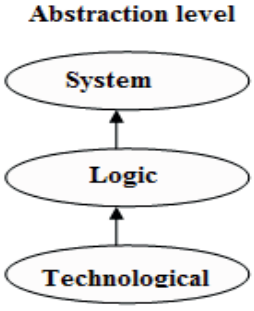

Figure 2. General design flow

Packaging and process technologies are addressed in low power technical level design. This includes:

i) Putting into practice a Silicon on Insulator (SOI) process development with partially or entirely depleted wells to minimize chip and package capacitances. Although this method is incredibly expensive, it has advanced at its own rate since it is so successful. ii) Reducing the supply voltage also reduces power consumption, but it demands new IC fabrication techniques, support circuits for low-voltage operation, such as level converters and DC/DC converters, as well as considerations for signal-to-noise.

Low power logic level [2] design is the level in the general design flow between technologically relevant issues and the system level. This level includes problems with state machines, clock gating, encoding, etc. The fundamental strategy in logic level optimization is reducing switching actions. The methods utilized in logic level design have a significant effect on a system's performance and power usage. Reducing power consumption through effective design techniques is relatively very less expensive than other alternatives, so that's the reason they are frequently adopted.

The system is developed using potential heterogeneous resources individually (electronic, optical, etc.) and will be coupled in a low power system level architecture. Connecting resources for proper functionality in an effective way is the focus of system level design. The chip can be a system if its individual parts are planned and optimized as distinct resources. Partitioning, memory organization, and power management are typical examples at these levels. Depending on the application, several static and dynamic power management approaches can result in significant power savings.

B. Dynamic Power Management

Techniques for reducing power [3] can be divided into two groups: static and dynamic. Static approaches can be used at design time and dynamic techniques during run time. Dynamic Power Management (DPM) [4] [5] [6] [7] refers to the technique of optimizing power consumption in electronic devices by dynamically adjusting the power consumption based on the current workload or usage pattern.DPM is commonly used in batteries, mobile devices and Computer systems to maximize battery life and reduce heat dissipation. In DPM,the system dynamically adjusts the clock frequency,voltage,and other parameters of a processor to minimize power consumption during periods of low activity. When workload or demand increase, DPM boosts performance by increasing frequency and voltage to ensure that the system meets user demands.DPM can be implemented at different levels of the system, including the processor, peripherals, memory and storage. The benefits of DPM include reduced energy consumption, extended battery life and reduced thermal stress, which can prolong the lifespan of components. Additionally, DPM can reduce the system noise, increase performance and decrease the cost of electronic devices by reducing the requirements for cooling and power supplies.

C. Referred Papers:Literature

Aaron P. Hurst [8] developed an approach called Observability Don't Care (ODCs), was used to add clock gating conditions into the design. This paradigm consists of either single-bit registers or single-output combinational logic nodes. This method results in a 7% reduction in the size of the logic network and a 14.5% reduction in dynamic power usage. The disadvantage of this approach is that it is difficult to downsize a large logic network utilizing ODCs.

RananFraer, et al. [9] suggested clock gating analysis, which extracts local or global gating conditions of the state elements that are gated in advance. In order to create a strong gating mechanism for state elements that are not or are gated improperly, certain conditions must be met [10]. Now, all of the state elements have the right propagation of gating conditions. For enabling the state elements, ODC - Observable Don't Care analysis is conducted. In this ODC method, the output from the clock-gated current cycle is an unobservable state. One of the two ways to ODC analysis is the STC approach. This technique allowed for power savings on microprocessor design of up to 28%. ODC and STC analysis have the following drawbacks: (i) they are not beneficial in the designers' approach since they require extra utilities for filtering and sorting; (ii) they must be included into the design cycle.

Macii.E et al. [11] showed leakage and dynamic power reductions might be obtained by combining clock gating (CG) with power-gating (PG). With this method, the same control signal is used to regulate both clock gating and power gating. This strategy results in a 20% reduction in leakage. This technique has two drawbacks: (i) not all circuits may be compatible with it, and (ii) in actual use, the temporal behaviors of the two signals differ.

Rani Bhutada et al. [12] proposed Automated Clock Gating [CG] method. In this case, Automated Clock Gating is implemented directly at the gate level in HDL coding. At different hierarchical levels, the fundamental Register-Based Clock Gating and Complex Clock Gating can be used. The findings indicate a remarkable power loss of roughly 28%.

Hai Li et al. [13] and Brooks D et al. suggested a Deterministic Approach and Value Based Clock Gating respectively. Modern pipeline stages are subjected to Deterministic Clock Gating (DCG). The most important finding is that, for a given cycle, a block's consumption is deterministically known a few cycles in advance for a modern pipeline. Applying DCG results in a 19.9% reduction in CPU power on average without sacrificing performance. This method makes the design verification process more difficult. It is challenging to lower the power using this strategy, especially in SoC designs.

Xiaotao Chang et al. [14] proposed a technique known as programmable clock gating, sometimes termed Intellectual Property (IP) level clock gating. The user can write to activate or disable the IP core clock by changing the flag bits in the control register. The user merely needs to set the control register to 0 to stop the clock when the IP core is not required. When the IP is required, users set the control register to 1, at which moment the clock is activated. The following problems with PCG: i) calls for software control ii) Accurate and efficient user configuration is necessary. System failures or high IP power consumption may be caused by incorrect user settings.

Hans M. et al. [15] suggested a Transparent Clock Gating technique [TCG]. Latches are transparent in this suggested technique. The idea of data partitioning is the basis of TCG. This method allows for a 30% reduction in dynamic power.

Yan Zhang et al. [16] discussed a clock gating approach for optimizing FPGA power. The control enable signal, which is used to turn on or off the clock for unnecessary modules, is received by this multiplexer.

Pi Zhou Ye et al. [17] and Piguet C [18] suggested RISC CPU hardware design core. The PIC 16C6X can use this basic instruction set. 8-bit RISC CPUs are created via a top-down design process. This CPU performs more efficiently than the CISC architecture. This core's shortcomings are that it needs more logic components. In order to lower the power consumption of the CPU core, the chip's frequency is low, low power techniques are not used, and there are fewer on-chip peripherals.

Nalan Erdas et al. [19] used Sea-of-Gates for the development of the 8- bit microcontroller. During the design stage, the logical design and system blocks are implemented at the gate level. The available clock systems are taken into account, and the architecture employs a buffered clock distribution tree. This design has two drawbacks: (i) it operates at a low frequency, and (ii) it uses more power.

Julio C. B. Mattos et al. [20] proposed a stack-based microcontroller. In this manner, a Stack code that uses less bits is required to encode one instruction. In comparison to CISC code, this code is smaller. There is a 31.46% reduction in power consumption possible. This controller's shortcomings include: i) executing fewer instructions ii) processing slowly iii) necessitating more program memory access and iv) generating greater heat.

Dilip Kumar et al. [21] specified a 5-stage MIPS pipelining to determine the delay that is caused by longer paths by employing different processing technologies. The fundamental idea is to shorten the critical path by improving hardware efficiency within the circuit, which leads to an increase in performance. To do this, the pipelines are set up so that high frequency clocks are required for pipelining [7]. Pipelining is the technique of breaking down a logic block into n smaller blocks and inserting latches in between them. This method executes several instructions concurrently. Depending on the processor, the pipeline may have fewer or more phases. Figure 3 depicts the Pipeline Technique's architecture. Multiple instructions are executed concurrently, which reduces power and delay, however, area is impacted.

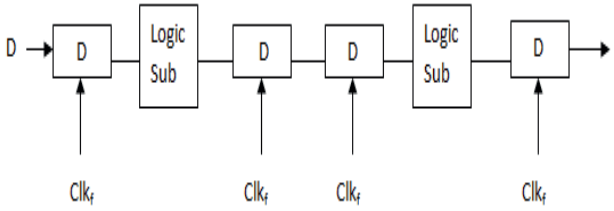

Figure 3. Implementation of Pipelining Technique

V.Prasanth, et al. [22] presented a 28nm, five-stage pipelined MIPS 32-bit CPU. Here, stage registers that toggle flip-flops in the design reduce switching activity between distinct stages. The Harvard architecture processor's speed and performance are improved in this research, which reduces the device's power consumption. In this paper, an innovative RTL clock gating mechanism is used to minimize dynamic power.

G. Jhansi [23] proposed that the power dissipation be taken as a major parameter to consider. Here, a 64-bit RISC CPU is used, and efficiency with great performance is prioritized as a key job. A Latch free based clock gating low power technology [24] is employed to reduce power dissipation.

Clock gating without a latch is depicted in figure 2.2. Basic gates like AND and OR gates can be used to implement this strategy. As long as the clock enable is turned on, the clock will here be triggered to the flip-flop. Clocks are turned off when the clock enable signal stops working [25].

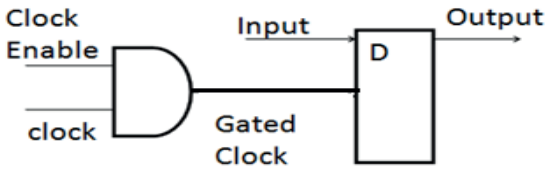

Figure 4. AND gate based Latch free clock gating.

Omkar, et al. [26] proposed the usage of a single precision floating point multiplier at the ALU which is in the execution block. A 32-bit RISC processor is composed of blocks like the instruction fetch, instruction decode, execute block, and write back unit. In this research, a specific power management strategy is applied to reduce static power. For low power applications, it's critical to reduce switching activity because CMOS devices only lose power when switching. One of the best methods for reducing switching activity is power management technique. This power-down method places the circuits in a sleep mode while not in use. It may be utilized at a number of hierarchical levels, including the level of a module, a chip, and even the printed circuit board.

Harpreet Kaur, et al. [27] proposed a MIPS processor with pipelining of five stage architecture that lowers the dynamic power consumption and raises the number of instructions per second for execution. By including NOP instruction, the risks that are introduced by pipelining are also removed. Given that this NOP instruction produces nothing beneficial, all of the power is wasted. As a result, this processor uses its dual write port register file to provide two right-back operations, which lessens the need for NOP in pipelining and results in further power savings. By utilizing a hazard detecting unit in the pipeline to eliminate unnecessary transitions, stalls are decreased.

P. Indira, et al. [28] proposed a MIPS 6 stage pipelined 64-bit RISC processor [29] for hazard free structure by employing a joint effort from the prefetch unit, forward unit, branch and jump prediction unit, and hazard unit. In this study, clock power is reduced using a Dual Edge Triggering Flip-Flop (DETFF) [30]. The Dual Edge Triggered Flip-flop is depicted in Figure 5.

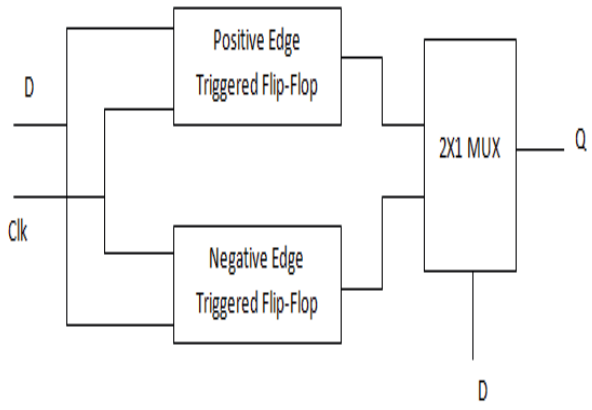

Figure 5: Dual Edge Triggered Flip-flop (DETFF)

Sneha Mangalwedhe, et al. [31] proposed the 5-stage pipelined 32 bit RISC processor [32] has as its primary goals to boost efficiency and decrease power dissipation. The multiplexer-based clock gating approach is used to reduce power dissipation. To improve the efficiency of pipelining a Hazard Detection unit is also included.

Hasan ErdemYantır et al. put [33] a hybrid approximation computing technique for association in memory processors. In order to optimize energy savings within certain rough bounds, this study focused on numerous distributed domains including image processing, machine learning, machine vision, and digital signal processing.

In addition, Duseok Kang et al. presented in [34] A novel method for scheduling deep learning applications on heterogeneous processors in an embedded device. This paper offered a scheduling method based on evolutionary algorithms for deploying deep learning applications on heterogeneous CPUs.

After that Ferran Reverter added [35] a three wire connected resistive sensor interface circuit based on a microcontroller. This article describes a prototype that was created using a commercial microcontroller to measure the resistances of a thermal sensor at various resistance values.

Additionally Cheng-Yao Hong et al. [36] proposed a variation resilient microprocessor with a two level timing error detection and correction system, in which the system was implemented on an ARM cortex- M10 microprocessor with a primary focus on energy savings through operation at lower supply voltages.

For embedded systems, Hyeonguk Jang et al. proposed [37] Integrating Memory Management units (MMU) inside networks on chips. A network on chip that supports multiprocessing and dual RISC-V processors is offered. It provides MMU capabilities without altering the processor design.

A concept for an 8 bit parallel RSFQ microprocessor was provided [38] in a further contribution from Pei- Yao Qu et al. This concept uses fast single flux quantum (RSFQ) circuit technology and a computer to process 8 bits every clock cycle. I also read a work by Swapnil Sayan Saha et al. [39] titled "Machine learning (ML) for microcontroller-class hardware." This emphasizes the prerequisites for enabling on-board machine learning for devices of the microcontroller class.

In addition, Vikkitharan Gnanasambandapillai et al. proposed [40] finding effective parallel instructions for ASIPs, In order to enhance the performance of complex applications. This fully automated approach created to locate parallel instructions for ASIPs also creates FINDER (Flexible Instructions Extensions Instructions), which enhances the performance of huge applications.

Mohammad Attari et al. contributed the work entitled an Application Specific Vector for Efficient Massive Multiple Input and Multiple Output (MIMO) processing [41]. This article introduces an application-specific instruction set processor (ASIP) with multiple inputs and multiple outputs (MIMO). In which the ASIP chip incorporates a parallel memory subsystem.

Further, Marco Crepaldi et al. contributed [42] an innovative multi one instruction set computer for microcontroller applications. a computer with a single instruction set and multiple execution modes that can only execute simple integer instructions are used. Along with RAM, it also has 8 bit I/O. Not all of the aspects of commercial ISA were targeted. On an FPGA, it has been synthesized.

Atef Ibrahim et al. presented [43] a work entitled Systolic processor core for finite field multiplication and squaring. In which the primary emphasis is on a single processor core that executes multiplication and square root operations simultaneously to conserve hardware resources.

In addition, a work challenging Single Instruction Multiple Data (SIMDS) and Very Long Instruction Word (VLIWS) with a reconfigurable architecture proposed by M. Wijtvliet et al. [44], In these reconfigurable architectures, this enables energy-efficient application-specific VLIW- SIMD processors by separating the control and data paths into separate blocks. It has been likened to CGRAC Coarse Grain Reconfigurable Architectures, VLIW, SIMD, low power microprocessors, and SIMD.

IV. Results

Numerous articles have been studied up to this point, and it is clear from them that a number of the strategies that have been described are being employed on MIPS RISC processors, which may be 32- or 64-bit machines with various pipeline topologies. These concepts use various modeling and synthesis techniques along with different processing technologies, such as 28nm, 40nm, 45nm, 60nm, and 90nm.

Let's compare all the parameter findings from the various ideas as indicated in the table to understand what these various strategies lead to in terms of MIPS development. 1.

CVR Journal of Science and Technology, Volume 25, December 2023
DOI: 10.32377/cvrjst2506

TABLE I.
POWER, DELAY AND FREQUENCY COMPARISON OF A PROCESSOR WITH DIFFERENT TECHNIQUES

S.No	Reference/Author Name	Total Power (W)	Delay (ns)	Frequency (MHz)
1	Ref [22] Dr. Dilip Kumar (Apr 2012)	0.031	6.57	178
2	Ref [28] HarpreetKaur (Mar 2013)	0.34	-	193.8
3	Ref [15] (Feb 2013)	0.829	14.348	179.092
4	Ref [27]Omkar (Jul2016)	0.21	0.562	-
5	Ref [24] G. Jhansi (Oct 2017)	0.177	-	-
6	Ref [32]Sneha Mangalwedha (Nov 2017)	0.363	-	401.881
7	Ref [31]P. Razak Hossai (Feb 2019)	0.023	1.143	420.028
8	Ref [29]P. Indira (Oct 2019)	3.60µ	1	255.88
9	Ref [23] Prasanth, V (Mar 2020)	0.129	11.18	285.583

Power, Delay and frequency comparison of processor with different techniques shown in table I. which compares the parameters of the many MIPS designs that have been suggested. Columns 2, 3, and 4 respectively display power usage, delay, and frequency. Table I shows a power reduction from 0.829W to 0.031W.Maximum dynamic power reduction of 90% was obtained for the most recent MIPS CPU.

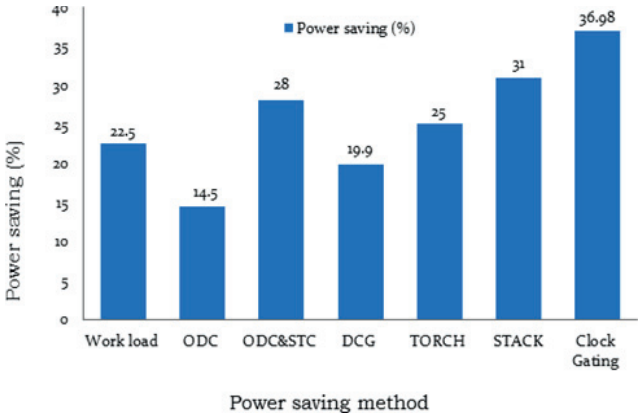

Figure 6. Percentage of Power saving of different MIPS processors using Low Power VLSI Techniques.

The figure 6 shows the percentage of power saving of different MIPS processors using Low power VLSI Techniques. Table II represents a comparison of power consumption with and without clock gating techniques. There is clear evidence from the table that using clock gating technique, there is a greatt possible reduction in the power consumption.

TABLE II.
COMPARISION OF POWER VALUES WITH AND WITHOUT CLOCK GATING TECHNIQUE

References	Clock Gating Technique	Power(W)	
		Without Clock Gating	With Clock Gating
Ref [32]	Multiplexer based Clock gating	0.463	0.363
Ref [30]	Circuit Partitioning	0.94	0.829
Ref [27]	Power Management unit	0.22	0.21
Ref [29]	Flip Flop based clock gating	0.577	0.34
Ref [31]	Dual Edge Triggered flipflop+Multi Vt	4.611 µ	3.60µ

V. CONCLUSIONS

In conclusion, low power RISC processors with low power techniques have become increasingly important in many applications that require energy-efficient computing, such as mobile devices, Internet of Things (IoT) devices, and wearable devices.

Low power RISC processors use reduced instruction set computing (RISC) architectures that have fewer and simpler instructions, which reduces the number of transistors needed and enables higher clock speeds. Low power techniques, such as Dynamic Voltage and Frequency Scaling (DVFS), clock Gating, and Power Gating, can further reduce power consumption by dynamically adjusting the voltage and frequency of the processor and turning off unused circuit blocks.

These techniques have been successful in reducing the power consumption of processors while maintaining acceptable levels of performance, making them well-suited for energy-constrained applications. Additionally, the development of advanced manufacturing processes, such as FinFET and FDSOI, has enabled the creation of low-power RISC processors with even better performance and power efficiency.

Overall, low power RISC processors with low power techniques are a promising area of research and development for energy-efficient computing and are likely to continue to be important for many years to come.

REFERENCES

1. Srinivas.D, and Malik.S, “A Survey of Optimization Techniques Targeting Low Power VLSI Circuits”, Proc. of 32nd ACM/IEEE Design Automation Conf., 1995, pp. 1-6.
2. Li-Chuan.W, Xiao Jun.W, and Bin.L, “A Survey of Dynamic Power Optimization Techniques”, Proc. of the 3rd IEEE Int’l workshop on System-on-Chip for Real-Time Applications (IWSOC) IEEE, 2003, pp. 48-52.
3. Rajesh.K.G, Irani.S and Sandee.K.S, “Formal Methods for Dynamic Power Management ", Proc. of int’l conf. on Computer Aided Design (ICCAD-2003), 2003, pp. 874 – 881
4. Hans Jacobson, Pradip Bose, Zhigang Hu, Rick Eickemeyer, Lee Eisen and John Griswel, “Stretching the Limits of Clock-Gating Efficiency in Server-Class Processors”, Proc. of the

11th Int'l Symposium on High-Performance Computer Architecture (HPCA- 2005) IEEE, 2005, pp. 238-242.
5. Aaron.P.H., "Automatic Synthesis of Clock Gating Logic with Controlled Netlist Perturbation", Proc. of 45th ACM/IEEE Design Automation conf. 2008 (DAC 2008), 2008, pp. 654 – 657.
6. Ranan.F, Gila.K, and Muhammad.K.M., " A New Paradigm for Synthesis and Propagation of Clock Gating Conditions", Proc. of Design Automation Conference 2008 (DAC2008) IEEE, 2008, pp. 658 – 663.
7. Hamid.M, Vishy.T, Matthew.C, and Kaushik.R, "Ultra Low-Power Clocking Scheme Using Energy Recovery and Clock Gating", IEEE Trans. on Very Large Scale Integration (VLSI) Systems, Vol 17, No. 1, 2009, pp. 33 - 44.
8. Aaron.P.H., "Automatic Synthesis of Clock Gating Logic with Controlled Netlist Perturbation", Proc. of 45th ACM/IEEE Design Automation conf. 2008 (DAC 2008), 2008,pp. 654 – 657.
9. Ranan.F, Gila.K, and Muhammad.K.M., " A New Paradigm for Synthesis and Propagation of Clock Gating Conditions", Proc. of Design Automation Conference 2008(DAC2008) IEEE, 2008, pp. 658 – 663
10. . Hamid.M, Vishy.T, Matthew.C, and Kaushik.R, "Ultra Low-Power Clocking Scheme Using Energy Recovery and Clock Gating", IEEE Trans. on Very Large Scale Integration (VLSI) Systems, Vol 17, No. 1, 2009, pp. 33 - 44.
11. Macii.E, Bolzani.L, Calimera.A, Macii.A and Poncino.M, "Integrating Clock Gating and Power Gating for Combined Dynamic and Leakage Power Optimization in Digital CMOS Circuits", Proc. of 11th Euro micro-Conference on Digital System Design Architectures,Methods and Tools, IEEE, 2008, pp. 298 – 303.
12. Rani Bhutada, and YiannosManoli, "Complex Clock Gating with Integrated Clock Gating Logic Cell", Proc. of Int'l conf. on Design and Technology of Integrated Systems in Nanoscale ERA2007, 2007, pp. 164-169.
13. Hai Li etc., "DCG: Deterministic clock-gating for low-power microprocessor design", IEEE Transactions on Very Large Scale Integration (VLSI) Systems 12(3), April 2004, pp: 245-254.
14. Xiaotao Chang , Mingming Zhang, Ge Zhang1, Zhimin Zhang and Jun Wang, "Adaptive Clock Gating Technique for Low Power IP Core in SoC Design", Proc. of IEEE Int'l symp. on Circuits and Systems (ISCAS 2007), 2007, pp. 2120 – 2123.
15. Hans.M.Jacobson, "Improved Clock-Gating through Transparent Pipelining", Proc. of the 2004 Int'l Symp. on Low Power Electronics and Design (ISLPED 04) ACM, 2004, pp. 26-31.
16. Yan Zhang, Jussi Toivanen, and Aarne.M, "Clock Gating in FPGAs: A Novel and Comparative Evaluation", Proc. of 9th EUROMICRO conf. on Digital System Design: Architecture, methods and Tools (DSD06) IEEE, 2006, pp.584-590.
17. Pizhou Ye and Chaodong Ling, "A RISC CPU IP Core", Proc. of 2nd Int'l Conf. on Anti-counterfeiting, Security and Identification(ASID 2008), 2008, pp. 356 – 359.
18. Piguet.C. "Low power design of 8-b embedded cool-RISC microcontroller cores", IEEE Journal of Solid-State Circuits, Vo.32, No.7, 1997, pp. 1067~1077.
19. Nalan.E., and Mustafa.G.C, "Design of an 8 Bit General Purpose Microcontroller with Sea-of-Gates Design Style ", Proc. Of eleventh Int'l conf. on Microelectronics (ICM1999) IEEE, 2002, pp. 177-180.
20. Júlio.C.B, Mattos, MárcioKreutz, and Luigi Carro, "Low-Power Control Architecture for Embedded Processors", Proc. of the 15th Symp. on Integrated Circuits and Systems Design (SBCCI'02) IEEE, 2002, pp. 221-226.
21. Dr.Dilip Kumar and Kiratpal , "Design of High performance MIPS-32 Pipeline Processor",Conference Paper • April 2012 DOI: 10.13140/RG.2.1.4883.6567.
22. V.Prasanth, V.Sailaja, P.Sunitha, B.Vasantha Lakshmi, "Design and implementation of low power 5 stage Pipelined 32 bits MIPS Processor using 28nm Technology", International Journal of Innovative Technology and Exploring Engineering (IJITEE) March, 20, Volume-8, Issue-4S2,ISSN: 2278-3075, pp.502-507.
23. G.Jhansi, " Design of MIPS based 64-bit RISC Processor", International Journal of Engineering and Advanced Technology (IJEAT), October 2017,Volume-7 ,Issue-1, ISSN: 2249 – 8958,pp.48-51.
24. Agineti. Ashok, and V. Ravi, "ASIC design of MIPSbased RISC processor for high performance"Proc.ofInternational Conference on Nextgen ElectronicTechnologies: Silicon to Software (ICNETS2), March2017, IEEE Proceedings, pp. 263-269.
25. Husainali S. Bhimani,. Hitesh N Patel and AbhishekA. Davda, "Design of 32-bit 3-Stage Pipelined Processorbased on MIPS in Verilog HDL and Implementation onFPGA Virtex7," International Journal of AppliedInformation Systems (IJAIS), May 2016.
26. Omkar A. Shastri, "Floating Point Parallel Processing Multiplier Based RISC (MIPS) Processor", International Journal of Advanced Research in Computer and Communication Engineering, July 2016, Vol. 5, Issue 7,ISO 3297:2007 Certified, ISSN: 2278 – 1021,pp.477-481.
27. Harpreet Kaur, Jaspal Singh, "MIPS Processor With Reduced Dynamic Power", IJCST, Jan - March 2013, Vol. 4, Issue 1, ISSN: 0976-8491 (Online) | ISSN: 2229-4333,pp.559-562.
28. P. Indira, M. Kamaraju, "Design and Implementation of 6-Stage 64-bit MIPS Pipelined Architecture", International Journal of Engineering and Advanced Technology (IJEAT), August 2019,ISSN: 2249 – 8958, Volume-8, Issue-6S2,pp.790-796.
29. Liang Geng, Ji-zhong Shen, Cong-yuan Xu "Power-efficient dual-edge implicit pulse-triggered flip-flop with an embedded clock-gating scheme", Frontiers of InformationTechnology and Electrical Engineering,Vol. 17,Issue 9.ISSN 2095-9184 (print); ISSN 2095-9230 (online) pp .962-972.
30. Razak Hossain, Leszek D. Wronski, and Alexander Albicki, "Low Power Design Using Double Edge Triggered Flip-Flops",Ieee Transactions On Very Large Scale Integration (VlSI) Systems, June 1994,Volume. 2, Issue No. 2, 1063-8210/94,pp-261-265.
31. Sneha Mangalwedha, RoopaKulkarni, S.Y.Kulkarni, "Low Power implementation of 32-bit RISC Processor with pipelining", Proc. of Second International Conference on Microelectronics, Computing & Communication Systems (MCCS),November 2017, springer, pp 307-320.
32. Nishant Kumar & Ekta Aggrawal, "General Purpose Six-Stage Pipelined Processor",International Journal of Scientific & Engineering Research, 2013, Vol. 4, Issue 9, pp.294-297.
33. Hasan Erdem Yantır, Ahmed M. Eltawil , and Fadi J. Kurdahi , "A Hybrid Approximate Computing Approach for Associative In-Memory Processors", IEEE Journal on Emerging and Selected Topics in Circuits and Systems, Vol. 8, No. 4, December 2018, PP- 758- 769.
34. Duseok Kang, Jinwoo Oh, Jongwoo Choi, Youngmin Y and Soonho Ha, "Scheduling of Deep Learning Applications onto Heterogeneous Processors in an Embedded Device",Volume 8, 2020 IEEE Access, PP- 43980- 43991.
35. Ferran Reverter, "A Microcontroller-Based Interface Circuit for Three-Wire Connected Resistive Sensors", IEEE

Transactions on Instrumentation and Measurement, Vol. 71, 2022,PP- 2006704.

36. Cheng-Yao Hong and Tsung-Te Liu, "A Variation-Resilient Microprocessor with a Two-Level Timing Error Detection and Correction System in 28-nm CMOS", IEEE JOURNAL of Solid-State Circuits, Vol. 55, No. 8, August 2020, PP- 2285-2294.
37. Hyeonguk Jang, Kyu Seung Han, Sukho Lee, Jae-Jin Lee and Woojoo Lee, "MMNoC: Embedding Memory Management Units into Network-on-Chip for Lightweight Embedded Systems", VOLUME 7, 2019 IEEE Access, PP- 80011- 80019.
38. Pei-Yao Qu, Guang-Ming Tang, Jia-Hong Yang, Xiao-Chun Ye, Dong-Rui Fan, Zhi-Min Zhang and Ning-Hui Sun, "Design of an 8-bit Bit-Parallel RSFQ Microprocessor", IEEE Transactions on Applied Superconductivity, Vol. 30, No. 7, October 2020, PP- 1302706.
39. S. S. Saha, S. S. Sandha and M. Srivastava, "Machine Learning for Microcontroller-Class Hardware: A Review," in IEEE Sensors Journal, vol. 22, no. 22, pp. 21362-21390, 15 Nov.,2022.
40. Vikkitharan Gnanasambandapillai, Jorgen Peddersen, Roshan Ragel, and Sri Parameswaran, "FINDER: Find Efficient Parallel Instructions for ASIPs to Improve Performance of Large Applications", IEEE Transactions on Computer-Aided Design of Integrated Circuits and Systems, Vol. 39, No. 11, November 2020, PP- 3577- 3588.
41. Mohammad Attari, Lucas Ferreira, Liang Liu, and Steffen Malkowsky, "An Application Specific Vector Processor for Efficient Massive MIMO Processing", IEEE Transactions on Circuits and Systems—I: Regular Papers, Vol. 69, No. 9, September 2022, PP- 3804- 3815
42. Marco Crepaldi, Andrea Merello and Mirco Di Salvo, "A Multi-One Instruction Set Computer for Microcontroller Applications", Volume 9, 2021 IEEE Access, PP- 113454-113474.
43. Atef Ibrahim, "Systolic Processor Core for Finite-Field Multiplication and Squaring in Cryptographic Processors of IoT Edge Devices", IEEE Internet of Things Journal, Vol. 9,No. 2, January 15, 2022, PP- 1354- 1360.
44. M. Wijtvliet, A. Kumar, and H. Corporaal, "Blocks: Challenging SIMDs and VLIWs with a Reconfigurable Architecture", IEEE Transactions on Computer-Aided Design of Integrated Circuits and Systems, Vol. 41, No. 9, September 2022, PP- 2915- 2928.

E-ISSN 2581 – 7957
P-ISSN 2277 – 3916
CVR Journal of Science and Technology, Volume 25, December 2023
DOI: 10.32377/cvrjst2507

Ubiquitous Tracking System: A Mobile and Versatile GPS-GSM Solution for Real-Time Vehicle and Asset Monitoring.

M. Ashok [1] Sura Rupendra [2] Pilli Sashank [3] Satvika Yannam [4]
[1] Sr. Asst. Professor, Department of ECE., CVR College of Engineering, Hyderabad, India
Email: m.ashok@cvr.ac.in
[2]UG Scholar, Department of ECE., CVR College of Engineering, Hyderabad, India
Email: sura.rupendra2002@gmail.com
[3] UG Scholar, Department of ECE., CVR College of Engineering, Hyderabad, India
Email: sashank.pilli@gmail.com
[4] UG Scholar, Department of ECE., CVR College of Engineering, Hyderabad, India
Email: satvikareddy2001@gmail.com

Abstract: **The Universal Tracking System is a cutting-edge technology that utilizes GPS and GSM modules to provide real-time tracking of assets, people, and vehicles. The system is versatile, offering a range of features and applications that cater to various needs, such as location tracking, asset management, and fleet monitoring. The system helps in reducing the chances of things getting lost, stolen, or misplaced by providing accurate and up-to-date location data. It is an affordable, easy-to-use, and reliable solution that can be accessed from anywhere, making it a valuable tool for personal and commercial use. With its wide range of benefits, the Universal Tracking System is an indispensable for anyone who needs to keep track of their assets or loved ones.**

I. Introduction

The GPS technology has become indispensable in our daily lives, so much so that we often use it involuntarily. We like to keep our essential items within our reach most of the time; when they are not mobile, we store them in a safe to keep them safe. However, what would be the scenario for those items that demand continuous monitoring? How can we know the status of an item when it is on the move? The proposed tracking system is designed to perform live tracking of the objects to which it is coupled. It enables us to have continuous monitoring of the item. [1]

In the late 1950s, the military developed the precursor to the current GPS. The Navy was responsible for the first two attempts, and the first satellite-based navigation system was called Transit. It was launched in 1959 and used radio signals and seven low-orbiting polar satellites to determine the locations of the ships. Transit measured distances using the Doppler Effect of radio waves, but it had limited accuracy, was only available in certain areas, and required constant monitoring. In 1964, the Timation system was introduced as the second attempt. It used two space satellites equipped with atomic clocks for more precise two-dimensional positioning.

The organization of rest of the article is as following:
II. Literature Survey
III. System Model
IV. Results and Discussion
V. Conclusion.

II. Literature Survey

Laipac S-911™ Personal Locator: The Laipac S-911™ Personal Locator is a compact device that can track personal safety and assets. It works on a global GSM/GPRS network and can function as an emergency phone with speed dialing for two-way communication. In an emergency, the device can silently call 911 or any other emergency number and reports its location and time stamp using a simulated voice. The device can also send SMS messages to a control center and be monitored in real time over the internet. The small device is 70 x 40 x 20 mm and has a rechargeable lithium-ion battery. An additional map database software is required to track the device in real time over the internet.

Star Finder I: The Automatic Vehicle Location (AVL) system is designed to be compatible with various communication methods, including cell phone modems, digital radios, and satellite modems (ORBCOMM), using CDMA/1X, GSM/SMS, and GPRS. The size of the AVL unit is compact, measuring 15 x 15 x 3.5 cm. The Star Finder AVL software is available to control the AVL system, which can track an unlimited number of vehicles in real-time. This software requires a map database like Microsoft MapPoint to function correctly.

Real Time Bus Track and Location Update System: The public transportation system is crucial to the development of the economy and is an integral part of people's lives. However, this tracking of the systems, monitoring, scheduling, and surveillance services are currently operating manually, which means the information is not easily accessible to the public. To address this issue, the "Real Time Bus Track and Location Update System" project aims at automation of these services by providing real-time tracking of buses. Each bus will have an RFID tag, and RFID readers will be placed at each bus stop. The central regulator of the system is Arduino. The GSM module will send location updates to authorized personnel for continuous monitoring, while GPS is used to track the buses. IoT will provide users

Received on 02-11-2022, Revised on 18-11-2022, Accepted on 30-11-2022.

CVR Journal of Science and Technology, Volume 25, December 2023
DOI: 10.32377/cvrjst2507

with information on bus trackers. Data from RFID readers will be processed using Arduino and sent to the cloud, which will act as an interface between the user and the system.

Location Tracking in GPS using Kalman Filter through SMS: The paper "Location Tracking in GPS using Kalman Filter through SMS," presented at IEEE EUROCON in 2009, explains a system in which 1' pixel depict areas suitable for bus travel, while 0' pixels depict other areas. Since there is always some margin of error and noise when measuring the location of the bus, the observations are revised utilizing a weighted average. This approach places greater weight on the estimations with higher accuracy.

III. System Model

Flowchart:

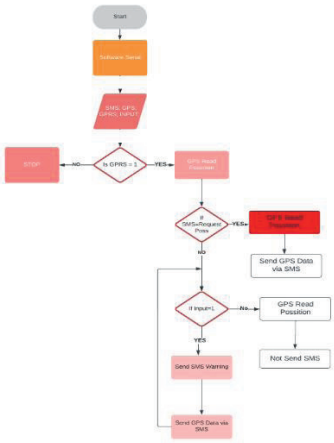

Figure1. Flow chart of universal tracking system

Figure 1 shows the flow of process of the tracking system happening before, after receiving the SMS to the module.

Component specifications:

1. **GY-NEO6MV2 GPS Modem:**
   - Power Supply Range: 3 V to 5 V.
   - Model: GY-GPS6MV2.
   - Ceramic antenna.
   - Antenna Size: 25 x 25 mm.
   - Module Size: 25 x 35 mm.
   - Mounting Hole Diameter: 3 mm.
   - Default Baud Rate: 9600 bps.

2. **Arduino board based on ATmega328P:**
   - A 16MHz crystal.
   - A 10K resistor.
   - Two 22pf capacitors
   - A 10uf capacitor.
   - Runs at clock speeds from 1MHz to 20MHz.
   - 32Kb Flash Memory.
   - 2Kb SRAM (Static Random Access Memory).
   - 1Kb EEPROM (Electrically Erasable Read Only Memory).

3. **SIM 900A GSM Module:**
   - Dual-Band 900/1800 Mhz.
   - GPRS multi-slot class 10/8GPRS station class B
   - Compliant to GSM phase2/2+
   - Dimensions: 24*24*3
   - Weight: 3.4g.
   - Supply voltage range: 5v.

A. GPS module:

A radio navigation system determining accurate latitude and longitude coordinates irrespective of the weather conditions. It works on land, air, and sea. The GPS modules are devices that allow your devices or circuits to receive the data of the GPS. It is a subcategory of satellite communication. The GPS provides different wireless services like navigation, positioning, location, and speed with the help of the dedicated GPS receivers and satellites. [1]

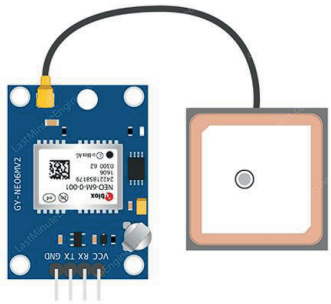

GY-NEO6MV2 GPS MODEM

B. Dual SIM band module:

Global system for mobile communication (GSM) is a standard describing the protocols for the second generation (2G) digital cellular network. It is developed by European Telecommunications standards institute. This module is responsible to communicate the location of the system that must be tracked via SMS. [2]

The GSM module uses standard AT (At Tension) commands to communicate with the host device and provides features such as voice and data communication, SMS (Short Message Service), GPRS (General Packet Radio Service), and GPS (Global Positioning System) functionality. It typically requires a SIM (Subscriber Identity Module) card to operate and can be powered by a battery or external power source.

GSM SIM900A Module

C. Arduino module:

Arduino is an open-source electronics platform that provides an easy and affordable way for people to create interactive projects. It consists of both hardware and software components, including microcontroller board and a programming environment that allows users to write code and upload it to the board. [3]

Arduino board based on ATmega328P

The Arduino board is equipped with input and output pins that can be used to connect to various sensors, actuators, and other electronic components. Users can write code to read input data from sensors, process that data algorithms and output control signal to actuators to perform various tasks.

One of the main advantages of Arduino is its accessibility. It is designed to be user friendly, even for those with little or no electronics experience. The programming language used in Arduino is based on C++, but it has a simplified syntax and a set of libraries that make it easier to use for the beginners. Arduino has a wide range of applications, from building robots and drones. It is also widely used in education as it provides a hands-on way for students to learn about electronics, programming, and engineering. It is overall a versatile and accessible platform that empowers individuals and communities to bring their ideas to life through electronics and programming.

D. System assembly:

GPS Module: The information related to the location (latitude and longitudinal coordinates) of the subject that must be tracked is gathered with the help of the satellite. [1]

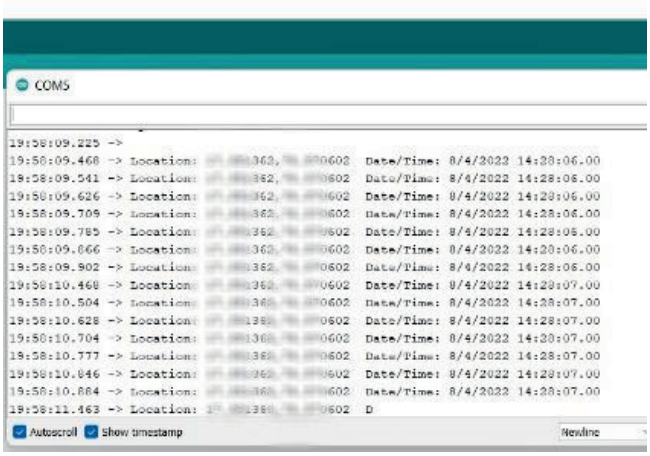

Figure 2. Tracked coordinates by GPS module.

The GPS tracker here is responsible for updating the information related to location, date, and time for about 6 times a second. The output of the GPS functioning is shown as in figure 2.

GSM module: The location of the subject that must be tracked is sent via SMS with the help of GSM module. This module waits for a coded trigger message and sends the programmed SMS. [2]

Some AT commands used for sending and receiving SMS using GSM SIM900A module are:

- To set module in SMS text mode: AT+CMGF = 1
- To send a SMS: AT + CMGS = "<recipient phone number>"

These commands are merely illustrative, and their precise syntax may differ based on the firmware version of your SIM900A module.

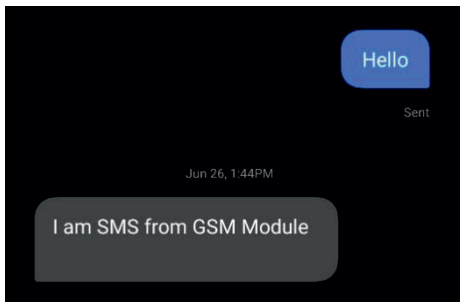

Figure 3. SMS response of GSM module.

Figure 3 shows the response SMS received from the GSM module when a trigger text is sent.

E-ISSN 2581 – 7957
P-ISSN 2277 – 3916

DOI: 10.32377/cvrjst2507

Arduino module: Arduino coordinates the action of the GPS and GSM modules. The system which runs on battery is deployed along with the subject that must be tracked. The GSM module waits for a coded triggered SMS from the user. The SMS when received is then validated by the Arduino module and then Arduino module access the latitude and longitudinal coordinates which is tracked by the GPS module.

The Arduino module validates the trigger SMS and append the latitude and longitudinal coordinates to the link, https://www.google.com/maps/?q= . The link generated after appending the latitude and longitudinal coordinates enables the user to access the location of the system using google maps app or through chrome.

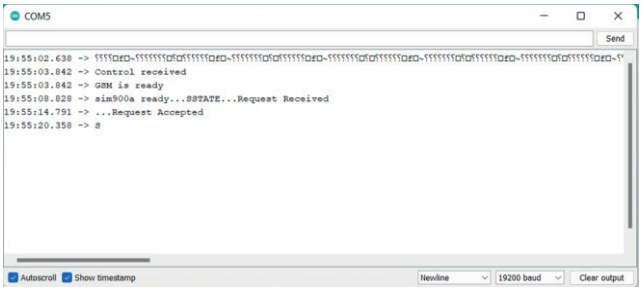

Figure 4. Terminal result when GPS and GSM are programmed.

An Arduino UNO is used with the GPRS+GPS(SIM900A) shield to send GPS coordinates to a mobile with an SMS and through HTTP when the module is called, and your number is correct.

When the person sends a message to the module and if the phone number is correct, the GPS obtains longitude and latitude, sends you an SMS with the position and sends the GPS data to the mobile in the form of a URL.

Load the next sketch into your Arduino and then assemble the GPRS+GPS shield with the antennas and the sim card installed. Remember, you must configure your APN, login, and password. If you don't do this, the GPRS+GPS cannot connect to the GPRS network. Also, you must set the URL with the IP address of the specific mobile. When the GPS fixes the GPS satellites, the GPRS+GPS shield will connect to the network, and it will send the GPS data through the Internet to the mobile in the form of a URL. After the arrival of URL., Search that URL in google then the details such as latitudes, longitudes, and position of the baggage by using this tracker.

IV. Result and Discussion

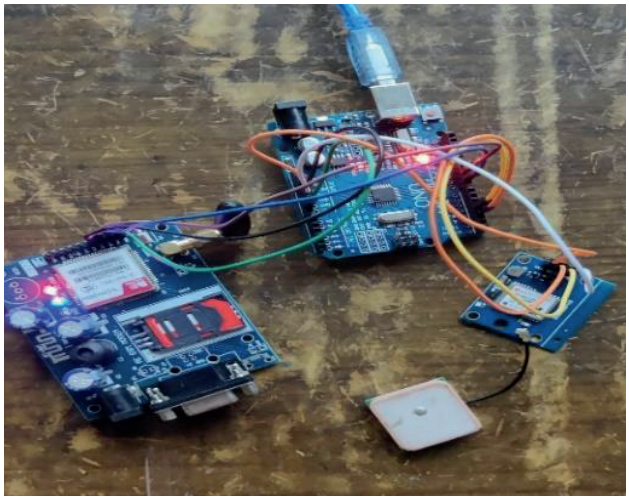

Figure 5. Components integration.

Figure 5 shows the system integration after assembly of components. The GSM and GPS modules will draw power from Arduino and are coordinated in the Arduino module. The Arduino module draws power from the secondary battery source. The code is dumped into the microcontroller from the Arduino software available in open source.

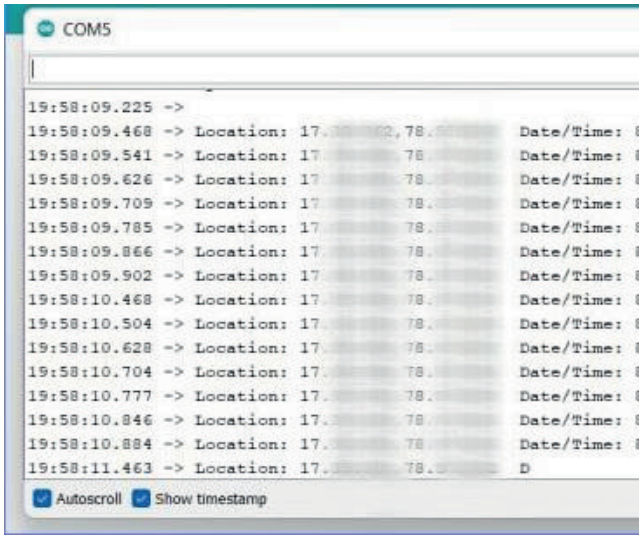

Figure 6. Terminal output.

Figure 6 shows the COMM port data which is been received when trigger message is received and acknowledge the location sent via SMS.

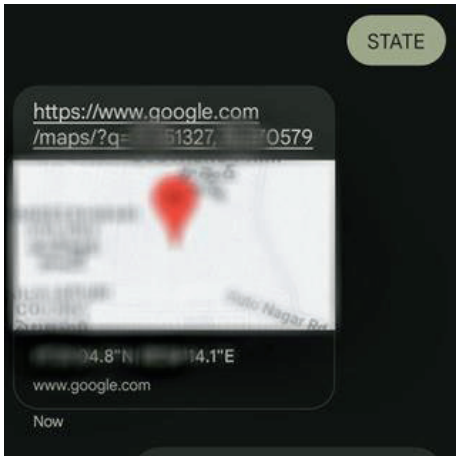

Figure 7. Final output SMS request and response.

Figure 7 shows the final output where the SMS, "STATE" which is said to be the coded text is sent to the module which contains SIM in GSM module. It reads the text and validates with pre-defined code and verifies the phone number and code and then access the location using GPS module and then append the coordinates to the link and send the appended text via SMS using GSM module.

V. Conclusions

In conclusion, the GPS and GSM-based tracking system has multiple benefits. It offers superior security compared to other systems and can be accessed from remote areas. The system helps prevent vehicle theft, and its installation is straightforward. Additionally, it is more dependable and cost-effective than other alternatives.

The utilization of GPS and GSM technologies enable the system to track vehicles in real-time and provides the latest details regarding ongoing trips. This technology can be utilized for real-time traffic surveillance and serves as a valuable resource for obtaining real-time information, monitoring congestion, and evaluating the performance of the systems.

References

[1] S H Bujang, H Suhaimi, Pg Emeroylariffion Abas "Performance of Global Positioning System (GPS) module "December 2020IOP Conference Series Materials Science and Engineering 991:012137

[2] Nur Aira Abdul Rahman, Noor Hisyam Ibrahim, Lojius Lombigit, Azraf Azman "GSM module for wireless radiation monitoring system via SMS" January 2018IOP Conference Series Materials Science and Engineering 298(1):012040

[3] Leo Louis "Working Principle of Arduino and Using it as a Tool for Study and Research." July 2018

[4] Zia Ur Rahman "GSM Technology: Architecture, Security and Future Challenges" February 2017

E-ISSN 2581 – 7957
P-ISSN 2277 – 3916
CVR Journal of Science and Technology, Volume 25, December 2023
DOI: 10.32377/cvrjst2508

Optimizing Hyper Parameters for Enhanced Performance: A Comparative Study on K-Nearest Neighbor and Support Vector Machine Models

Arun Kumar Katkoori[1] and R. Prakash Kumar[2]
[1]Sr. Asst. Professor, CVR College of Engineering/ECE Department, Hyderabad, India
Email: arun.katkoori@gmail.com
[2]Sr. Asst. Professor, CVR College of Engineering/ECE Department, Hyderabad, India
Email: prakash.rachmagdu@gmail.com

Abstract: **Numerous applications and areas benefit from the use of machine learning algorithms. The hyperparameters needed to fit a suitable model must be tuned to address different issues. The choice of the best configuration directly affects the performance of the model. User-defined hyper-parameters are those that are set before the training process is carried out. In machine learning, optimizing the hyperparameters is a process that can reduce the cost function. This paper presents a couple of methods that are used to optimize the K-Nearest Neighbor algorithm and the Support Vector Machine model. We have performed several experiments on the different optimization techniques to evaluate their accuracy and complexity.**

Index Terms: **Hyper parameters, Optimization Techniques, KNN, SVM, Random Search, Grid Search.**

I. Introduction

Machine learning has been widely used in various applications, such as advertising and recommendation systems. These algorithms are generally good at handling data analytics-related challenges. ML techniques can be used for different kinds of datasets or issues [1]. Developing an efficient model can be a time-consuming process, as it involves choosing the best algorithm and tuning its hyperparameters. There are two kinds of parameters that are used in developing machine learning models. The first is called model parameters, which can be updated and initialised through the learning process. The other is called hyper-parameters, which are defined by the model architecture. ML models cannot directly be estimated from data learning, and these must first be set [2].

One of the most important factors that are considered when developing machine learning algorithms is hyperparameters [3]. These are settings that are set before the training process, and they can be used to control the model's behavior. They also help determine how well the model can learn from new data. A hyperparameter is different from a machine learning model's parameter, which are acquired from data gathered during the training phase. For instance, the learning rate, the number of trees in a randomly generated forest, and the regularisation term are examples of hyperparameters [4].

In machine learning, optimizing hyperparameters is an important step. Doing so can significantly affect the model's performance. There are various techniques for doing so, such as random search [5], grid searching [6], and Bayesian optimization [7], among others. Grid searching is a type of algorithm that involves trying out a set of predefined hyperparameters and picking the one that gives you the best validation set performance. Random search, on the other hand, is a process that involves randomly sampling the combinations. For instance, in Bayesian optimization, a probabilistic model is used to guide the search.

There are many advantages to implementing HPO techniques in machine learning frameworks.

By utilizing HPO to identify the ideal set of hyperparameters, user can greatly enhance the performance and accuracy of ML model. User can also fine-tune the parameters to make the model more capable of learning from and generalising new data.

One of the most common issues that an ML model encounters when it comes to training data is overfitting. This occurs when the model fails to perform well on fresh data. With the help of HPO, you can identify the appropriate hyperparameters that will help minimize overfitting.

Utilizing hyperparameter optimization (HPO) techniques can help find the ideal hyperparameters efficiently, resulting in reduced training times for models. This is especially advantageous when dealing with large datasets or complex models. The use of HPO techniques can help ensure the consistency and reproducible nature of your ML models, even if the same set of parameters is used by different developers. This is because their hyperparameters are precisely optimized, utilizing an objective and systematic approach.

Hyperparameter optimization techniques are different from standard optimization methods in several aspects.

- Traditional optimization techniques are commonly used to improve a single function with a small number of variables. On the other hand, HPO involves optimizing several hyperparameters in a search area, which can be more challenging.
- An objective function that is well-defined can be improved through traditional optimization techniques. In HPO, an objective function is usually focused on the performance of a machine learning model in a validation set.
- The computational cost of implementing traditional optimization methods is typically high when there are many factors involved. Due to the complexity of the training pipeline, it can

Received on 17-10-2023, Revised on 11-11-2023, Accepted on 09-12-2023.

also have a significant impact on the overall cost of computing.

Decision-theoretic approaches are used to define a search space for hyper-parameters. They allow users to identify the ideal combination of these characteristics inside the search space and choose the most effective one. A particular type of search method known as grid search is used to find the optimal configuration of these characteristics.

Due to the limited number of resources and the time needed to perform a search, a decision-theoretic method known as random search is used. It randomly chooses the most appropriate hyper-parameters from the search space.

II. Literature Survey

The paper [8] analyzed the various algorithms used in the development of neural networks to find the best hyperparameters. The three algorithms used in the study were the Genetic Algorithm, the Grid Search, and the Bayesian Algorithm. The experiments were conducted on a dataset from Santander for customer transaction prediction. The parameters used in the analysis included the number of hidden layers, size, loss function, optimizers, activation function, and drop-out. The results indicated that the grid search performed better than the genetic algorithm, while the latter performed better than the Bayesian algorithm. The best hyperparameters were found in the first two algorithms, the Grid Search, and the Bayesian. The former performed well because it had the same number of secret layers and an identical optimizer.

Another paper [9] proposes an IDS framework that uses the k-nearest-neighbor tuning method to improve the performance of its semi-supervised learning. The first step is to identify the nearest neighbor of each unlabeled datapoint. After that, the data points are classified into either attack or normal classes according to the statistical information collected from these neighboring data points. The paper presents a comprehensive analysis of the model's robustness using a standard dataset NSL-KDD. The results of the study show that the proposed framework performs better than the KNN algorithms that are based on IDS.

Authors [10] introduced several advanced techniques and discussed their application to the algorithms. It also provides a variety of frameworks and libraries for addressing the issue. The paper conducted experiments to evaluate the effectiveness of different optimization techniques and presents practical optimization examples. The results of these studies will help researchers and industrial users identify the optimal configurations of their models.

Authors [11] evaluated six machine-learning and statistical models in terms of their predictive performance. The results revealed that the former outperformed the latter, except for SVM. In addition, non-spatial partitioning models exhibited overoptimistic performance when paired with spatial autocorrelation.

This paper [12] aims to analyze the various popular algorithms for optimizing hyperparameters in a grid search, random search, and genetic algorithm for building a neural network framework. The results of the study are based on the proposed models' accuracy and execution time.

The general method for choosing SVM hyperparameters is known as the CMA evolution strategy. It can handle various kernel parameters and doesn't require the availability of differentiable kernels or the separability of data. In addition, the selection criteria typically have multiple local optima, making it more suited for model selection than the gradient-based approach [13].

To improve the SVM parameters, authors [14] used two different methods: grid search and genetic algorithm. In their experiment, it was revealed that the grid search method is very reliable when it comes to finding optimal combinations within the given ranges, but it was very slow when it came to performing optimization in low dimensional datasets. The use of GA in SVM parameter optimization can help solve the issue of grid search. Compared to grid search, GA is more stable. The average running time of this method on nine datasets was 16 times faster. In fact, the results of the GA were significantly better than those of grid search in eight of the datasets.

Manual and grid searches are commonly used for optimizing hyper-parameters. In this paper, the authors [15] show that trials that are randomly chosen are more efficient than those conducted on a grid. We also compare the effectiveness of these two strategies with a previous study that used both to configure deep belief networks and neural networks. They found that random searches are more efficient than neural networks that are configured with a grid search. They can find better models in a fraction of the time. In contrast, random searches are more effective when they are granted the same computational budget.

III. Methodology

Fig. 1 illustrates the key components and the flow of hyperparameter tuning using optimization techniques within the context of building and evaluating machine learning models. These techniques help you systematically explore and optimize hyperparameters to improve the model's performance on dataset.

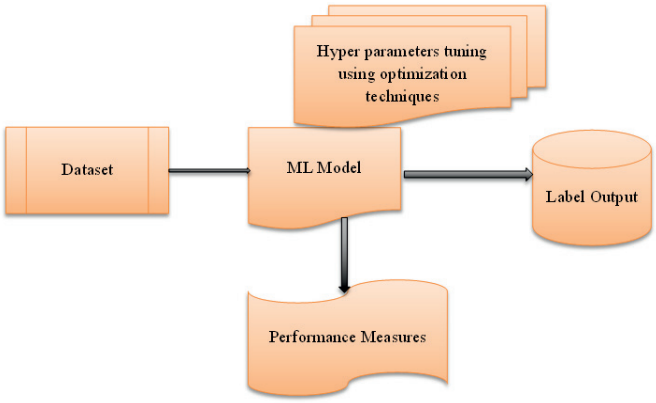

Figure 1. Block diagram of proposed method

The dataset represents the collection of data points with features and labels, serving as the foundation for training and evaluating machine learning models. The machine learning model that takes the input data from the dataset and

produces predictions as output. The ML model generates predictions based on the input data. These predictions are then compared to the actual labels in the dataset to assess the model's performance. Performance measures [16] are metrics used to evaluate the quality of the model's predictions, such as accuracy, precision, recall, F1-score, mean squared error, etc.

Here four datasets are used i.e., balance scale dataset, IRIS dataset, breast cancer dataset, and digits dataset. They are frequently utilized to test and benchmark the performance of various algorithms and models in the evaluation of classification-related tasks.

i) Balance Dataset:

It displays a balanced scale with varying weights on its sides to determine its fairness. The dataset features four attributes, which represent the distance and weight of objects on the balance's right and left sides. The target variable of the dataset is the class that determines whether or not the scale is balanced.

ii) IRIS dataset:

This dataset is used in the research of statistics and machine learning. It contains the measurements of various features of an iris flower, such as its sepal width, length, and petal width. The four features represent the iris flower's dimensions. The target is the species.

iii) Breast Dataset:

This dataset is frequently utilized for classification purposes related to the diagnosis of breast cancer. It features digitized images of a fine needle as an FNA. The attributes of this dataset include various features such as the mean radius, texture, and smoothness. The classification parameter target determines whether the tumor is benign or malignant.

iv) Digits Dataset:

The Digits dataset is frequently utilized for identifying handwritten digits. It comprises images of the digits. The features that represent them have pixel values. The target digit is the one depicted in the image.

Hyperparameters are model settings or configurations that are not learned from the data but must be specified before training. Examples include learning rates, the number of hidden layers in a neural network, regularization strength, etc. Hyperparameter tuning is the process of finding the optimal combination of hyperparameters to maximize the model's performance on the given task. This is important because different hyperparameter settings can have a significant impact on the model's effectiveness.

The KNN [17] and SVM [18] models were then created using the scikit-learn framework. We identified the necessary hyperparameters for each model. For SVM, the hyperparameters are gamma, C, and kernel. On the other hand, for KNN, the hyperparameters are n neighbors.

A. Q-Random Search

Here, Random Search [19] is utilized to find the optimal hyperparameters suitable for SVM and KNN models. A quick-random search introduces various constraints and refinements. For instance, the range or intervals that random sampling may be restricted to may be considered more meaningful for the analysis.

The three hyperparameters of SVM that are used in the decision function are "C," "gamma," and "kernel." The "C" parameter determines the optimal balance between the training points correctly classified and the smooth decision boundary. The "gamma" parameter indicates how far the influence of one training example can go.

TABLE I.
PSEUDO CODE FOR Q-RANDOM SEARCH USING SVM

```
INPUT: maximum number of iterations( maxitr)
1.  param_grid = {'c': [1, 3, 5,7],
    'gamma': [0.1, 0.01, 0.001],
     'kernel': ['linear', 'rbf'}
2.best_para={'c':lst['c'][1],'gamma':lst['gamma'][1],'kernel':lst['kernel'][0]}
3.svm_model=svm.SVC(C=best_para['c'],gamma=best_para['gamma'],
  kernel=best_para['kernel'])
4.  best_acc=accuracy(svm_model )
5.  For i in maxitr :
                c=random(param_grid[‘c’])
                gamma=random(param_grid[‘gamma’)
                    kernel=random(param_grid[‘kernel’])
                    model=svm(c,gamma,kernel)
                    present_acc=accuracy(model)
                      if(present_acc)> best_acc:
                            best_acc= present_acc
                            best_para={'c':c,'gamma':gamma,'ker
nel':kernel}
                    End if
                End for
6.  Return best_para
```

The optimal combination of hyperphys will be determined by evaluating each iteration through a loop called "maxitr". The random value of each parameter will be used in the creation of a new SVM. Its accuracy is then calculated by using the function "accuracy”.

TABLE II.
PSEUDO CODE FOR Q-RANDOM SEARCH USING KNN

```
INPUT: maximum number of iterations( maxitr)
1.  para_grid = {'n_neighbors': [1:10]}
2.  Random Search for KNN
    def random_search_knn(maxitr, para_grid_knn):
3.   Initialize the best accuracy and best parameters
       best_acc = 0
       best_para = {}
4.  for in range(maxitr)
        n_neighbors =
    random.choice(para_grid_knn['n_neighbors'])
        model = KNeighborsClassifier(n_neighbors=n_neighbors)
5.  present_acc = accuracy_knn(model)
6.  if present_acc > best_acc:
          best_acc = present_acc
         best_para = {'n_neighbors': n_neighbors}
    End if
    End for
7.  Return best_para
```

CVR Journal of Science and Technology, Volume 25, December 2023
DOI: 10.32377/cvrjst2508

The function "accuracy" updates the hyperphys' values if the new model's accuracy exceeds the current best. It then returns the most accurate set.

The given table II pseudocode provides a method that can be used to search for hyperparameter values in a KNN algorithm. It randomly chooses the optimal values for the n_neighbors parameter from the grid "para_grid_knn". Each iteration of the KNN algorithm, a model is created with a randomly chosen n_neighbors value. The algorithm's accuracy is calculated by using a hypothetical accuracy-knn function. If the current model exceeds the previous best, its corresponding hyperparameters and accuracy are updated. The algorithm then returns the best configuration after the random search.

B. Q-Grid Search

For Grid Search, a set of parameters are created that are used to train the models. Then select the best ones for the validation set and random sampling for the training.

The Q-grid (Quick) search strategy adopts a more efficient approach, which eliminates the need to evaluate every possible combination within a predefined grid. Instead, it uses a randomized sampling method to evaluate each combination. This method helps reduce the computational demands while maintaining a level of exhaustiveness. The new strategy avoids the need to analyze every possible combination in each grid, especially when dealing with large search spaces. It focuses on exploring different hyperparameter configurations to find promising ones.

The first value of each hyperparameter in the dictionary of "param grid" is the initial value of the model that will be used to create a SVM. The model's accuracy is then calculated using the "accuracy" function. The best acc parameter is used to represent the initial accuracy. The algorithm iterates through the various hyperparameters in the grid and creates new SVM models with the current set of values. The model's accuracy is then calculated using the "accuracy" function.

The function considers the new model's accuracy and updates the hyperparameters with the new values. It then returns the best set of values, which gives the highest accuracy.

Table IV pseudocode describes a method that can be used to search for hyperparameter values in a KNN algorithm. It takes into account the maximum number of iterations that can be performed to find the most appropriate values for the n_neighbors parameter from the grid "para_grid_knn".The KNN algorithm creates a model with the chosen n_neighbors value in every iteration. Its accuracy is computed by using a function known as an accuracy_knn. If the current model's accuracy exceeds the previous best, the corresponding hyperparameters are updated. The algorithm then performs an iterative process to find the optimal configuration.

TABLE III.
PSEUDO CODE FOR Q-GRID SEARCH USING SVM

```
INPUT: maximum number of iterations( maxitr)
1.  param_grid = {'c': [1, 3, 5,7],
                  'gamma': [0.1, 0.01, 0.001],
                  'kernel': ['linear', 'rbf']
2.  best_para={'c':lst['c'][1],'gamma':lst['gamma'][1],'kernel':lst['k
    ernel'][0]}
3.  svm_model=svm.SVC(C=best_para['c'],gamma=best_para['ga
    mma'],
    kernel=best_para['kernel'])
4.  best_acc=accuracy(svm_model )
    For c in param_grid[‘c’]
        For gamma in param_grid[‘gamma’]
            For kernel in param_grid[‘kernel’]
                model=svm(c,gamma,kernel)
                present_acc=accuracy(model)
                if(present_acc)> best_acc:
                    best_acc= present_acc

best_para={'c':c,'gamma':gamma,'kernel':kernel}
                End if
            End for
        End for
    End for
5.  Return best_para
```

TABLE IV.
PSEUDO CODE FOR Q-GRID SEARCH

```
INPUT: maximum number of iterations( maxitr)
1. param_grid = {'n_neighbors': [1:10]}
2.  Grid Search for KNN
    def grid_search_knn(maxitr, para_grid_knn):
3.   Initialize the best accuracy and best parameters
       best_acc = 0
       best_para = {}
4.  for in range(maxitr)
       n_neighbors = grid.choice(para_grid_knn['n_neighbors'])
       model = KNeighborsClassifier(n_neighbors=n_neighbors)
5.  present_acc = accuracy_knn(model)
6.  if present_acc > best_acc:
        best_acc = present_acc
       best_para = {'n_neighbors': n_neighbors}
    End if
    End for
7.  Return best_para
```

CVR Journal of Science and Technology, Volume 25, December 2023
DOI: 10.32377/cvrjst2508

IV. Results

Tables V and VI provide a comparative analysis of different SVM configurations, KNN and their performance on the different datasets. It demonstrates the impact of hyperparameter tuning on accuracy and computation time, which can be crucial when selecting the best SVM model for a particular problem.

TABLE V.
SVM Classifier's Performance on Different Datasets

Dataset	Name	Accuracy	Computation time (sec.)	c	gamma	kernel
Balance Scale Dataset	Default	0.87	0.004115	1.0	scale	rbf
	grid search	0.872	0.39201	1	0.01	rbf
	Random	0.884	0.20400	4.64158	0.00599	linear
	Q-grid search	0.884	0.13948	5	0.1	linear
	Q-random search	0.884	0.2372	5	0.1	linear
IRIS Dataset	Default	0.85833	0.00373	1.0	Scale	rbf
	grid search	0.96666	0.362037	3	0.1	linear
	Random	0.925	0.14787	215.4434	0.35938	linear
	Q-gird search	0.9666	0.1012547	3	0.01	linear
	Q-random search	0.96666	0.124896	3	0.01	linear
Breast Cancer	Default	0.90789	0.00808	1.0	scale	rbf
	grid search	0.94736	19.35496	5	0.1	linear
	Random	0.96052	17.96333	1.291549	2.7825	linear
	Q-gird search	0.95614	13.00778	3	0.01	linear
	Q-random search	0.95614	15.81649	3	0.01	linear
Digits Dataset	Default	0.97496	0.013361	1.0	scale	rbf
	grid search	0.98817	0.86540	3	0.001	rbf
	Random	0.96105	0.446697	1.29154	0.04641	linear
	Q-gird search	0.988178	0.913914	3	0.001	rbf
	Q-random search	0.988178	0.940677	7	0.001	rbf

E-ISSN 2581 – 7957
P-ISSN 2277 – 3916

CVR Journal of Science and Technology, Volume 25, December 2023
DOI: 10.32377/cvrjst2508

TABLE VI.
KNN CLASSIFIER'S PERFORMANCE ON DIFFERENT DATASETS

Dataset	Name	Accuracy	Computation time (sec.)	No. of neighbours
Balance Scale Dataset	Default	0.838	0.004738	3.0
	grid search	0.86	1.6074438	18
	Random	0.86	0.58122706	23
	Q-gird search	0.874	0.63590097	16
	Q-random search	0.872	0.62832236	15
IRIS Dataset	Default	0.925	0.0060422	3.0
	grid search	0.933333	1.6042816	1
	Random	0.9333	1.08904	1
	Q-gird search	0.9333	0.71362185	1
	Q-random search	0.93333	0.2778687	1
Breast Cancer Dataset	Default	0.61538	0.0025372	3.0
	grid search	0.65034	1.5867512	5
	Random	0.66433	1.0021665	19
	Q-gird search	0.69930	0.4683482	4
	Q-random search	0.69930	0.6204957	4
Digits Dataset	Default	0.93421	0.0049138	3.0
	grid search	0.93421	2.0322103	3
	Random	0.93421	1.2464041	3
	Q-gird search	0.93421	1.5173799	3
	Q-random search	0.93421	0.6609208	3

Fig. 2 shows the SVM Classifier's C and gamma value, which are optimized using Q-random and Q-grid search techniques for 5 datasets. Also, the KNN Classifier is evaluated using Q-random and Q-grid-based search optimization techniques for 5 datasets. Red color dot indicates the optimum value.

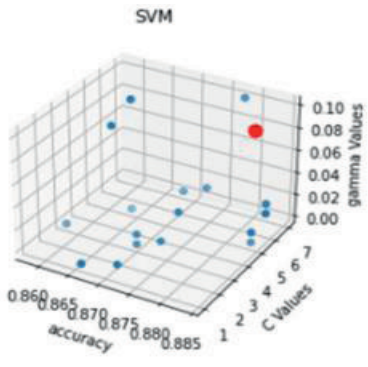

a) Balanced dataset

E-ISSN 2581 – 7957
P-ISSN 2277 – 3916

CVR Journal of Science and Technology, Volume 25, December 2023
DOI: 10.32377/cvrjst2508

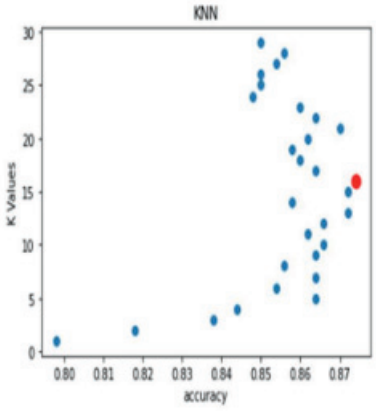

b) Balanced dataset

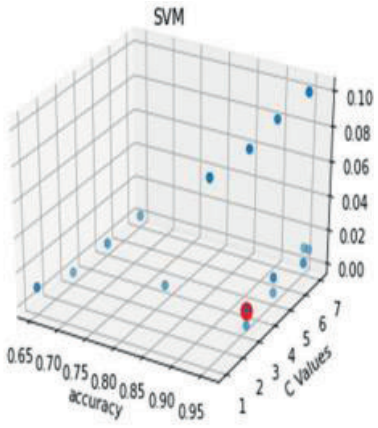

c) Iris Dataset

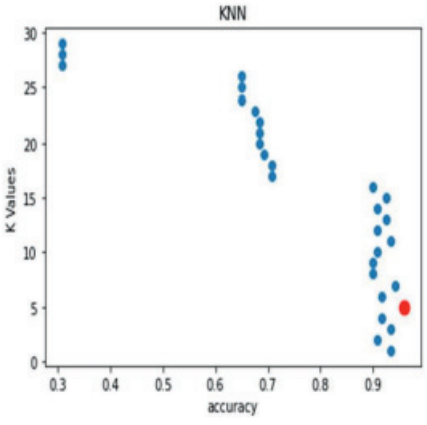

d) Iris dataset

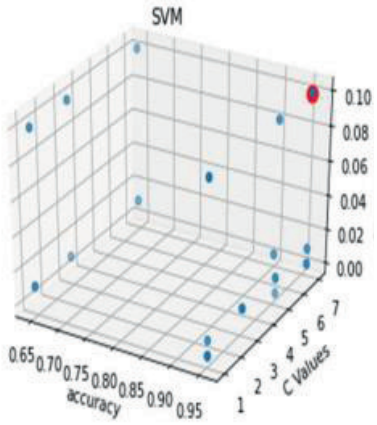

e) Breast Cancer Dataset

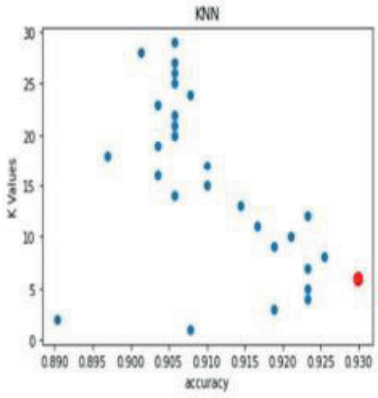

f) Breast Cancer Dataset

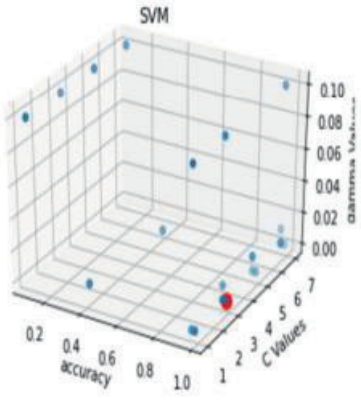

g) Digits dataset

CVR Journal of Science and Technology, Volume 25, December 2023
DOI: 10.32377/cvrjst2508

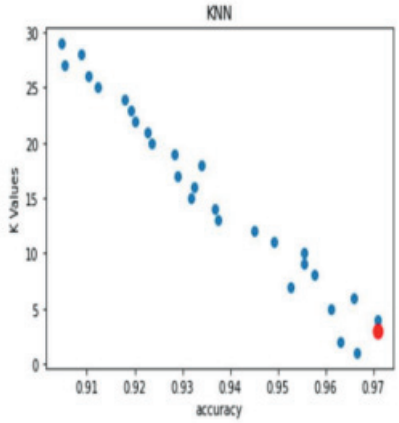

h) Digits dataset

Figure 2. SVM's and KNN's classifiers hyper parameters optimization using Q-random and Q-grid Search techniques applied on Balanced, Iris, Breast cancer and Digits datasets.

The results of the study revealed that the Q-random algorithm is better than the grid and random search methods when it comes to tuning hyperparameters in ML models. The accuracy of the models that were trained using the different algorithms was evaluated.

According to the findings, the Q-search optimization algorithm is more accurate than the grid or random search methods. This can be attributed to the algorithm's low number of iterations, which aids in achieving improved hyperparameter tuning.

It is noted that since the Q-random optimization algorithm only iterates around 30 times, it is more accurate and efficient than the random search method. It also has better performance in terms of tuning time and processing resources. The researchers attributed the improved accuracy of the Q-random algorithm to its intelligent sampling technique, which helps it focus on ideal hyperparameters at a faster rate than the random search method.

V. Conclusions

The importance of tuning machine learning models is acknowledged in this study, as it directly affects their performance in various applications. The study also analyzed the different KNN and SVM configurations on different datasets.

- The study investigated optimizing hyperparameters using various optimization techniques, such as random and grid searches. It found that the q-random algorithm performed better than both random and grid searches in tuning accuracy.
- The efficiency and accuracy of the training models were found to be better with the q-random algorithm. This was due to its low number of iterations. This algorithm can effectively fine-tune hyperparameter values.
- The efficiency of the q-random algorithm when it comes to tuning time and computational resources was also better than that of random searches. Its ability to sample various hyperparameters allowed it to improve its accuracy and convergence.
- The findings of this study have practical applications in the areas of machine learning. It shows that the q-random algorithm can be utilized to optimize hyperparameters, which makes it an ideal alternative to traditional techniques.

The study demonstrates that optimizing the performance of learning models involves considering the various hyperparameters. The q-random approach is an ideal choice, as it offers high efficiency and accuracy. As machine learning advances, more effective optimization techniques will be needed to help develop AI applications that can be used in various sectors.

References

[1] Cherian, I. ., Agnihotri, A. ., Katkoori, A. K. ., & Prasad , V. . (2023). Machine Learning for Early Detection of Alzheimer's Disease from Brain MRI. International Journal of Intelligent Systems and Applications in Engineering, 11(7s), 36–43.

[2] Rajesh, Dr. V. and Bhanuprakash Dudi. "Performance analysis of leaf image classification using machine learning algorithms on different datasets." (2021).

[3] Dudi, Bhanuprakash, and V. Rajesh. "Medicinal plant recognition based on CNN and machine learning." International Journal of Advanced Trends in Computer Science and Engineering 8.4 (2019): 999-1003.

[4] Prakash, D. Bhanu, K. Arun Kumar, and R. Prakash Kumar. "Hyper-parameter optimization using metaheuristic algorithms." CVR Journal of Science and Technology 23.1 (2022): 37-43.

[5] Li, B. (n.d.). Random Search Plus: A more effective random search for Random Search Plus: A more effective random search for machine learning hyperparameters optimization machine learning hyperparameters optimization.

[6] Liashchynskyi, P., & Liashchynskyi, P. (2019). Grid Search, Random Search, Genetic Algorithm: A Big Comparison for NAS.

[7] Zhang, Y., Apley, D.W. & Chen, W. Bayesian Optimization for Materials Design with Mixed Quantitative and Qualitative Variables. Sci Rep 10, 4924 (2020).

[8] Alibrahim, Hussain & Ludwig, Simone. (2021). Hyperparameter Optimization: Comparing Genetic Algorithm against Grid Search and Bayesian Optimization. 1551-1559. 10.1109/CEC45853.2021.9504761.

[9] Wazirali, R. An Improved Intrusion Detection System Based on KNN Hyperparameter Tuning and Cross-Validation. Arab J.Sci Eng 45, 10859–10873(2020).

[10] Li Yang, Abdallah Shami, On hyperparameter optimization of machine learning algorithms: Theory and practice, Neurocomputing, Volume 415, 2020, Pages 295-316, ISSN 0925-2312.

[11] Patrick Schratz, Jannes Muenchow, Eugenia Iturritxa, Jakob Richter, Alexander Brenning, Hyperparameter tuning and performance assessment of statistical and machine-learning algorithms using spatial data, Ecological Modelling, Volume 406, 2019, Pages 109-120, ISSN 0304-3800.

[12] Liashchynskyi, Petro B. and Pavlo Liashchynskyi. "Grid Search, Random Search, Genetic Algorithm: A Big Comparison for NAS." ArXiv abs/1912.06059 (2019).

[13] Frauke Friedrichs, Christian Igel, Evolutionary tuning of multiple SVM parameters, Neurocomputing, Volume 64, 2005, Pages 107-117, ISSN 0925-2312.
[14] Syarif, Iwan & Prugel-Bennett, A. & Wills, Gary. (2016). SVM Parameter Optimization using Grid Search and Genetic Algorithm to Improve Classification Performance. TELKOMNIKA (Telecommunication Computing Electronics and Control). 14.
[15] James Bergstra and Yoshua Bengio. 2012. Random search for hyper-parameter optimization. J. Mach. Learn. Res. 13, null (3/1/2012), 281–305.
[16] Kumar, K.A., Boda, R. A computer-aided brain tumor diagnosis by adaptive fuzzy active contour fusion model and deep fuzzy classifier. Multimed Tools Appl 81, 25405–25441 (2022).
[17] L. R. Somula and M. Meena, "K-Nearest Neighbour (KNN) Algorithm based Cooperative Spectrum Sensing in Cognitive Radio Networks," 2022 IEEE 4th International Conference on Cybernetics, Cognition and Machine Learning Applications (ICCCMLA), Goa, India, 2022, pp. 1-6, doi: 10.1109/ICCCMLA56841.2022.9988996.
[18] Katukuri Arun Kumar, Ravi Boda, A Multi-Objective Randomly Updated Beetle Swarm and Multi-Verse Optimization for Brain Tumor Segmentation and Classification, The Computer Journal, Volume 65, Issue 4, April 2022, Pages 1029–1052.
Esmaeili, Ahmad, Zahra Ghorrati, and Eric T. Matson. 2023. "Agent-Based Collaborative Random Search for Hyperparameter Tuning and Global Function Optimization" Systems 11, no. 5: 228.

E-ISSN 2581 – 7957
P-ISSN 2277 – 3916

CVR Journal of Science and Technology, Volume 25, December 2023
DOI: 10.32377/cvrjst2509

Development of 'Cloud and IoT based' Online Condition Monitoring System for Analytical Instruments

K.V.N.S. Sriveena[1] and K.V.N.S.V.P.L. Narasimham[2]
[1]BITS-Pilani, Pilani Campus, Vidya Vihar, Pilani-333031, Rajasthan, India
Email: ksriveena7@gmail.com
[2] Scientific Officer (G), NCCCM/BARC, ECIL Post, Hyderabad-500062, Telangana, India
Email: kvnarasimham@gmail.com

Abstract: **Analytical Instrumentation Systems are very much essential for compositional characterization of materials and form part of instrumental methods of analysis. Most of the analytical instrumentation systems are highly expensive and sophisticated in nature. Performance of these systems can be optimized by operating them in a controlled laboratory environment and precise monitoring of process parameters of the system. Hence continuous monitoring of ambient parameters of the laboratory, in which these systems are located, and process parameters related to each instrument is very important for obtaining the best out of these instruments. This paper describes an innovative application that has been designed using Cloud and IoT based Online Condition Monitoring of sophisticated laboratory instrumentation systems. Implementation of the thought process, involved in the realization of the objectives, has been described at length.**

Index Terms: Cloud Computing, IoT, Analytical Instruments, Mass Spectrometers, Embedded Systems, Sensors.

I. Introduction

The Internet of Things (IoT) has been a new revolution and a fundamental facilitator for modern industrial technological advancements. The Pandemic (Covid-19) impact has transformed the conventional method of monitoring into a digitalized way, which led to the unprecedented growth of the Industrial IoT sector globally. Thus, technologies like IoT, Cloud computing, Embedded System Design, Networking, Wireless Communications, and Smart devices paved the way and made our lives faster, efficient, and quicker to communicate between people-people, people-machine & machine-machine. Analytical instruments such as Mass spectrometers, Spectrophotometers, and Gas Chromatography systems etc., are well known for their usefulness in material characterization. Mass spectrometry systems are widely used in laboratories for identification and quantification of compounds/elements in different types of materials. A typical Inductively Coupled Plasma Quadrupole Mass Spectrometer (ICPQMS) system has various sub- systems such as Sample introduction, Ionisation source, RF generator, Lens supplies, Mass analyser, Control electronics, and Data acquisition system etc. A number of process parameters need to be continuously monitored and controlled for achieving optimum utilization of these instruments. The details of the process parameters, considered in this work, are described in the subsequent sections.

II. Need For the Development of Proposed System

Care must be taken to protect mass spectrometry systems, indigenous or imported instruments, as they are highly sensitive and expensive products. Any deviation from ambient parameters will lead to malfunctioning of instruments. These instruments operate in certain conditions and if the conditions are deteriorating, it is very important to switch off and protect expensive detectors and critical subsystems at the right time. Hence, it is vital to monitor RH, ambient temperatures, vacuum etc., and read the necessary parameters of laboratories and analytical instruments through sensors. For example, in an Inductively Coupled Plasma Quadrupole Mass Spectrometer (ICPQMS) system, vacuum (of the order of 2E-8 mbar) is crucial and is required for accurate and precise results. Similarly gas flow rates such as COOL GAS, NEBULISER, and AUX GAS need to be monitored. The inventory monitoring of various consumables is also an important activity for maximizing the utilization of the instrument. Hence there is a need for continuous monitoring of these process parameters for the optimum performance of the instruments. In this regard, an attempt has been made to develop a smart remote process monitoring system for laboratories in general and Mass Spectrometer Systems in particular.

III. Literature Survey

Yohanes et al., proposed an IoT server platform called Smart Environmental Monitoring and Analytical Real-time (SEMAR) [1] for integrating many IoT application systems. This paper provided in-depth technical end-to-end implementation of IoT application systems. Raghuvaran K. and J. Thiyagarajan [2] described how Raspberry Pi and wireless communications can be used for industrial remote process monitoring systems. They proposed RPi based global process monitoring of parameters such as light intensity, current, water level, and voltage are tracked and

Received on 01-12-2023, Revised on 04-12-2023, Accepted on 08-12-2023.

controlled. Seema et al., described the role of IIoT in manufacturing units [3]. Rajeswari et al., achieved a reduction in power consumption [4] through the

Lakkundi [9] proposed an industrial gas monitoring system using Arduino and Linux based OS. Review paper by Perigisetty Vedavalli et al., [10] was published on Automated Monitoring Systems based on R-Pi. Banagar et al., [11] proposed smart IoT systems but limited to offline and not online based.From the above literature survey, it is understood that there are some smart IoT systems that monitor the parameters such as temperature, humidity, smoke etc., in an industry or laboratory ambient conditions only. All the systems proposed were limited to demo only. But, the condition of the highly- expensive and high end scientific instruments was not being monitored such as capturing of vacuum real time signals from the instruments etc., Also, continuous live streaming of the Instruments facility was not proposed earlier. Hence there is a need for continuous online monitoring of highly sophisticated and imported Analytical instruments which need to be monitored round the clock and the monitoring system should be smart enough to generate alerts in case any parameter crosses its threshold. Hence the present work proposes "Development of 'Cloud and IoT based' Online Condition Monitoring System for Analytical Instruments". The Methodology has been described in the following section.

IV. Methodology Description

An online condition monitoring system for Mass Spectrometer Systems using IoT and cloud-based tech stacks, has been developed and presented in this paper at length. The hardware is designed using a Raspberry Pi microcontroller and various sensors such as vacuum gauges, temperature and humidity sensors for monitoring instruments and ambient conditions. The readings of all deployed sensors are stored, analyzed, processed, and aggregated in the IoT cloud platform. When any unintended situation arises, alarms and email notifications are triggered to the user and they monitor the statistics using Web interfaces like mobile or login onto a website. This system will help in minimizing or eliminating the need for manual readings and

frequent on-site visits to Laboratories. This development work also enables timely and early detection of events round

implementation of ESP8266 based smart system. Referenced papers from [5-8] described monitoring of process parameters using Arduino microcontroller. Naveen the clock by tracking various parameters like temperature, humidity, and vacuum etc., remotely through virtual tools & applications.

V. Experimental Work

The architecture of the IoT based system is depicted as shown in Figure 1. The system consists of the following modules: (i) Sensor modules – Sensors or components like Vacuum gauge (combo) for Vacuum levels, DHT22 sensor for temp & RH, are deployed in the premises. Sensors have high self-configuring reading capabilities based on the surrounding conditions and they are the sources of capturing physical entities of the environment at fixed periods. (ii) Hardware and Sensor interfacing – Raspberry Pi 4 acts as an Hardware IoT device (microcontroller) that has CPU, RAM, ROM, 40 GPIO pins and several external interfaces like USB, language software that runs on OS of RPi. All the sensors are interfaced using GPIO pins and then powered on in order to read the sensor values locally. The RPi uses Wi-Fi and lightweight MQTT protocol to connect to 'ThingsBoard' Cloud using python programming and then sends the processed meaningful data. (iii) IoT Cloud – The readings of all deployed sensors are stored, analyzed, and processed. Here, the virtual entity having attributes of temperature, humidity, and vacuum are created in the Things Board where data is collected and stored in the dashboard. The ThingsBoard has a Transport layer that carries the data through the other nodes for successful propagation. It has a rule engine that is the heart of ThingsBoard where the functions can be configured. It supports many kinds of Widgets on which Realtime information can be displayed. (iv) End users/Web – when any unintended situation arises, alarms and email notifications are triggered for the user and the concerned users monitor the statistics using web interfaces like mobile or they login into the ThingsBoard website/portal.

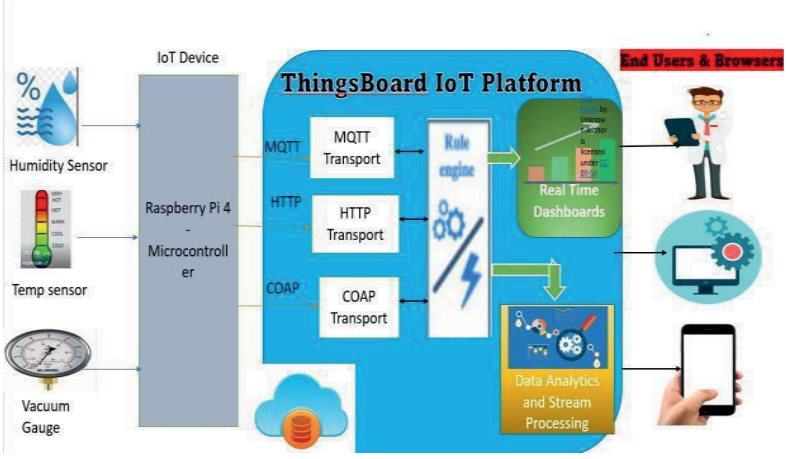

Figure 1. Functional block Diagram /Description of IoT based Instrument Condition Monitoring System

E-ISSN 2581 – 7957
P-ISSN 2277 – 3916

DOI: 10.32377/cvrjst2509

VI. Results and Discussion

The entire experiment has been carried out in the laboratory by deploying the hardware circuit and software program. The instrument's ambient Temperatures,

Humidity, and Vacuum levels are captured by the Web Dashboard that has been designed and developed in the IoT Cloud Platform for user interaction. If any of the values exceed the set threshold values, alert notifications are triggered continuously to take appropriate action as shown in the Figure 2 and Figure 3 below. Table-1 shows the theoretical vacuum level calculated using the Eq (1), instrument gauge display and the values sent to the IoT cloud. Theoretical Formula to convert o/p voltage from gauge to pressure (mbar) is given by

Figure 2. Humidity Readings on UI and Alert

Figure 3. Vacuum Readings (mbar) on UI and Alert

CVR Journal of Science and Technology, Volume 25, December 2023
DOI: 10.32377/cvrjst2509

Vacuum Pressure =10 pow[(Vout–6.8/0.6] Eq (1)

Dashboard output format can be defined as per the user requirement. In this project, an attempt has been made to display the real time parameter readings on the dashboard. Customization of the trends can be done based upon the users' requirements and interests.SMS alerts can be generated to take appropriate actions if the process parameter value exceeds safe value defined by the user.

TABLE 1.
Vacuum Gauge and IoT Cloud Readings

Gauge O/P Voltage (Volts)	Vacuum Level (mbar) shown in IoT cloud	Vacuum Level (mbar) shown on gauge	Error
6.06	5.84 E-2	5.84 E-2	0
5.897	3.06 E-2	3.14 E-2	0.08
4.043	2.1E-5	2.54E-5	0.44
3.785	9.5 E-6	9.44 E-6	0.5
2.89	3 E-7	3.04 E-7	0.04
2.87	3 E-7	2.8 E-7	0.2

VII. Conclusions

This proposed work demonstrated the design and implementation of an IoT Level-4 end-to-end system called "Development of 'cloud and IoT based' online condition monitoring system for analytical instruments" from 'Data collection' to 'Data Dissemination'.

The implemented system transformed a traditional lab into a Smart laboratory where the data management process improved by leaps and bounds. This development work also enabled timely and early detection of events by tracking various parameters like temperature, humidity and instrument vacuum remotely through virtual tools & applications. If any instrument parameter value exceeded the 'SET' limit, this system generated an alert and a real-time/live image of the lab would be sent to the email of authorized users. This system minimized the need for manual readings and frequent on-site visits to Laboratories. The result of the transformation helped in the advancement of Quality Control (QC) labs and production plants using IoT and Cloud-based tech stacks and made a way for Digital India.

References

[1] Yohanes Yohanie Fridelin Panduman, Nobuo Funabiki, Pradini Puspitaningayu, Minoru Kuribayashi, Sritrusta Sukaridhoto and Wen-Chung Kao, "Design and Implementation of SEMAR IoT Server Platform with Applications", Sensors 2022, 22(17), 6436. https://doi.org/10.3390/s22176436.

[2] Raguvaran. K. and J. Thiyagarajan, "Raspberry PI based global industrial process monitoring through wireless communication", Proceedings of 2015 International Conference on Robotics, Automation, Control and Embedded Systems (RACE)Publisher: IEEE, 18-20 February 2015.

[3] Seema, M R Pavithra Rubini, S Rajashree, and P Shanthi, "Literature survey on smart manufacturing in industrial internet of things (IIOT), Proceedings of the International Research Journal of Engineering and Technology (IRJET) e-ISSN: 2395- 0056, Volume: 08, Issue: 06 June2021.

[4] A.Rajeswari, M. Poongothai, and P. Muthu Subramanian, "Design and Implementation of IoT Based Smart Laboratory", Proceedings of 5th International Conference on Industrial Engineering and Applications, Publisher IEEE;2018.

[5] M.Patki1, and Anjali V. Patil, "Raspberry Pi based industrial process monitoring by using wireless communication", International Journal of Advance Engineering and Research Development Volume 4; Issue 4, April -2017.

[6] Rizky pratama hudha janto, Nurul Fahmi, Eko Prayitno, and Rosmida, "Real-Time Monitoring for Environmental Through Wireless Sensor Network", Publisher: IEEE, International Conference on Applied Engineering (ICAE).

[7] B.C Kavitha, and R Vallikannu, "IoT Based Intelligent Industry Monitoring System", Proceedings of 2019 - 6th International Conference on Signal Processing and Integrated Networks (SPIN); Publisher: IEEE; 07-08 March 2019.

[8] Aravind R, Yadikiumarani, Meghna, Harshitha, and Naregowda, "IoT based Real Time Data Monitoring for Industry", Department of Electronics and Communication Engineering GSSSIETW Mysore, Karnataka, India.

[9] Naveen Lakkundi, "Remote Monitoring and Controlling of Industry using IoT", SKYFILABS.

[10] Perigisetty Vedavalli, Hari Kishan Kondaveeti, and Deepak Ch, "A Review on Automated Monitoring Applications of Raspberry Pi", Proceedings of 2022 - 8th International Conference on Advanced Computing and Communication Systems, ICACCS 2022; 25-26 March 2022.

[11] N. Banagar, "IoT based Smart Laboratory System", IJERT Vol. 9 Issue 01, January 2020.

E-ISSN 2581 – 7957
P-ISSN 2277 – 3916
CVR Journal of Science and Technology, Volume 25, December 2023
DOI: 10.32377/cvrjst2510

GSM based Patient Healthcare Monitoring System

Gopisetty Ramesh[1] and V. Sreelatha Reddy[2]
[1]Sr. Asst. Professor, CVR College of Engineering/EIE Department, Hyderabad, India
Email: ramesh.g@cvr.ac.in
[2]Sr. Asst. Professor, CVR College of Engineering/EIE Department, Hyderabad, India
Email: v.sreelatha@cvr.ac.in

***Abstract*: Modern healthcare monitoring system necessitate immediate data acquisition, accurate predictions, and swift medication responses. These systems are equipped with sensors to measure vital parameters like body temperature, heart rate and oxygen levels. The collected data is transmitted to a central control system for remote patient health analysis, effectively reducing the workload of medical professionals and ensuring precise results. Additionally, these systems employ GSM technology to enable parameter monitoring via mobile phones. Data from patients is processed through a microcontroller platform, typically Arduino Uno. Any anomalies reported by the patient trigger the system to send a message to the designated caretaker or physician providing essential data for future health assessments. Further enhancements such as timed medication remainders can transform this system into a real time application focused device, advancing patient care systems. When considering factors such as cost, configuration and efficiency, this system emerges as the most effective and cost-efficient solution compared to alternatives worldwide. Moreover, it offers invaluable assistance to patients residing in remote areas.**

***Index terms*: Heartbeat, Arduino Uno, GSM technology, Real time clock**

I. Introduction

Heart disease is the primary cause of mortality among men and women in many countries. Within this category, heart attack, coronary heart disease, congestive heart failure and congenital heart diseases represent significant health challenges. The elderly, especially those requiring round the clock monitoring, are particularly susceptible to heart related issues. Many of them live alone, often without continuous care and support, further exacerbating their vulnerability.

Furthermore, healthcare services in remote areas of many countries are often undeserved, lacking the necessary infrastructure to provide adequate medical attention. There is a compelling case for the development and implementation of a remote monitoring system by considering all the above factors into account. The primary goal of this system is to transmit a patient's vital symptoms including body temperature and heart rate using the short message service (SMS) in conjunction with cost effective hardware components.

One of the distinctive features of this system is its ability to not only measure heart rate and body temperature but also display the recorded values on LCD screen. This innovative feature empowers patients to independently monitor their heart rate and body temperature. The system achieves this by employing heartbeat sensor circuit for heart rate detection and LM35 temperature sensor for accurate body temperature measurement. Arduino uno serves as the interface between these sensors and the system, collecting the necessary signals and processing them to generate valuable output.

The output data are subsequently transferred through the transmitter utilizing GSM module to send this information from the Arduino uno to the recipient, often medical expert in the form SMS messages. In terms of cost effectiveness, ease of setup and overall efficiency, this system shines as a highly efficient and profitable solution when compared to alternative systems worldwide.

Additionally, the advantages of this system extend to patients living in remote or isolated areas, providing them with essential healthcare support that might otherwise be challenging to access. If not only improves care of patients but also addresses that pressing issue of monitoring elderly individuals, enhancing their quality of life and overall well-being.

A. Objective

The main objective of this proposed system is:

i. Real-time calculation of the heart rate of a patient.
ii. Real-time calculation of the temperature of the human body.
iii. Display the calculated heart rate and temperature on the LCD module and send via SMS.
iv. Set the Alarm using a Real-time clock module for patient pill monitoring on a time-to-time basis.

B. Motivation

In a hospital setting, either a nurse or a doctor is required to physically move from one patient to another to conduct health checks. However, this approach may not enable continuous monitoring of patients and critical situations may go unnoticed until healthcare professional assesses the patient's health during their rounds. This can pose a significant challenge, especially for doctors who are responsible for patients in the hospital.

Our system addresses this issue by providing continuous monitoring of patient's health and ability to detect any abnormalities. The system continually collects and analyzes data from the patients under supervision. When it identifies any irregularities or concerning health parameters, it promptly notifies the designated caretaker or a doctor. This proactive approach ensures that critical situations are detected and acted upon in a timely manner, relieving the burden on healthcare providers and enhancing the level of care provided to patients in the hospital.

II. Literature Review

[1] studied research on patient's health monitoring system that is both flexible and scalable within the context of a 6LowPAN network. One significant limitation of

Received on 18-08-2023, Revised on 19-09-2023, Accepted on 03-11-2023.

CVR Journal of Science and Technology, Volume 25, December 2023
DOI: 10.32377/cvrjst2510

existing approaches is the integration of various technologies and networking solutions. The Internet of Things (IoT) represents an outcome of synergistic collaboration across multiple fields, including telecommunications, computer science and electronics. Additionally developed CDMA- based ubiquitous disease management system tailored chronic illness. This innovative system aims to improving healthcare of patients by utilizing an expanded, simplified electrocardiogram (ECG) mobile phone diagnostic algorithm within the hospital, home or travel settings suggested by [2,3] and developed significant emerging trend is the expansion of Machine-to-Machine (M2M) capabilities into the wireless technology. Vendors are incorporating radio chips or modules that can be easily connected to nearly any device or machine, marking a notable shift in the industry. [4] developed a personal health diagnosis system that has been created based on a patient's symptoms, utilizing a variety of datasets to access both disease and patient's risk and pointed out that the innovations in the latest generation systems revolve around two key aspects. The introduction of continuous monitoring capabilities for patients and enhancement of workflow and productivity for medical staff. [5] also underscored the significance of various technologies and their advantages in facilitating rapid communication. [6] developed a related development, a wearable sensor system designed for monitoring the movements of the patient. This system has been fine tuned to maintain an error rate below 5% by setting a threshold level. [7] developed IoT based system for monitoring of driver drowsiness and alert message to the driver to avoid accidents.

The proposed system measures human body temperature by placing fingers on a temperature sensor and monitoring the heartbeat by placing a fingertip on heartbeat sensor module. Moreover, the system can perform multiple functions including temperature measurement, real time clock (RTC) and alarm functionalities as well as monitoring heartbeat. It is equipped to send SMS notifications to the predefined mobile numbers stored within the system.

To implement this system, the hardware components are interfaced with an Arduino uno. The block diagram of the proposed system is shown in figure 1 and illustrating the various hardware components and their connections within the system.

III. Implementation

A. Block Diagram

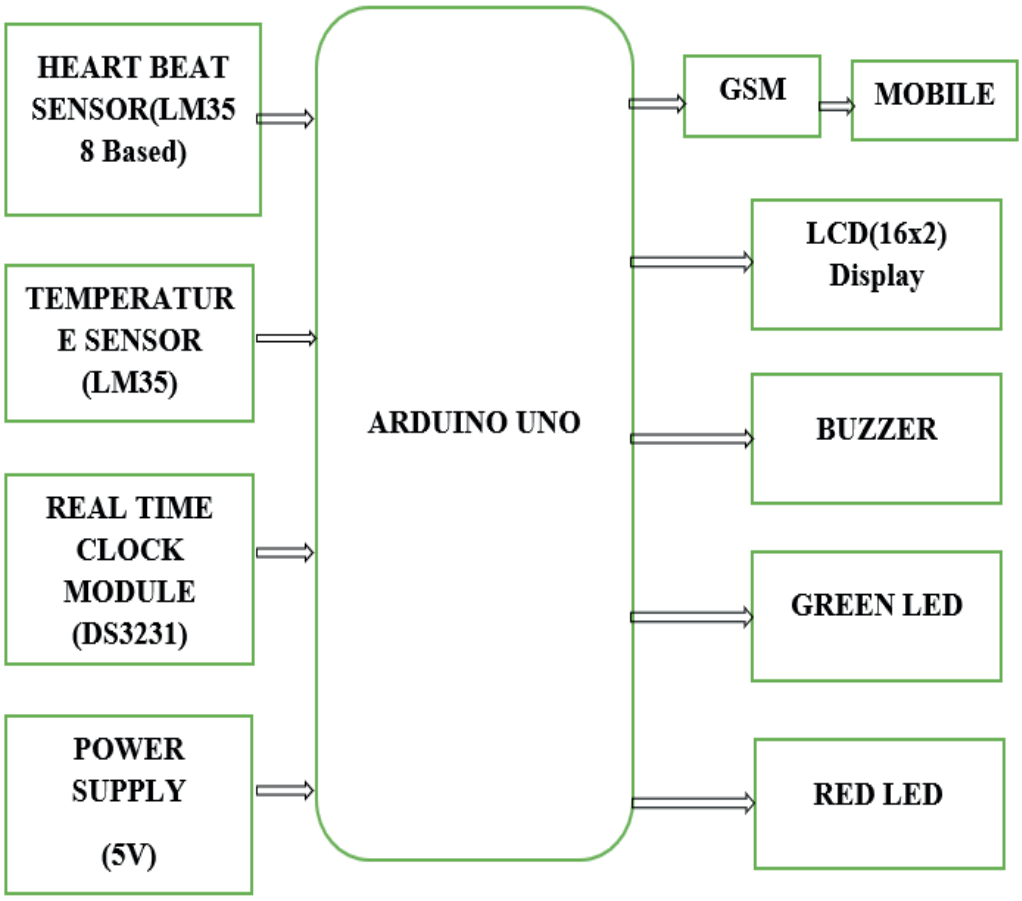

Figure 1. Block diagram of the Proposed System

CVR Journal of Science and Technology, Volume 25, December 2023
DOI: 10.32377/cvrjst2510

Initially the Arduino Uno is interfaced with the heartbeat sensor which is based on the LM358 IC. Similarly, the Temperature Sensor (LM35) and Real Time Clock Module (DS321) are interfaced with Arduino in the appropriate way. These act as input sensors to the Arduino. The GSM, LCD Display, Buzzer, and LED (red, green) interface with Arduino. These sensors act as output Devices in the module. Here, the Arduino is the microcontroller-based controller that controls the whole process. Like Reading the inputs initializing the devices or sensors and turning off the sensors. Further, The GSM Module is responsible for sending the SMS to the concerned phone Number. The required code is dumped in the Arduino using Arduino IDE software.

The complete methodology of the system is explained by seeing the above block diagram. The system commences operation by establishing the connection between the power supply and the central control unit, Arduino. The input configuration includes the integration of a set of sensors comprising the heartbeat sensor, SPO2 sensor, temperature sensor, and real-time clock sensor. To enable data capture, an initial step involves placing a finger on the heartbeat sensor and the temperature sensor. Subsequently, the gathered data undergoes tailored processing before being simultaneously relayed to both the LCD display and the GSM module for the purposes of display and communication. In case of any abnormalities, the system sends an alert message to the doctor or caretaker's mobile device. To ensure timely medication, the RTC module (DS3231) monitors the schedule and sets alarms when the patient needs to take prescribed medicines. When the patient's temperature exceeds 35°C, the RED LED activates and sends an alert message to the respective doctor for immediate attention. If the patient's heart rate falls below 60 or exceeds 100, the system triggers the buzzer and illuminates the RED LED. Furthermore, when the patient takes medication at the specified times, the GREEN LED lights up. Figure 2 illustrates the flowchart of the proposed system.

B. Flow Chart

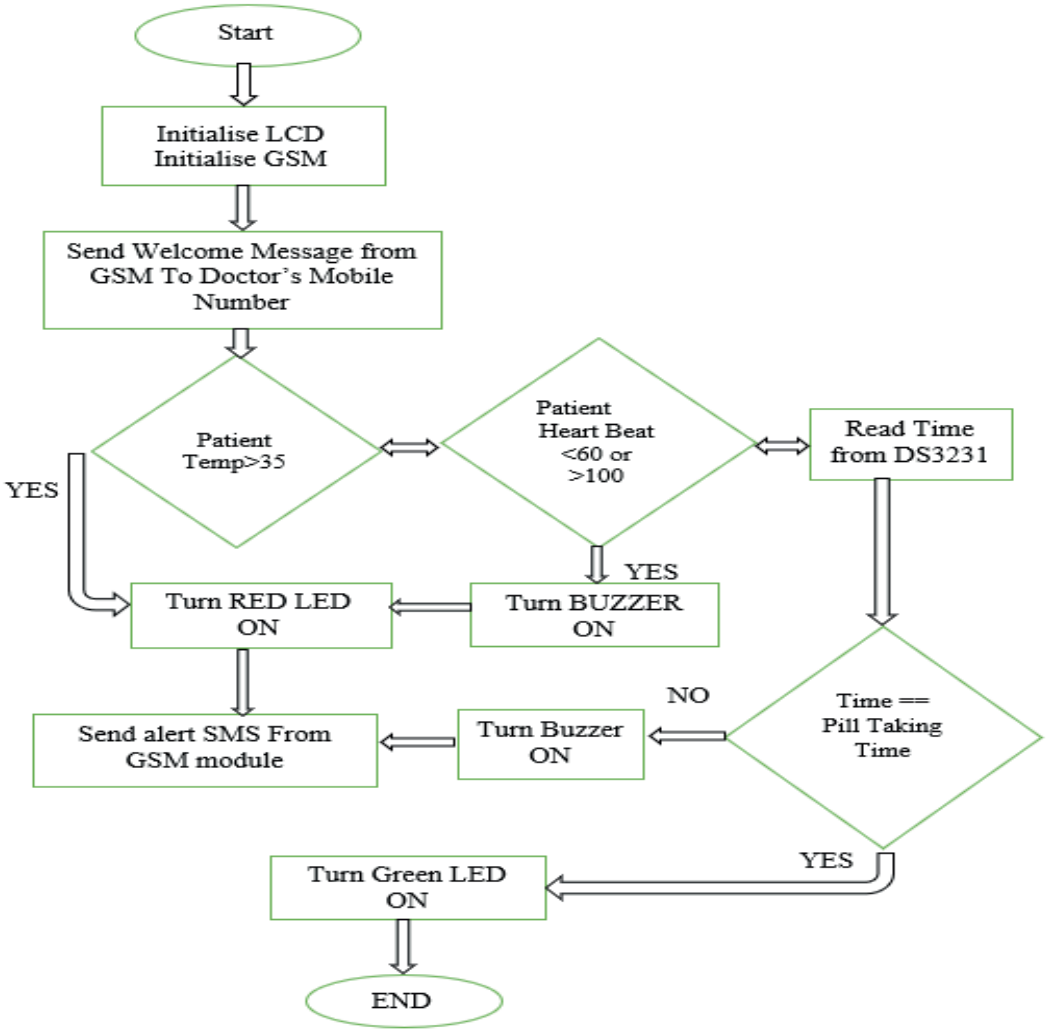

Figure 2. Flow chart of the proposed system

First, initialize the LCD monitor, enable the GSM module, and send the welcome message to the doctor's mobile number. The temperature sensor continuously monitors the patient's body temperature, and the heartbeat sensor continuously measures the heartbeat of the patient which is attached to the fingertip of the patient. If the patient's temperature is above the specified temperature i.e., 35°C or their heartbeat is above the normal heart rate i.e., below 60 or above 100, RED LED will glow and simultaneously get the sound from the buzzer which alerts the abnormal condition of the patient. The GSM module sent an alert message to the doctor and set a time for the patient to take proper medicine in order the maintain the body temperature and normal heartbeat.

IV. Results

The proposed system demonstrates significant potential for applications within the healthcare industry, given its utilization of a compact controller and a diverse array of biosensors for remote data transmission. This system serves as a valuable tool for healthcare professionals to closely monitor the well-being of their patients. Harnessing data collected through comprehensive patient health assessments enables continuous monitoring of the overall health of individuals in need of ongoing care. Additionally, the system can be configured to set alarms for medication adherence, and it measures vital signs such as temperature and heart rate through various biosensors. Table 1 provides a record of the patient's heart rate and temperature readings. Hardware setup is shown in figure 3 and figure 4 displays the patient's body temperature and heart rate on an LCD screen.

TABLE I.
Body Temperature and Heartbeat of the Patient

BODY TEMPERATURE (°C)	HEART-RATE (BPM)
35	73
34	74
36	69
35	79
36	73
31	73
34	73

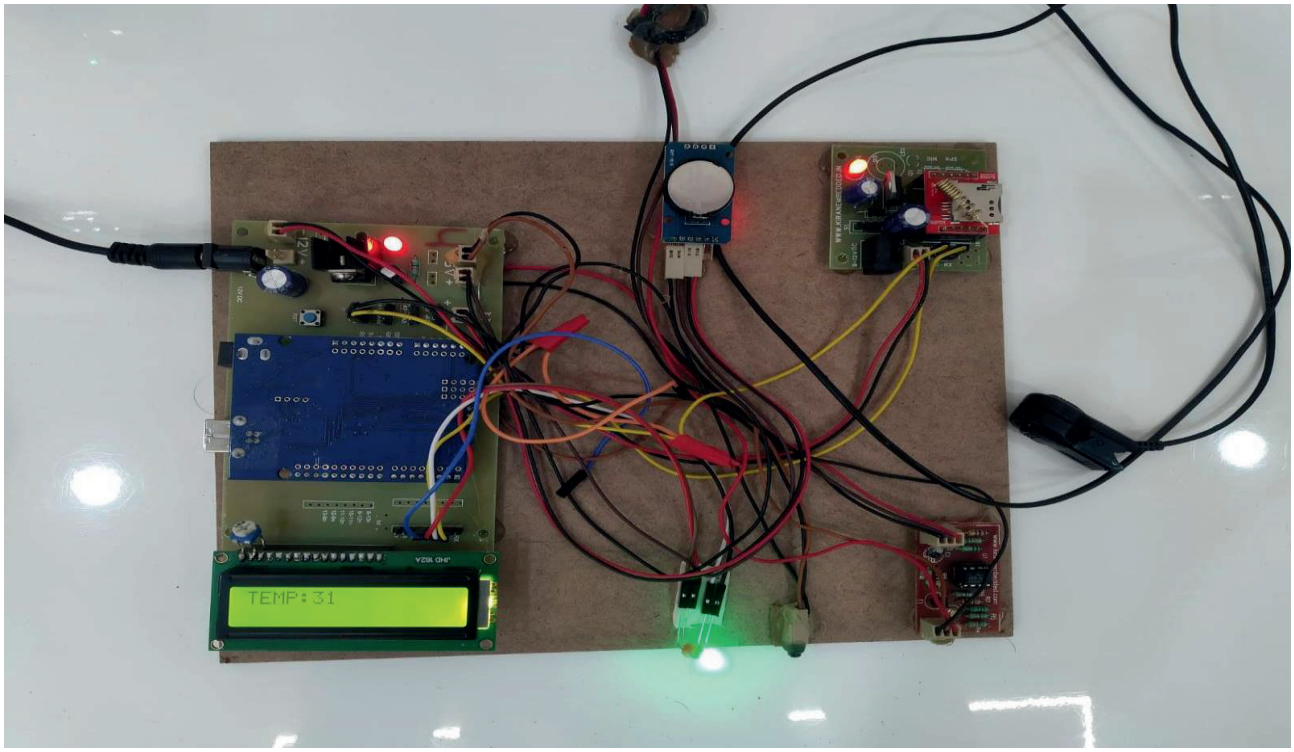

Figure 3. Hardware Setup of the system

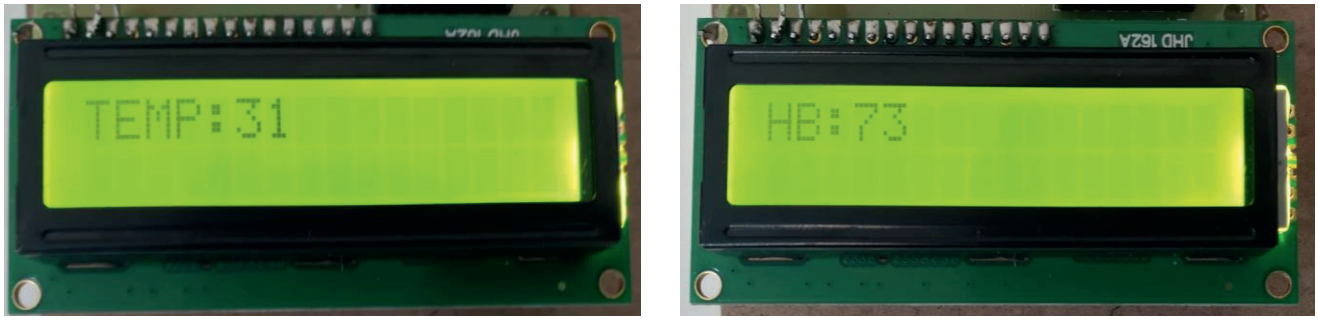

Figure 4. Display of body temperature and heartbeat of the patient

V. Conclusions

The proposed system not only allows for the evaluation of doctor's performance within hospital but also ensures that patients receive accurate and potentially life-saving treatments. Future enhancements to the system could involve the integration of blood pressure sensors and dental care monitoring systems, thus advancing its capabilities in monitoring of health. With precise experimentation, the system could transition into a real-time hospital environment, potentially saving numerous lives. Implementing quick, accurate, and real-time methodologies can further enhance the efficiency of the proposed system. An additional focus is on cost reduction, making it feasible for patients at all levels of disease severity to benefit from this system. The system measures body temperature by placing a finger on a temperature sensor and records the heartbeat by placing the fingertip on the Heartbeat sensor module. It then calculates both the temperature and heartbeat data, sending SMS messages to pre-stored mobile numbers in the system. Additionally, SMS is the optimal method for data transmission in critical situations, especially in rural areas where broadband communication is scarce.

The incorporation of both a blood pressure sensor and dental care monitoring systems represents a significant advancement in the ongoing development of the health monitoring system. This methodology can be extended to encompass various healthcare services and applications, including disease management and eldercare.

References

[1] Bhoomika, Dr. K. N. Muralidhara, "Secured Smart Healthcare Monitoring System Based on IoT", International Journal on Recent and Innovation Trends in Computing and Communication Volume 3, Issue 7, 2015.

[2] W. Y. Chung, C. Yau, K. S. Shin "A cellphone-based health monitoring system with self-analysis processor using wireless sensor network technology," in Proc. 29th Annu. Int. Conf. Eng. Med. Biol. Soc., Lyon, France, 2007.

[3] Adivarekar, J.S., Chordia, A.D., Baviskar, H.H., Aher, P.V. And Gupta, S. "Patient Monitoring System Using GSM Technology". International Journal of Mathematics and Research, 1(2). 2013.

[4] Vara Prasad Rao Mangu, "Patient health monitoring with doctor alert reporting over IOT", Journal of Interdisciplinary Cycle Research 12(4):1380-1391, 2020.

[5] M. Babu Prasad, "GSM based health care monitoring system" International Journal of Innovative Technology and Exploring Engineering (IJITEE) ISSN: 2278-3075, Volume 8, Issue 2, December 2018.

[6] Amna Abdullah, Asma Ismael, Aisha Rashid, Ali Abou-ElNour, and Mohammed Tarique, "Real-time wireless health monitoring application using mobile devices", International Journal of Computer Networks & Communications (IJCNC) Vol.7, No.3, May 2015.

[7] Dr. Gopisetty Ramesh "IoT based driver drowsiness and pothole detection alert system", International Journal on Recent and Innovation Trends in Computing and Communication (IJRITCC), Volume 11, Issue 7, 2023.

[8] Purnima, P. S. "Zigbee and GSM based patient health monitoring system", International Conference on Electronics and Communication Systems (ICECS), pp. 1–5. 2014.

E-ISSN 2581 – 7957
P-ISSN 2277 – 3916
CVR Journal of Science and Technology, Volume 25, December 2023
DOI: 10.32377/cvrjst2511

A Cost Effective Approach to Design A Portable Mobile Charging Device using Wind Energy

S. Harivardhagini
Professor, CVR College of Engineering/EIE Department, Hyderabad, India
Email: harivardhagini@cvr.ac.in

Abstract: **Renewable energy is energy from renewable resources that are naturally replenished on a human timescale. Renewable resources include sunlight, wind, the movement of water, and geothermal heat. This project is designed to create a portable mobile charging device that is chargable through wind energy. This portable device system utilizes a small, lightweight wind turbine that can be easily carried or attached to various objects, such as backpacks or bicycles, to harness the power of wind and convert it into electrical energy. The generated energy is stored in a portable battery pack, which can be used to charge mobile devices, such as smartphones, tablets, or other USB-powered devices, anytime and anywhere. This project also discusses the performance evaluation of our system, including the power output, charging time, and energy efficiency, under different wind conditions and usage scenarios. Our project helps in accessing affordable, reliable, sustainable energy which in turn assists in achieving the 'sustainable development goal 7[SDG], that is ensuring access to affordable and clean energy'. This technology has the potential to provide a reliable and eco-friendly energy source for mobile devices, reducing the dependence on traditional electricity sources and contributing to a greener and more sustainable future.**

Index Terms: **Renewable Energy, Wind Energy, Sustainable Development, Portable, Affordable & Reliable Energy**

I. Introduction

In today's world, mobile phones have become an essential part of our daily lives and keeping them charged all the time is crucial. However, in many remote areas or during outdoor activities, access to a stable power source for mobile charging can be limited. This project aims to develop a portable mobile charging system that utilizes wind energy to provide a sustainable and convenient solution for charging mobile devices on-the-go. In recent years, there has been a growing global concern regarding the environmental impact of conventional energy sources, such as fossil fuels. The increasing demand for energy, coupled with the urgent need to mitigate climate change, has spurred extensive research into harnessing renewable energy as a sustainable path to power the future. This literature review aims to provide an overview of key findings from five relevant papers published in reputable journals, highlighting the advancements and challenges in the field of renewable energy. Overview of the global energy crisis and climate change concerns. Need for renewable energy sources to mitigate environmental impact. Importance of sustainable energy solutions for a sustainable future. Types of Renewable Energy Sources are Solar energy: Photovoltaic and solar thermal systems. Wind energy: Onshore and offshore wind turbines. Hydropower: Conventional hydroelectric plants and small-scale hydropower. Biomass energy: Conversion of organic matter into biofuels. Geothermal energy: Utilizing heat from the Earth's interior. Tidal and wave energy: Harnessing the power of ocean currents and waves. As the global demand for energy continues to rise, the need for sustainable and clean sources of power has become increasingly urgent. Harnessing renewable energy has emerged as a promising solution to meet this demand while reducing the environmental impact of traditional fossil fuel-based energy systems. This literature review aims to explore the current state of research on harnessing renewable energy and its potential to power the future sustainably. By analyzing and synthesizing findings from five selected papers, this review provides valuable insights into the advancements, challenges, and future prospects of renewable energy technologies. Harnessing renewable energy has emerged as a critical solution to address the challenges posed by climate change and the limited availability of fossil fuels. This synopsis provides an overview of the current state of renewable energy technologies, their benefits, and the challenges associated with their implementation. It explores various sources of renewable energy, including solar, wind, hydroelectric, biomass, and geothermal, highlighting their potential as sustainable alternatives to conventional energy sources. The synopsis examines the significant environmental advantages offered by renewable energy, such as reduced greenhouse gas emissions, improved air quality, and minimized ecological impact. It emphasizes the potential for renewable energy to contribute to global efforts in mitigating climate change, achieving energy security, and promoting sustainable development. Furthermore, the synopsis delves into the technological advancements and innovations driving the growth of renewable energy systems. It discusses key components such as solar panels, wind turbines, hydroelectric generators, and biomass conversion technologies, shedding light on their efficiency, reliability, and scalability. The role of energy storage systems and smart grids in integrating intermittent renewable sources into the existing energy infrastructure is also explored. Despite the numerous advantages, several challenges hinder the widespread adoption of renewable energy. This synopsis highlights the economic barriers, including initial installation costs and intermittency issues, as well as the need for supportive policies and incentives to facilitate the transition towards renewable energy. The role of research and development in improving efficiency, cost-effectiveness, and energy storage technologies is also emphasized. The synopsis concludes by emphasizing the need for a comprehensive and integrated approach to harnessing renewable energy. It highlights the

CVR College of Engineering
Received on 30.09.2023, Revised on 09.11.2023, Accepted on 20.11.2023.

importance of collaboration between governments, industries, and research institutions to drive innovation, policy formulation, and investment in renewable energy projects. By leveraging the potential of renewable energy sources, societies can pave the way for a sustainable, clean, and resilient energy future, while mitigating the adverse impacts of climate change and promoting environmental stewardship.

II. Literature Survey

This paper presents a design and implementation of a small-scale low speed wind power based portable mobile phone charger. The implementation includes a savonius wind turbine and a controller.[1]

In this work, the researcher came up with a solution of maintaining sustainability of energy stored in the phone battery exploration that has been carried out with mobile phones. This concept utilizes wind generated electrical Energy to charge the mobile phone's battery. The model consists of four main components that are propeller, generator, chip integrated on PCB, and mobile set suitable charging pin. [2]

In this paperwork they develop a small compact and easy to carry mobile charger which utilizes wind energy to charge mobile phones with ease during travelling. It minimizes the dependability on conventional chargers. It utilizes a fan connected to a DC generator, a bridge rectifier which minimizes fluctuations. It works effectively between vehicle/wind speed of 40kmph and 80kmph. It can be easily installed in the window of the car/bus/train etc. and the mobile phone can be charged directly. [3]

In their paperwork, wind energy is used to get 6V with the help of generator and solar energy is used to 8 V with the help of solar panel. The proposed charger will solve the problem of mobile charging during traveling, power cut and non-availability of power in remote areas. [4]

A prototype of battery charger is developed for application with mobile phones as an example to address the design considerations, plus demonstrates the performance of the charger adapted to a practical application system. This mobile charger is better than normal mobile charging as it uses wind power as a renewable energy source. [5]

III. Design And Implementation

In today's fast-paced digital age, mobile devices have become an integral part of our lives, providing us with constant connectivity and access to a plethora of information and services. However, the ever-increasing reliance on these devices often leads to a common problem - limited battery life. This issue is particularly challenging in situations where a power source is not readily available, such as during outdoor activities, emergencies, or in remote areas. To address this problem, harnessing renewable energy sources has emerged as a viable solution. Among these sources, wind energy stands out as a promising option due to its abundance and accessibility in various environments.[6] [7].

Portable mobile charging systems that utilize wind energy present a compelling solution, [8] [9] [10] allowing users to recharge their mobile devices on the go while simultaneously leveraging a clean and sustainable energy source. The design and implementation of a portable mobile charging system powered by wind energy requires careful consideration of various factors. These include the efficiency of energy conversion, the portability and durability of the system, and the user experience. This synopsis aims to explore the design and implementation aspects of a wind-powered mobile charging system, discussing the key components, technologies, and considerations involved in its development. By utilizing wind energy, not only can we extend the battery life of our mobile devices, but we can also reduce our carbon footprint and promote the adoption of renewable energy solutions. [11] [12] This paper delves into the intricacies of designing an efficient and practical wind-powered mobile charging system, presenting a sustainable and portable solution for powering our devices in diverse settings.

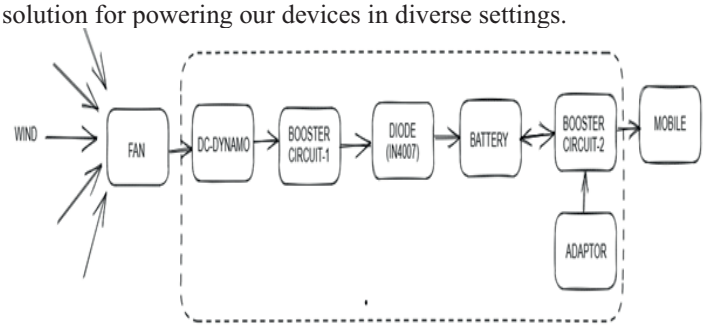

Figure 1. Block diagram of portable mobile charger using wind energy

Figure 1 represents the block diagram presents an efficient and self-sustaining portable mobile charging system that harnesses wind energy through a fan and DC-dynamo, regulates the output voltage using a booster converter, and incorporates a battery to store and supply power to charge mobile devices. With this innovative solution, users can stay connected and charge their devices anytime, anywhere, relying on clean and renewable wind energy. [13] [14] [15]

The portable mobile charging system using wind energy consists of the following key components:

1. Wind Fan
2. Dc-Dynamo
3. Booster Converters
4. Diode
5. Battery
6. Adapter
7. Load (Mobile)

Below is a detailed description of each block in the diagram:

1. Wind Fan:

The project begins with a wind fan, which serves as the primary source of wind energy. The fan is designed to capture the kinetic energy from the wind and direct it towards the DC dynamo. The size and shape of the fan are optimized for portability and efficient energy capture, making it suitable for on-the-go use.

2. DC-Dynamo:

The wind fan is connected to a DC-dynamo, also known as a small-scale wind turbine generator. The DC-dynamo's main function is to convert the mechanical energy from the rotating fan blades into electrical energy in the form of direct current

CVR Journal of Science and Technology, Volume 25, December 2023
DOI: 10.32377/cvrjst2511

(DC). As the wind spins the fan blades, the dynamo's internal coils and magnets generate an electric current.

3. Booster Converter:

The output of the DC-dynamo generates variable voltage levels depending on wind speed. To ensure a stable and optimal charging voltage for mobile devices, a booster converter is incorporated into the system. The booster converter regulates the incoming DC voltage, stepping it up or down as necessary, to provide a consistent output voltage suitable for charging mobile devices efficiently.

4. Diode:

In the charging circuit, a diode is placed to prevent any reverse current flow from the battery to the generator during low wind speed or no wind conditions. This ensures that the battery remains charged and ready to supply power to the mobile device when required, without wasting energy back to the generator.

5. Adapter:

The regulated output from the booster converter is connected to an adapter, which acts as an interface between the charging system and the mobile device. The adapter typically includes USB ports or other standard charging connectors to support various mobile devices, such as smartphones and tablets.

6. Battery:

To provide a continuous power supply even in the absence of wind or during periods of low wind, the system includes a battery. The battery stores the excess electrical energy generated by the DC-dynamo and the booster converter. During periods of low wind or when the mobile device is actively drawing power, the battery discharges its stored energy to ensure a consistent charging experience for the mobile device.

Figure 2 shows the schematic of portable mobile charger using wind energy. The connections of the setup is seen in the same. Figure 3 shows the flowchart of the process. The user unfolds the wind turbine and secures it in an open area with sufficient wind flow. As wind flows through the turbine blades, they rotate, generating mechanical energy. The rotating motion of the turbine's shaft drives the generator, converting mechanical energy into electrical energy. The generated electrical energy is stored in the battery pack, ensuring a constant power supply for charging mobile devices. Users connect their mobile devices to the USB charging ports provided by the system.

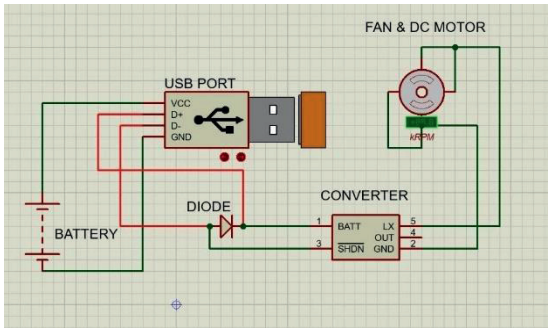

Figure 2. Schematic of the portable mobile charger using wind energy

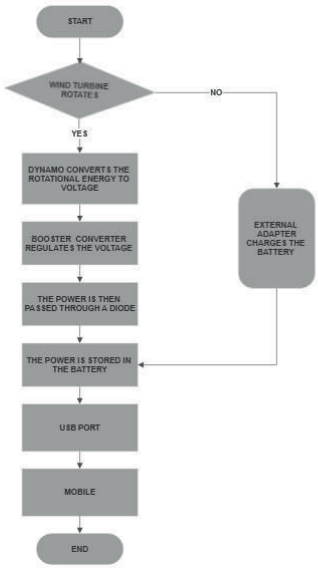

Figure 3. Flowchart of the process

The regulated electrical energy from the battery pack is used to charge the connected devices. The figure 4 depicts the prototype of the system. It was successfully operated to get the required output.

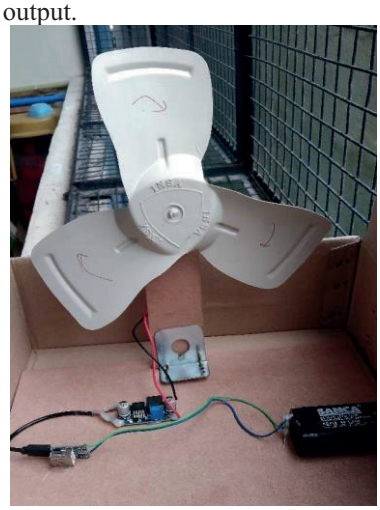

Figure 4. Prototype of the process

IV. Result

Figure 5 shows the mobile charging rate with the wind charger and the conventional charger are monitored and compared for every 5 min and recorded. The details are mentioned in the table below.

S. No	TIME (in Min)	CHARGE BY WIND CHARGER (in %)	CHARGE BY CONVENTIONAL CHARGER (in %)
1	5	1	3
2	10	2	8
3	15	4	13
4	20	8	17
5	25	12	23
6	30	15	28

Figure 5. Mobile Charging Percentage with Time (in min)

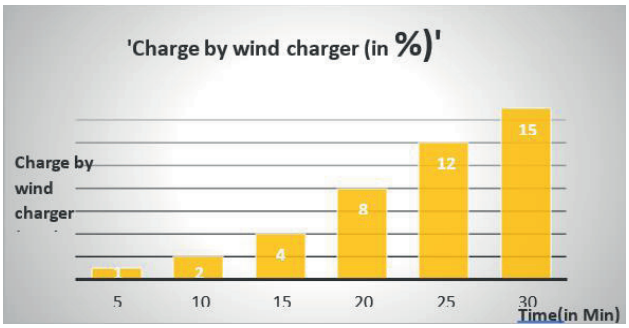

Figure 6. Mobile Charging using wind energy in percentag &time (in min)

The figure 6 shows the graph of rate of charging of wind based charger with respect to time. Figure 7 shows the comparison of Mobile Charging Rate for Wind charger & Conventional Charger Vs Time (in min)

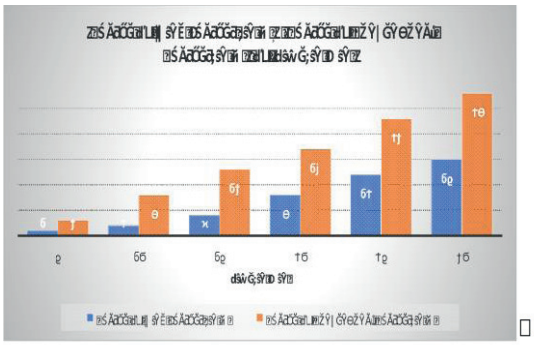

Figure 7. Mobile Charging Rate for Wind charger & Conventional Charger Vs Time(in min)

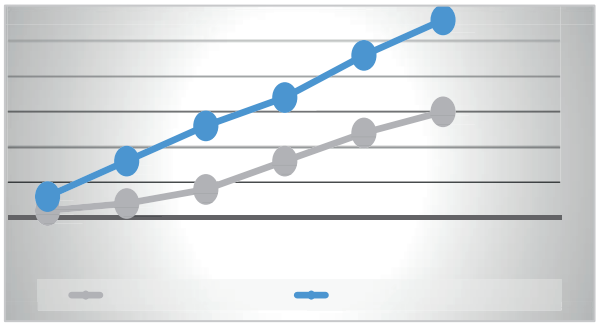

Figure 8. Trends Between Charging Rate of Wind Charger and Conventional Charge

The above graph in figure 8 clearly describes the difference between the charging rates of both the Wind Powered charger and the Conventional Charger. However, the conventional charger charges the mobile quickly. But it works with the help of electric power. Where the Wind -Powered charger harness the wind energy, which is a natural resource to charges the mobile. Thus, this portable wind-powered charger provides a sustainable and eco-friendly method to charge electronic devices.

V. Conclusions

The use of wind energy for portable mobile charging presents an innovative and sustainable solution to address the increasing demand for mobile power [16]. By utilizing wind power, we can reduce our reliance on traditional energy sources and contribute to a greener future. Portable wind turbines offer a flexible and convenient way to generate electricity, [17] [18] enabling users to charge their mobile devices even in remote locations or during outdoor activities. Wind power is an abundant and inexhaustible energy source that does not produce harmful emissions or contribute to climate change. Furthermore, the use of wind energy for portable mobile charging promotes energy independence [19] and empowers individuals to take control of their power needs. With the advancements in technology, portable wind turbines have become more efficient, compact, and affordable, making them accessible to a wider range of users.[20] However, it is important to acknowledge the challenges associated with portable wind charging, such as the variability of wind resources and the need for appropriate wind conditions for optimal charging efficiency. It combines the benefits of renewable energy with the convenience of portable technology, paving the way for a cleaner and more environmentally conscious future.

The utilization of wind energy for portable mobile charging has gained significant momentum in recent years [21] [22]. As we look towards the future, there are several exciting possibilities and potential advancements in this field. Here are some future scopes for portable mobile charging using wind energy:

1. Technological Improvements: With ongoing advancements in renewable energy technology, we can expect the development of more efficient and compact wind energy harvesting devices specifically designed for portable mobile charging. These devices may incorporate innovative materials, enhanced aerodynamic designs, and optimized power conversion systems to maximize energy generation.
2. Miniaturization and Integration: Future developments may lead to the miniaturization and integration of wind energy harvesting technologies into portable mobile charging solutions. This could involve the incorporation of small wind turbines directly into mobile devices or the development of compact wind energy harvesting accessories that seamlessly integrate with smartphones and other portable electronics.
3. Energy Storage Solutions: One of the key challenges in portable mobile charging using wind energy is the intermittent nature of wind resources. Future research may focus on improving energy storage technologies, such as advanced batteries or supercapacitors, to efficiently store excess energy generated by wind turbines. This would enable continuous and reliable charging of mobile devices, even when wind resources are limited.
4. Hybrid Energy Systems: The integration of multiple renewable energy sources into hybrid energy systems holds great potential. In the future, we may witness the combination of wind energy harvesting with other renewable sources like solar or kinetic energy to create more robust and efficient portable charging solutions. Such hybrid systems could offer greater charging capacity and increased reliability, ensuring uninterrupted power supply for mobile devices.

5. Application Diversification: As the technology matures, portable mobile charging using wind energy could find application beyond personal devices. Industries such as outdoor recreation, emergency response, and remote areas with limited access to electricity could benefit from ruggedized and efficient wind energy-based charging solutions. These could include portable charging stations for multiple devices or specialized chargers for specific purposes, catering to a wide range of user needs.

6. Environmental Impact: In the future, there may be a greater emphasis on sustainable and environmentally friendly solutions. Portable mobile charging using wind energy aligns well with this objective, as it harnesses a clean and renewable energy source. As awareness and demand for eco-friendly technologies increase, the future scope of wind energy-based mobile charging could expand significantly.

The future of portable mobile charging using wind energy holds immense potential for technological advancements, miniaturization, integration, energy storage solutions, hybrid energy systems, application diversification, and environmental impact. These developments will not only enhance the convenience and reliability of portable charging but also contribute to a more sustainable and greener future.

REFERENCES

[1] R. Rajan, V. Panchalogaranjan, V. Aravinthan, T. Thiruvaran and V. Shanmugarajah, "Low- Cost Portable Wind Power Generation for Mobile Charging Applications," 2018 IEEE International Conference on Information and Automation for Sustainability (ICIAfS).

[2] Saikumar.P, Thamaraikannan.D, Yuvaraj.G, Yuvaraj.C, “Wind Energy Based Mobile Battery Charging and Battery Applications”, International Journal for Research and Development in Engineering (IJRDE).

[3] Shafiur Rahman, Dr.M.G. Patil, “Development of wind powered mobile charger”, International Journal of Research in Aeronautical and Mechanical Engineering.

[4] Pawan Vijay, Tanuj Manglani, Pankaj Kumar, Ramkishan Meena, Anita Khedia, “Wind and Solar Mobile Charger”, International Journal of Recent Research and Review, Vol. VII, Issue 4, December 2014.

[5] Kharudin Ali, Wan Syahidah Wan Mohd, Damhuji Rifai, Muaz Ishtiyaq Ahmed, Asyraf Muzzakir and Tg Ammar Asyraf, “Design and Implementation of Portable Mobile Phone Charger using Multi-directional Wind Turbine Extract”, International Journal of Science and Technology, Vol. 9(9), March 2016.

[6] Rajesh, R., & Sudhakar, M. (2020). Portable wind energy harvesting using a hybrid win turbine for mobile charging applications. International Journal of Green Energy, 17(2), 96-104.

[7] Xie, X., & Xiao, B. (2018). Study on the portable wind power generation device based on dualrotor wind turbine. Applied Sciences, 8(8), 1423.

[8] Prakash, B., & Ravi, V. (2021). Design and optimization of portable wind turbine charger. IOP Conference Series: Materials Science and Engineering, 1010(1), 012060.

[9] Verma, A., & Mittal, S. (2019). Portable wind turbine: A sustainable solution for mobile charging. International Journal of Innovative Technology and Exploring Engineering, 8(12S3), 218-220.

[10] Kalyani, R., & Saravanan, S. (2018). Portable wind energy harvesting using vertical axis wind turbine for mobile charging. International Journal of Mechanical Engineering and Technology, 9(11), 1744-1751.

[11] Prasad, P., & Shrivastava, A. (2021). Design and analysis of a portable wind turbine charger. International Journal of Renewable Energy Research, 11(4), 2027-2036.

[12] Banik, D., & Bhattacharya, B. (2019). A compact and portable wind turbine system for mobile charging. International Journal of Renewable Energy Technology, 10(2), 156-173.

[13] Weng, X., Qian, Y., & Li, Y. (2020). Development of a portable wind energy harvesting system for mobile charging. In 2020 IEEE Energy Internet and Energy System Integration Conference (EI2) (pp. 1-6). IEEE.

[14] Brännström, F., Leijon, M., & Bernhoff, H. (2017). Wind energy harvesting using small-scale wind turbines for battery charging. Energies, 10(9), 1413.

[15] Radziemska, E., Bogacz, A., & Markowski, P. (2018). The assessment of the possibility of charging the phone battery with the use of portable wind turbines. Energies, 11(6), 1523.

[16] Agrawal, P., & Sharma, S. (2022). Portable wind turbine for mobile charging: A review. In IOP Conference Series: Materials Science and Engineering, 1234(1), 012003.

[17] Zhang, Y., Tan, Z., & Zou, Z. (2019). Design and performance evaluation of a portable wind turbine for mobile charging. Energies, 12(13), 2565.

[18] Maqsood, M., Hussain, S., & Khalid, Z. (2021). Design and analysis of portable wind turbines for mobile charging. International Journal of Advanced Computer Science and Applications, 12(1), 442-449.

[19] Doye, D., & Sharma, P. K. (2020). Design and simulation of portable wind turbine for mobile charging. In 2020 2nd International Conference on Intelligent Computing and Control Systems (ICICCS) (pp. 309-314). IEEE.

[20] Afolabi, O., Adegboye, F., & Olugbayode, S. (2021). Design and development of portable wind turbine for mobile charging. International Journal of Mechanical and Production Engineering Research and Development, 11(1), 267-276.

[21] Zhang, J., Huang, W., & Zhang, H. (2022). Research on portable wind turbine for mobile phone charging. In 2022 7th International Conference on Energy Science and Electrical Engineering (ICESEE) (pp. 464-469). IEEE.

[22] Han, W., & Li, H. (2021). Design and optimization of a portable wind turbine for mobile charging. In 2021 International Conference on Mechatronics, Robotics and Automation (ICMRA) (pp. 260-265). IEEE.

E-ISSN 2581 – 7957
P-ISSN 2277 – 3916
CVR Journal of Science and Technology, Volume 25, December 2023
DOI: 10.32377/cvrjst2512

IoT Enabled Power Theft Detection System

N. Swapna[1] and V. Sreelatha Reddy[2]
[1]Asst. Professor, Guru Nanak Institutions Technical Campus/ECE Department, Hyderabad, India
Email: swapnan.ecegnitc@gniindia.org
[2]Sr. Asst. Professor, CVR College of Engineering/EIE Department, Hyderabad, India
Email: srilathareddy.cvr@gmail.com

***Abstract*: The unauthorized appropriation of electrical power poses a significant challenge within global power system networks, and it is strictly prohibited by legal regulations. The imperative to discern the location of power theft is crucial for enabling legal recourse against perpetrators. The system consists of an ESP32 module, a Long-Range Communication Module, an OLED display, and current transformers. Given the limitations of conventional meters in handling high currents, current transformers are employed for their detection. One current transformer measures the load's current, while the other measures the supply current, both connected to the power supply terminals to ascertain the electrical power output by the source. An IoT-based power theft detection system has been successfully deployed, complemented by Long-Range Communication for enhanced backup protection, as detailed in this research paper.**

***Index Terms*: power theft, Internet of Things (IoT), Sensors, protocol.**

I. Introduction

The issue of power theft is of contemporary significance, inflicting substantial financial losses upon electricity providers, with particular prominence in countries like India where such incidents are alarmingly frequent. Implementing proactive strategies to curb power theft holds the potential for substantial power *conservation. The* application of an electrical power theft detection system plays a pivotal role in the identification of unauthorized tapping on distribution lines, extending its utility to local neighborhoods and broader distribution networks within the electrical power supply system. The existing system grapples with shortcomings in accurately pinpointing the precise location of unauthorized taps. In contrast, the proposed system is meticulously designed to locate the specific electrical line subject promptly and accurately to tampering in *real time*. The paramount importance of a stable and dependable power grid in modern society cannot be overemphasized. The blackout that transpired in India in July 2012 serves as a poignant example, affecting over 60 million individuals and plunging 20 out of 28 Indian states into darkness. This incident served as a stark reminder of the inadequacies of the traditional power grid, which astonishingly still adheres to designs dating back more than a *century. In* response to the advancements in data systems and communication technology, numerous countries are actively engaged in the modernization of their aging power grids, ushering in the era of smart grids. These smart grids offer bidirectional energy transmission, unwavering reliability, and real-time functionalities, empowering them to facilitate demand response, self-healing capabilities, and heightened security. Smart grids encompass a spectrum of operational and energy measures, including the deployment of smart meters, *and* intelligent appliances, harnessing renewable energy resources, and enhancing energy efficiency. This research paper embarks on an exploration of these critical dimensions and their implications.

A. Objective

The fundamental objective of this research project is to detect cases of power theft, dissuade unauthorized power consumption, and ultimately ensure the secure and lawful utilization of electrical power.

Automated Operation: The power theft system aims to automate the authorized power utilization, eliminating the need for manual protection of power systems. By utilizing sensors, actuators, and IoT connectivity, the system can collect data, analyze it, and alert the surroundings and complaints of the electricity board based on predefined algorithms. The objective of a power theft system is to save the power there, enhancing the nation's wealth.

Remote Monitoring and Control: Another objective of a power theft system based on IOT technology is to enable remote monitoring of power security. By integrating with cloud platforms, the electricity board receives notifications and alerts.

Energy Efficiency: As soon as power energy theft occurs the load gets disconnected, and the system sends the signals to the authorized power station hence utilizing the power energy efficiently.

power theft systems also focus on optimizing energy usage.

B. Motivation

Power burglary alludes to the unlawful or unapproved utilization of power without appropriate installment to the service organization. This can happen through different means, like messing with meters, utilizing sidesteps, or controlling the wiring to keep away from meter readings. Power burglary can have critical unfortunate results for service organizations, purchasers, and society all in all. Here are a few inspirations for executing tasks to battle power burglary.

Monetary Misfortune Counteraction: Influence burglary prompts significant income misfortunes for service organizations, as they can't charge clients precisely for the power consumed. These misfortunes can affect the organization's monetary security and capacity to put resources into framework upgrades.

Received on 18-08-2023, Revised on 02-11-2023, Accepted on 28-11-2023.

Decency and Value: Power robbery puts uncalled-for trouble on fair purchasers who cover their bills instantly. Tending to drive robbery guarantees that all shoppers contribute their reasonable portion toward the expense of power age and appropriation.

Administration Quality: Power burglary can strain the power matrix and lead to blackouts or diminished help quality for authentic clients. By tending to control burglary, service organizations can further develop administration dependability and generally speaking network execution.

Energy Protection: Unapproved utilization of power adds to the wastage of important assets. Tending to drive robbery is in accordance with energy preservation endeavors, advancing reasonable energy rehearse.

Lawful and Administrative Consistence: Power burglary is unlawful and frequently abuses utility guidelines. Carrying out measures to forestall power burglary guarantees consistent with regulations and guidelines overseeing the energy area.

Mechanical Development: Power burglary avoidance projects frequently include the turn of events and sending of cutting-edge innovations, for example, shrewd meters, information investigation, and remote observing frameworks. These activities drive mechanical advancement in the energy business.

Financial Turn of events: Addressing power robbery can add to a steady and solid energy supply, which is critical for monetary development and improvement. Organizations and businesses require a reliable and reasonable energy supply to work proficiently.

Decreasing Carbon Impression: Forestalling power burglary can prompt more exact energy utilization information, which thusly helps service organizations better arrange and upgrade energy age. This can add to a more productive utilization of assets and a decrease in ozone-depleting substance discharges.

Purchaser Training: Power burglary avoidance projects frequently incorporate instructive missions to bring issues to light about the unfortunate results of forcible robbery. Teaching buyers about the significance of paying for the power they use can assist with cultivating a feeling of obligation.

By and large, the inspiration driving power burglary counteraction projects is to make a fair, productive, and maintainable energy dissemination framework that benefits both service organizations and shoppers while advancing capable energy utilization rehearses.

II. Literature Review

[1] The proposed system employs two methods for detecting power theft: the measurement and comparison of current. Current is measured at the distributor box and transmitted to a server database via GSM/GPRS for each household. Simultaneously, electric meters within individual homes gauge and transmit current data to the server, accompanied by user information and a photograph of the residence via a mobile app. Upon detecting a marginal variance between the distributor box and electric meter current readings, the server identifies power theft. Subsequently, user particulars, including the address and an area photograph, are relayed to an authorized mobile app, while latitude and longitude data are utilized to pinpoint the location of the theft on Google Maps. This process is also applied to uncover instances of hooking on individual electric poles.

[2] Muhammad Badar Shahid and colleagues discussed the significant issue of non-technical power losses, primarily resulting from electricity theft in countries like Pakistan. These thefts lead to substantial financial losses and jeopardize the nation's economic stability. The prevalent forms of theft include consumer-side tampering, like meter bypassing, and line-side theft through the "Hooking" system. In order to address these thefts and mitigate their economic repercussions, we introduce an innovative solution. Our theft detection algorithm has the capability to recognize unauthorized power consumption at both the consumer's end (meter tampering) and within the distribution lines (hooking) by means of consumer load profiling. When instances of theft are identified, our prevention algorithm takes prompt action by disconnecting all legitimate consumers and delivering a high-voltage pulse to the distribution line, rendering illicit connections nonfunctional.

[3] This paper discusses the controller-based system that gathers voltage and current data from the LT side of distribution transformers and household energy meters. The energy meter data is wirelessly transmitted to the main control unit on the LT side of the distribution transformer. By analyzing voltage drops and current changes in the distribution line caused by power theft, the system detects and locates the theft. It then signals the circuit breaker to interrupt power and rechecks for theft. In case theft persists even after four attempts, the system initiates a complete system reset and dispatches an alert message to the electricity provider or the nearest substation, providing precise information about the location of the theft. Testing of this system using MATLAB has yielded satisfactory results.

[4] This paper presents an inventive approach to measuring and billing energy consumption, offering an alternative to conventional methods. In light of the growing adoption of renewable energy sources and decentralized power generation, the advancement of smart grid technologies has become ever more crucial. The proposed smart energy meter system seamlessly integrates an embedded controller and a GSM module to transmit data, including energy consumption in kilowatt-hours (kwh), billing information, and security alerts, over GSM mobile networks. This system also maintains continuous monitoring of energy meter readings and sends notifications such as low balance and zero balance alerts to designated phone numbers via a GSM modem.

[5] Discussed the various kinds of Electricity theft have been a persistent problem and emerged as a significant issue, particularly in developing countries like India. This illicit activity has adverse effects on the economy and hampers the

overall growth of the nation, as the progress of the power sector is intricately linked with the country's economic development. In India, power theft takes various forms, with tapping into power lines being a common method. To address this challenge, a system based on Arduino Uno has been developed for the automatic detection and measurement of power theft. Whenever unauthorized power consumption is detected by this system, it promptly alerts the relevant authorities.

[6] Proposed that Energy theft is a significant problem in developing countries like India, Pakistan, and Sri Lanka. Illicit electricity use can severely disrupt a country's economy. Detecting and addressing such theft at the individual level in real-time applications is challenging. Various methods of energy theft, such as meter tampering, meter bypassing, and direct line hooking exist. This paper presents a solution for detecting energy theft using Arduino and a GSM module. An LCD displays power usage data, including the discrepancy between legitimate consumption and theft, which is then transmitted via GSM to the electricity board and the consumer, along with transformer details. The system is equipped with power backup, ensuring uninterrupted message transmission even during power failures, streamlining the reporting process to the electricity board.

[7] The paper addresses the critical issue of electricity theft, which is on the rise, especially in developing nations such as India, leading to various challenges. In response, this paper proposes a method for identifying theft, notifying users, and discontinuing the power supply upon detecting unauthorized activities. The system utilizes GSM technology to send SMS notifications to users and is integrated with a specialized energy meter equipped with a relay, effectively tackling non-technical losses, billing discrepancies, and voltage fluctuations.

[8] To address power theft, a system has been proposed that relies on current measurement and comparative analysis. The process of current distribution initiates from the electric pole, extending to an intermediary distributor box, and ultimately reaching individual residences. The distributor box periodically measures current and forwards this data to the respective server database for each household via the GSM/GPRS network. Simultaneously, each household is equipped with an electric meter for current measurement, and this data is regularly transmitted to the server database through the use of GSM/GPRS technology. Additionally, during the installation of the electric meter, user information is entered into the database using a user-friendly mobile application. This information encompasses the user's address, latitude, and longitude, which are obtained from the mobile GPS, and includes a photographic record of the user's residence or the surrounding area.

[9] Discussed that the importance of electrical energy in both industrial and household contexts cannot be overstated. However, the escalating demand for electricity has given rise to a pressing concern – the rampant issue of power theft. In nations like India, power theft contributes to a substantial 30%-40% of the total generated power, resulting in significant financial losses for electricity boards. This paper introduces an innovative approach to tackle power theft by detecting unauthorized activities, promptly notifying consumers, and disconnecting the supply as needed. The system is designed to automatically send SMS alerts to users via a GSM module. Moreover, the system incorporates a distinctive energy meter equipped with a relay to effectively address non-technical losses, billing discrepancies, and voltage fluctuations.

[10] This paper addresses power theft issues in low-voltage distribution using smart meters and IoT. The system utilizes real-time power theft detection through linear regression, complemented by Android applications to monitor consumer data and promptly notify relevant authorities. The system detects theft from meter bypass, tampering, and line hooking. Additionally, it enables distribution authorities to control the power supply for individual consumers using a prototype circuit with ATmega328P and NodeMCU.

[11] Proposed a method in Southeast Asian countries experiencing rapid economic growth, largely driven by power generation. However, transformer theft is a prevalent issue hindering progress. To address this, a GSM-based system has been developed to protect distribution transformers from theft and monitor their health parameters using sensors like magnetic, IR, and weight sensors. The system alerts authorities via SMS about theft attempts and provides real-time information on transformer health, including temperature and oil level.

III. Implementation

An IoT-enabled power theft detection system that utilizes IoT technology requires various hardware components to detect the power theft. The key components of this system include the ESP32, meter reading, current, voltage sensors, OLED, Zigbee, Relay Driver, and buzzer. By integrating these hardware components, the power theft detection system effectively oversees, identifies, and manages power theft incidents. The integration of IoT technology empowers efficient authorized power usage, leading to the country's economic growth.

Figure 1 illustrates a block diagram for an IoT-based power theft detection system. The system includes the following components.

Sensors: Different sensors are sent into the framework to gather pertinent information. These sensors can incorporate meter perusing, current, and voltage sensors. They give continuous data about the power essential for compelling power robbery and control frameworks.

IoT: The Internet of Things (IoT) represents yet another breakthrough technology in the field of Information Technology. It facilitates the interconnection of a wide array of devices, including sensors, actuators, PLCs, and various smart embedded electronic devices and controls, as well as diverse software applications. This connectivity and network infrastructure enable seamless communication among these diverse devices, facilitating the exchange of information.

CVR Journal of Science and Technology, Volume 25, December 2023
DOI: 10.32377/cvrjst2512

ESP32: The ESP32 is a series of robust, energy-efficient, cost-effective microcontrollers equipped with integrated Wi-Fi and dual-mode Bluetooth capabilities. It is a single 2.4 GHz WIFI-and-Bluetooth combination chip developed using TSMC's super low-power 40 nm technology. Designed to deliver optimal power and RF performance, it exhibits resilience, versatility, and reliability across a wide range of applications and power scenarios.

A. Block diagram

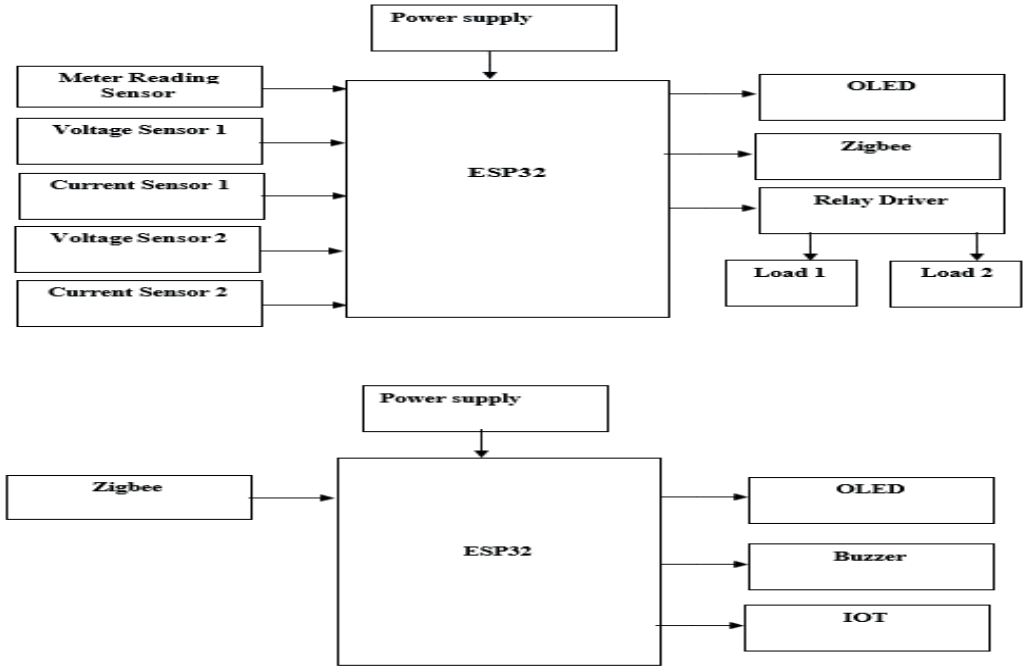

Figure 1. Block Diagram for Power Theft Detection System

OLED: OLED, which stands for Organic Light Emitting Diodes, is a flat-panel light-emitting technology achieved by placing a series of organic thin films between two conductors. When an electrical current is applied, it emits vibrant light. OLEDs are self-illuminating displays that do not require a backlight, making them thinner and more efficient compared to LCD displays, which rely on a white backlight. Notably, OLED displays offer not only slimness and efficiency but also the highest image quality, with the potential for transparency, flexibility, foldability, and even rollability and stretchability in the future. OLEDs represent the future of display technology.

Actuators (Relay Driver): The ULN2003 is a solid IC comprised of seven NPN Darlington semiconductor matches with high voltage and flow capacity. It is commonly employed in various applications such as relay drivers, motor drivers, display drivers, LED light drivers, logic buffers, line drivers, solenoid drivers, and other high-voltage current applications. The ULN2003 is extensively utilized in relay control and stepper motor control applications.

Zigbee: Zigbee is a specification for the establishment of high-level communication protocols utilized to establish functioning personal area networks from small, low-power digital radios. Based on the IEEE 802.15 standard, Zigbee devices, while low-powered, can often transmit data over extended distances by relaying information through intermediate devices to reach more distant ones, creating a mesh network. This network operates without centralized control or a high-power transmitter/receiver capable of reaching all of the networked devices.

The decentralized nature of these wireless ad-hoc networks makes them well-suited for situations where reliance on a central node is not feasible. Zigbee protocols are designed for embedded applications that demand low data rates and minimal power consumption. As a result, the resulting network operates with minimal power requirements, with individual devices expected to have a battery life of at least two years to meet Zigbee certification standards.

A bell or beeper is a signaling device, typically electronic, commonly found in vehicles, household appliances like microwaves, or game shows. It typically consists of multiple switches or sensors connected to a control unit that determines if a button has been pushed or a preset time has elapsed. It often illuminates a light on the corresponding button or control panel and emits a warning signal in the form of a continuous or intermittent buzzing or beeping sound. Initially, this device was based on an electromechanical system, similar to an electric bell without the metal gong that produces the ringing noise. These units were frequently mounted on walls or ceilings and used the structure as a resonating surface.

Another approach, especially with some air conditioner-related devices, involved implementing a circuit to capture

CVR Journal of Science and Technology, Volume 25, December 2023
DOI: 10.32377/cvrjst2512

the air conditioner's current noise, amplifying it to the extent it could drive a speaker, and then connecting this circuit to an inexpensive 8-ohm speaker. Nowadays, it's more common to use a ceramic-based piezoelectric sounder like a son alert, which generates a high-pitched tone. Typically, these sounders were linked to "driver" circuits that could modify the sound's pitch or toggle it on and off.

The power supply section is responsible for providing +5V to the components for their operation. The LM7805 IC is employed to deliver a stable +5V power source. To ensure the power theft system functions effectively, it necessitates a consistent power supply to operate sensors, IoT devices, technical equipment, and actuators. This can be achieved through a combination of mains power, batteries, solar chargers, or other sustainable energy sources.

B. Schematic Diagram

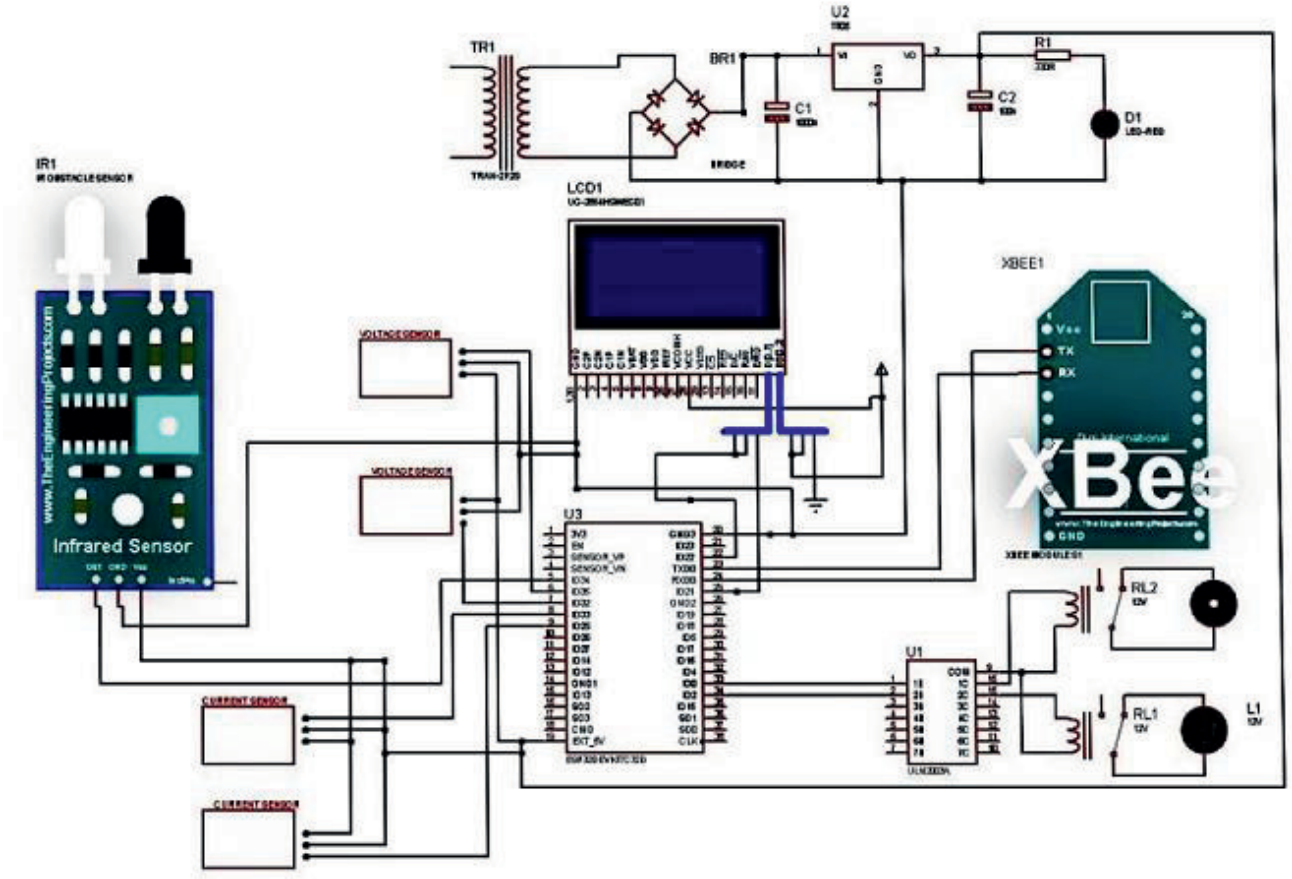

Figure 2. Schematic diagram of the System

The schematic diagram of the system is depicted in Figure 2. An IoT-based power theft detection system typically comprises multiple components and sensors working collaboratively to safeguard power from unauthorized usage. Below is an overview of a standard schematic diagram for this system:

1. IR sensor: The framework starts with an IR sensor. Working on IR sensors is extremely straightforward, and the working standard is completely founded on a change in the obstruction of the IR recipient. Here in this sense, we associate IR recipient in switch predisposition, so it gives exceptionally high obstruction on the off chance that it isn't presented to IR light. The obstruction for this situation is in the scope of the Super ohms, however when the IR light is considered back and falls IR recipient. The opposition of Rx comes in a range between Kilo ohms to many ohms. We convert this adjustment of protection from a change in voltage. Then, at that point, this voltage is applied to a comparator IC which contrasts it and an edge level. On the off chance the voltage of the sensor is more than the limit, the yield is high it is low which can be utilized straightforwardly for microcontrollers.

2. Voltage Sensor: A Voltage Sensor is a device that converts the voltage measured between two points in an

E-ISSN 2581 – 7957
P-ISSN 2277 – 3916

DOI: 10.32377/cvrjst2512

electrical circuit into a physical signal proportional to that voltage. The voltage sensor circuit is a combination of various electronic components, allowing the precise measurement of voltage values. Potentiometers and ADC (Analog-to-Digital Converter) are key components commonly used in voltage sensors.

3. A current sensor is a device that detects and transforms current into a readily measurable output voltage, directly proportional to the current passing through the measured path. This output can be utilized to display the measured current on an ammeter, stored for further analysis in a data acquisition system, or employed for control purposes.

4. Microcontroller: Upon detecting power theft, the controller supplies a 5V operating voltage to the relay, disconnects the load from the power source, and halts any further power theft attempts. Consequently, this system automatically alerts and isolates the supply from the load, effectively preventing theft.5. Driver: at whatever point the transfer driver gets the high voltage from the regulator, the ringer makes a blaring sound, and the bulb (load) gets detached from the supply.

6. OLED: The situation with activity is shown obviously on OLED i.e., when power robbery happens, we can notice the text "power burglary occurred" on OLED. Simultaneously, the signal makes a blaring sound.

7. Zigbee: Finally, the Zigbee convention is liable for correspondence among every one of the parts of the power-robbing framework.

C. Flowchart

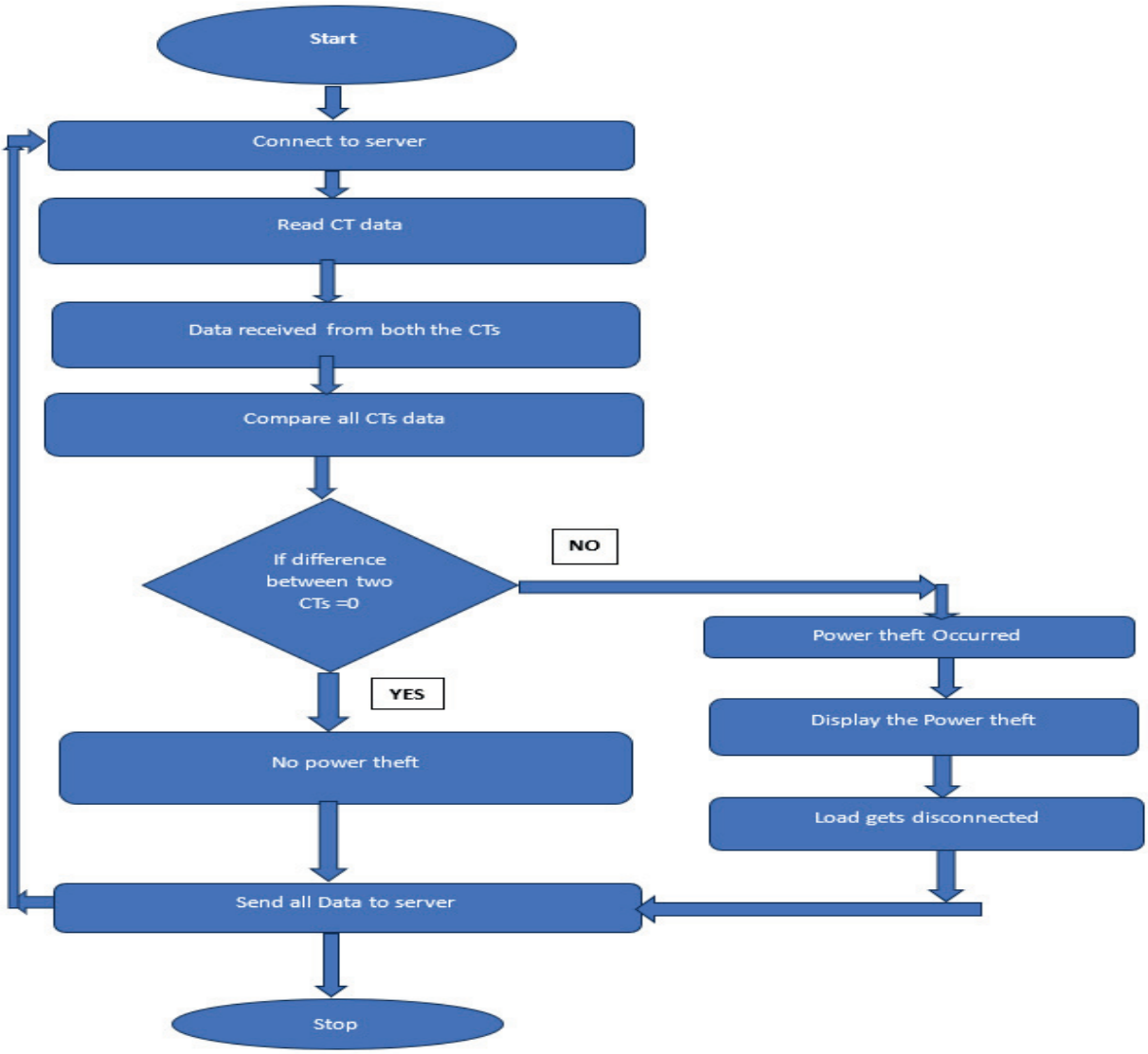

Figure 3: System Flowchart

CVR Journal of Science and Technology, Volume 25, December 2023
DOI: 10.32377/cvrjst2512

IV. RESULTS

The implementation of an efficient power theft system using IoT technology can yield several positive outcomes. Here are some potential results:

1. Real-time monitoring: The power theft system monitors the power theft and used in various fields like Utility companies, Residential and commercial buildings, Law Enforcement Agencies, and Electrification.

2. Wireless connectivity: As the technology used here is IOT so much wiring equipment is avoided.

3. Timely Alerts and Notifications: Using the Zigbee protocol integrated with IoT technology and different actuators, whenever the power theft occurs it not only protects the unauthorized power usage but also alerts the people surrounding and the electricity board in time.

4. Efficient Resource Allocation: As the power theft system uses different components and due to the automation process the manual intervention was reduced. This saves time and effort for users, allowing them to focus on other important tasks. Enhanced Security Measures: The IoT-based power theft system provides more security for the electricity by alerting authorized persons. The system also protects the unauthorized usage of power in an illegal manner. Overall, the power theft system using IoT technology can result in power protection, Acknowledgment the authorized persons, cost savings, improved national property and yield, and time efficiency. These outcomes demonstrate the potential of IoT-enabled power theft systems. The complete hardware setup is shown in Figure 4

This system also used in

1. Utility companies- used to monitor and detect instances of power theft within theirdistribution networks.
2. Residential and commercial buildings- used to monitor electricity consumption anddetect any unauthorized tapping.
3. Law Enforcement Agencies- utilized to support their investigations and crack down on illegal activities related to power theft.
4. Electrification- used to curb power theft effectively ensures the availability to all consumers and promotes fair electricity distribution in underserved regions.

A. Abbreviations

TABLE I.
ABBREVIATIONS

Abbreviation	Definition
CT	Current Transformer
OLED	Organic Light Emitting Diode.

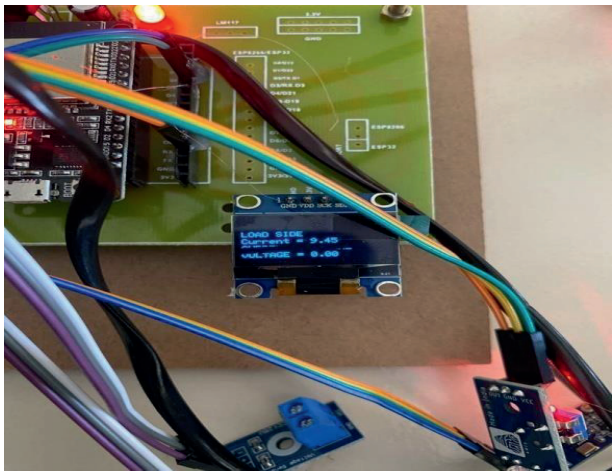

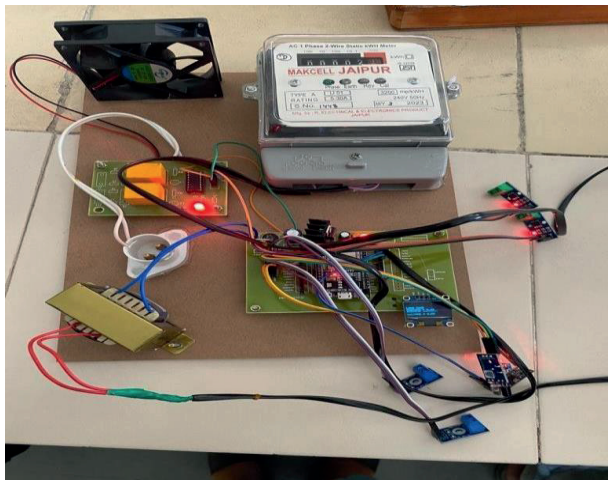

Figure 4. Hardware Setup of the system

V. CONCLUSIONS

In summary, the deployment of an IoT-based power theft system presents notable advantages within the realm of smart city advancements. This research project places a primary emphasis on bolstering connectivity and networking elements within the IoT framework. Over the course of this study, we have achieved successful power theft detection, fault identification, and precise fault location tracking, enabling the implementation of necessary corrective measures. The proposed system adeptly tackles various prominent challenges inherent in the current Indian grid infrastructure, encompassing energy conservation, power theft prevention, and cable fault management. It is worth highlighting that the system's efficient power utilization leads to substantial cost reductions, establishing its economic viability for the electricity board.

The project demonstrated that utilizing Internet of Things (IoT) technologies for power theft detection can significantly enhance accuracy compared to traditional methods. By integrating smart meters, sensors, and data analysis techniques, the system achieved a high level of precision in

identifying and distinguishing between legitimate power consumption and unauthorized usage.

Future Directions: The project identified potential avenues for further research and development, such as exploring advanced machine learning techniques to enhance detection accuracy, integrating renewable energy sources into the IoT framework, and investigating novel approaches to user-friendly interfaces for end-users.

REFERENCES

[1] N. K. Mucheli *et al.*, "Smart Power Theft Detection System," *2019 Devices for Integrated CircuitDevIC)*, March 2019.

[2] Muhammad Badar Shahid, Muhammad Osama Shahid, T. Hasan, and S. Saleem, "Design and Development of An Efficient Power Theft Detection and Prevention System through Consumer Load Profiling," *2019 International Conference on Electrical, Communication, and Computer Engineering (ICECCE)*, Jul.2019.

[3] Mohd Uvais, "Controller Based Power Theft Location Detection System," *International Conference on Electrical and Electronics Engineering*, Feb.2020,

[4] C. Santhosh, S. V. Aswin Kumar, J. Gopi Krishna, M. Vaishnavi, P. Sairam, and P. Kasulu, "IoT based smart energy meter using GSM," *Materials Today: Proceedings*, vol. 46, Mar. 2021, doi: Accessed: Oct. 30, 2023.

[5] V. R. Pawar, J. J. Jadhav, J. Saha, and S. S. Jadhav, "Arduino Uno Based Automatic Power Theft Detection," *Journal For Basic Sciences*, vol. 23, no. 5, May 2023.

[6] T. Shahzad Gill *et al.*, "IoT Based Smart Power Quality Monitoring and Electricity Theft Detection System," *IEEE Xplore*, Dec. 01, 2021.

[7] Bandarupalli Deepthi, V. Naga, and P. V. Naidu, "Detection of Electricity Theft in the Distribution System using Arduino and GSM," 2019 International Conferenceon Computation of Power, Energy, Information and Communication (ICCPEIC), Mar. 2019.

[8] V. Jaiswal, Hritik Kumar Singh, and K. Singh, "Arduino GSM based Power Theft Detection and Energy Metering System," 2020 5th International Conference on Communication and Electronics Systems (ICCES), Jun. 2020.

[9] M. J. Jeffin, G. M. Madhu, A. Rao, G. Singh, and C. Vyjayanthi, "Internet of Things Enabled Power Theft Detection and Smart Meter Monitoring System," 2020 International Conference on Communication and Signal Processing (ICCSP), pp. 0262–0267, Jul. 2020.

[10] X. Feng et al., "A Novel Electricity Theft Detection

[11] Scheme Based on Text Convolutional Neural Networks," Energies, vol. 13, no. 21, p. 5758, Nov. 2020.

[12] R. E. Ogu and G. A. Chukwudebe, "Development of a cost-effective electricity theft detection and prevention system based on IoT technology," Nov. 2017.

E-ISSN 2581 – 7957
P-ISSN 2277 – 3916

CVR Journal of Science and Technology, Volume 25, December 2023
DOI: 10.32377/cvrjst2513

Effective Event Exposure Classifier (E3C) in Wireless Sensor Network through SVM

G. Malleswari[1], A. Srinivasa Reddy[2]
[1]Asst. Professor, CVR College of Engineering/CSE Department, Hyderabad, India
Email: gkmalleswari@gmail.com
[2]Asst. Professor, CVR College of Engineering/ET Department, Hyderabad, India
Email: srinivas.asr@gmail.com

Abstract: **A Wireless Sensor Network (WSN) is composed of distributed nodes designed for environmental monitoring and event detection. To optimize energy usage during correlated data gathering, the Correlated Data Gathering (CDG) scheme utilizes the Adaptive Routing algorithm. While this approach effectively conserves energy, it introduces a significant energy-delay tradeoff when securing data within the sensor network. In response to this challenge, the E3C-SVM system leverages Support Vector Machine (SVM) classification with minimal energy consumption to assess event significance. E3C-SVM also employs the Doppler Effect method for efficient sensing data event recovery, particularly in identifying periodic events caused by moving objects. By reducing classification time, E3C-SVM mitigates the energy-delay tradeoff. Furthermore, E3C-SVM incorporates a mechanism for generating event-specific keys, reducing energy consumption during key generation, and enhancing security when broadcasting notifications to sensor nodes. This feature elevates the security level of object collection. Experimental evaluations primarily assess classifier performance, security levels, and energy consumption rates.**

Index Terms: **Correlated Data Gathering, Wireless Sensor Network, Support Vector Machine, Classification time, Adaptive Routing.**

I. Introduction

Due to the different positions of items in Wireless Sensor Networks (WSNs), the presence of several sensor nodes frequently results in significant correlations. Occasionally, transmitting data from all these sensors to the destination can result in heightened network traffic and congestion. This practice not only increases network congestion but also leads to congestion at the destination nodes, subsequently elevating the overall energy consumption of the network. To tackle these challenges, several researchers have proposed object classification techniques that leverage data aggregation within WSNs to alleviate network traffic. A multi-hop data aggregation strategy has been introduced to enhance energy efficiency and reduce energy consumption throughout the entire network. This strategy primarily focuses on optimizing data aggregation times. To facilitate this, researchers have introduced an integrated algorithm called the Adaptive and Distributed Routing Algorithm, operating within a game theoretic framework to enable efficient data gathering. However, despite achieving a reduction in energy consumption across the network, it's important to note that the energy-delay tradeoff remains a concern when it comes to securing data within the sensor network.

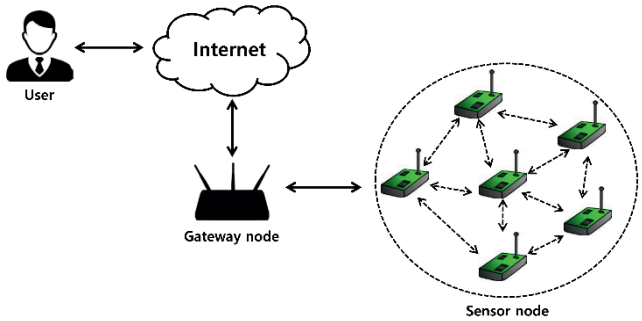

Figure 1. WSN architecture

WSNs encompass networks comprising diminutive, independent sensor nodes endowed with wireless communication capabilities. These nodes are engineered to amass and dispatch data originating from their immediate surroundings. Below, you will find some vital characteristics and constituents of wireless sensor networks:

Sensor Nodes: Sensor nodes serve as the fundamental building blocks within WSNs. They typically take the form of small, cost-effective devices equipped with sensors designed to gauge diverse physical parameters, including temperature, humidity, light, sound, or motion. These nodes often grapple with limited processing capabilities, memory, and energy reservoirs.

Wireless Communication: Sensor nodes engage in wireless communication, both amongst themselves and with a central base station or sink node, using various wireless communication protocols such as Zigbee, Bluetooth, Wi-Fi, or tailor-made protocols. Communication in WSNs can take on the form of single-hop (direct communication with the sink node) or multi-hop (data relayed through intermediary nodes).

Data Collection: Sensor nodes operate in a continuous cycle of gathering data from their immediate surroundings, subsequently transmitting it to a central hub or sink node. This collected data encompasses a wide spectrum, ranging from environmental measurements and surveillance data to any pertinent information relevant to the specific application.

Energy Constraints: Arguably one of the most pivotal challenges confronting WSNs pertains to energy efficiency. Sensor nodes are typically reliant on battery power and possess only finite energy reservoirs. Striking a balance between maximizing the network's operational lifespan and ensuring dependable data transmission constitutes a paramount design consideration.

Received on 26-09-2023, Revised on 20-10-2023, Accepted on 03-11-2023.

Distributed Deployment: Sensor nodes are commonly deployed across an expansive area in a distributed fashion, often in remote or hard-to-access locales. These nodes typically self-organize and must adapt to dynamic changes in network conditions.

Data Processing: Depending on the application, data processing may take place at the sensor nodes themselves, or alternatively, the data can be transmitted to a central base station for processing. The decision hinges on the specific requirements of the application.

WSNs are made up of widely dispersed sensor nodes that oversee gathering and sending environmental data to predetermined locations. This study delved into bandwidth allocation by distributing data slots among multiple users at a significant rate, aiming to ensure Quality of Service (QoS). Furthermore, a mathematical model was developed to evaluate delay metrics for Service Data Units (SDUs) in a multiuser scenario. However, it's crucial to remember that the transmission of the recognition of the effectiveness of this distribution came with a sizable delay. The utilization of wireless sensor networks is experiencing a remarkable surge in applications across various domains, including healthcare, environmental monitoring, and surveillance, among others. While numerous research efforts have introduced data aggregation techniques, these methods often encounter limitations. These constraints were effectively addressed through the inventive design of a base station capable of recovering all aggregated sensing data objects, aptly termed as "recoverable." Although these aggregation techniques successfully reduced transmission overhead, they did so at the cost of a higher energy consumption ratio.

II. Literature Study

Tao Cui et al. [1] investigation “focused on enhancing High-Speed Downlink Packet Access (HSDPA) single-user throughput. In their research, offline and online optimization methods were developed that modified the Channel Quality Indicator (CQI) used by the network to schedule data transmission. By adjusting the CQI in the offline algorithm based on the acknowledgment/negative acknowledgment (ACK/NAK) history, the team was able to reach a particular target block error rate (BLER). They discovered the target BLER that maximizes throughput offline by experimenting with different target BLER values. This technique helps HSDPA allocate resources fairly among many users while simultaneously improving throughput. On the other hand, the online approach does not require a specified goal BLER because it changes the CQI offset using an expected short-term throughput gradient. Additionally, they suggested an adjustable step size device to monitor environmental changes over time. Both algorithms' convergence behavior was examined, and some of the research' conclusions were generalizable to other stochastic optimization methods. Simulations that were used to validate the study's findings also helped to shed light on the ideal BLER target value. When compared to the typical strategy of aiming for a 10% BLER, both the offline and online algorithms showed the potential for up to a 25% improvement in throughput.”

Engin Zeydan et al. [2] investigated that "With the use of energy-efficient data aggregation trees, our study implements multi-hop data aggregation in an effort to reduce the overall energy consumption in wireless sensor networks. We offer an adaptive and distributed routing method designed for the aggregation of correlated data to accomplish this. This algorithm is based on game theory and takes advantage of data correlations between nodes. In this plan, routes are carefully chosen to reduce the network's overall energy consumption. To modify routes in response to local data features, we use the best response dynamics technique. Our routing algorithm's cost function considers a number of variables, such as energy consumption, interference, and in-network data aggregation. Our iterative technique also shows convergence in a finite number of steps, which is significant."

Liang Liu et al. [3] introduced “a fresh method of looking at the coverage issue that centers on target localization in wireless camera sensor networks. They first introduced a special localization-focused sensing model that makes use of camera sensors' capacity for perspective projection. The authors developed a brand-new idea known as "Localization-oriented coverage" (abbreviated as L-coverage) on the foundation of this innovative sensing paradigm. Bayesian estimating theory was employed in the creation of this idea. Additionally, they carried out a thorough research to comprehend the connection between camera sensor density and the likelihood of reaching L-coverage in scenarios of random deployment, where camera sensors are dispersed according to a 2-dimensional Poisson process. The authors set density requirements to get a desired level of L-coverage probability based on their findings regarding the relationship between camera sensor density and L-coverage probability. Detailed simulations were run to validate and rate the efficacy of their proposed models and strategies.”

A.S. Reddy et al. [4] stated that “A Wireless Sensor Network (WSN) is made up of sensor nodes that are responsible for tracking and gathering information about the physical environment and storing it in one place. WSN technology serves as the foundation for emerging network paradigms such as the Internet of Things, Sensor Control Networks, Ubiquitous Sensor Networks, and Machine-Oriented Communications. It is essential to develop an energy-efficient routing protocol in order to carry out the sensing, communication, and processing functions within a WSN. A protocol of this kind is essential for controlling network energy consumption, reducing traffic, and lowering overhead during data transmission phases. Clustering is a crucial strategy for attaining energy balance between the sensor nodes. We use bio-inspired methods, notably the Firefly and Spider Optimization algorithms, to create an ensemble method in our suggested strategy. By routinely recycling data from the source node to the sink, this cutting-edge protocol assists in preventing the development of redundant routing messages, which can cause significant energy waste. The best route path can be chosen more easily thanks to this routing technology. In order to determine the ideal cluster heads in each iteration, our proposed algorithm takes into account a number of factors, including node residual energy, inter-cluster distances to the sink, and cluster overlaps. Furthermore, the parameters of the suggested solution can be dynamically changed when clustering in order

to meet the unique needs of the network and achieve optimal performance."

III. Support Vector Machine

A supervised machine learning approach called Support Vector Machine (SVM) is used for classification and regression. SVMs are notably acclaimed for their prowess in tackling classification tasks, excelling at discerning an optimal decision boundary to segregate data points into distinct classes. The foundation of SVMs hinges on the notion of pinpointing a hyperplane, a flat affine subspace, that achieves the most effective separation of data points across classes. Central to this concept is the maximization of the margin, representing the minimum distance between the hyperplane and its closest data points, known as support vectors. Typically, the margin is denoted as "2/||w||," where "w" signifies the weight vector associated with the hyperplane. An inherent strength of SVMs lies in their capacity to address datasets that are not linearly separable. This capability is realized through the application of kernel functions, which implicitly project the original feature space into a higher-dimensional realm where data points become linearly separable. Various kernel functions serve distinct purposes:

Linear Kernel: Suited for data that can be readily separated by straight lines.

Polynomial Kernel: Ideal for data separable by polynomial curves or surfaces.

RBF Kernel: Effective in handling intricate, non-linearly separable data.

Sigmoid Kernel: Often employed in neural network applications.

In essence, SVMs, bolstered by their kernel functions, provide a versatile and robust tool for a wide spectrum of classification tasks, accommodating both linear and non-linear data separation challenges.

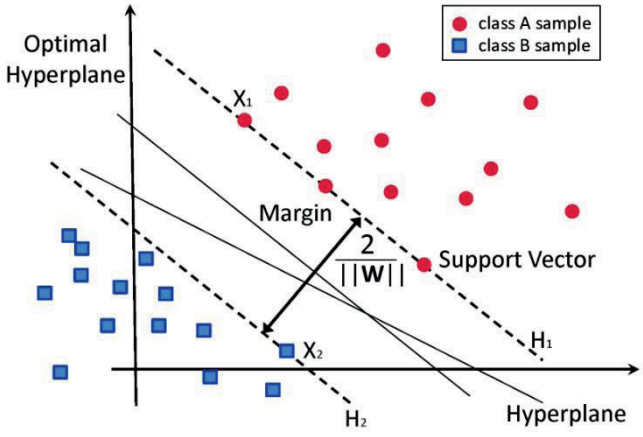

Figure 2. SVM overview

IV. Proposed Methodology

In this specific context, we present a specialized solution known as the Predetermined Event Weight-Based Support Vector Machine, or E3C-SVM, designed for enhancing the efficiency and security of data collection in wireless sensor networks. The core principle underlying our proposed system is the E3C-SVM's capacity to assign event weights in advance within the wireless sensor network, enabling highly efficient node classification with minimal energy consumption. E3C-SVM identifies objects by grouping events differently and establishing decision boundaries to classify events within the sensor network. Our E3C-SVM approach identifies events in the sensor network by maximizing the margin length of hyperplanes, as illustrated in Figure 3. For example, in situations where sensor network nodes are dispersed across a region, monitoring vehicle activities becomes crucial. This system tracks vehicle activities in the designated area while also collecting and categorizing events from various users. E3C-SVM categorizes events related to vehicles based on attributes such as size, shape, and load, all while consuming an exceedingly small amount of energy. Considering that vehicle movements are dynamic within the network, the events in the wireless sensor network also evolve over time.

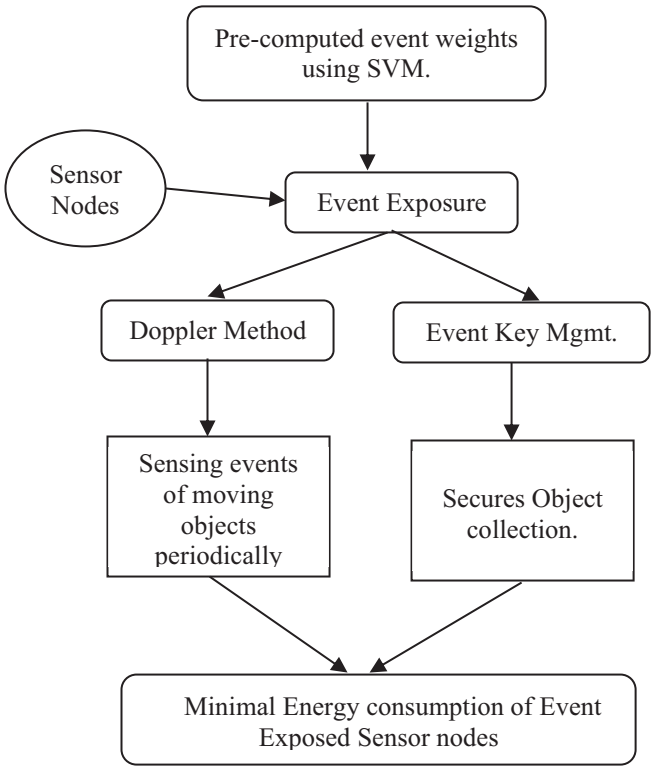

Figure 3. Proposed methodology

Vehicle events are classified by attributes such as shape, load, and size through the utilization of an SVM, where the optimal hyperplane value is chosen to maximize the margin length. Additionally, we introduce the Doppler Effect technique, which can be applied for identifying periodic events across a broad spectrum of frequency ranges. This approach is employed to detect events with diverse frequency characteristics as they propagate from the source object node to the target node. The integration of the Doppler Effect method within E3C-SVM offers efficient event detection with minimal processing time. Despite an increase in frequency values compared to previous iterations, this method minimizes processing time while accurately pinpointing nodes. Additionally, it facilitates the categorization and grouping of similar events, resulting in

reduced energy consumption. E3C-SVM employs security measures through event section key management, ensuring the establishment of sensor node keys for safeguarding collected objects with minimal energy consumption. It excels at event detection within sensor networks and effectively utilizes an SVM classifier with predetermined weights, accommodating networks of varying sensor node sizes. These predetermined weights significantly contribute to the precise classification of objects within the sensor network. The system proficiently identifies periodic events through the Doppler Effect method, followed by secure collection and grouping of the detected objects via the event section key management system. The primary goal of E3C-SVM is to both protect and optimize energy utilization within the sensor network during event exposure.

A. Doppler Effect

Within Wireless Sensor Networks (WSNs), the Doppler Effect refers to the change in signal frequency received by a sensor node, resulting from the relative motion between the sensor node and the source of the signal. This concept bears a resemblance to the well-known Doppler Effect encountered in the field of physics, which is observable in occurrences involving sound waves or electromagnetic waves, including light. Although sensor nodes within WSNs are generally static or have limited mobility, there are situations in which the Doppler Effect becomes a pertinent factor to consider.

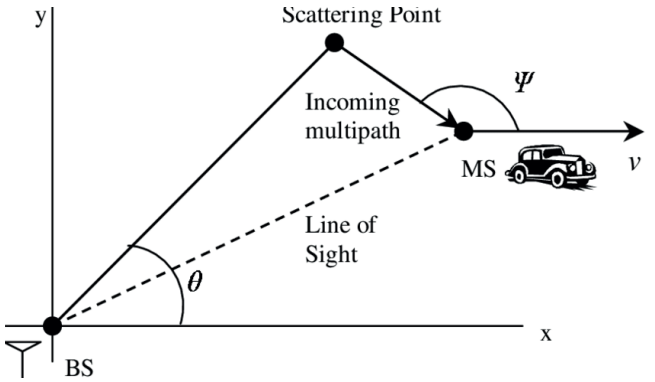

Figure 4. Illustration of Doppler effect

Relative Motion: Whenever a sensor node experiences motion, like a moving vehicle with embedded sensors, or when the signal source is in motion, the relative movement between the node and the source induces a change in the received signal's frequency.

Frequency Shift: If the signal source is approaching the sensor node, the received signal exhibits a higher frequency compared to the source's original signal. This occurrence is termed a positive Doppler shift or a blue shift. Conversely, when the source moves away from the sensor node, the received signal features a lower frequency, denoted as a negative Doppler shift or a red shift.

Communication Reliability: Frequency shifts can influence the reliability of communication among sensor nodes. Significant shifts may result in signal degradation or data loss.

Localization: In WSNs, the Doppler Effect finds application in localization. By analyzing the frequency shift in signals received from various sensor nodes, it becomes feasible to estimate node positions and relative motion.

Energy Efficiency: Understanding the Doppler Effect aids in optimizing energy usage within WSNs. For instance, sensor nodes can adapt their transmission power or duty cycle based on their relative motion, conserving energy.

Adaptive Modulation and Coding: Employing adaptive modulation and coding schemes that adjust signal parameters according to estimated Doppler shifts.

Frequent Updates: Ensuring regular updates of location information to accommodate changes in node positions.

Antenna Diversity: Utilizing multiple antennas or antenna arrays to mitigate fading resulting from Doppler shifts.

B. Pre-computed Event Weight-SVM

Let's examine an object denoted as P, $P = \{x_i, y_i\}$. This object employs the Support Vector Machine (SVM) to determine the optimal hyperplane value, using a weight vector 'w' that has been predetermined. The 'i' value in the E3C-SVM is calculated starting from the hyperplane:

$$\min(w) = \frac{1}{2}|w|^2 + E * \sum_{i=1}^{n}(x_i, y_i) \qquad (1)$$

The pre-computed weight vector 'w' is applied to the objects x_i and y_i correspondingly. 'E' represents the energy consumption rate within the context of E3C-SVM. The indeterminate vector within the Support Vector Machine is characterized as follows:

$$y_i * (w * x_i + u) \qquad (2)$$

The number of vectors used for object classification is dependent on obtaining maximum marginal length, and the sensor network reflects the Lagrange multipliers ρ_i used to find the best hyperplane value. The E3C-SVM judgment function for classifying objects is written as,

$$Fun_{Decision} = CL\{\sum_{i=1}^{n}(\rho_i . x_i . y_i), (x_i, u)\} \qquad (3)$$

Objects detected as events are categorized through the decision classifier, and 'CL' is employed to denote their classification. The classification procedure makes use of the optimal hyperplane in conjunction with Lagrange multipliers, treating undetermined vector points distinctly within the sensor network. In the E3C-SVM system, the hyperplane value is harnessed, and the Doppler Effect method is employed through a sequence of incremental steps to discern events within the sensor network. To adapt to the diverse frequency ranges present in the sensor network, the Doppler Effect approach in E3C-SVM contributes to a reduction in energy consumption rates.

For event detection in E3C-SVM, the Doppler Effect technique is used from the source sensor node to the destination sensor node. The frequency 'f', which stands for the velocity of the source sensor node's motion:

CVR Journal of Science and Technology, Volume 25, December 2023
DOI: 10.32377/cvrjst2513

$$Freq\ f = \frac{E + V_t}{E + V_s} * f_0 \qquad (4)$$

In Equation 4, 'E' signifies the energy expenditure related to event detection within the sensor nodes with v_t and v_s the target node velocity 't' and source node velocity 's' for detecting events with the optimal hyperplane value.

V. Result Analysis

The Predetermined Event Weight-Based Support Vector Machine (E3C-SVM), an efficient Event Detection Classifier designed for wireless sensor networks, undergoes experimental assessment using the NS2 simulator. The current Correlated Data Gathering (CDG) and Energy-Efficient and High-Accuracy (EEHA) schemes are compared with E3C-SVM. These simulations employ a network environment comprising 150 sensor nodes. The sensor nodes employ the AODV routing protocol to conduct tests involving randomly moving objects. All nodes' movements occur within a sensor field measuring 750 m × 750 m, with nodes traveling at random speeds of 40 m/s and pausing for an average duration of 0.01 s. Various metrics, including throughput, energy consumption rate, processing time, classifier rate, mean classification time, and other variables, are evaluated in the experimental setup. In the context of E3C-SVM, the classifier rate gauges the speed at which events are classified and captured, with higher rates indicating lower energy consumption. The classifier rate is expressed as a percentage (%). Considering a range of objects, the mean classification time measures the duration required to identify periodic events based on attributes such as shape, size, and load.

TABLE I.
Rate of Classification

Sensor Nodes	Rate of Classification		
	E3C-SVM	CDG	EEHA
20	69	62	57
50	73	65	61
80	76	67	63
120	79	70	66
150	83	74	69

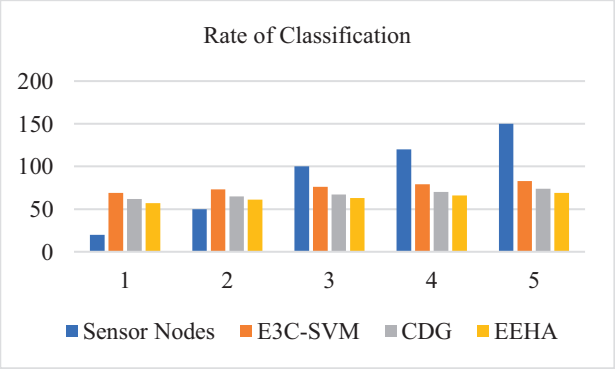

Figure 5. Rate of Classification

TABLE II.
Consumption of Energy

Sensor Nodes	Consumption of Energy		
	E3C-SVM	CDG	EEHA
20	23	28	31
50	30	32	35
80	32	39	42
120	35	46	49
150	39	50	56

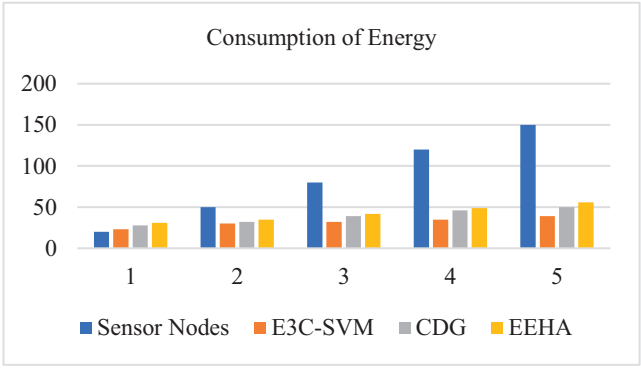

Figure 6. Energy Consumption

VI. Conclusions

Focusing on the detection and categorization of periodic events, the energy-efficient event detection framework offers a comprehensive approach to effectively identify events within a wireless sensor network. This approach reduces energy consumption across diverse sensor nodes by implementing event section key generation techniques, utilizing an SVM classifier. Each sensor node possesses a unique section key, enhancing security through information sharing among sensor nodes. To achieve efficient object classification, this research combines Lagrange classifiers with optimal hyperplanes to propose a decision function classifier. The Doppler Effect method is also employed for swiftly detecting periodic events associated with moving objects, minimizing processing time. By leveraging the Doppler Effect method, the wireless sensor network establishes a theoretical model that enhances classification rates and energy efficiency. Through simulations and real-world applications, it is demonstrated that this energy-efficient approach outperforms state-of-the-art techniques in terms of energy conservation.

References

[1] T. Cui, F. Lu, V. Sethuraman, A. Goteti, S. P. N. Rao and P. Subrahmanya, "Throughput Optimization in High Speed Downlink Packet Access (HSDPA)" in IEEE Transactions on Wireless Communications, vol. 10, no. 2, pp. 474-483, February 2011, doi: 10.1109/TWC.2010.120610.091294.

[2] Engin Zeydan., Didem Kivanc., Cristina Comaniciu., Ufuk Tureli., (2012): "Energy-efficient routing for correlated data in wireless sensor networks" Ad Hoc Networks., Elsevier journal.

[3] Liang Liu, Xi Zhang, and Huadong Ma.(2011):"Localization-Oriented Coverage in Wireless Camera Sensor Networks",

IEEE Transactions on Wireless Communications, Vol. 10, No. 2.

[4] G. Malleswari, "Adaptive Energy Routing Protocol using Spider Optimization in Wireless Sensor Networks," 2023 International Conference on Computer Communication and Informatics (ICCCI), Coimbatore, India, 2023, pp. 1-6, doi: 10.1109/ICCCI56745.2023.10128603.

[5] P. C. Reddy and P. C. S. Reddy, "Performance Analysis of Adhoc Network Routing Protocols," 2006 International Symposium on Ad Hoc and Ubiquitous Computing, Mangalore, India, 2006, pp. 186-187, doi: 10.1109/ISAHUC.2006.4290671.

[6] Engin Zeydan., Didem Kivanc., Cristina Comaniciu., Ufuk Tureli., (2012): "Energy-efficient routing for correlated data in wireless sensor networks," Ad Hoc Networks., Elsevier journal.

[7] Hongjuan Li., Kai Lin, Keqiu Li.(2012): "Energy-efficient and high-accuracy secure data aggregation in wireless sensor networks," Computer Communications., Elsevier journal.

[8] Qu, Z., Wang, L. (2006). A Spatial Clustering Algorithm Based on SOFM. In: Li, X., Zaïane, O.R., Li, Z. (eds) Advanced Data Mining and Applications. ADMA 2006. Lecture Notes in Computer Science(), vol 4093. Springer, Berlin, Heidelberg.

[9] Kumar Gourav, Dr. Amanpreet Kaur, "A Study of Reinforcement Learning Applications & Its Algorithms:, International Journal of Scientific & Technology Research Volume 9, Issue 03, March 2020.

[10] Reddy, A. Srinivasa. "Effective CNN-MSO method for brain tumor detection and segmentation." Materials Today: Proceedings 57 (2022): 1969-1974.

[11] D. A. Vidhate and P. Kulkarni, Enhanced Cooperative Multi-agent Learning Algorithms using Reinforcement Learning, published in the proceedings of IEEE International Conference on Computing, Analytics and Security Trends, pp 556-561, 2016.

[12] Srinivasa Reddy, A., Chenna Reddy, P. (2020). Enhanced Image Segmentation Using Application of Web Optimization for Brain Tumor Images. Smart Intelligent Computing and Applications . Smart Innovation, Systems and Technologies, vol 159.

[13] J. Hou, Huali, J. Hu, C. Zhao, Y Guo, S. Li, and Q. Pan, A Review of the Applications and Hotspots of Reinforcement Learning, published in the proceedings of IEEE International Conference on Unmanned Systems (ICUS), October, 2017, DOI: 10.1109/ICUS.2017.8278398.

[14] G Malleswari, "Significance of Genetic Algorithms in Image Segmentation", International Journal of Signal Processing, Image Processing and Pattern Recognition,9(4), 177-184.

[15] Srinivasa Reddy, A., Chenna Reddy, P. MRI brain tumor segmentation and prediction using modified region growing and adaptive SVM. Soft Comput 25, 4135–4148 (2021).

[16] A. S. Reddy and G. Malleswari, "Efficient Brain Tumor Segmentation using Kernel Representation," 2023 7th International Conference on Intelligent Computing and Control Systems (ICICCS), Madurai, India, 2023, pp. 1006-1011.

[17] A. S. Reddy and P. C. Reddy, "Novel Algorithm based on Region Growing Method for Better Image Segmentation," 2018 3rd International Conference on Communication and Electronics Systems (ICCES), Coimbatore, India, 2018, pp. 229-234.

[18] A. S. Reddy, "Performance of VANET over MANET in Mobile Computing Environment," 2022 7th International Conference on Communication and Electronics Systems (ICCES), Coimbatore, India, 2022, pp. 659-664.

E-ISSN 2581 – 7957
P-ISSN 2277 – 3916
CVR Journal of Science and Technology, Volume 25, December 2023
DOI: 10.32377/cvrjst2514

Extraction and Characterization of Furcraea Fiber for Textile Applications – An exploratory Investigation

Yasin Pathan
Asst. Professor, CVR College of Engineering/ Mechanical Engg. Department, Hyderabad, India
Email: p.yasin339@gmail.com

Abstract: **The aim of this paper is to study the use of Furcraea plant leaves as a potential source of lignocellulose fibers with an emphasis on textile applications. The plant leaves are retted in water, squeezed and beaten to collect the fibers. According to National Standard 08-1113-1989, the length of the fibers measures in the range of 60 to 100 cm. Bundle strength, color, fineness, root content, defects and bulk density are measured to be 19.0 g tex^{-1}, 36%, 34.44 tex, 1.52%, 16.75% and 0.37 g cc^{-1} respectively. The extracted fiber grade has also been estimated in accordance with commercial natural fiber standard IS 271 (2003). The findings revealed that these fibers are viable substitutes for jute fibers of TD-4 grade to produce packaging bags of food grains.**

Index Terms: **Furcraea, Composite, Leaf fiber, Extraction, Fiber properties, Textile.**

I. Introduction

Over the last few years, researchers have been exploring new natural fibers that can be used as raw materials for various applications. The main factors encouraging the investigation of these environmentally friendly materials are the rapidly expanding environmental consciousness, restrictions on the use of petroleum based Man-made materials, and high processing costs [1].

While natural fibers can be used in a wide range of applications, including textiles and composites, there is currently more research being conducted on the use of natural fibers in composites compared to textiles. Sreenivasan et al [2], characterized s. cylindrica fibers but primary textile parameters i.e., bundle strength, bulk density and defects were not evaluated [3]. Shinoj S R et al [4] collated information on the aptness of oil palm fruit for bio composite formation in various polymer matrices but did not explore its suitability for textile applications. Similarly, many researchers reported characterization of novel plant based fibers with primary objective of investigating the degree of suitability for composite application [5-7]. On the other hand, recent research has increasingly focused on exploring new natural fibers specifically for textile applications. Bauhinia Vahlii bark fiber has been characterized and found suitable for yarn production through blending with existing cellulosic fibers [8]. Recent investigations on Furcraea foetida plant leaf fibers have revealed their potential as an alternative material for existing textile fibers, specifically yarns [9]. The fiber extracted from the stalk portion of the Etlingera elatior plant has undergone unprecedented investigations, revealing its spinnability and successful utilization as a raw material for textile applications [10]. Similarly, the exploration of Agave vera-cruz [11], Euphorbia tirucalli [12], and Canna edulis [13] plants fibers has yielded encouraging results, particularly in the realm of textile applications.

TABLE I.
FEW FLFS PROPERTIES COMPARED TO OTHER NATURAL FIBERS

Sl. No.	Fiber/plant name	Fineness (tex)	Bundle strength (g/tex)
1	Furcraea foetida [19]	8.3	21
2	Cotton [19]	0.1-0.3	26.6-28.7
3	Pineapple leaf [19]	3.5-4.3	23-30
4	Sisal [27]	30-32	28-30
5	Abaca [28]	20-35	20-35
6	Ramie [28]	0.4-0.8	28-40
7	Coconut fruit [27,28]	50-55	11-12
8	Banana [28]	3-25	20-30
9	FLF	34.44	19

Agave fourcroydes, also referred to as Furcraea, is a plant that is indigenous to Mexico and Guatemala. It is closely related to the sisal fiber crop and is a member of the asparagus family. The plant has rosette of sword shape leaves rows up to 100 cm length. Growing from the sturdy stalk, the leaves are a greyish green color and 10 to 15 cm wide. Cazaurang-Martinez MN et al [14] reported chemical, few physical and mechanical properties of the Furcraea fiber. A chemical analysis of Furcraea leaf fibers revealed that cellulose comprises the largest portion (59%) of the fiber composition. Following cellulose, hemicellulose accounts for 28% of the fibers, while lignin makes up approximately 8%. The tensile strength of Furcraea fiber, determined through mechanical testing, is measured at 570 MPa. Additionally, the Young's modulus of Furcraea fiber, which represents its stiffness or elasticity, is found to be 14.7 GPa. The true density of the fiber was 1.2 kg/m3. These properties are comparable to many existing natural fibers and attracted many researchers. As a result, this natural fiber had predominantly been investigated and utilized in non-textile applications, such as composite materials [15-17]. The present work emphasizes the extraction and assessment of Furcraea leaf fiber for its textile qualities, which were previously underappreciated due to a lack of awareness.

Received on 23-05-2023, Revised on 20-09-2023, Accepted on 15-10-2023.

CVR Journal of Science and Technology, Volume 25, December 2023
DOI: 10.32377/cvrjst2514

II. Material and Methods

A. Collection of leaves and Extraction of fibers

The process of water retting, as detailed by Madival AS et al. [18], was employed to effectively separate the fibrous bundles from the Furcraea leaves. This method involved submerging the leaves or bast in water for a specific duration to initiate the natural decomposition and separation of the fibers. In the present work, healthy Furcraea leaves were harvested from the Hyderabad Forest area in Telangana state, India. The selected leaves had almost equal sizes and colors. The length and width of the leaves were around 60–100 cm and 6–7.5 cm, respectively. These leaves were water retted for 20 days, followed by careful squeezing, and battering to separate the fibers from non-fibrous tissues. These fibers were sun-dried for four days

Figure 1. Extracted FLFs

before being kept in a polythene bag for future usage. Figure 1 shows its well-retted and dried Furcraea leaves fibers (FLFs).

B. Determination of Textile properties

The fiber length measurements were performed in accordance with National Standard 08-1113-1989 for the Measurement of FLFs Length. Twenty bunches of fiber strand samples, each comprising at least 100 fibers, were put out loosely on a flat surface. The largest sample among the bunches was measured using the established methodology.

Color is one of the important characteristics of any fiber, and it can vary in appearance, including shades of grey, creamy pink, ivory, white, cyan, and more. In the case of FLFs, the color assessment was performed using the method developed by the Indian Jute Industries Research Association (IJIRA). This method involves the use of a whiteness index measurement device to quantify the color percentage in terms of different categories, ranging from creamy pink to brownish white (superior), brownish to reddish white with some light grey, brownish to light grey, and grey to dark (inferior). By employing this IJIRA method, the color characteristics of the FLFs samples were effectively evaluated and categorized based on their color variations.

Fineness is a crucial measurement that quantifies the thickness, diameter, breadth, or weight per unit length of the fiber. In this study, the fiber's fineness was assessed following the BIS Standard IS 271 (2003) using air flow equipment. To determine the fineness, chopped FLFs samples were precisely weighed and placed into a two-ended open cylindrical chamber attached to a manometer. The fibers were then crushed to achieve a consistent volume within the chamber. Compressed air was subsequently pumped into the chamber, and the amount of air flow was controlled. If a significant amount of air passed through the chamber, it indicated that the fiber was coarser. Conversely, if minimal air passed through, it indicated that the fiber was finer. By conducting extensive testing and analyzing the data, the average fineness of the fiber samples was expressed in Tex units. The diameter of the fiber could be determined by calculating the ratio of air flow pressure to differential pressure, providing valuable insights into the size and thickness of the fibers.

Strength refers to the fiber's capacity to withstand external forces such as tearing or stretching. In this study, the bundle strength, also known as the tenacity of the fiber, was evaluated following the guidelines of IS 271 (2003) using tensile strength testing equipment with a capacity of 100 kgf. Well-prepared test samples of the fiber were fed into the testing machine, which subjected the fiber to tension until it broke. The time taken for the fiber to break was recorded, with a duration of 20 ± 5 seconds. By analyzing the test results, the strength of the FLFs bundle was measured and expressed in g Tex^{-1}. This measurement provides valuable information about the fiber's ability to resist external forces and helps in assessing its overall strength and durability.

The bulk density, also referred to as the weight or body measure of the fiber, was determined by calculating the mass-to-volume ratio, including airspaces. The measurement followed the guidelines of IS 271 (2003) and utilized specialized devices for assessing bulk density. For the study, five samples of FLFs were prepared, each weighing 40 g and measuring 100 mm in length. These samples were placed between metal plates in a bulk density measuring device. A 10 kg weight was applied to apply pressure, and the volume of the fibers was recorded. By calculating the ratio of mass to volume, the bulk density of the FLFs was determined and expressed in g cc^{-1}. A higher bulk density is often regarded as an indicator of higher fiber quality, suggesting increased compactness and weight of the fiber.

C. Morphological properties

SEM (Scanning Electron Microscopy) was employed to examine the cross-section and surface characteristics of FLFs. The fractured samples of FLFs, which underwent sputter coating with gold, were analyzed using a SEM device manufactured by ZEISS in Germany. This equipment allowed for detailed imaging and analysis of the fiber's structure and surface morphology, providing valuable insights into its microstructure and properties.

III. Results and Discussion

The length of the FLFs was found to vary within the range of 60 to 100 cm. The FLFs extracted from the plant closely matched the length of the leaves being processed. This similarity in length suggested that the fiber length

could be influenced by the size of the leaves being processed. The FLFs can be categorized as "extra-long staple fiber" based on its length. When it comes to producing high-quality yarn, longer raw fibers are favored over shorter ones. This preference is rooted in the understanding that longer fibers provide several advantages during the spinning process. One significant advantage is the increased surface area of longer fibers, which promotes better friction and reduces slippage between the fibers [19]. Longitudinal and Cross-sectional Microstructures of FLF shown in Figure 3 and Figure 4, it is evident that uneven surface with impurities and lumen spaces will promote requisite friction and reduced slippage while spinning. In accordance with Murthy H V S [20], utilizing long staple yarns in fabric production results in fabrics that are stronger, smoother, and more functional and are also valuable compared to fabrics made from short staple yarns. This indicates that high quality yarn can be produced using FLFs. It is recommended that the length of the fiber used should be

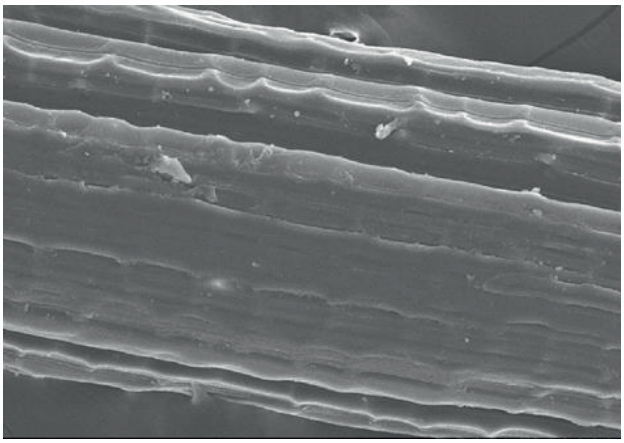

Figure 2. Microstructural analysis of FLFs: Longitudinal view.

at least 5 mm, ensuring a substantial length-to-diameter ratio to facilitate the manufacturing of yarn that maintains the integrity of individual fibers [20]. The configuration factor of spinning machines employed in fiber treatment is influenced by the length of the fiber, as it plays a crucial role in determining the suitability of the spinning process. This can be attributed to FLFs easy spinnability. The industrial handling of textile fibers is a crucial stage in the processing for making various products. The length of the fiber plays a significant role in the spinning system, as it determines the placement of rollers and helps prevent excessive twisting during processing. In the case of jute fiber, the required minimum length according to BIS systems IS 271 (2003) and IS 271 (2020) is approximately 100 cm. This length is considered optimal as it facilitates efficient feeding on breaker cards and minimizes handling operations [21]. According to Reddy N et al. [22], fibers should be at least 2 cm long to be suitable for textile applications. Based on a replicated study mentioned earlier, it can be concluded that the HFLs are suitable for use in textile applications. Due to the lower stiffness of the fibers, processing finer fibers for fabrics results in softer fabrics and has the potential to yield yarn with a greater thread count [21].

The HFLs were evaluated for their fineness in accordance with the IS 271 (2003) standard for jute fiber where its fineness is divided into four categories: very fine, fine, well-separated, and separated fibers. The testing of the fibers revealed that HFLs have a fineness of 34.44 tex, placing them in the 'separated fibers' range. This fineness is unusual and significantly coarser compared to jute fiber. Table 1, which compares the FLFs' characteristics with those of other lignocellulose fibers, clearly shows their notably high fineness value. According to Murthy H V S [20], fiber fineness plays a significant role in various crucial yarn qualities, such as packing and flexural rigidity. Coarser fibers have a lower specific surface area, which leads to decreased fiber cohesion and capillary activity within the yarn structure. As the yarn count decreases, the torsional resistance of the fiber worsens. Coarser fibers are generally more challenging to twist, but once twisted, they store more strain energy compared to finer fibers. This can lead to undesirable kinks and snarls in the relaxed state of the yarn.

The performance of the finished product heavily depends on the mechanical characteristics of textile fibers, such as their response to loads and deformations. Factors such as plant type and growth pattern determine fiber strength.

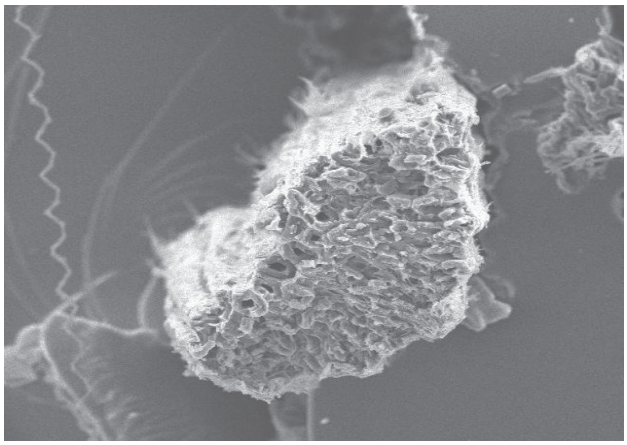

Figure 3. Microstructural analysis of FLFs: Cross-sectional view.

Tenacity, sometimes referred to as bundle strength, is a crucial characteristic that indicates the fiber's capacity to withstand stresses and significantly influences grading evaluation [21]. According to IS 271(2003), there are six classifications for bundle strength: weak mixed, average, fair average, fairly good, excellent, and very good. The bundle strength of the extracted FLFs was measured to be 19.0 g tex^{-1} (i.e., 2.11 g den^{-1}). This measurement clearly confirms that the FLFs possess a notable level of average strength. This FLFs bundle strength value highlights their robustness and suggests that they are well-suited for various applications that require moderately strong and durable fibers. It is evident from Table 1 that FLFs are comparable to a variety of lignocellulosic fibers. The strength of the FLFs surpasses the minimum bundle strength requirement of 1 g den^{-1}, making them suitable for textile applications [19,20]. These fibers can also be used in clothing and home applications since their strength level almost matches the advised range of 3 to 7 g den-1 [19,20]. This suggests that the raw FLFs have a strength profile that makes them

suitable for a variety of textile goods, assuring their viability and efficiency in a variety of situations, such as apparel and household items.

Bulk density is categorized as either heavy-bodied (compact and heavier) or medium-bodied (loose and lighter) by IS 271 (2003). FLFs extracted from leaves, and its bulk density was determined to be 0.37 g cc-1 which is less than a common jute fiber bulk density of 0.45 g cc-1 [23]. This demonstrates the medium-bodied nature of the FLFs. However, it is important to note that the most recent BIS systems (IS 271(2020)) no longer considers bulk density as one of the criteria for classifying mother jute fiber [24].

The capacity of a fiber to distinguish between appearances of redness, whiteness, yellowness, blueness, and other colors is known as its color. Its aesthetic value is influenced by this trait. FLFs color was easily measured using a hand-held color meter with indicators. According to the BIS method, the color of FLFs was determined to be 36%, which is a fairly good color (grey to dark grey). This demonstrates that FLFs, whose color comes from the natural pigmentation of the plant, grows in a range of hues ranging from brown to green and may be utilized for textile, clothing, and craft applications [25]. Dyeing textile items is one of the costliest steps in the finishing process since it uses a lot of water and energy, generates a lot of reject, and emits a lot of pollutants. Up to 50% of the overall cost of producing textiles may be saved by eliminating the dying step for naturally colored fibers. The textiles that will be made from FLFs don't need to be dyed since they already have a good color [25, 26].

According to recent research on ramie fiber [21] and banana fiber [29], grading any new or potential natural fiber is critical for predicting how it will behave during the manufacturing process, determining its best use in the development of various types of yarns, and determining its blending compatibility with other commercial natural fibers. Since FLFs is a novel natural fiber, there are no recognized grading criteria. The current study investigated the criteria of fiber fineness, bundle strength, bulk density, and color which are a few of the parameters used to assess the grade of jute fiber (BIS system) has been utilized for FLFs. The remaining two variables as per the BIS system are root content and defects. Because FLF is a leaf fiber, Tis BIS system was not used to determine root content or defects as they vary from bast fiber to leaf fiber. If root content and defects are eliminated, FLFs evaluated according to BIS method IS 271(2003) will yield at least W-2 grade fibers, which are useful for producing packaging bags of food grains. Also, this type of grade evaluation could certainly aid in blending of jute fiber and FLFs [30].

IV. Conclusions

This study was conducted to investigate the viability of utilizing FLFs as textile fibers. The research demonstrated that FLFs can be efficiently produced from plants using a cost-effective water retting method. While FLFs were observed to possess a coarser fineness compared to many natural fibers, they showcased a natural color range from grey to dark grey, negating the necessity for additional dyeing processes in textile production. Furthermore, FLFs were categorized as long staple fibers and exhibited adequate bundle strength, positioning them as comparable to well-established textile fibers suitable for yarn spinning. These findings strongly suggest that FLFs have the potential to emerge as a compelling alternative to traditional yarns within the textile industry. In conclusion, this study indicates that FLFs can effectively function as textile fibers, offering benefits such as cost-effectiveness, ease of production, natural coloration, and competitive performance when compared to established fibers. Consequently, FLFs present promising prospects as a sustainable and feasible option in textile manufacturing.

References

[1] Prabhu, K. H., M. D. Teli, and N. G. Waghmare. 2011. Eco-friendly dyeing using natural mordant extracted from Emblica officinalis G. fruit on cotton and silk fabrics with antibacterial activity. Fibers and Polymers 12(6): 753–759.

[2] Sreenivasan VS, Somasundaram S, Ravindran D, et al. Microstructural, physico-chemical and mechanical characterization of Sansevieria cylindrica fibers – An exploratory investigation. Mater Des, 2011; 32: 453–461.

[3] Indian standards specifications IS: 271, Textiles - Grading of White, Tossa and Daisee uncut Indian jute. Bureau of Indian Standards, New Delhi, 2003.

[4] Shinoj, S., R. Visvanathan, S. Panigrahi, and M. Kochubabu. 2011. Oil palm fiber (OPF) and its composites: A review. Industrial Crops and Products 33(1): 7–22.

[5] Paiva M, Ammar I, Campos A, et al. Alfa fibers: Mechanical, morphological and interfacial characterization. Compos Sci Technol, 2007; 67: 1132–1138.

[6] Binoj JS, Edwin Raj R, Sreenivasan VS, et al. Morphological, physical, mechanical, chemical and thermal characterization of sustainable Indian Areca fruit husk fibers (Areca Catechu L.) as potential alternate for hazardous synthetic fibers. J Bionic Eng, 2016; 13: 156–165.

[7] Béakou A, Ntenga R, Lepetit J, et al. Physico-chemical and microstructural characterization of "Rhectophyllum camerunense" plant fiber. Compos Part A Appl Sci, 2008; 39: 67–74.

[8] Bar G, Chaudhary K. Characterization of Textile Grade Novel Bauhinia Vahlii Fiber. Journal of Natural Fibers; 20. Epub ahead of print November 14, 2022. DOI: 10.1080/15440478.2022.2143464.

[9] Totong T, Wardiningsih W, Al-Ayyuby M, et al. Extraction and Characterization of Natural Fiber from Furcraea Foetida Leaves as an Alternative Material for Textile Applications. Journal of Natural Fibers 2021; 19: 6044–6055.

[10] Wardiningsih W, Sopyan M, Pradana S, et al. Characterization of Natural Fiber Extracted from Etlingera elatior Stalk for Textile Applications. Journal of Natural Fibers 2021; 19: 9384–9395.

[11] Kanimozhi M, Vasugi N. Characterization of Agave vera-cruz Mill Leaf Fiber for Textile Applications–An Exploratory Investigation. Journal of Natural Fibers 2012; 9: 219–228.

[12] Azanaw A, Ketema A. Extraction and Characterization of Fibers from Ethiopian Finger Euphorbia (Euphorbia Tirucalli) Plants. Journal of Natural Fibers 2022; 19: 11885–11895.

[13] Mulyani RrW, Wardiningsih W, Wahyudiana T, et al. Characterization of Agro Waste Fiber Extracted from the Stem of Canna Edulis Plant and Its Potential in the Textiles. Journal of Natural Fibers 2021; 19: 8909–8922.

[14] Cazaurang-Martinez MN, Herrera-Franco PJ, Gonzalez-Chi PI, et al. Physical and mechanical properties of Furcraea

fibers. Journal of Applied Polymer Science 1991; 43: 749–756.
[15] Han SO, Ahn HJ, Cho D. Hygrothermal effect on Furcraea or silk fiber reinforced poly(butylene succinate) biocomposites. Composites Part B: Engineering 2010; 41: 491–497.
[16] Yasin P, Venkata Ramana M, Krishna Vamshi C, et al. A study of continuous Furcraea/Epoxy composites. Materials Today: Proceedings 2019; 18: 3798–3811.
[17] Herrera-Franco PJ, Valadez-González A. A study of the mechanical properties of short natural-fiber reinforced composites. Composites Part B: Engineering 2005; 36: 597–608.
[18] Madival AS, Doreswamy D, Maddasani S, et al. Processing, Characterization of Furcraea foetida (FF) Fiber and Investigation of Physical/Mechanical Properties of FF/Epoxy Composite. Polym. 2022; 14: 1476.
[19] Totong Totong, Wiah Wardiningsih, Muhammad Al-Ayyuby, Ria Wanti & Ryan Rudy (2022) Extraction and Characterization of Natural Fiber from Furcraea Foetida Leaves as an Alternative Material for Textile Applications, J Nat Fibers, 19:13, 6044-6055.
[20] Murthy, H. V. S. 2016. Introduction to Textile Fibers. (WPI publishing), 2016, 1-36.
[21] S.C. Saha, A. Sarkar, G. Sardar, D.P. Ray & G. Roy. Grading system of ramie fiber. Int J Bioresour Sci. 2017;4(1): 9-12.
[22] Reddy N and Y Yang. Preparation and characterization of long natural cellulose fibers from wheat straw. J Agric Food Chem. 2007;55 (21):8570–75.
[23] Rana MN, Islam MN, Nath SK, et al. Properties of low-density cement-bonded composite panels manufactured from polystyrene and jute stick particles. Journal of Wood Science; 65. Epub ahead of print October 17, 2019. DOI: 10.1186/s10086-019-1831-3.
[24] S. Banik, M. K. Basak, S. C. sil. Effect of inoculation of pectinolytic mixed bacterial culture on improvement of ribbon retting of jute and kenaf. J Nat Fibers, 2007; 4: 33-50.
[25] Matusiak M and Frydrych I. Investigation of naturally coloured cotton of different origin–analysis of fiber properties. Fibers Text East Eur. 2014; 5(107): 34–42.
[26] Święch T, Frydrych I. Naturally coloured cottons: Properties of fibers and yarns. Fibers Text East Eur.1999; 7, 4: 25–29.
[27] Basu, G., A. N. Roy, K. K. Satapathy, J. Sk Md, L. M. Abbas, and R. Chakraborty. Potentiality for Value-Added technical use of Indian sisal. Ind Crops Prod, 36;1:33–40.
[28] Das, P. K., D. Nag, S. Debnath, and L. K. Nayak. Machinery for extraction and traditional spinning of plant fibers. Indian J Tradit Knowl. 2010; 9(2): 386-393.
[29] Balakrishnan S, Wickramasinghe GD, Wijayapala US. A novel approach for banana (Musa) Pseudo-stem fiber grading Method: Extracted fibers from Sri Lankan Banana Cultivars. J Eng Fibers Fabrics, 2020;15: 1-9.
[30] Basu G, Roy AN. Blending of Jute with Different Natural Fibers. J Nat Fibers. 2008;4:13–29.

E-ISSN 2581 – 7957
P-ISSN 2277 – 3916

CVR Journal of Science and Technology, Volume 25, December 2023
DOI: 10.32377/cvrjst2515

Simulation Study on Building Energy Management in HVAC Control System for House Building

Sk Mohammad Shareef
Asst. Professor, CVR College of Engineering/Mechanical Engg. Department, Hyderabad, India
Email: shareefshaik4@gmail.com

Abstract: **House buildings usually consume high energy and the operation efficiency of air conditioning system in house buildings is still far from agreeable. Thus, it is important to break down the data and suggest recommendations on energy usage. In the current work, an energy simulating instrument termed e-Quest was applied to model the thermal, ventilation and different energy in taking processes in a three storeyed building to predict its energy performance. In order to precisely compute the energy usages in building, the instrument considered the outer climate of the building, warmness resources within the building and the use of structure materials. This building energy imitating approach was arguably established as an influential practice for observing energy pattern of building, evaluating architectural design, decide upon proper structural resources and system demanded as well.**

Index Terms: **House building, e-QUEST, HVAC (Heating, Ventilation and Air-Conditioning) and Energy usage**

I. Introduction

Main objective of this work is to analyze the different parameters which affect the power consumption using HVAC (Heating, Ventilation and Air-Conditioning) system before constructing the building because reconstruction is a long and hard process.

Buildings are complicated physical things. They interact with their instant surroundings while trying to supply a comfortable living and working out environment to the residents. The way a building behaves and performs is affected by the attachments framed in taking building materials and factors while aiming the building envelope (fences, windows, ceilings), and other systems (lighting, HVAC,etc.). Buildings deliver easy inner atmosphere provisions like thermal, visual, and auricular by devouring energy.

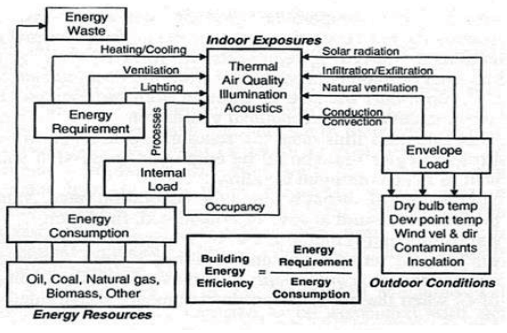

Figure 1. Energy Flow and Concepts in Buildings.

Fig .1 shows the Energy flow and concepts in Building.

An energy simulation implement models are thermal, visual, ventilation and different energy consuming procedures taking place within a building to forecast its energy and environmental performance. During its computation process, it takes the outside climatic factors, inner heat sources, building materials and systems into consideration to exactly model the building. Building energy simulation is an important method to acquire knowledge about energy performance of buildings and to assess architectural design opinions as well as to find options in construction materials and methods. Moreover, the sophisticated design effects also can be questioned, and their performance can be quantified and estimated.

A. About e-QUEST

e-QUEST is a simple employment building energy deconstruction instrument which provides high grade developments by joining a building creation charmer, an energy effectiveness measure wizard and pictorial results display module with a perfected DOE-2.2 decided building energy simulation program. Within-QUEST, DOE-2.2 performs an hourly simulation of the building predicated on fences, windows, glass, people, pack loads, and ventilation.

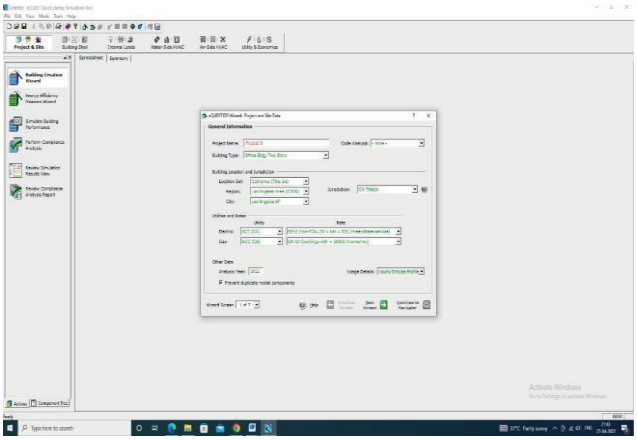

Figure 2. e-QUEST Software Interface.

Fig 2 shows the interface of e-QUEST software.

e-QUEST allows users to bring many simulations and review the indispensable results in side- by side graphics. It offers energy charge estimating, day lighting and lighting system regulator, and mechanic perpetration of energy effectiveness expedients (e-QUEST, 2008).

Received on 17.10.2023, Revised on 02.11.2023, Accepted on 25.11.2023.

CVR Journal of Science and Technology, Volume 25, December 2023
DOI: 10.32377/cvrjst2515

II. Literature Survey

Yamin Zhu et al [1] conducted a case study on pertaining computer- based simulation to do energy auditing. They finished the task by associating the power of the portfolio manager which is elaborated by the Environmental Protection Agency and eQuest DOE2.com. The stimulation has broken down the job of an existing facility in setup to express methods for attaining the Energy Start designation.

R. Pacheco et al [2] written a review on energy efficient design of building energy and concluded that energy consumption in the domestic building sector makes it compulsory not only to convey out fundamental examination on the thermodynamic detail of the colorful systems but also allows to deliver energy. Still, it's also compulsory to express project grades associated with the sustainability of these buildings.

M. Santamouris et al [3] conducted trial on ceiling system inducted in a nursery academy structure. The simulations were carried out for the building in both non-insulated and insulated structures. Consisting to the effects, the investment of the green ceiling system significantly contributed to the structure energy efficiency.

Florides et al [4] modelled and analyzed on new businesses of cyprus and energy consumption and concluded that that the fence isolation pays back in a twenty- span period whereas the ceiling isolation has significant profitable advantage with life round savings up to EUR 22,374 turning on the place temperature and the isolation consistence.

Yi Zhitong et al [5] conducted analysis on crystalline radiative cooling flick for structures with ceiling glazing and concluded that when the T- RC flick is appertained on a1.0 m ×0.6 m ×1.2 m (L × W × H) model box with ceiling glazing, the inner side air temperature of the model box was demoted by an utmost valuation of 21.6 °C.

Hee et al [6] has conducted analysis on window glazing on daylighting and energy delivering in structures and concluded that both glazing kinds; it involves offerings on some sides to open occasion for different sides in setup to give the ideal equilibrium among the accounted features while minimizing the paradox.

Zhaosong Fang et al [7] has conducted experiment on constructing envelope isolation on refrigerating energy consumption in summer and concluded that during devouring the same quantum of refrigerating energy, the inner temperature of the energy effective room was significantly less than the introductory room. This means refrigerating energy has been wasted and it also could route to thermal discomforting.

III. Energy Modelling

A. Building Details

In this present work, the building which is taken for analysis is located in Hyderabad, India. It is a three storeyed house building with a total floor area of 1800 sft.

The floor height is 12’ with a floor to ceiling clear space of 9’. The Walls are of the type of insulated concrete block with interior finish of lay-In acoustic tile with no batt insulation. The Ground Floor consists of a Parking Place, Garden, Kitchen, 2 Bedrooms, 2 Rest Rooms, Living Space and one Guest Room. The Ground Floor consists of a Parking Place, Garden, Kitchen, 2 Bedrooms, 2 Rest Rooms, Living Space and one Guest Room.

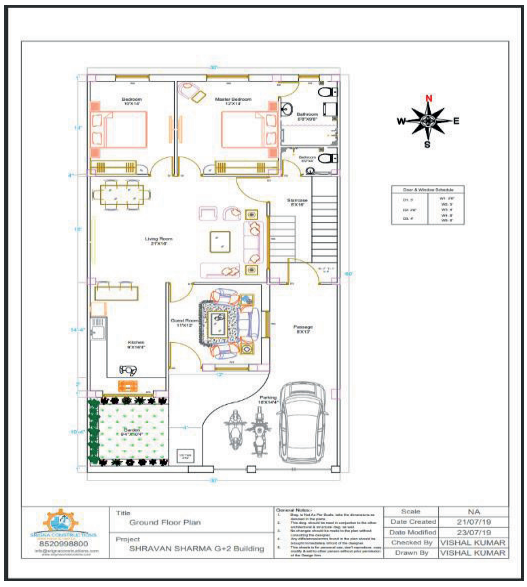

Figure 3. Ground Floor layout

First Floor consists of Balcony, Kitchen, 2 Bedrooms, 2 Rest Rooms, Guest Room, and Living Room is shown in Fig.3

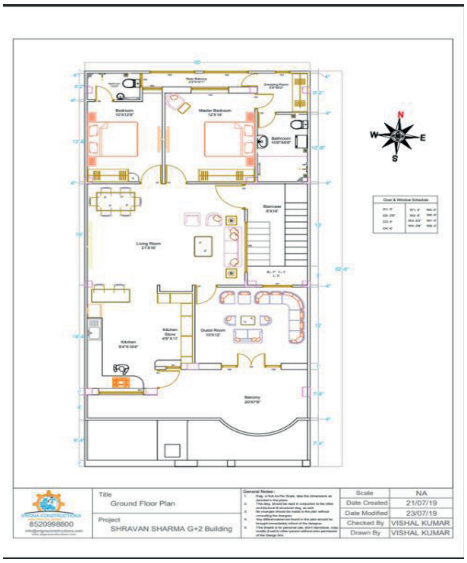

Figure 4. First Floor layout

Second Floor Consists of Staff Room, CEO Office, Meeting Room, Reception Area, 2 Bathrooms and Balconyis shown in Fig.4

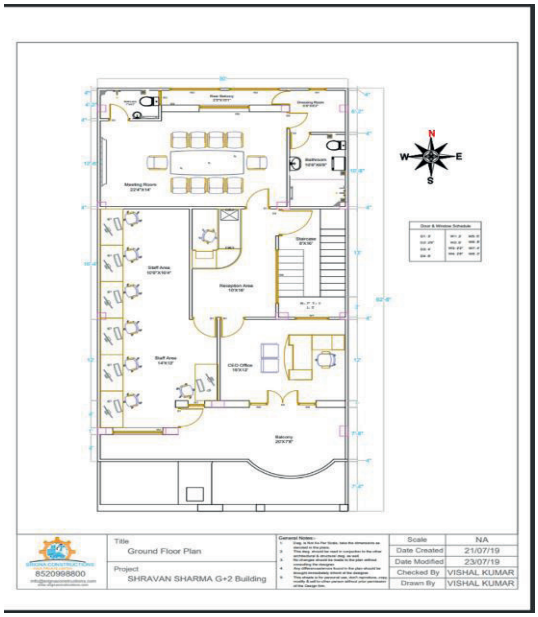

Figure 5. Second Floor layout

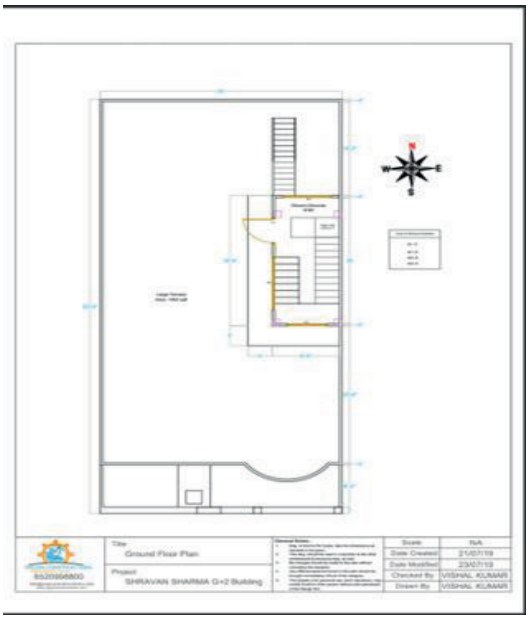

Figure 6. Terrace layout

Fig 5 and Fig.6 show Second and Terrace layout.

IV. E-QUEST PROJECT

A. Steps for building 3D Model

The first step is to open e-Quest and choose "Create New Project via the Wizard."

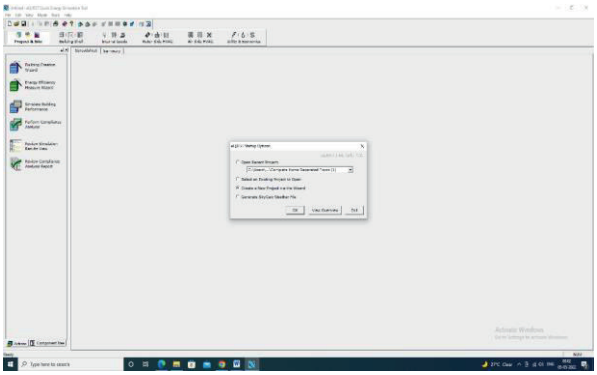

Figure 7. Create New Project Wizard

Fig 7 shows, how create a new project wizard in e-QUEST Software

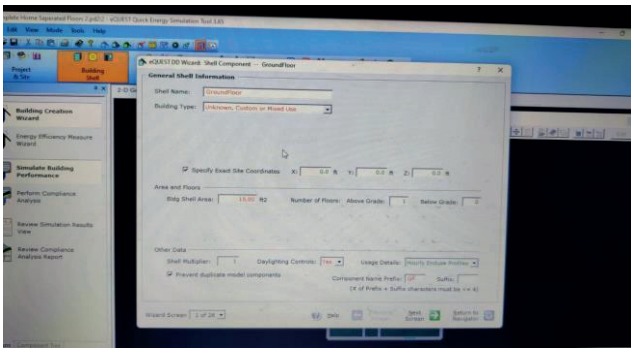

Figure 8. General Information of Building Wizard

This screen will collect general information about building such as size, location, etc shown in Fig.8

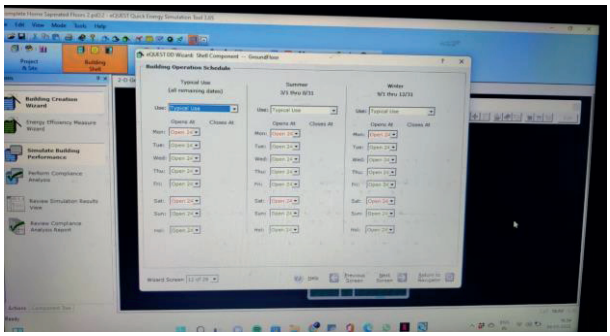

Figure 9. Building Operational Schedule Wizard

This step gathers information about operation timings of the building which is shown in Fig.9

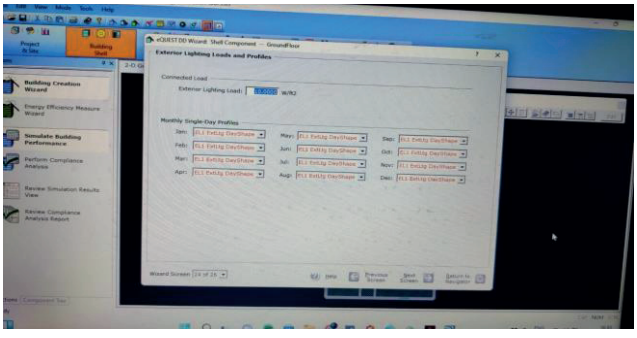

Figure 10. Exterior Lighting Loads

CVR Journal of Science and Technology, Volume 25, December 2023
DOI: 10.32377/cvrjst2515

Fig 10 shows the collecting information about exterior lighting loads.

V. About HVAC

Heating [1], ventilation, and air conditioning is the usage of different technologies to constrain the temperature and moisture of the air in a boxed place. Its goal is to provide thermal consolation and adequate inner air quality.

Heating devices generally include boaster motors which move the air throughout the range. An HVAC network usually contains an A.C or Heat pump [2] as a cooling equipment. An AC only cools but H.P can cool and heat the air. The main goal of HVAC [5] system is to circulate air throughout the room according to human comfort. An A.C, Heat pump and furnace absorbs heat or creates it and circulates through the passages called ducts inside the room. A boaster motor and ductwork assist to grease the motion of the air. Duct work directly connects to heating and cooling system.

Fig 11 shows the air-side HVAC system layout.

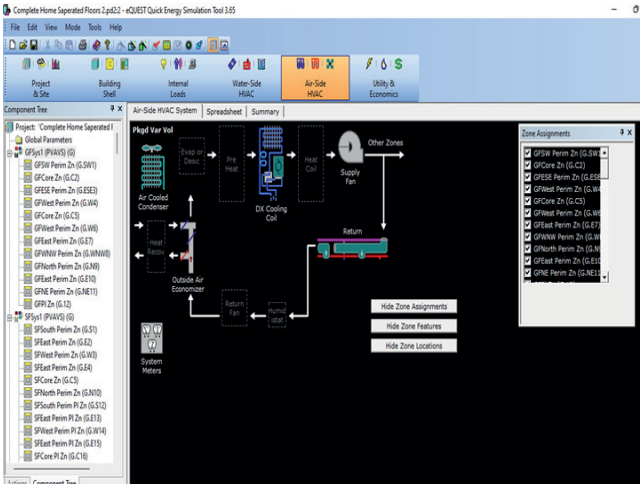

Figure 11. Air side HVAC system Layout

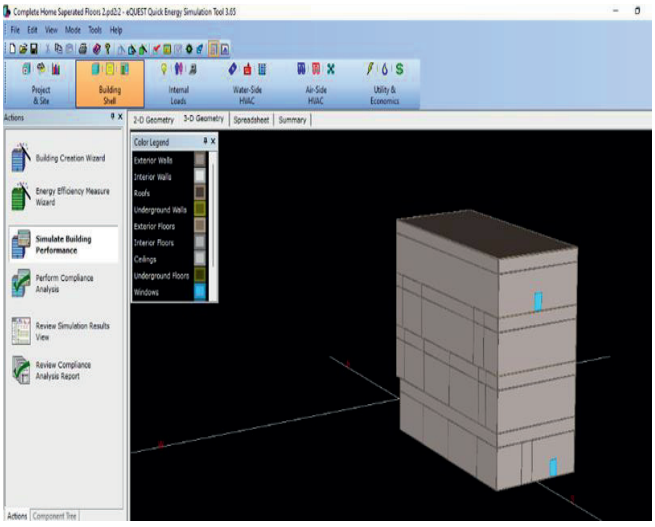

Figure 12. Side view of Building 3D Model

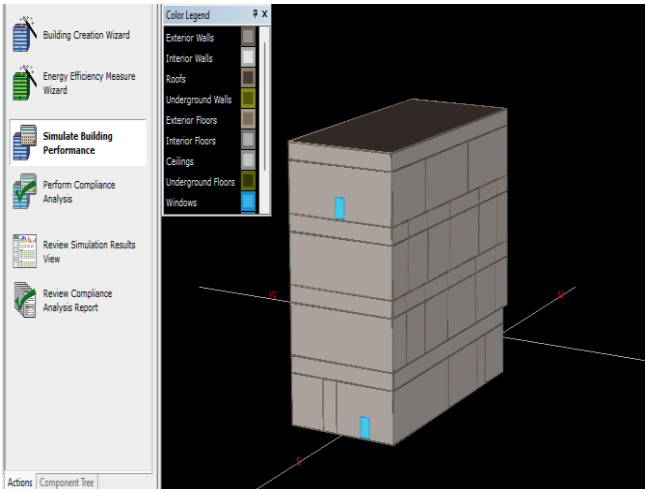

Figure 13. Front view of Building 3D Model

After successfully executing all the building creation and HVAC system steps, it will get a 3D model [3][4] of this building layout which is shown in Fig.12 and 13.

VI. Results and Discussions

During summer based on the setting parameters in the building creation steps, the simulation conclusions are displayed in Fig 14 and Fig 15. It gives results that more power [6][7] is up to 10080Kw-h that was consumed in the month of May. However, the lowest power is consumed in the month of January was only 6130Kwh, which was almost 40% less than the total power consumption in May.

Electric Consumption (kWh x000)

	Jan	Feb	Mar	Apr	May	Jun	Jul	Aug	Sep	Oct	Nov	Dec	Total
Space Cool	1.80	2.14	3.62	4.65	5.24	4.27	3.59	3.47	3.44	3.23	2.16	1.83	39.44
Heat Reject.	-	-	-	-	-	-	-	-	-	-	-	-	-
Refrigeration	-	-	-	-	-	-	-	-	-	-	-	-	-
Space Heat	0.01	-	-	-	-	-	-	-	-	-	-	-	0.01
HP Supp.	-	-	-	-	-	-	-	-	-	-	-	-	-
Hot Water	-	-	-	-	-	-	-	-	-	-	-	-	-
Vent. Fans	0.43	0.50	0.69	0.78	0.85	0.72	0.64	0.63	0.61	0.61	0.50	0.45	7.42
Pumps & Aux.	0.29	0.26	0.29	0.28	0.29	0.28	0.29	0.29	0.28	0.29	0.28	0.29	3.39
Ext. Usage	-	-	-	-	-	-	-	-	-	-	-	-	-
Misc. Equip.	2.24	2.11	2.52	2.32	2.34	2.42	2.24	2.52	2.33	2.24	2.23	2.34	27.87
Task Lights	-	-	-	-	-	-	-	-	-	-	-	-	-
Area Lights	1.37	1.32	1.51	1.37	1.36	1.38	1.27	1.45	1.34	1.33	1.36	1.43	16.48
Total	6.13	6.34	8.63	9.40	10.08	9.06	8.03	8.36	8.00	7.71	6.53	6.33	94.60

Figure 14. Electric consumption with respect to different months

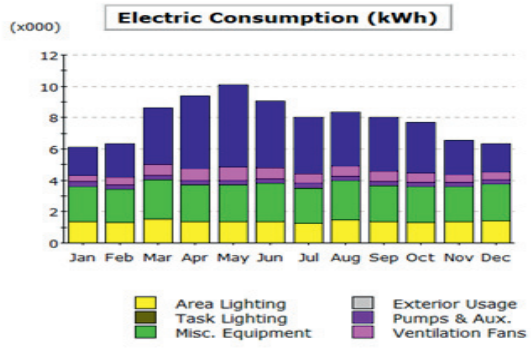

Figure 15. Electric consumption rate

During winter season, especially in Hyderabad region, the ambient air and temperature conditions are usually favorable to human comfort. So, the energy used for circulation of hot air outside is reduced amicably such that the total energy consumption rate is reduced drastically in January and also February. In May, the building payload increases with open-air temperature, so air conditioning power consumption reaches the greatest number. computed by the entire building region of 1800 square feet, the yearly energy consumption of per unit region is52.55 Kw h/(ft2).

VII. Conclusions

From these results, it is concluded that the energy consumption in summer is very high. Therefore, in this present work, it is focused on different parameters affecting energy consumption and tried to optimize it to the best of its ability by using different HVAC systems such as the following.

- Lighting device design: - To use this device, the variety of building shouldn't surpass the defined value. Corresponding to the simulation conclusions, it is recommended that 0.57W/ft2 (6.5W/m2) is more reasonable.
- In summer, the influence of stock air temperature on building electricity consumption is higher than the inner program temperature. For this purpose, DX cooling coils are suggested to improve energy optimization conditions and human comfort.

References

[1] Yimin Zhu. “Applying computer-based simulation to energy auditing: A case study”. Energy and Buildings, 38: 421—428, 2006.

[2] R. Pacheco, J. Ordónez, G. Martínez, “Energy efficient design of building”. A review, Renewable and Sustainable Energy Reviews - 2012.

[3] M. Santamouris, C. Pavlou, P. Doukas, G. Mihalakakou, A. Synnefa, A. Hatzibiros, “Investigating and analyzing the energy and environmental performance of an experimental green roof system installed in a nursery school building in Athens”, Energy -(2007)

[4] G.A. Florides, S.A. Kalogirou, S.A. Tassou, L.C. Wrobel, “Modeling of the mod-ern houses of Cyprus and energy consumption analysis”, Energy-(2000).

[5] Yi Zhitong, lv Yingyan , Xu Dikai , Xu Jingtao , Qian Hua, Zhao Dongliang , Yang Ronggui “Energy saving analysis of a transparent radiative cooling film for buildings with roof glazing” Energy and Built Environment Volume 2, Issue 2, April 2021, Pages 214-222.

[6] W.J. Hee, M.A. Alghoul, B. Bakhtyar, OmKalthum Elayeb , M.A. Shameri , M.S. Alrubaih , K. Sopian “The role of window glazing on daylighting and energy saving in buildings”, Renewable and Sustainable Energy Reviews Volume 42, February 2015, Pages 323-343.

[7] Zhaosong Fang, Nan, Baizhan Li, Guozhi Luo and Yanqi Huang “The effect of building envelope insulation on cooling energy consumption in summer”, Energy and Buildings Volume 77, July 2014, Pages 197-205.

E-ISSN 2581 – 7957
P-ISSN 2277 – 3916
CVR Journal of Science and Technology, Volume 25, December 2023
DOI: 10.32377/cvrjst2516

Crude Oil Price Forecasting – ARIMA Model Approach

V. Swapna
Sr. Asst. Professor, CVR College of Engineering/H&S(Statistics)Department, Hyderabad, India
Email: swapnacvr82@gmail.com

Abstract: **The price of crude oil forecasting has become more significant in the trade of day-to-day services of energy. A good predicting model increases the efficiency of producers, and consumers, and their prices are also playing a vital role in the investment process of financial trade. To analyze and forecast time series, a well-known ARIMA model is used in this paper to model month-ahead spot prices. The proposed model has been applied a series of times which consists of the monthly prices of crude oil from the Information of the U.S. Energy Administration.**

Index Terms: **Crude oil, Box-Jenkins Methodology, MAPE, and Forecasting**.

I. Introduction

In the terminology of economics, "energy" includes all the commodities and the resources of energy by providing the ability to accomplish work. The resources of Energy commodities like crude oil, diesel fuel, gasoline, natural gas, etc., could be used to offer the services of energy as per the requirements of human actions, namely cooking, electricity, electronic activity, lighting, motive power, space, and water heating. The resources of Energy played a basic role in shaping the human lifestyle. In the present days, the need of energy has become very important for the survival of people, so the production and the consumption of energy are the utmost dwelling needs of human survival on the earth.

A. About the data

This study employed the methodology of the data series with monthly crude oil prices beginning from Jan. 1986 to Nov. 2022. The data was taken from the Department of Energy, US: Administration in Energy Information: http://www.eia.doe.gov/

II. The Methodology

In this paper, the technique of traditional time series prediction, Auto-Regressive Integrated Moving Average (ARIMA) has been discussed. It is emphasized how the best suitable ARIMA models are to be applied in the forecasting price of crude oil.

A. ARIMA Modeling

Box and Jenkins presented the model, ARIMA, for the first time in 1976, then onwards, it became one of the most widely used forecasting strategies. [11] In the model of ARIMA, it has been assumed that the value of a variable in the future will be a linear combination of values and errors of the past.

$$Y_{t=}$$
$$\theta_0 + \emptyset_1 Y_{t-1} + \emptyset_2 Y_{t-2} + - - - + \emptyset_p Y_{t-p} + \epsilon_T - \theta_1 \epsilon_{t-1} - \theta_2 \epsilon_{t-2} - \cdots - \theta_q \epsilon_{t-q}$$
$$\theta_0 + \emptyset_1 Y_{t-1} + \emptyset_2 Y_{t-2} + - - - + \emptyset_p Y_{t-p} + \epsilon_T - \theta_1 \epsilon_{t-1} - \theta_2 \epsilon_{t-2} - \cdots - \theta_q \epsilon_{t-q}$$
__(1)

Here y_t is a real value, and φ, Θ are the coefficients, p, and q are integers that are repeatedly offered as autoregressive, ϵ_t has been the casual error at time t and moving average polynomials, in that order. Basically, the procedure has three phases: (i) Model classification, (ii) Parameter estimation, and (iii) Diagnostic examination. E.g., the model, ARIMA (1, 0, 1) ought to be characterized as follows. [1]

Equation (2):

$$Y_{t=}\theta_0 + \emptyset_1 Y_{t-1} + \epsilon_T - \theta_1 \epsilon_{t-1}$$
$$\theta_0 + \emptyset_1 Y_{t-1} + \epsilon_T - \theta_1 \epsilon_{t-1} \quad \_\_\_\_\_ (2)$$

The first Equation is a particular case of the family of ARIMA models. In equation (1), If q = 0, it becomes an AR model of order p, and when p = 0, it reduces to a MA model of order q. The important project of the model, [3] ARIMA construction will have to decide the appropriate order of the model (p, q). Box and Jenkins (1976) established an approach in the construction of the models of ARIMA, that has been a central effect on the prediction of applications and the analyzation of time series. [2]

The Partial Autocorrelation Function (PACF) and the Autocorrelation Function (ACF) of the collected data serve as the basic tools for recognizing the order of the model, ARIMA as stated by Box and Jenkins. Stationarity is the cornerstone of time series analysis as the essential phase to grow a new model which is to be applied for estimation. When creating an ARIMA [8] model that is used for prediction. A mean and variance of a stationary time series are constant. When the time series of experimentation exhibits trend, and heteroscedasticity. The collected data is subjected to power transformation and differencing to remove the trend and to maintain a frequent variance before fitting a model, ARIMA.

A general univariate model known as Auto Regressive Integrated Moving Averages (ARIMA) was developed on the presumption that the forecasted time series is stationary and linear.

Received on 26-04-2023, Revised on 05-10-2023, Accepted on 30-09-2023

The statistical records of data collection between July 1995 and November 2016 showed the average weekly price of crude is mapped as in Figure 1.

B. Time series plot

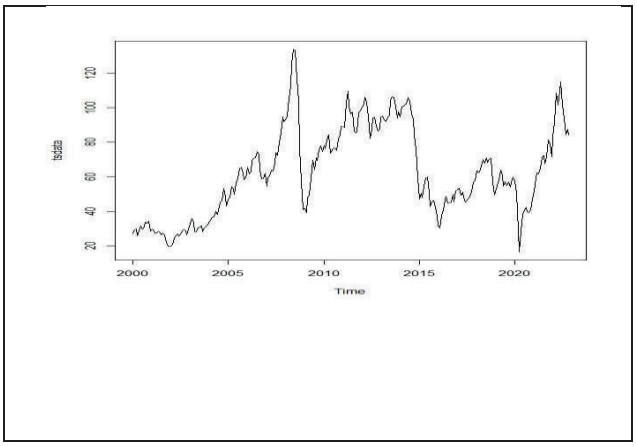

Figure 1. Time series plot of crude oil prices

It is observed as in Figure 1 that the series of time plot shows on average an increasing trend means non-stationary data. The model, ARIMA has been assessed only after converting the variable into a static series for forecasting. The natural transformation of the log is used to correct non-stationary variance and non-stationarity is corrected in an average by using suitable differentiating the data. Here, the variation of order 1 (i.e. d=1) can make data stationary in the mean. [6]

To identify the model parameters of the time series, normally we use ACF, PACF of the time series. ACF and PACF functions are used to determine the ARIMA model of a time series data. [9]

The ACF helps to identify the MA(q) hyper parameter, whereas PACF helps to identify the AR(p) hyper parameter. The difference between ACF, PACF shows the correlation between the point x(t) and a log function.

C. The time series data of ACF plot:

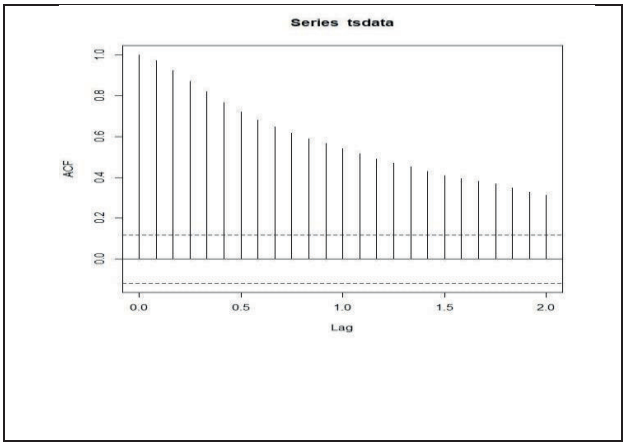

Figure 2. The prices of crude oil of the ACF plot.

D. The time series plot of PACF:

In the AR(p) process, the PACF has a significant spike at a certain lag q and PACF decay shows a sinusoidal behavior.

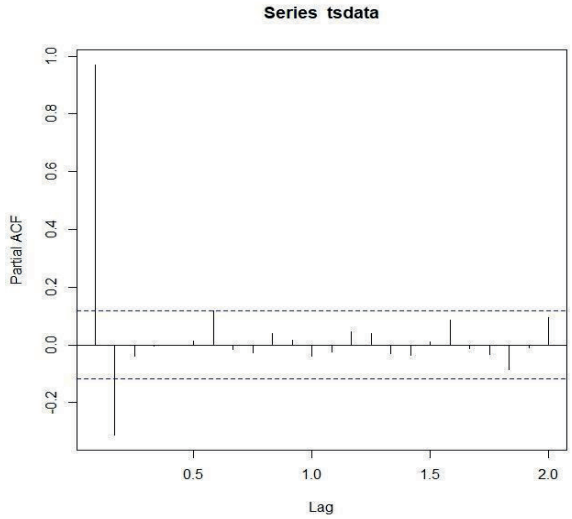

Figure 3. The prices of crude oil of PACF plot:

The above Figures 2,3 stated ACF and PACF plots show that the data is not stationary.

The given time series data is stationary at the variation of order 1 (d=1) and which is used for prediction of time series data for the year 2023.

The stationary time series data projection as follows at d=1

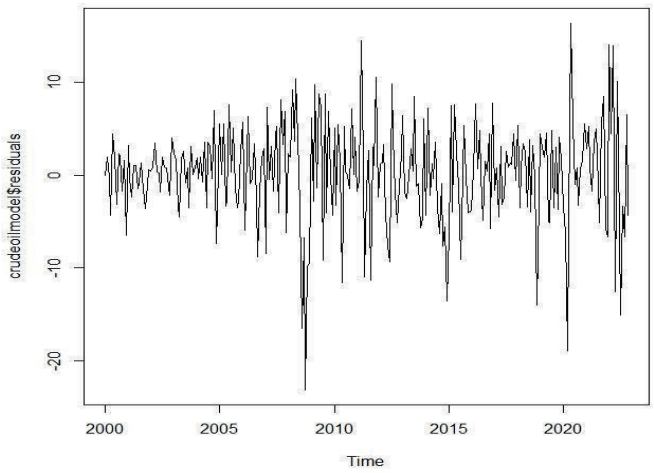

Figure 4. Residual plot of the crude oil prices

The Figure 4 shows that that the data has become stationary. The p value as 0.01 which proves this data has become stationary as given by Dickey-Fuller Test. Plotting from the ACF to the above differencing is given in Figure 5. [3].

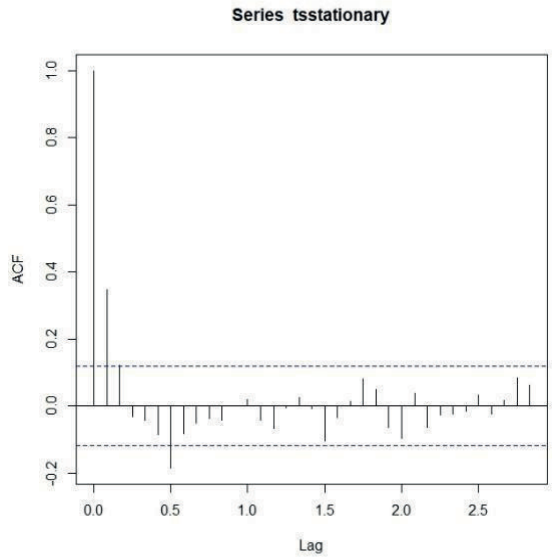

Figure 5. ACF of first difference data

For checking correlation between residuals, it gets the ACF. ACF has a significant spike at a certain lag p and ACF decay shows a sinusoidal behavior.

TABLE I.
ERROR MEASURES

Ljung Box Q test	Error measures						
Statistics	DF	P-value	MAPE	MAE	RMSE	BIC	AIC
17.058	20	0.6492	7.186	4.111	5.443	1718.39	1711.16

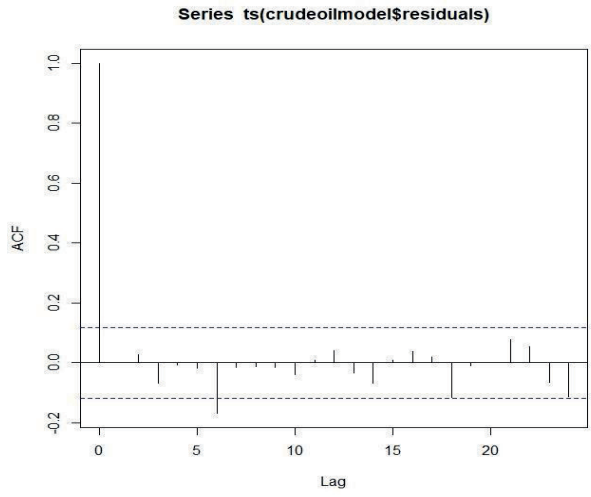

Figure 6. ACF of Residuals

The Figure 6 shows clearly that there is a little correlation between the residuals, hence, this forecasting is a good model.

Crude oil forecast:

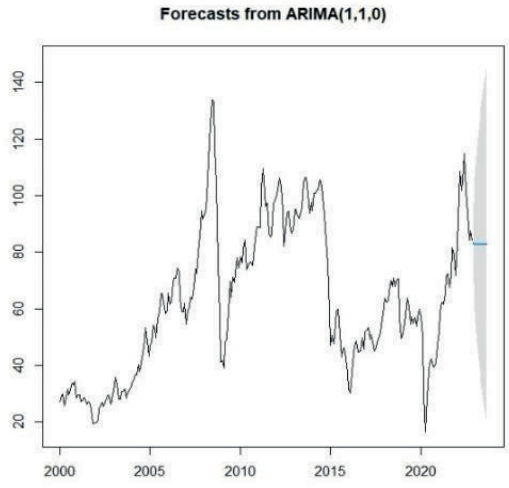

Figure 7. The prices of crude oil forecast:

The forecast values are given in Figure 7.

TABLE II.
ARIMA MODEL PARAMETERS

Model	AIC
ARIMA(1,1,0)	1711.16
ARIMA(0,1,1)	1715.99
ARIMA(0,1,0)	1744.41
ARIMA(1,1,1)	1713.16

From the above Table II of the ARIMA model parameters, it is observed that ARIMA (1,1,0) is fitting well for the data. [8] The parameters of the selected model are given in Table III.

TABLE III.
ARIMA MATHEMATICAL MODEL PARAMETER

Model	Parameter	P-value	Significance
AR(1)	0.3470	0.01	significant
MA(1)	0.0565	0.01	significant

The Mathematical model of ARIMA time series data for forecasting time series is

$$Yt = \mathbf{0.3470}Y_{t-1} + \mathbf{0.0565}$$

[8] For forecasting the prices of crude oil, the suitable model is.

TABLE IV.
FORECASTS OF THE PRICES OF CRUDE OIL

Year & Month	Prices (Dollars per Barrel)	Lower limit	Upper limit
Dec 2022	83.26	69.19	97.33
Jan 2023	82.88	59.27	106.48
Feb 2023	82.75	51.38	114.11
Mar 2023	82.70	44.82	120.57
Apr 2023	82.68	39.16	126.21
May 2023	82.68	34.13	131.23
Jun 2023	82.68	29.57	135.79
Jul 2023	82.68	25.36	139.99
Aug 2023	82.68	21.45	143.90
Sep 2023	82.68	17.76	147.59

From Table IV, it is observed from the forecasts that crude oil prices would reach 83 dollars per Barrel by September 2023 with the maximum scope of 147.59 Dollars per Barrel.

III. CONCLUSIONS

Among all the models used ARIMA (1,1,0) gave the best execution. There are theoretical reasons on why the model, ARIMA is a good prediction of Time Series data: [9]

The model, ARIMA, includes an amalgamation of both components of Auto Regressive (AR) and Moving Average (MA). The parameters of the ARIMA model have been estimated by minimizing the fitting errors. The ARIMA also determines the level of differencing used in making the data stationary to some extent.

Time series data forecasts may be accurate using a variety of sophisticated methods, but there are times when they significantly over fit the data. Additionally, most of them are deficient in flexibility. [11] The ARIMA has the advantage of being adaptable enough in capturing observed trends and associations as per the collected data while remaining simple enough but not to over fit the collected data.

The best prediction is provided by the neural network model when the analysis is extended to R.

In the proposed ARIMA model it is observed from the value of RMSE (5.443).

REFERENCES

[1] Ashok K. Nag and Amit Mitra (2002): “Forecasting Daily Foreign Exchange Rates Using Genetically Optimized Neural Networks”, Journal of Forecasting, 21, 501-511.
[2] Box, G.E.P. and G.M. Jenkins (1970): “Time series analysis: Forecasting and control”, San Francisco: Holden-Day.
[3] C.M. Kuan and T.Liu, “Forecasting exchange rates using feedforward and recurrent neural networks,” J. Appl. Econometrics, vol. 10, 1995, pp. 347–364.
[4] Ciobanu Dumitru, Vasilescu Maria, Advantages and Disadvantages of Using Neural Networks for Predictions (https://ideas.repec.org/a/ovi/oviste/vxiiy2012i1p444449.html)
[5] Honlun Yip, Hongqin Fan, Yathung Chiang (2014): "Predicting the maintenance cost of construction equipment: Comparison between general regression neural network and Box–Jenkins time series models", Automation in Construction, Vol.38, Pages. 30–38.
[6] Kanthala Sampath Kumar, V. Swapna, S.A. JyothiRani , V.V. Hara Gopal, (2018). Volatility of daily and Weekly Crude Oil Prices – A Statistical Perspective. International Journal of Scientific Research in Mathematical and Statistical Sciences, 5(5), 108-113.
[7] Makridakis, S., S.C. Wheelwright, and R.J. Hyndman (1998): “Forecasting: Methods and Applications”, New York: John Wiley & Sons.
[8] Raghavender, M., & Guguloth, R. (2015). Forecasting of maize production in Telangana.Rani, S. J., & Haragopal, V. V. Forecasting Exchange Rates using Neural Neworks.
[9] Ruslana Dalinina, Introduction to Forecasting with ARIMA in R https://blogs.oracle.com/datascience/introduction-to-forecasting-with-arima-in-r)
[10] V. Swapna, Kanthala Sampath Kumar, V.V. Hara Gopal, (2020). Statistical An alysis of the Costs of OPEC Crude Oil. International Journal of Scientific Research in Mathematical and Statistical Sciences, 7(4), 1-9.

E-ISSN 2581 – 7957
P-ISSN 2277 – 3916

CVR Journal of Science and Technology, Volume 25, December 2023
DOI: 10.32377/cvrjst2517

Recent Advances of Rhodium Catalyzed Coupling Reactions

Satyanarayana Battula
Asst. Professor, CVR College of Engineering/H&S (Chemistry) Department, Hyderabad, India.
Email: satyamssd@gmail.com

Abstract: **Rh-catalyzed few recent reactions including C–H activation (*sp2* and *sp3*), carbene insertion and boronic acid activations are reviewed. These strategies mostly assist to the development of a widely applicable and efficient protocol to the formation of various C-C (C*sp2*-C*sp2* and C*sp3*-C*sp2*) and C-X bonds in their particular domain; in addition, these new bonds perhaps incorporate important tandem cyclization to produce valuable heterocycles. These reactions highlight the innate nature of rhodium in selectivity as well as reactivity in the C-H bond functionalizations through the generation of organo-rhodium reactive intermediates.**

Index Terms: Rh-Catalysis, C-H activation, Carbene insertion, Heterocycles, C-X bonds, MCR

I. Introduction

Transition metal catalyzed cross-coupling reactions have been well familiar and are being essential tools in modern organic synthesis. Amongst, rhodium complexes are peculiar and most important for organic synthesis due to their ability to catalyze a variety of useful transformations [1-9]. The organic synthesis through rhodium catalysis associates the most recent progress and developments including in the field of cyclization reactions, C-H arylation reactions of arenes/ heteroarenes, multi component reactions and carbene coupling reactions by using rhodium(I) and rhodium(III) complexes [10-12]. In particular, carbene coupling reactions through trans-metalation & C-C activations catalyzed by rhodium(I) catalysts [3-9], additionally, C-H activation centered carbene coupling reactions are catalyzed by rhodium(III) catalysts [10-12]. Apart from its functionality, Rh(I) complexes are efficiently employed for C-X bond formations [13-16], especially in the challenging area bond formations, viz., C-S [17,18], C-Se [18], C-Si [19], and C-P [20] formations. On the other hand, rhodium (II) complexes are very prominent to catalyze C-H bond activations & insertions [21], classical carbene cross coupling reactions, cyclopropanations [22,23], and ylide formations [24]. Generally coupling reactions need a nucleophile and an electrophile as the coupling partners. The transition metal can connect both the fragments of the nucleophile as well as electrophile. Researchers worldwide focus on developing coupling reactions through expanding the new coupling partners.

II. Rhodium Catalyzed Coupling Reactions

Allylation of allylic ethers **1**/**5** with allyl magnesium chloride **2** was carried out by $RhCl(L)_2$ (L may be, nbd-norbornanediene, cod- 1,5-cycloocatdiene) in THF solvent under refluxing conditions to produce corresponding dienes **3** & **4**, and the product ratio depends on the conditions of the reaction and the nature of catalyst (Scheme 1). Apart from Grignard based reagent, $RhCl(cod)_2$ produces similar products of dienes with allylic zinc chloride substrate **6**, wherein the reaction was found to be facilitated by the presence of TMEDA ligand [25].

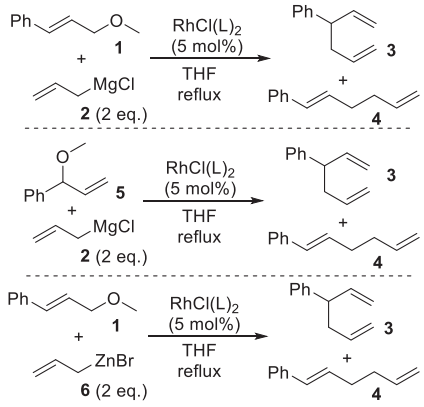

Scheme 1. Allylation of allyl ethers by Rh (I) complexes

In 2006, Kenichiro Itami and group developed a rhodium complex contains strongly π-acceptor ligands and also found its utility in the C-H arylations of hetero arenes with aryl iodides **8a** (Scheme 2) [26]. This Rh complex is very stable for long time; no decomposition of the material was detected even after 8 months. X-ray studies of this complex revealed that this might have happened as rhodium perhaps completely covered with two bulky ligands, viz., $P[OCH(CF_3)_2]_3$. In addition, this method also applied for the direct arylation of benzene, but with low efficacy and produces mixture of regio isomers.

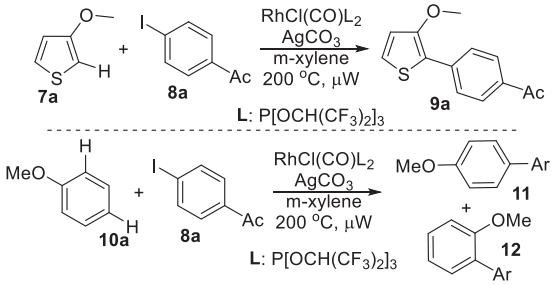

Scheme 2. Arylation of arenes/ heteroarens

Rhodium catalysts are also useful for multi component reactions (MCRs), Hayashi et. al. developed rhodium catalyzed MCR that involves cross coupling of organic halides. Reaction of alkyne tethered iodoarene **13** with organic zinc halide **6** in the presence of rhodium catalyst

Received on 02-05-20230, Revised on 19-08-2023, Accepted on 27-09-2023.

$RhCl(cod)_2$ in dioxane at 40 °C produces the cyclic compound **14** through carborhodation, oxidative addition and followed by reductive elimination. It was mechanistically proved that, this rhodium catalytic cycle is different to palladium catalyzed reaction of Pd(0)/Pd(II) catalytic cycle (Scheme 3) [27].

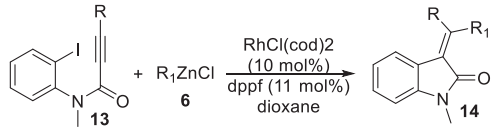

Scheme 3. Rhodium catalyzed arylation followed by cyclization.

In another multi component reaction, it involves rhodium(I) complex [of 1,5-Cyclooctadiene (cod) ligand] catalyzed the cross-coupling reaction of α-aryldizaoacetates **15** with different boronic acids **16** and alkyl halides **17** in the presence of a base KO*t*Bu to generate α,α-heterodiaryl carboxylic esters **18** (Scheme 4) [28]. Initially boronic acid forms organo-rhodium with rhodium complex and it produces allyl complex with diazo compound which finally undergoes alkylation with alkyl halide with the assistance of base to produce α,α-heterodiaryl carboxylic esters.

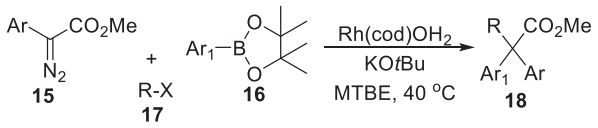

Scheme 4. Rhodium catalyzed cross coupling reaction of diazocarboxylate with boronic acid

Wang, J., et. al. developed a multi component reaction of tertiary propargyl alcohol **19a**, diazo ester **15** and alkyl halide **17** and that was catalyzed by $Rh(cod)OH_2$ with BINAP ligand in the presence of a base NaOMe in toluene solvent produces the product **20** through simultaneous alkyl and alkynyl coupling reactions (Scheme 5) [29]. These two coupling partners are linked with carbene moiety leads to produce C(*sp*)-C(*sp3*) and C(*sp3*)-C(*sp3*) chemical bonds. These reactions are helpful to construct quaternary centers with readily available materials.

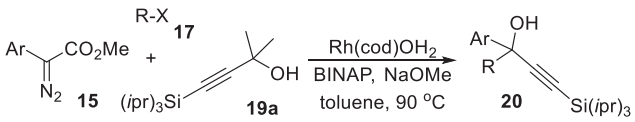

Scheme 5. Rhodium catalyzed successive C(sp)-C(sp3) and C(sp3)-C(sp3) bond formations

In addition, carbene mediated coupling of diazoester **15** with arylstannane **21a** was being developed by the same Wang, J., group (Scheme 6) [30]. The reaction is carried out between diazoester and arylstannane with the aid of the same catalyst $Rh(cod)OH_2$ (2 mol%) and ligand XPhos (10 mol%) in the presence of an additive KF (1 equiv) and in THF/H_2O solvent mixture at 70 °C leads to generate Stille like coupling product **22**. The process of this reaction is very easy and mild and this reaction offers a good method for the synthesis of α-aryl esters molecules.

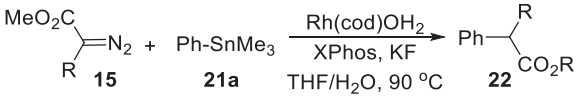

Scheme 6. Rhodium catalyzed Stille type coupling reaction

They also found the utility of diazoesters **15** in the reaction with arylsiloxane reagents **23** in presence of 2 mol% $Rh(cod)OH_2$, 10 mol% of $PCy_3.HBF_4$ and 1 equiv TBAF (Scheme 7) [31]. It is also another example for Csp3-Csp2 coupling reaction and produces the same compound/ α-aryl esters **22**. This reaction was the initial example for arylsiloxanes as coupling agents. This reaction is proceeded through the Rh(I) carbene migratory insertion.

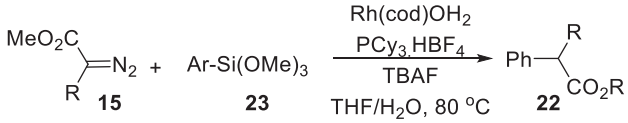

Scheme 7. Rhodium catalyzed diazoester coupling reaction with arylsiloxane

Jiang and his coworkers developed a method to the synthesis of densely functionalized benzo[b]flourenes and 2-napthalenylmethanones through a synergistic bimetallic catalytic pathway, which involves 1.5 mol% $(RhCp^*Cl_2)_2$ and 10 mol% CuI from the reaction of 1,5-eneyn **23** with aryl diazoacetate **15** in the presence of 4 equiv additive TIBN (triisobutylamine) in DMF solvent at 60 °C (Scheme 8) [32]. Amongst, the former reaction happened with aryl diazoester **15a** produces functionalized benzo[b]flourenes **24**; while the second reaction involves the use of ethyl diazoacetate **15b** to generate functionalized napthalenes **25**. The reaction was proved to start with in-situ formed rhodium carbenoids.

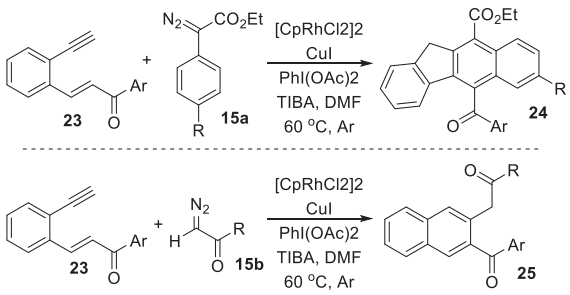

Scheme 8. Rhodium catalyzed synthesis to benzo[b]flourenes and 2-napthalenylmethanones

A coupling reaction of alkyltrifluoroborate **26** with α-diazomalonates **15** was being developed by Yu, W. -Y., and his group through the C(*sp3*)-C(*sp3*) coupling and these coupled products **27** were formed up to 97% yields and it was shown in Scheme 9 [33]. Cp*Rh(III) catalyst along with an additive AgOAc were used for the reaction in methanol solvent. For the diazo partners, useful functional groups, including ketone, ester, amide, ether, sulfonyl, and thiophenes were tested successfully. Mass spectrometry (ESI-MS) study of the reaction clearly indicated that the formation of a distinct molecular species corresponding to σ-alkylrhodium(III) complexes. The successful diazo

coupling reaction may be attributed to the coordination of the amide group and that promotes stability of the alkylrhodium (III) complex through the formation of a five membered metallacycle.

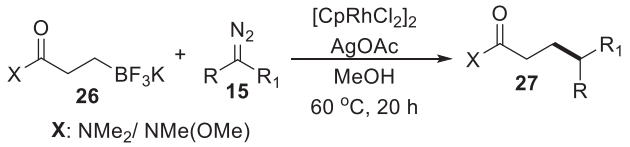

Scheme 9. Rh(III)-catalyzed cross coupling of alkyl trifluoroborate with α-diazomalonates

In one more diazoacetate reaction, cross coupling was observed through rhodium catalyzed reaction between 2-bromoethyl aryldiazoacetates **15c** with tertiary propargyl alcohol **28a** (Scheme 10) [34]. This cross coupling occurred with the assistance of 2 mol% $Rh(cod)OH_2$ catalyst and 1 equiv of NaO*t*Bu, 10 mol% of TBAI phase transfer catalyst in mixture of solvent (water and toluene) to afford carbene involved lactonization to produce **29**. It proceeds through a sequential cleavage of C-C bonds followed by the formation of C(sp2)-C(sp) and C-O bonds.

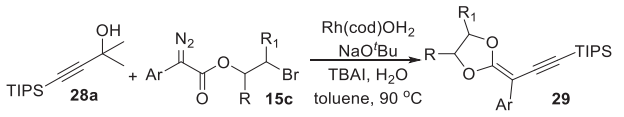

Scheme 10. Rh(III)-catalyzed cross coupling of tertiary propargyl alcohol with diazoacetates

Zhao, Y. L. and his workers reported coupling of diazoacetate followed by cyclization in presence of rhodium catalyst (Scheme 11) [35]. This cyclization occurred between alkenyldiazoacetates **15** with o-alkenyl arylisocyanides **15** with 3 mol% $[Rh(cod)Cl_2]$ and 0.3 equiv of $Cu(MeCN)_4BF_4$ in chlorobenzene at 55 °C for 16 h to produce carbazoles **31**. During this reaction, intramolecular [4+2] cycloaddition/ oxidative aromatization process leads to produce carbazoles.

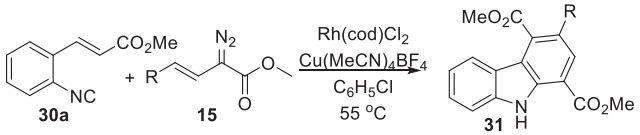

Scheme 11. Rh(III)-catalyzed synthesis to carbazoles

Ellmann, J. A., and coworkers reported a Rh(III) catalyzed multicomponent coupling reaction between aldehydes **32a**, 2-aminopyridines **33** and diazoesters **15d** to produce pyrido[1,2-a]pyrimidine-4-ones **34** (Scheme 12) [36]. This reaction proceeds through imine formation between 2-aminopyridine and aldehyde, and followed by imine C-H activation by Rh(III), carbene insertion and cyclization to generate the final product **34**. The reaction is very comfort with aromatic aldehydes and enolizable aldehydes; in addition, trimethyl orthoformate and DMF dimethyl acetals are also used for the substitute of aldehyde to launch –OMe and dimethylamino functional groups on pyrimidine ring.

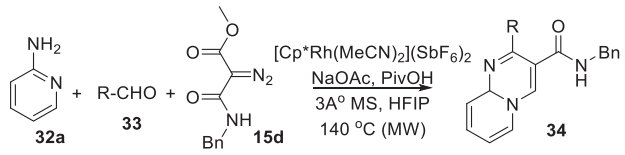

Scheme 12. Rh(III)-catalyzed synthesis to pyrido[1,2-a]pyrimidine-4-ones

Tech-Peng Loh and co-workers developed a rhodium catalyzed direct oxidative cross coupling of acrylamides **35** with olefins **36** to produce (Z,E) dienamides **37**, wherein they used a co-oxidant $Cu(OAc)_2.H_2O$ along with rhodium complex $[RhCl_2Cp^*]_2$. This reaction indicates the rhodium complex ability in the generation of Csp2- Csp2 cross coupling reaction, and it had shown a wide substrate flexibility and functional group compatibility (Scheme 13) [37].

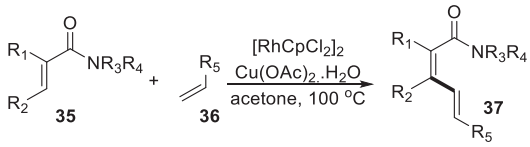

Scheme 13. Rhodium catalyzed sp2-sp2 cross coupling reaction

A similar sort of coupling was achieved by Miura and group in a reaction between aryl boronic acids **38** and alkenyl dihalides **36** and that was catalyzed by 3 mol% of $Rh(cod)OH_2$ and 6 mol% of 1,4-bis(diphenylophosphino)butane (DPPB) in presence of K_3PO_4 in dioxane solvent and refluxed at 100 °C for about 8 to 15 h produces mono-arylated olefins **39** (Scheme 14) [38]. This reaction is worked well with 1,2-dichloro and 1,2-dibromo alkenes, and yielded products in appreciable yields with regioselectivity wherein it produces E-isomer majorly rather Z-isomer. Moreover, the reaction of 1,1-dihalo alkene under the said conditions produces corresponding di-arylated product with aryl boronic acids but with less yield.

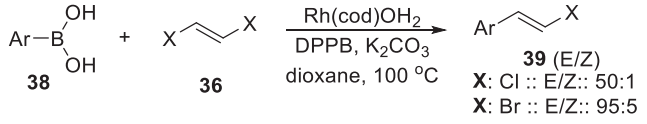

Scheme 14. Rhodium catalyzed mono-arylation of alkenylhalides with aryl boronic acids

Yu and his group developed a rhodium catalyzed C-H arylation of arenes with phenyl boronic acid esters **38** (Scheme 15). In this reaction, the ability of $[Cp^*RhCl_2]_2$ catalyzed reaction was considerably increased by bidentate phosphine ligand (BINAP). The reaction is initiated by the presence of an easily labile donating group N-pentafluorophenylbenzamide **40** for the first time as an auxiliary. The reaction offers a practical and general method to this C-H arylation of versatile benzamide and boronic ester substrates [39].

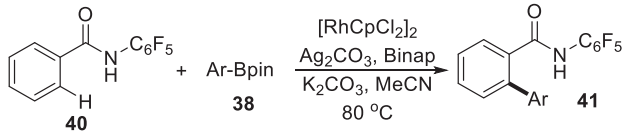

Scheme 15. Rhodium catalyzed C-H arylation

Apart from diazo compounds as carbene precursors, Wang and coworkers are being used conjugated enynones **42** as a carbene precursor with boronic acids **38** in the synthesis of furyl containing triarylmethanes **43** through a rhodium catalyzed method (Scheme 16) [40], wherein 2 mol% of $Rh(cod)(OH)_2$ and 1 equiv of base KOtBu were used in MeOH solvent at 80 °C. These mild reaction conditions are facilitated to the synthesis of functionalized furan compounds. The reaction involves Rh(I) carbene formation, migration, insertion in a sequence in the generation of products.

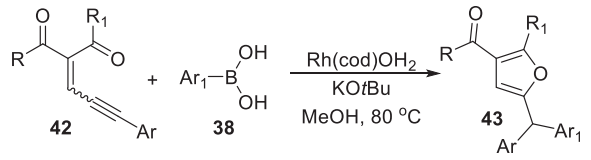

Scheme 16. Rhodium catalyzed synthesis to furan compounds

Regioselective synthesis of phenanthridinone heterocycles **45** were achieved from N-methoxy benzamides **44** and aryl boronicacids **38** through the Rh(III) catalysis (Scheme 17). It involves one pot C-C/C-N bond formation leads to a (4+2) cyclization in a milder approach. This transformation was initiated by Ag^+ through the removal of halide ion from the catalyst in presence of ligand, during process Rh(III) converted to Rh(I) and which is re-oxidized to the required catalyst by the oxidation of Ag2O to further catalytic action [41].

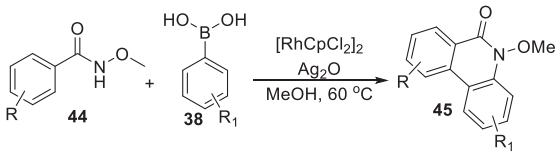

Scheme 17. Rhodium (III) catalyzed synthesis of phenanthridinones

Along with regular C-H activations/ functionalizations, rhodium could produce C-C activation and utilization of this protocol into a new bond formation with boronic acids. Wang, J., and coworkers discovered rhodium catalyzed direct exchange of the methyl/ aryl group of a ketone with another aryl group from boronicacid (Scheme 18) [42]. In this reaction 1-(quinolin-8-yl)ethanone substrates **46** were treated with boronicacids **38** in the presence of $Rh(PPh_3)Cl$, CuI, and a base K_2CO_3 refluxed at 130 °C in xylene. The reaction was initiated directly with C-C activation through Rh(I) complex formation and subsequent boronicacid transmetalations by Rh(I)/Rh(III) catalytic cycle produces the coupling product **48**.

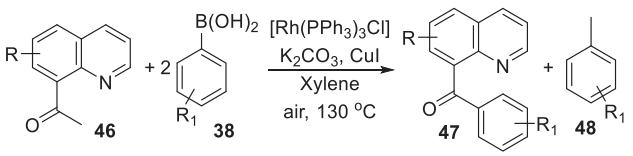

Scheme 18. Rhodium (I) catalyzed C-C activation with boronicacids

Wang, Z., and his group developed the rhodium catalyzed C-P cross coupling reaction by the reaction of aryl iodides **8** with acylphosphines **49** which served as reagent as well as ligand in this reaction. Generally, these C-P cross coupling reactions are familiar with transition element catalysis, but Rh(I) catalyzed C-P formations are rare. This reaction was the foremost example for rhodium catalyzed C-P bond formation (Scheme 17) [20].

Scheme 19. Rh(I) catalyzed C-P cross coupling reaction

Li, X., and his coworkers were being used 4-acyl-1-sulfonyltriazoles **52** as carbene source in $Cp^*Rh(III)$ catalyzed C-H bond activation of ortho-selective coupling reaction and described in Scheme 18. This coupling reaction produces olefin and later with further feasibility, undergoes cyclization to generate cyclized product **57** (on the basis of nature of arene) [43].

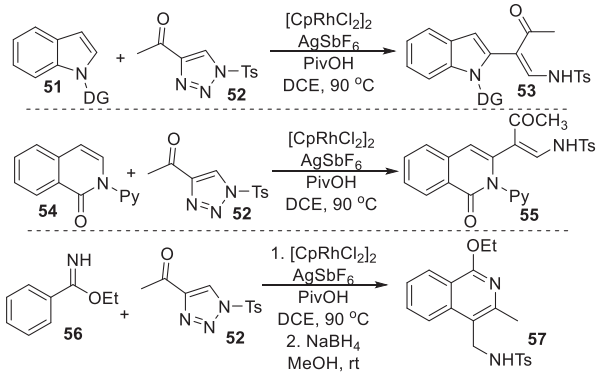

Scheme 20. Rh(III) catalyzed C-C coupling of arenes with sulfonyltriazoles

III. Conclusions

In summary, we present the recent reaction profile and scope of the rhodium catalyzed coupling reactions that are important in the synthetic organic chemistry as its selective reactivity and carbene insertion reactions by its feasible organometallic intermediate formation. Particularly, these mild approaches afford a wide range of powerful, general and efficient methods for the construction of intricate aza-fused heterocycles, polycyclic structures and heterocyclic scaffolds. However, the noteworthy achievements have been made, still challenging rhodium catalyzed reactions associates multiple C-H bond activations, direct C-H bond activation without the involvement of metal chelation and innate *sp3*C-H activations remains offer a great scope to chemists worldwide. Eventually, these rhodium catalyzed reactions are to be a tool in future to construct various stimulating organic structural frameworks.

References

[1] K. Fagnou and M. Lautens. Rhodium-Catalyzed Carbon−Carbon Bond Forming Reactions of Organometallic Compounds. *Chem. Rev.*, **2003**, *103*, 169-196. https://doi.org/10.1021/cr020007u.

[2] F. Chen, T. Wang and N. Jiao. Recent Advances in Transition-Metal-Catalyzed Functionalization of Unstrained Carbon–Carbon Bonds. *Chem. Rev.*, **2014**, *114*, 8613-8661. https://doi.org/10.1021/cr400628s.

[3] L. Souillart and N. Cramer. Catalytic C–C Bond Activations via Oxidative Addition to Transition Metals. *Chem. Rev.*, **2015**, *115*, 9410-9464. https://doi.org/10.1021/acs.chemrev.5b00138.

[4] G. Fumagalli, S. Stanton and J. F. Bower. Recent Methodologies That Exploit C–C Single-Bond Cleavage of Strained Ring Systems by Transition Metal Complexes. *Chem. Rev.*, **2017**, *117*, 9404-9432. https://doi.org/10.1021/acs.chemrev.6b00599.

[5] P. Chen, B. A. Billett, T. Tsukamoto and G. Dong. "Cut and Sew" Transformations via Transition-Metal-Catalyzed Carbon–Carbon Bond Activation. *ACS Catal.*, **2017**, *7*, 1340-1360. https://doi.org/10.1021/acscatal.6b03210.

[6] Y. Zeng, H. Gao, Y. Zhu, Z. Jiang, Z. Jiang. Site-Divergent Alkenyl C–H Fluoroallylation of Olefins Enabled by Tunable Rhodium Catalysis. *ACS Catal.,* **2022**, *12*, 8857–8867. https://doi.org/10.1021/acscatal.2c00540.

[7] D. A. Colby, A. S. Tsai, R. G. Bergman and J. A. Ellman. Rhodium Catalyzed Chelation-Assisted C–H Bond Functionalization Reactions. *Acc. Chem. Res.*, **2012**, *45*, 814-825. https://doi.org/10.1021/ar200190g.

[8] G. Song, F. Wang and X. Li. C–C, C–O and C–N bond formation via rhodium(iii)-catalyzed oxidative C–H activation. *Chem. Soc. Rev.,* **2012**, *41*, 3651-3678. https://doi.org/10.1039/C2CS15281A.

[9] N. Kuhl, N. Schröder and F. Glorius. Formal SN-Type Reactions in Rhodium(III)-Catalyzed C-H Bond Activation. *Adv. Synth. Catal.*, **2014**, *356*, 1443-1460. https://doi.org/10.1002/adsc.201400197.

[10] A. Vigalok and D. Milstein. Direct Synthesis of Thermally Stable PCP-Type Rhodium Carbenes. *Organometallics*, **2000**, *19*, 2061-2064. https://doi.org/10.1021/om990764r.

[11] R. Cohen, B. Rybtchinski, M. Gandelman, H. Rozenberg, J. M. Martin and D. Milstein. Metallacarbenes from Diazoalkanes: An Experimental and Computational Study of the Reaction Mechanism. *J. Am. Chem. Soc.*, **2003**, *125*, 6532-6546. https://doi.org/10.1021/ja028923c.

[12] C. Werle, R. Goddard, P. Philipps, C. Fares and A. Fu¨rstner. Structures of Reactive Donor/Acceptor and Donor/Donor Rhodium Carbenes in the Solid State and Their Implications for Catalysis. *J. Am. Chem. Soc*., **2016**, *138*, 3797-3805. https://doi.org/10.1021/jacs.5b13321.

[13] L. Vilella-Arribas, M. García-Melchor, D. Balcells, A. Lledós, J. A. López, S. Sancho, B. E. Villarroya, M. P. d. Río, M. A. Ciriano and C. Tejel. Rhodium Complexes Promoting C−O Bond Formation in Reactions with Oxygen: The Role of Superoxo Species. Chem. Eur. J, **2017**, *23*, 5232-5243. https://doi.org/10.1002/chem.201605959.

[14] A. M. Geer, Á. L. Serrano, B. d. Bruin, M. A. Ciriano and C. Tejel. Terminal Phosphanido Rhodium Complexes Mediating Catalytic P-P and P-C Bond Formation. *Angew. Chem. Int. Ed.*, **2015**, *54*, 472-475. https://doi.org/10.1002/anie.201407707.

[15] V. Varela-Izquierdo, A. M. Geer, J. Navarro, J. A. López, M. A. Ciriano, and C. Tejel. Rhodium Complexes in P–C Bond Formation: Key Role of a Hydrido Ligand. *J. Am. Chem. Soc*., **2021**, *143*, 349–358. https://doi.org/10.1021/jacs.0c11010.

[16] D. A. Colby, R. G. Bergman and J. A. Ellman. Rhodium-Catalyzed C−C Bond Formation via Heteroatom-Directed C−H Bond Activation. *Chem. Rev.*, **2010**, *110*, 624-655. https://doi.org/10.1021/cr900005n.

[17] M. Arisawa, T. Suzuki, T. Ishikawa and M. Yamaguchi. Rhodium-Catalyzed Substitution Reaction of Aryl Fluorides with Disulfides: p-Orientation in the Polyarylthiolation of Polyfluorobenzenes. *J. Am. Chem. Soc.*, **2008**, *130*, 12214-12215. https://doi.org/10.1021/ja8049996.

[18] K. Ajiki, M. Hirano and K. Tanaka. Rhodium-Catalyzed Reaction of Thiols with Polychloroalkanes in the Presence of Triethylamine. *Org. Lett.*, **2005**, *7*, 4193-4195. https://doi.org/10.1021/ol0501673.

[19] J. P. Morales-Ceron, P. Lara, J. Lopez-Serrano, L. L. Santos, V. Salazar, E. Álvarez and A. Saurez. Rhodium(I) Complexes with Ligands Based on N-Heterocyclic Carbene and Hemilabile Pyridine Donors as Highly E Stereoselective Alkyne Hydrosilylation Catalysts. *Organometallics*, **2017**, *36*, 2460-2469. https://doi.org/10.1021/acs.organomet.7b00361.

[20] J. Yang, H. Wu and Z. Wang. Rhodium-catalyzed triarylphosphine synthesis via cross-coupling of aryl iodides and acylphosphines. *J. Saudi Chem. Soc.*, **2018**, *22*, 1-5. https://doi.org/10.1016/j.jscs.2016.07.002.

[21] Y. Shi, A. V. Gulevich and V. Gevorgyan. Rhodium-Catalyzed NH Insertion of Pyridyl Carbenes Derived from Pyridotriazoles: A General and Efficient Approach to 2-Picolylamines and Imidazo[1,5-a]pyridines. *Angew. Chem. Int. Ed.*, **2014**, *53*, 14191-14195. https://doi.org/10.1002/anie.201408335.

[22] L. R. Collins, S. Auris, R. Goddard and A. Fürstner. Chiral Heterobimetallic Bismuth–Rhodium Paddlewheel Catalysts: A Conceptually New Approach to Asymmetric Cyclopropanation. *Angew. Chem. Int. Ed.*, **2019**, *58*, 3557-3561. https://doi.org/10.1002/anie.201900265.

[23] K. O. Marichev, Y. Wang, A. M. Carranco, E. C. Garcia, Z.-X. Yu and M. P. Doyle, Rhodium(ii)-catalysed generation of cycloprop-1-en-1-yl ketones and their rearrangement to 5-aryl-2-siloxyfurans. *Chem. Commun.*, **2018**, *54*, 9513-9516. https://doi.org/10.1039/C8CC05623D.

[24] Z.-S. Chen, X.-Y. Huang, L.-H. Chen, J.-M. Gao and K. Ji. Rh(II)/Pd(0) Dual Catalysis: Regiodivergent Transformations of Alkylic Oxonium Ylides. *ACS Catal.*, **2017**, *7*, 7902-7907. https://doi.org/10.1021/acscatal.7b02909.

[25] H. Yasui, K. Mizutani, H. Yorimitsu and K. Oshima. Cobalt- and rhodium-catalyzed cross-coupling reaction of allylic ethers and halides with organometallic reagents. *Tetrahedron*, **2006**, *62*, 1410-1415. https://doi.org/10.1016/j.tet.2005.11.032.

[26] S. Yanagisawa, T. Sudo, R. Noyori and K. Itami, Direct C−H Arylation of (Hetero)arenes with Aryl Iodides via Rhodium Catalysis. *J. Am. Chem. Soc.*, **2006**, *128*, 11748-11749. https://doi.org/10.1021/ja064500p.

[27] R. Shintani, T. Yamagami and T. Hayashi. Rhodium-Catalyzed Multicomponent-Coupling Reactions Involving a Carborhodation−Cross-Coupling Sequence. *Org. Lett.*, **2006**, *8*, 4799-4801. https://doi.org/10.1021/ol061858h.

[28] Y.-T. Tsoi, Z. Zhou and W.-Y. Yu. Rhodium-Catalyzed Cross-Coupling Reaction of Arylboronates and Diazoesters and Tandem Alkylation Reaction for the Synthesis of Quaternary α,α-Heterodiaryl Carboxylic Esters. *Org. Lett.*, **2011**, *13*, 5370-5373. https://doi.org/10.1021/ol2022577.

[29] Y. Xia, S. Feng, Z. Liu, Y. Zhang and J. Wang. Rhodium(I)-Catalyzed Sequential C(sp)-C(sp3) and C(sp3)-C(sp3) Bond Formation through Migratory Carbene Insertion. *Angew. Chem*., **2015**, *127*, 8002-8005. https://doi.org/10.1002/ange.201503140.

[30] Z. Liu, Y. Xia, S. feng, S. Wang, D. Qui, Y. Zhang and J. Wang. RhI-Catalyzed Stille-Type Coupling of Diazoesters with Aryl Trimethylstannanes. *Aust. J. Chem.*, **2015**, *68*, 1379-1384. https://doi.org/10.1071/CH15218.

[31] Y. Xia, Z. Liu, S. Feng, F. Ye, Y. Zhang and J. Wang. Rh(I)-Catalyzed Cross-Coupling of α-Diazoesters with Arylsiloxanes. *Org. Lett.*, **2015**, *17*, 956-959. https://doi.org/10.1021/acs.orglett.5b00052.

[32] Y.-N. Wu, T. Xu, R. Fu, N.-N. Wang, W.-J. Hao, S.-L. Wang, G. Li, S.-J. Tu and B. Jiang. Dual rhodium/copper catalysis: synthesis of benzo[b]fluorenes and 2-naphthalenylmethanones via de-diazotized cycloadditions. *Chem. Commun.*, **2016**, *52*, 11943-11946. https://doi.org/10.1039/C6CC06320A.

[33] Y.-S. Lu and W.-Y. Yu. Cp*Rh(III)-Catalyzed Cross-Coupling of Alkyltrifluoroborate with α-Diazomalonates for C(sp3)–C(sp3) Bond Formation. *Org. Lett.*, **2016**, *18*, 1350-1353. https://doi.org/10.1021/acs.orglett.6b00283.

[34] Z. Liu, Y. Xia, S. Feng, Y. Zhanga and J. Wang. Rh(i)-Catalyzed coupling of 2-bromoethyl aryldiazoacetates with tertiary propargyl alcohols through carbene migratory insertion. *Org. Chem. Front.*, **2016**, *3*, 1691-1698. https://doi.org/10.1039/C6QO00453A.

[35] L. Zhang, T. Liu, Y.-M. Wang, J. Chen and Y.-L. Zhao. Rhodium-Catalyzed Coupling–Cyclization of Alkenyldiazoacetates with o-Alkenyl Arylisocyanides: A General Route to Carbazoles. *Org. Lett.*, **2019**, *21*, 2973–2977. https://doi.org/10.1021/acs.orglett.9b00307.

[36] G. L. Hoang, A. J. Zoll and J. A. Ellman. Three-Component Coupling of Aldehydes, 2-Aminopyridines, and Diazo Esters via Rhodium(III)-Catalyzed Imidoyl C–H Activation: Synthesis of Pyrido[1,2-a]pyrimidin-4-ones. *Org. Lett.*, **2019**, *21*, 3886–3890. https://doi.org/10.1021/acs.orglett.9b00779.

[37] J. Zhang and T.-P. Loh. Ruthenium- and rhodium-catalyzed cross-coupling reaction of acrylamides with alkenes: efficient access to (Z,E)-dienamides. *Chem. Commun.*, **2012**, *48*, 11232-11234. https://doi.org/10.1039/C2CC36137J.

[38] T. Matsuda, K. Suzuki and N. Miura. Rhodium-Catalyzed Cross-Coupling of Alkenyl Halides with Arylboron Compounds. *Adv. Synth. Catal.*, **2013**, *355*, 3396-3400. https://doi.org/10.1002/adsc.201300482.

[39] H.-W. Wang, P.-P. Cui, Y. Lu, W.-Y. Sun and J.-Q. Yu. Ligand-Promoted Rh(III)-Catalyzed Coupling of Aryl C–H Bonds with Arylboron Reagents. *J. Org. Chem.*, **2016**, *81*, 3416-3422. https://doi.org/10.1021/acs.joc.6b00083.

[40] Y. Xia, L. Chen, P. Qu, G. Ji, S. Feng, Q. Xiao, Y. Zhang and J. Wang. Rh(I)-Catalyzed Coupling of Conjugated Enynones with Arylboronic Acids: Synthesis of Furyl-Containing Triarylmethanes. *J. Org. Chem*., **2016**, *81*, 10484-10489. https://doi.org/10.1021/acs.joc.6b00730.

[41] J. Karthikeyan, R. Haridharan and C.-H. Cheng. Rhodium(III)-Catalyzed Oxidative C□H Coupling of N-Methoxybenzamides with Aryl Boronic Acids: One-Pot Synthesis of Phenanthridinones. *Angew. Chem. Int. Ed.*, **2012**, *51*, 12343-12347. https://doi.org/10.1002/anie.201206890.

[42] J. Wang, W. Chen, S. Zuo, L. Liu, X. Zhang and J. Wang. Direct Exchange of a Ketone Methyl or Aryl Group to Another Aryl Group through C□C Bond Activation Assisted by Rhodium Chelation. *Angew. Chem. Int. Ed.*, **2012**, *51*, 12334-12338. https://doi.org/10.1002/anie.201206693.

[43] M. Tian, B. Liu, J. Sun and X. Li. Rh(III)-Catalyzed C–C Coupling of Diverse Arenes and 4-Acyl-1-sulfonyltriazoles via C–H Activation. *Org. Lett.*, **2018**, *20*, 4946-4949. https://doi.org/10.1021/acs.orglett.8b02078.

E-ISSN 2581 – 7957
P-ISSN 2277 – 3916

CVR Journal of Science and Technology, Volume 25, December 2023
DOI: 10.32377/cvrjst2518

Ecological Studies on Safilguda Lake with Reference to Water Quality

A. Rohini[1] and P. Manikya Reddy[2]
[1]Sr. Asst. Professor, CVR College of Engineering/H&S (Env.Sc.) Department, Hyderabad, India
Email: rohini.escience@gmail.com
[2]Professor, CVR College of Engineering/H&S (Env.Sc.) Department, Hyderabad, India
Email: reddymanikyap@gmail.com

Abstract: ***In this paper, the*** **Ecological studies on Safilguda lake were carried out. For this purpose, the physico-chemical parameters and phytoplankton were taken into consideration. The physico-chemical parameters showed some variation in the lake. The lake water is alkaline and dissolved oxygen was always recorded in low concentration. Bicarbonates, chlorides, organic matter, total hardness and total dissolved solids have been reported in high concentrations. In the lake, four groups of algae were recorded. Among these, Euglenophyceae was dominant followed by Cyanophyceae. On the basis of the physico-chemical and biological parameters, the assessment of water quality has been made.**

Index Terms: **Safilguda lake, Ecological studies, Water quality, Physico-chemical parameters and Phytoplankton**

I. Introduction

Water is the most valuable blessing to humankind and life on earth is not conceivable without water. Life on land, in the lakes, rivers and other freshwater habitats of the earth is vitally dependent on renewable fresh water, a resource that comprises only a tiny fraction of the global water pool. About 71 percent of the Earth's surface is covered with water and the distribution of water on the earth is uneven. The oceans hold about 97 percent of all Earth's water which is saline. Only 3% of Earth's water is freshwater, the amount needed for life to survive. A small portion of fresh water, less than one percent, is in lakes, rivers and streams. Lakes have environmental significance as sources of surface and ground water recharge, controls runoff, moderate the hydrological events drought and floods, host variety of flora and fauna and provide a wide array of recreational activities and aesthetic benefits for humans to enjoy.

Water is a scarce and precious resource which is not only being overexploited but also is seriously degraded due to anthropogenic activities. Water is a synonym for life without which life would not have emerged. Water, an indispensable requisite in natural state is free from contamination. Humans due to over usage, improper management and pollution have modified the quality and quantity of water resources to the greater extent. Release of waste waters from industries, household, agricultural runoff and urban waste alters the characteristics of water making it unfit and unsuitable for various purposes.

Water quality is a term used to describe the physical, chemical and biological characteristics of water, usually in respect to its suitability for a particular purpose. Potable or drinking water is defined as having acceptable quality in terms of its physical, chemical, and bacteriological parameters so that it can be safely used for drinking. Physical, chemical and biological properties which make the water quality change due to water pollution and affect the aquatic ecosystem. The aquatic organisms respond to these changes. Thus, water quality leads to the changes in distribution and composition of the species of aquatic environment. Presence or absence or dominant growth of some aquatic organisms is an indicator of water quality. Water pollution not only affects water quality but also threatens human health, economic development and social prosperity. By physico-chemical analysis, the water quality can be assessed. Chemical analysis in testing the water quality can reveal the concentration and type of pollutants present in the water. Biological analysis talks about the effects of pollutants on aquatic life.

Physico-chemical and biological factors are very important for ecological studies of water bodies. Better quality of water is described by its physical, chemical and biological characteristics [1]. Pollution alters the physical, chemical and biological parameters of water resources and deteriorates the water quality. Phytoplankton and various physico-chemical parameters help in assessing the water quality and pollution. Physico-chemical analysis is the prime consideration to assess the quality of water for its best use for drinking, irrigation and industrial purposes. The phytoplanktonic algae are the aquatic flora which grow in different aquatic ecosystems. Many taxonomic groups of algal communities are present. The study of phytoplankton gives their number, variety and distribution [2]. The variations and distribution of phytoplankton in freshwater depend on physico-chemical features. Phytoplankton are sensitive to the changes in aquatic environment and therefore act as indicators of water quality. Some phytoplankton dominate in polluted, eutrophic waters like blue-green algae and euglenoids whereas diatoms grow profusely in fresh waters. Blue greens grow abundantly and form algal blooms during summer.

II. Materials and Methods

Hyderabad, the capital of Telangana which is the newly formed and youngest Indian state is one of the major urban cities in India. Aside from historical monuments, Hyderabad is popular for its lakes and was called as Limnological capital of India which provide a perfect escape from the hustle and bustle of city life.

Safilguda lake, originally named Nadimi cheruvu is a natural lake located in Safilguda, Hyderabad. The lake was the source of irrigation for the farmers and the Hyderabadi nawabs and the military authorities used to quench their

Received on 16.10.2023, Revised on 09.11.2023, Accepted on 20.11.2023.

thirst. The lake was spread over 17acres. Due to gradual dwellings around the lake since 1975, the ill-effect on the lake has started. The lake is now spread over 5acres with a depth of 5metres.

Water samples were collected from the sampling stations of Safilguda lake. The entrance of the lake is the first monitoring station on the left side of the lake for immersion of Ganesh idols. Centre of the lake is taken as second sampling station. The lake's right side is the station III which is surrounded by residential areas.

From the sampling stations of Safilguda lake, water samples were collected every month during May 2017 to April 2018. The samples were tested in the laboratory for different physical and chemical parameters following APHA, 2005 [3] procedures. For Phytoplankton study, collected water samples of one litre were added with 2-3 ml of 4% formaldehyde solution and were kept in the sedimentation column undisturbed. Settling of the organisms in the samples takes about a month. For frequency measurements and identification of algal species, the samples were concentrated to 100 ml. At each station, the drop method of Pearsall et.al. (1946) [4] was followed for frequency measurement of different species of phytoplankton.

III. Results and Discussion

Physico-chemical parameters: The average values of physico-chemical parameters of the three stations are incorporated in Table 1.

TABLE I.
AVERAGE VALUES OF PHYSICO-CHEMICAL PARAMETERS OF SAFILGUDA LAKE. (ALL VALUES ARE EXPRESSED IN MG/L EXCEPT PH AND TEMPERATURE)

S.No	Parameters	Station I	Station II	Station III
		Average	Average	Average
1	Temperature	21.4	21.3	21.4
2	pH	8.3	8.4	8.4
3	Carbonates	17.5	23.3	24.5
4	Bicarbonates	285.6	215.14	247.23
5	Chlorides	301.25	338.62	333.11
6	DO	3.5	3.1	3.3
7	OM	8.4	8.6	8.8
8	COD	350.8	355.6	274.5
9	Total hardness	422.2	454.6	495.7
10	Calcium	43.3	35.9	26.12
11	Magnesium	20.2	9.5	13.8
12	Phosphates	10.2	10.9	10.98
13	Sulphates	30	14.4	24.9
14	Silicates	0.91	0.94	0.91
15	Nitrites	0.003	0.0037	0.003
16	TDS	845	834	870

From the table, it is evident that the lake exhibits alkalinity with pH ranging from 8.0 to 8.8 at all the stations. 6 to 48.0 mg/L is the range for carbonates. Bicarbonates ranged from 132.0 to 295.67 mg/L. The range of Chlorides was 140.0 to 365.8 mg/ L. 1.6 to 4.2 mg/L is the range of DO. The range of Organic matter was 1.5 to 18.5 mg/L. Chemical oxygen demand ranged from 100.0 to 560.0 mg/L. Total hardness was in the range of 210.0 to 500.0 mg /L. Ca and Mg ranged from 13.0 to 64.3 mg/L and 6.0 - 32.0 mg/L respectively. Phosphates were in the range of 8.98 - 13.89 mg /L. Nitrites were recorded in trace amounts ranging from 0.002 - 0.006 mg/L. Sulphates ranged from 11.45 to 28.89 mg/L. Silicates were in the range of 0.45 to 1.56 mg/L. Total dissolved solids ranged from 600 to 870 mg/L.

During the year, monthly analysis of water samples taken from Safilguda lake was done for physico-chemical parameters to study seasonal fluctuations, variations and interrelationships. There are certain correlations between the physico-chemical parameters.

The physico-chemical parameters exhibit certain interrelationships. The life of aquatic species is influenced by water quality characteristics. They have an impact on the variety, distribution and species makeup of the organisms. Water bodies undergo seasonal changes in their physico-chemical characteristics.

Surface water temperature regulates various physico-chemical and biological activities in the aquatic environment and has a major influence on the growth and distribution of aquatic organisms. The rate of chemical reactions in aquatic living forms can be influenced by the changes in water temperature. Hence, temperature is one of the most significant parameters for the aquatic ecosystem. In the present study, the lowest temperature was found during winter while the highest during summer.

In the present study, pH and carbonates are directly correlated. The pH and carbonates are inversely proportional to bicarbonates.

Chlorides play an important role in determining the quality of water. High concentration of chlorides indicates water pollution. The sources of chlorides in drinking water are municipal waste water discharge called sewage. High chlorides were reported in the present investigation due to sewage. Chlorides showed a positive correlation with organic matter. The release of sewage and domestic waste into the lake led to the growth of organic matter. The presence of organic matter increases the chloride content in water. Hence, chloride content in water bodies is an indicator of organic pollution.

The parameters water temperature, dissolved oxygen and organic matter are strongly related to each other and a change in one parameter has an effect on the other. Increase in water temperature and organic matter has led to decrease in dissolved oxygen. Organic matter, dissolved oxygen and chemical oxygen demand are all inversely correlated.

Water hardness and pH are strongly related. Water that is considered hard is alkaline having a pH greater than 8. Total hardness is high due to the alkaline nature of water. A decrease in magnesium levels and an increase in calcium concentrations were observed.

Phosphates in larger quantities designate the lake as polluted and eutrophic. Municipal waste water increases the phosphate levels in water. Excess phosphates lead to the profuse growth of algae and aquatic weeds. Algal blooms

results in decreased levels of dissolved oxygen and effects the aquatic organisms.

Excess nitrates in water causes Eutrophication which changes the physical, chemical and biological characteristics of water.

TDS is an important parameter in assessing the water quality. At higher concentration, TDS influences the taste, hardness and corrosive property of water. Higher TDS effect aquatic life forms and renders the water unfit and unsafe for drinking and domestic use.

In Safilguda lake, the parameters bicarbonates, chlorides, total hardness, total dissolved solids and phosphates were high and low levels of dissolved oxygen were noted.

Phytoplankton: In the lake, four different groups of planktonic algae Euglenophyceae, Cyanophyceae, Chlorophyceae and Bacillariophyceae were encountered. Euglenophyceae was the dominant algae followed by Cyanophyceae, Chlorophyceae and Bacillariophyceae.

The percentage of Phytoplankton at all the stations is incorporated in Table 2.

The phytoplanktonic algae are the aquatic flora which grow in different aquatic ecosystems of ponds, lakes, rivers as well as oceans. Phytoplankton are seen floating, suspended or attached to other substrata. These can be single celled, grow in colonies or occur as filaments. These are small chlorophyllous plants and are of many taxonomic groups. Different phytoplanktonic algae found in various aquatic ecosystems include green algae, blue-green algae, euglenoid flagellates, desmids and diatoms. Many taxonomic groups of algal communities have been discovered so far which are present in diverse habitats. Phycological studies deal with the microscopic plant like organisms distribution, abundance and diversity. In all the habitats, phytoplankton is affected by biotic and abiotic factors. Hence, the change in the aquatic ecosystem can be predicted by phytoplanktonic algae. Planktic life in aquatic habitats indicates water quality. The environmental parameters affect the seasonal abundance and distribution of plankton types.

One of the significant groups of phytoplankton is euglenophytes which are free living, phototrophic and unicellular flagellates. Euglenoids are found in large numbers in aquatic environments that contain more organic matter. Euglenophycean members are used as markers for organic contamination. Their occurence in fresh waters indicates the possibility of eutrophication and acts as pollution indicator organisms. Euglenophyceae account for the highest percentage of algal population in the lake. It is the dominant group of phytoplankton at all the stations. Euglenoid flagellates reached high peaks during summer and the number reduced during winter. *Euglena, Phacus, Trachelomonas and Lepocinclis* are dominant in the lake. Among these, *Euglena and Phacus* showed high species diversity. High temperature, organic matter and low DO favoured good growth of euglenoids which was in conformity with Cynthia [5], Sudha Rani [6], Amin et.al.[7] Veerendra babu et.al.[8], Seeta and Manikya Reddy [9] and Padma priya et.al.[10].

Blue-green algae, also called Cyanobacteria, are commonly found in diverse habitats, mostly in all the aquatic ecosystems. These are the oldest photosynthetic organisms on the earth and occur in many diversified forms like single celled, filamentous and coccoid. These can be free living or found in symbiotic association with plants, fungi etc. Cyanophyceae is the second predominant algae. Cyanophycean members were maximum during summer and low during winter. Diversified species of *Arthrospira, Oscillatoria and Microcystis* were identified at all the stations. High temperatures, warm water and intense sunlight in summers with low dissolved oxygen and high organic matter makes blue greens to grow abundantly which is according to Manikya Reddy and Venkateshwarlu [11], Pulla Reddy [12], Sudha rani [13], Ananthaiah [14], Amin et.al. [15], Padmapriya et.al.[16] and Veerendra babu et.al.[17]. Cyanobacteria thrive well in eutrophic waters rich in organic matter having high temperatures, inadequate dissolved oxygen and poor water quality.

Chlorophyceae is the third dominant group. Green algae are the largest algal class and are closely related to higher plants due to the presence of similar photosynthetic pigments. They occur as filaments, colonies or unicellular forms and are omnipresent in all the ecosystems either fresh, marine or terrestrial habitats. These are abundant and diverse in fresh waters but sometimes form blooms under eutrophic conditions. Among Chlorophycean members, Chlorococcales dominate during the entire study period. The species of *Scenedesmus, Coelastrum, Chlorococcum, Pandorina, Eudorina* and *Pyrobotrys* were present. Many diverse species of *Scenedesmus* were identified in the lake. More organisms from chlorophycean group were encountered during summer and the number was lowest during winter. Distribution and variety of chlorophytic phytoplankton are influenced by physico-chemical factors. Growth of chlorophycean members require different physico-chemical factors which vary from other groups of phytoplankton. Cynthia [18], Sudha rani [19], Ananthaiah[20], Ruth et.al [21], Amin et.al.[22], Padmapriya et.al.[23], Veerendra babu et.al.[24], Ramadevi [25] and Harini [26] proved that high content of organic matter and low dissolved oxygen influence green algal growth. Water temperature, dissolved oxygen, organic matter, nitrites and phosphates mostly influence the chlorophycean growth, composition and abundance.

TABLE II.
PERCENTAGE OF PHYTOPLANKTON

Algal Groups	Station I	Station II	Station III
Euglenophyceae	40.55	40.73	38.56
Cyanophyceae	30.68	30.57	31.37
Chlorophyceae	17.8	18.46	18.92
Bacillariophyceae	10.95	10.23	11.13

Diatoms are the members of the class Bacillariophyceae which are widely distributed microscopic unicellular algae. These can grow in fresh and marine waters. Diatoms have a silica based cell wall and are often referred to as "jewels of the sea" due to their optical properties. These are the most beautiful microscopic algae due to their structure and sculpturing of their walls. Diatoms constitute a small portion of the phytoplanktonic algae in the present study. This group is represented in lesser numbers when compared to other groups of algae throughout the study period. Diatoms were observed in good numbers during winter and the number decreased during summer. The species of *Cyclotella, Nitzschia, Navicula, Gomphonema and Synedra* were reported in the present study. Sudha Rani [27], Amin et.al.[28], Padma priya et.al.[29], Navatha and Manikya Reddy [30], Seeta and Manikya Reddy [31] and Srinivas et.al [32] observed that diatoms are in good number in winter and low in summer season. Diatoms are crucial in biomonitoring of aquatic ecosystems since these react to environmental changes and act as bioindicators of water quality. Safilguda lake is a polluted habitat. Due to this, the development and survival of diatoms are affected.

The common and dominant algal species of Safilguda lake are represented in Table 3.

TABLE III.
COMMON AND DOMINANT ALGAL SPECIES

Group	Dominant Species
Euglenophyceae	*Euglena acus, E.polymorpha, E.tripteris, Phacus orbicularis, Ph.longicauda, Ph.acuminatus, Trachelomonas hispid and Lepocinclis ovum.*
Cyanophyceae	Arthrospira platensis, Oscillatoria animalis, Oscillatoria chalybea, Merismopedia punctata, Chroococcus minutus and Microsystis aereginosa.
Chlorophyceae	*Scenedesmus dimorphus, S.quadricauda, S.armatus, S.quadricauda var.quadrispina, . Coelastrum microporum, Chlorococcum, Pandorina morum, Eudorina and Pyrobotrys.*
Bacillariophceae	*Cyclotella menegheniana, Nitzschia palae, Navicula rhynchocephala, Gomphonema parvulum and Synedra Ulna.*

IV. CONCLUSIONS

Based on the Physico-chemical parameters, Ecological studies have been made. The physico-chemical and phytoplanktonic parameters indicate that the water in Safilguda lake is polluted. The species of *Euglena polymorpha, E. acus, E. tripteris, Phacus orbicularies, P. longicauda, Arthrospira platensis, Pandorina morum, Cyclotella menegeniana and Nitzchia palea* were present in the lake and they can be considered as good ecological indicators of water quality and pollution.

REFERENCES

[1] Rohini.A,"Ecological studies on Safilguda lake with reference to water quality", Ph.D Thesis, Osmania University, Hyderabad, 2023.
[2] [2,7,15,22,28] Amin, Navatha and Manikya Reddy, "Ecological studies of Mir Alam Lake with reference to water quality" Nature Environment and Pollution Technology, vol.12, issue no.2, pp. 355-358, 2013.
[3] [3] American Public Health Association (APHA), "Standard methods for examination of water and waste water", 21st edition, Washington D C.2005.
[4] [4] Pearsall, "Freshwater biology and water supply in Britain". Sci. Publ. Freshwater Biol. Assoc., pp. 1-90, 1946.
[5] [5] [5,18] Cynthia, "Ecological Investigations on phytoplankton of two small lakes situated in Hyderabad Development area", Ph.D. Thesis, Osmania University, Hyderabad, 1980.
[6] [6] [6,13,19,27] Sudha Rani," Environmental monitoring of Hussain Sagar lake water", Ph.D Thesis. O.U. Hyderabad, 2004.
[7] [7] [8,17,24] Veerendra Babu A, Seeta Y, Manikya Reddy P, "Ecological studies on Alisagar lake with reference to water quality",International Journal of Current Research, 10(6), pp 69989-69992, 2018.
[8] [8] [9,31] Seeta.Y and Manikya Reddy.P "Ecological Studies of the River Krishna near Gadwal, Telangana with reference to Water Quality", G- Journal of Environmental Science and Technology ,5(4), pp 37-39, 2018.
[9] [9] [10,16,23,29] Padma Priya.K.T., Seeta.Y and Manikya Reddy.P, "Impact of Physico-Chemical Parameters on distribution and diversity of Euglenophyceae in Saroornagar Lake", Hyderabad, International Journal of Scientific Research in Science and Technology, 9(2), pp 16-24, 2022.
[10] [10] [11] Manikya Reddy.P and Venkateswarlu.V, "Assessment of water quality and pollution in the river Tungabhadra near Kurnool", Andhra Pradesh, Jr. Environ.Biol., 8(2), pp 109-119, 1987.
[11] [11] [12] Pulla Reddy.P, "Limnological studies on Ramanpad lake with reference to water quality", Ph.D. Thesis, Osmania University, Hyderabad, 2004.
[12] [12] [20] Ananthaiah, "Ecological studies on temple tanks of Ananthagiri and Sarpanpally project with reference to water quality", Ph.D. Thesis, Osmania University, Hyderabad, 2010.
[13] [13] [21] Ruth O.K, Johnson M.E.C and Shailaja. K, "Water Quality of Nadami Lake", Hyderabad, A.P., India, Journal of Aquatic Biology, 27, pp 48-50, 2012.
[14] [14] [25] Ramadevi.A, "Ecological Study on the Phytoplankton of Ibrahimpatnam lake", Ph.D Thesis, OU, Hyderabad, 2019.
[15] [15] [26] Harini.T, "The Impact of Urbanization on the Ecology of Durgham Cheruvu", Hyderabad, Ph.D Thesis, OU, Hyderabad, 2020.

[16] [16] [30] Navatha.K and Manikya Reddy.P, “Influence of Physico-chemical factors on the growth of Bacillariophyceae in two lakes of Hyderabad”, India. International education and research journal, 2(7), pp 105-108, 2016.
[17] [17] [32] Srinivas.L, Seeta.Y and Manikya Reddy.P, “Studies on algal diversity in Lower Manair Dam, Karimnagar”, Telangana, India. Journal of algal biomass utilization, 8(2), pp 11-15, 2017.

In the next issue (Vol. 26, June 2024)

1.	*Area-Delay-Power Efficient VLSI Architecture 2D FIR Filter using Modified Multipliers and Adders*	*Dr. Venkata Krishna Odugu* *Dr. B. Janardhana Rao* *Dr. G. Harish Babu*
2.	*An IoT based Low-cost Artificial Mechanical Ventilator for Patients*	*V. Sreelatha Reddy* *Dr. D. Gopisetty Ramesh*
3.	*A Survey on Recent Approaches for Image Captioning*	*Qazi Anwar* *Ch V S Satyamurty*

E-ISSN 2581 – 7957
P-ISSN 2277 – 3916

CVR Journal of Science and Technology, Volume 26, June 2024
DOI: 10.32377/cvrjstxxxx

Template for the Preparation of Papers for Publication in CVR Journal of Science and Technology

First A. Author[1] and Second B. Author[2]
[1]Designation, Name of Institution/Department, City, Country
Email: first.author@hostname1.org
[2]Designation, Name of Institution/Department, City, Country
Email: second.author@hostname2.org

Abstract: **These instructions give you basic guidelines for preparing camera-ready papers for CVR College journal Publications. Your cooperation in this matter will help in producing a high-quality journal.**

Index Terms: **first term, second term, third term, fourth term, fifth term, sixth term**

I. Introduction

Your goal is to simulate the usual appearance of papers in a Journal Publication of the CVR College. We are requesting that you follow these guidelines as closely as possible. It should be original work. Format must be done as per the template specified. Diagrams with good clarity with relevant reference within the text are to be given. References are to be cited within the body of the paper. Number of pages must not be less than five with minimum number of 4000 words and not exceeding eight pages. The journal is published in colour. Colours used for headings, subheadings and other captions must be strictly as per the template given in colour.

A. Full-Sized Camera-Ready (CR) Copy

Prepare your CR paper in full-size format, on A4 paper (210 x 297 mm or 8.27 x 11.69 in). No header or footer, no page number.

Type sizes and typefaces: Follow the type sizes specified in Table I. As an aid in gauging type size, 1 point is about 0.35 mm. The size of the lowercase letter "j" will give the point size. Times New Roman has to be the font for main text. Paper should be single spaced.

Margins: Top and Bottom = 24.9mm (0.98 in), Left and Right = 16 mm (0.63 in). The column width is 86mm (3.39 in). The space between the two columns is 6mm (0.24 in). Paragraph indentation is 3.7 mm (0.15 in).

Left- and right-justify your columns. Use tables and figures to adjust column length. On the last page of your paper, adjust the lengths of the columns so that they are equal. Use automatic hyphenation and check spelling. Digitize or paste down figures.

For the Title use 24-point Times New Roman font, an initial capital letter for each word. Its paragraph description should be set so that the line spacing is single with 6-point spacing before and 6-point spacing after. Use two additional line spacings of 10 points before the beginning of the double column section, as shown above.

TABLE I.
TYPE SIZES FOR CAMERA-READY PAPERS

Type size (pts.)	Appearance		
	Regular	Bold	Italic
6	Table caption, table superscripts		
8	Tables, table names, f irst letters in table captions, figure captions, footnotes, text subscripts, and superscripts		
9	References, authors' biographies	Abstra ct	
10	Section titles ,Authors' affiliations, main text, equations, first letters in section titles		Subheading
11	Authors' names		
24	Paper title		

Each major section begins with a Heading in 10 point Times New Roman font centered within the column and numbered using Roman numerals (except for REFERENCES), followed by a period, two spaces, and the title using an initial capital letter for each word. The remaining letters are in SMALL CAPITALS (8 point). The paragraph description of the section heading line should be set for 12 points before and 6 points after.

Subheadings should be 10 point, italic, left justified, and numbered with letters (A, B, …), followed by a period, two spaces, and the title using an initial capital letter for each word. The paragraph description of the subheading line should be set for 6 points before and 3 points after.

For main text, paragraph spacing should be single spaced, no space between paragraphs. Paragraph indentation should be 3.7mm/0.21in, but no indentation for abstract & index terms.

II. Helpful Hints

A. Figures And Tables

Position figures and tables at the tops and bottoms of columns. Avoid placing them in the middle of columns. Large figures and tables may span across both columns. Leave sufficient room between the figures/tables and the main text. Figure captions should be centered below the figures; table captions should be centered above. Avoid placing figures and tables before their first mention in the

Received on xx-xx-xxxx, Revised on xx-xx-xxxx, Accepted on xx-xx-xxxx.

text. Use the abbreviation "Fig. 1," even at the beginning of a sentence.

To figure axis labels, use words rather than symbols. Do not label axes only with units. Do not label axes with a ratio

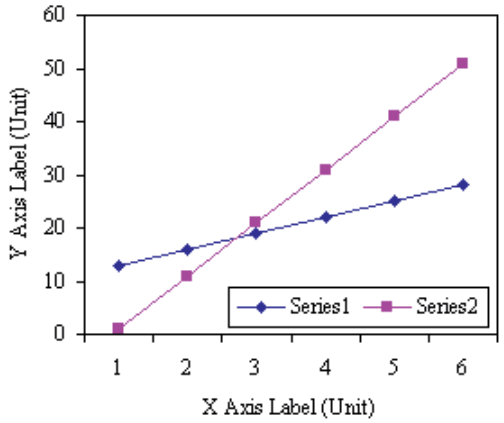

Figure 2. Note how the caption is centered in the column.

of quantities and units. Figure labels should be legible, about 8-point type.

All figures, tables and references must be cited in the text.

Please indicate the broad area/specializations into which the research paper falls, in the covering letter/mail to the Editor, so that reviewers with those specializations may be identified.

B. References

Number citations consecutively in square brackets [1]. Punctuation follows the bracket [2]. Use "Ref. [3]" or "Reference [3]" at the beginning of a sentence:

Give all authors' names; use "et al." if there are six authors or more. Papers that have not been published, even if they have been submitted for publication, should be cited as "unpublished" [4]. Papers that have been accepted for publication should be cited as "in press" [5]. In a paper title, capitalize the first word and all other words except for conjunctions, prepositions less than seven letters, and prepositional phrases. Good number of references must be given.

Latest references in the area must be included and every refence must be cited in the text of the research article.

C. Footnotes

Number footnotes separately in superscripts [1, 2, ⋯]. Place the actual footnote at the bottom of the column in which it was cited, as in this column. See first page footnote as an example.

D. Abbreviations and Acronyms

Define abbreviations and acronyms the first time they are used in the text, even after they have been defined in the abstract. Do not use abbreviations in the title unless they are unavoidable.

E. Equations0

Equations should be left justified in the column. The paragraph description of the line containing the equation should be set for 6 points before and 6 points after. Number equations consecutively with equation numbers in parentheses flush with the right margin, as in (1). Italicize Roman symbols for quantities and variables, but not Greek symbols. Punctuate equations with commas or periods when they are part of a sentence, as in

$$a + b = c\,. \tag{1}$$

Symbols in your equation should be defined before the equation appears or immediately following. Use "(1)," not "Eq. (1)" or "equation (1)," except at the beginning of a sentence: "Equation (1) is ..."

F. Other Recommendations

Use either SI (MKS) or CGS as primary units. (SI units are encouraged.) If your native language is not English, try to get a native English-speaking colleague to proofread your paper. Do not add page numbers.

III. Conclusions

The authors can conclude on the topic discussed and proposed, future enhancement of research work can also be briefed here.

References

[1] G. Eason, B. Noble, and I. N. Sneddon, "On certain integrals of Lipschitz-Hankel type involving products of Bessel functions," Phil. Trans. Roy. Soc. London, vol. A247, pp. 529–551, April 1955.

[2] J. Clerk Maxwell, *A Treatise on Electricity and Magnetism*, 3rd ed., vol. 2. Oxford: Clarendon, 1892, pp.68–73.

[3] I. S. Jacobs and C. P. Bean, "Fine particles, thin films and exchange anisotropy," in *Magnetism*, vol. III, G. T. Rado and H. Suhl, Eds. New York: Academic, 1963, pp. 271–350.

[4] K. Elissa, "Title of paper if known," unpublished.

[5] R. Nicole, "Title of paper with only first word capitalized", *J. Name Stand. Abbrev.*, in press.

[6] Y. Yorozu, M. Hirano, K. Oka, and Y. Tagawa, "Electron spectroscopy studies on magneto-optical media and plastic substrate interface," *IEEE Transl. J. Magn. Japan*, vol. 2, pp. 740–741, August 1987 [Digests 9th Annual Conf. Magnetics Japan, p. 301, 1982].

[7] M. Young, *The Technical Writer's Handbook*. Mill Valley, CA: University Science, 1989.

[8] T. Ali, B.K. Subhash and R.C. Biradar, "A Miniaturized Decagonal Sierpinski UWB Fractal Antenna", PIERS C, vol. 84, pp. 161-174, 2018.

ABOUT THE COLLEGE

CVR College of Engineering, an autonomous institution under the UGC, was established in the Year 2001, the first college in Telangana to be promoted by NRI technology professionals resident in the USA. The NRI promoters are associated with cutting-edge technologies of the computer and electronics industry. They also have strong associations with other leading NRI professionals working for world-renowned companies like IBM, Intel, Cisco, Facebook, AT & T, Google, and Apple who have agreed to associate with the College with a vision and passion to make the College a state-of-the-art engineering institution.

All B. Tech Programmes which are eligible are accredited three or four times by the NBA since 2007. Two UG Programmes namely ECE & EEE are accredited for Six years by the NBA under Tier-I. As of now, 7 B. Tech Programmes and 2 P.G Programmes are accredited. NAAC reaccredited the college for five years with grade 'A' with effect from 2022. Two M. Tech Programmers of AI and Data Science in 2018-2019 and three B. Tech CSE Programmes (AI & ML, DS & CS) in 2020-2021 and 3 new branches in Emerging Technologies namely B. Tech AI & ML, AI & DS and CSBSs Are the Recent Programs in 2023-24.

As formulated by the IQAC, many FDPs and workshops are organized by departments. College has MoUs with organizations such as Virtusa, Mitsubishi, NRSC, COMSAT, CADENCE, IIIT. Under innovation activities faculty have published 38 patents so far. Projects from NRSC under the RESPOND programme of ISRO, AICTE-RPS, TEQIP-III from JNTU, MODROBS-AICTE worth Rs.71 Lakhs are some of the recent projects funded by central agencies. Total funds received are Rs. 160 lakhs. Newgen IEDC of Government of India (DST) has sanctioned Rs.287 Lakhs for a period for five years in 2018-19, for Innovative Entrepreneurship Development Programmes by students and staff. 10 Projects were completed in 2019-20, 16 in 2020-21, 20 in 2021-22 and 21 projects in 2022-23. An exclusive Innovation Centre of 5000 Sqft. has been created for practical work and counseling.

The college has been creating records year after year. With more than 100 companies visiting CVRCE and 1000+ placements for the 2022 - 2023 academic year, it is the highest among the peer group of colleges. The highest offer is **57 Lakhs** at Deutsche Bank and next being **44 Lakhs** by 4 students at AMAZON and several students received offers higher than **Rs. 25 Lakhs**. More than **100 students** received offers higher than **Rs. 10 Lakhs**. About **200 offers** are higher than **Rs. 7 Lakhs**. With this, CVRCE becomes one of the leading colleges in the state in terms of offers with higher salaries. The placement percentage continues to be 100% since 5 years. The college has made huge progress in a short span of time and is preferred by the students and parents during the EAMCET counseling this year and is among the **top 3 colleges** in the state. College has been consistently in the range of 101-150 by NIRF over last five years. Many students have received special cash prizes in competitions like Hackathon, Mitsubishi etc., worth 1 to 2 Lakhs.

CVR is rated amongst the top 100 engineering institutions in the country by Outlook and holds many more recognitions.

CALL FOR PAPERS:

Papers in Engineering, Science and Management disciplines are invited for Publication in our Journal. Authors are requested to mail their contributions to Editor, CVR Journal of Science and Technology (Email Id: journal@cvr.ac.in). Authors can also submit their papers through our online open journal system (OJS) www.ojs.cvr.ac.in or www.cvr.ac.in/ojs. Papers are to be written using a Standard Template, which may be obtained on request from the Editor. It is also available on the college website www.cvr.ac.in

CVR JOURNAL OF SCIENCE AND TECHNOLOGY

CVR COLLEGE OF ENGINEERING

(UGC Autonomous- Affiliated to JNTU Hyderabad)
Mangalpalli (V), Ibrahimpatnam (M),
R.R. District, Telangana - 501510
http://cvr.ac.in